



AUSTRALIA
University of Southern Queensland
Faculty of Health, Engineering and Sciences

**Wear and Frictional Performance of Metals under
Dry/Waste Cooking Oil Lubricant Conditions**

For the award of

Doctor of Philosophy

A dissertation submitted by

Jasem Alotaibi
Master in Engineering

2014

Abstract

The development of recycled, renewable and sustainable products to replace fossil products is a vital concern from industrial, environmental and academic viewpoints. Lubricants are one of the synthetic products widely used in numerous fields of the manufacturing and industrial sectors. Furthermore in 2005, more than 38 million metric tons of oils were used in the lubrication techniques of various industrial applications in the United States (US). In other words, the need for alternative friendly lubricants needs to increase by about 36 billion gallons to meet expected demands in 2022. This need motivates the current investigation of the potential use of waste cooking oil as a lubricant for tribological applications. A review of the available literature reviewed no work related to this topic. However, many works have been conducted on vegetable oils and their potential as lubricant. The current study establishes the basis for the research in the area of waste cooking oil as a lubricant; focusing on the oil and its blend characteristics and applications in journal bearings.

At the first stage of this study, comprehensive experiments were conducted on the wear and the frictional behaviour of brass, aluminium and mild steel metals sliding against a stainless steel counterface under dry contact condition for comparison purposes with the lubricant results. Furthermore, predicting the tribological performance of materials is a very complex task and many attempts to model the wear and frictional behaviour of materials have failed. In this study, the artificial neural networks approach is used as a tool to predict wear, roughness, interface temperature and the frictional behaviour of metals under different operating parameters.

For the wear experiments under dry contact conditions, the wear and frictional performance of brass, aluminium and mild steel metals was investigated at different operating parameters: sliding distances (0 – 10.8 km) and applied loads (0 – 50 N) against a stainless steel counterface at a sliding velocity of 2.8 m/s. Experiments were performed using a block-on-ring (BOR) machine. To categorise the wear mechanism and damage features on the worn surfaces and the collected debris, scanning electron microscopy was used. A thermal imager was used to measure the interface temperature between the contacted bodies.

The results of the dry tests revealed that the operating parameters significantly influence the wear and frictional behaviour of all the metals. Brass metal exhibited better wear and frictional behaviour compared to the other metals tested. This is mainly due to the presence of 4% of Pb which helped reduce the aggressiveness of the material removal. Three different wear mechanisms were observed: two-body abrasion (brass), three-body abrasion (mild steel) and adhesive (aluminium). Friction coefficient trends were almost steady for brass and mild steel, however, aluminium/stainless steel exhibited slight fluctuations due to the modifications of the worn surface due to the sliding.

A biolubricant extracted from waste cooking oil (WCO) was developed in this study. Different blends of lubricant were prepared: fully synthetic 100%SO, 75%SO+25%WCO, 50%SO+50%WCO 25%SO+75%WCO and 100%WCO. The prepared waste cooking oil was blended with 5% (wt) of EVA copolymer and 2%

(wt) of EC and synthetic oils. Viscosity, pour point and flash points of the blends were examined and compared with industrial lubricants, (10W-50, 15W-40, 5W-40, and 5W-30).

The possibility of using WCO with its blend as a lubricant was tested using two techniques. First, a new tribology machine was designed and fabricated locally to study the wear and frictional performance of brass, aluminium and mild steel under lubricant conditions considering different sliding distances (up to 10.8 km), applied loads (10 N – 40 N) and sliding speed of 2.8 m/s at different lubricant temperatures (22°C, 40°C, 80°C). For consistent comparison purposes with the dry data, 113 kPa applied pressure was used as the dry contact condition was conducted mainly on 50N applied load which is equivalent to 113 kPa.

This study found promising potential for the use of WCO as a lubricant from a viscosity viewpoint. The viscosity of the waste cooking oil was significantly enhanced with the addition of 5% (wt) of EVA copolymer and 2% (wt) of EC. Blending the waste cooking oil with the fully synthetic oil also showed good improvement in performance. Based on the viscosity data, it is found that the pure waste cooking oil is very comparable with W5-30 oil which is recommended for gasoline and diesel engines. Increasing the applied load reduced the specific wear rate due to the presence of the lubricant which assisted to absorb the heat in the interface and clear (polish) the rubbed surfaces. The lubricant temperature was the key in determining the wear behaviour of the materials. Increasing the temperature reduced the viscosity, leading to less lifting during the experiments (i.e. a high specific wear rate). Conversely, the lubricant temperature showed no remarkable influence on the frictional behaviour. This is mainly due to the chemical adsorption of the fatty acids on the worn surfaces which acted as coated layer. From the journal bearing testing results, the waste cooking oil and its blends exhibited a similar trend in oil pressure values to the ones obtained for the fully synthetic oil, thus demonstrating the potential of waste cooking oil and its blends for journal bearing applications.

The complexity of predicting the wear and frictional performance of the materials motivates the tribologist to adopt an artificial neural network (ANN) approach, as it can be used to make such predictions with caution. In developing an ANN for this study, training function, performance and adopting functions were found to be the keys to predicting wear, roughness and interface temperature. The large input data of the friction coefficient (12009 x 3 x 3) made the prediction of friction coefficient difficult and led to poor ANN performance. Using individual inputs for each parameter and training the ANN in several steps improved the performance. About 95.5% prediction performance was recorded, particularly for the wear, roughness and interface temperature.

List of Publications

- Alotaibi, J, Yousif, B & Yusaf, T 2014, 'Wear behaviour and mechanism of different metals sliding against stainless steel counterface', *Proceedings of the Institution of Mechanical Engineers, Part J: Journal of Engineering Tribology*, p. 1350650114527072.
- Alotaibi, J, Yousif, B & Yusaf, T (in press), 'Brass, aluminium, and mild steel sliding against stainless steel under dry conditions', *International Journal of Precision Technology, Inderscience*.
- Alotaibi, J, Yousif, B & Yusaf, T (under review), 'Review on biolubricants and the potential of waste cooking oil', *Renewable and Sustainable Energy Review*.
- Alotaibi, J, Yousif, B & Yusaf, T (forthcoming), 'The potential of using waste cooking oil as lubricant', paper to be presented at Wear of Materials (WOM), Toronto, Canada, 12–16 April 2015.
- Alotaibi, J, Yousif, B & Yusaf, T (in progress), 'Designing a new lubrication tribology machine and the possibility of using waste cooking oil as lubricant, paper to be submitted to *Tribology Letter*.

Certification of Thesis

I certify that the ideas, designs and experimental work, results, analyses and conclusions set out in this thesis are entirely my own effort, except where otherwise indicated and acknowledged.

I further certify that the work is original and has not been previously submitted for assessment in any other course or institution, except where specifically stated.

Jasem Alotaibi
0061039057

Signature of Candidate

Date

Endorsement

Signature of Principal Supervisor

Signature of Associate
Supervisor

Date

Date

Acknowledgements

I would like to express my most sincere appreciation to my PhD project supervisors Dr B. F. Yousif and Dr. Talal Yusaf for their support, encouragement, valuable input and guidance at every stage of this thesis. I would also like to extend my gratitude towards the entire departmental and technical staff for their assistance and support in using the facilities and materials for conducting the experimental work for this thesis.

In addition, I wish to express my deepest appreciation to my family members for their constant support throughout this study, especially my mother and my son Ghanim. I would also like to thank my friends for their encouragement.

For the English editing services, I would like to thank Elite editing company (academic English editing) and Ms. Sandra Cochrane from the library of University of Southern Queensland.

Finally, I wish to extend my sincere gratitude to the University of Southern Queensland for their financial support during this study.

Contents

Abstract	ii
List of Publications	iv
Certification of Thesis	v
Acknowledgements	vi
Contents	vii
List of Tables	xvi
List of Figures	x
List of Abbreviations	xvii
Chapter 1: Introduction	1
1.1 Introduction	1
1.2 Research Question.....	2
1.3 Objectives of the Project	2
1.4 Significance and Contributions	2
1.5 Organisation of the Thesis	3
Chapter 2: Literature Review	5
2.1 Introduction	5
2.2 Lubricants and Biolubricants	5
2.2.1 Biolubricants in the Recent Era.....	6
2.2.2 Characteristics of Biolubricant Oils	9
2.3.1 Edible and Inedible Oils.....	11
2.3 Waste Cooking Oil.....	12
2.4 Tribological Test Rig	13
2.4.1 Operating Parameters Effects.....	14
2.4.2 Effect of Lubricant Temperature on the Wear and Frictional Behaviour of Metals.....	14
2.4.3 Influence of additives on characteristics of lubricants	15
2.4.4 Dry Adhesive Wear Behaviour of Common Metals	16
2.5 Artificial Neural Networks.....	17
2.6 Summary of the Literature	18
Chapter 3: Methodology and Newly Designed Machine	19
3.1 Introduction	19
3.2 Preparation of Materials	19
3.2.1 Waste Cooking Oil Preparations	19
3.2.2 Metals Selection	21
3.3 Hybrid Tribological Machine.....	21
3.3.1 The Block-on-ring Concept.....	21
3.3.2 Integration of Lubricant Temperature in the New Machine	22
3.3.3 Verification of the New Hybrid Tribological Machine.....	28
3.4 Experimental Procedure	29
3.4.1 Dry Adhesive Wear Testing.....	29
3.4.2 Adhesive Wear Testing Under Lubricant Condition	31
3.5 Properties of Waste Cooking Oil	33
3.5.1 Pour Point and Flash Points	33
3.5.2 Viscosity of the Waste Cooking Oil and its Blends.....	34
Chapter 4: Wear Behaviour and Mechanism of Different Metals Sliding Against Stainless Steel Counterface	41
4.1 Introduction	41
4.2 Background	41
4.3 Dry Wear Behaviour of Selected Metals	42

4.3.1 Specific Wear Rate against Sliding Distance	42
4.3.2 Dry Frictional Behaviour of Selected Metals.....	46
4.3.3 Worn Surface Observation on Selected Metals Subjected to Dry Sliding	49
4.4 Chapter Summary.....	60
Chapter 5: The Potential Use of Waste Cooking Oil as a Lubricant	61
5.1 Introduction	61
5.2 Influence of Waste Cooking Oil on the Tribological Performance of the Metals	61
5.2.1 Wear Behaviour of Metals Under Waste Cooking Oil Lubricant Conditions	61
5.2.2 Frictional Performance of Metals Wear under Waste Cooking Oil Lubricant Conditions.....	65
5.2.3 Observations of Worn Surface Tested Under Waste Cooking Oil.....	67
5.3 Wear and Frictional Behaviour of Metals Using Different Blends of Lubricant	72
5.3.1 Wear Behaviour of Selected Metals using Different Blends of Lubricant	72
5.3.2 Frictional Wear Behaviour	77
5.3.3 Surface Observations.....	80
5.4 Influence of the Lubricant Temperature on the Wear and Friction Behaviour of the Metals	85
5.4.1 Wear Behaviour.....	85
5.4.2 Frictional Behaviour.....	87
5.4.3 Surface Observation	89
5.5 Chapter Summary.....	97
Chapter 6: The Performance of Waste Cooking Oil in Journal Bearings.....	99
6.1 Introduction	99
6.2 Working Mechanism of Journal Bearings.....	99
6.3 Lubricant Preparation and Experimental Procedure	101
6.3.1 Lubricant Selection and Preparation for Journal Bearing Tests.....	101
6.3.2 Journal Bearing Setup	101
6.3.3 Experimental Procedure	104
6.4 Results and Discussion.....	105
6.4.1 Pressure Distribution	106
6.4.2 Lubricant Temperature in Journal Bearing	108
6.4.3 Friction Coefficient	110
6.5 Chapter Summary.....	111
Chapter 7: Prediction of Dry Wear Performance Using Artificial Neural Networks	112
7.1 Introduction	112
7.2 Development of the ANN Model	112
7.2.1 Selection of the Model	112
7.2.2 Experimental Data and ANN Development Method	114
7.2.3 Selection of the ANN Parameters	115
7.2.4 Training the ANN Model	116
7.2.5 Scope of Prediction	119
7.3 Optimisation of the ANN Model.....	119
7.3.1 ANN for Wear, Temperature And Roughness Prediction.....	119
7.3.2 Optimum ANN Model for Friction Coefficient	125

7.4 Prediction of Specific Wear Rate	132
7.5 Chapter Summary.....	137
Chapter 8: Conclusions and Recommendations	138
8.1 Conclusions	138
8.2 Recommendations	140
References	141
Appendix A: Detailed Drawings of the Components of the Hybrid Tribology Machine	160
Appendix B: Details of the ANN models	174
B.1 The Performance of Different Training Functions	174
B.2 Optimum Performance Function	185

List of Figures

Figure 1.1: Layout of the thesis.....	4
Figure 2.1: Data extracted from an international database (www.sciencedirect.com) showing the number of publications in the area of biolubricants.	6
Figure 3.1: Waste cooking oil extraction, preparation and blending	20
Figure 3.2: Block-on-ring technique	22
Figure 3.3: Three-dimensional view of the hybrid tribology machine	23
Figure 3.4: The custom-made load cell sensing frictional force	24
Figure 3.5: Leakage and sealing sections in the lubricant container.....	25
Figure 3.6: Assessment stage of the hybrid tribology machine before operation	26
Figure 3.7: Photos of the hybrid tribological machine integrated with the computer	27
Figure 3.8: Specific wear rate of the selected materials at 113.7 kPa applied stress using the new hybrid and laboratory machines at 2.8m/s sliding distance	28
Figure 3.9: Tribological machine with block-on-ring configuration (Yousif (2013a))	29
Figure 3.10: Roughness profiles of sections on the polished samples before testing* <i>the scale of the figures are different since they are auto-generated by Mahr roughness machine.</i>	30
Figure 3.11: Extraction of the debris from the lubricant.....	33
Figure 3.12: Viscosity vs. temperature of different blends of waste cooking and synthetic oils.....	35
Figure 3.13: Viscosity of the blends at 40°C and 80°C.....	36
Figure 3.14: Waste cooking oil viscosity with industrial lubricant.....	38
Figure 3.15: Viscosity index of waste cooking oil and its blend with W 5-30	39
Figure 4.1: Specific wear rate vs. sliding distance of brass, aluminium and mild steel materials under dry contact conditions.....	43
Figure 4.2: Specific wear rate vs. sliding distance of brass, aluminium and mild steel materials under dry contact conditions.....	44
Figure 4.3: Weight loss vs. sliding distance of brass, aluminium and mild steel materials under dry contact conditions.....	45
Figure 4.4: Summary of specific wear rate at steady state of brass, aluminium and mild steel materials under dry contact conditions at different applied loads after 10.8 km sliding distance	45
Figure 4.5: Friction coefficient vs. sliding distance of brass, aluminium and mild steel materials under dry contact conditions.....	46
Figure 4.6: Summary of friction coefficient at steady state of brass, aluminium and mild steel materials under dry contact conditions at different applied loads after 10.8 km sliding distance	47
Figure 4.7: Heat distribution in the rubbing area of the metals with the counterface after 2.5 km sliding distance under 30 N applied load * <i>The arrow points out the main measurement spot.</i>	49
Figure 4.8: Samples of the roughness profile of the specimens after the tests showing the maximum reading at different applied loads after 10.8 km sliding distance..	50
Figure 4.9: Average worn surface roughness after the test at different applied loads after 10.8 km sliding distance	51
Figure 4.10: Micrographs of the steel surface after the sliding showing different wear mechanisms	53
Figure 4.11: Micrographs of the aluminium surface after the sliding showing adhesive, abrasive and ploughing wear mechanisms	54

Figure 4.12: Micrographs of the brass surface after the sliding showing purely adhesive associate with small area of abrasive wear mechanisms.....	55
Figure 4.13 Micrographs of the collected debris after stainless steel sliding against mild steel, aluminium and brass under the applied load of 50 N for 10.8 km sliding distance.....	56
Figure 4.14: Schematic drawing showing different wear mechanisms exhibited when stainless steel rubbed against a) brass, b) aluminium and c) mild steel.....	57
Figure 5.1: Specific wear rate of the metals against sliding distance under different applied loads using waste cooking oil as a lubricant at 22°C	63
Figure 5.2: Specific wear rate of the metals against applied load using waste cooking oil as a lubricant at 22°C after 10.8 km sliding distance.....	64
Figure 5.3: Friction coefficients of the metals against sliding distance using waste cooking oil as a lubricant at 22°C under the applied load of 30 N.....	66
Figure 5.4: Mean friction coefficients of the metals against applied load using waste cooking oil as a lubricant at 22°C	66
Figure 5.5: Counterface temperature against applied load using waste cooking oil as a lubricant at starting temperature of 22°C	67
Figure 5.6: Sample of the roughness of the worn surfaces under the condition of waste cooking oil as a lubricant at a temperature of 22°C	68
Figure 5.7: Ra of the worn surfaces at different applied loads under the condition of waste cooking oil as a lubricant at a temperature of 22°C at the applied load of 30N.....	69
Figure 5.8: Micrographs of a) brass surface before tests b-e) the worn surface of the brass after testing at different applied loads under the condition of waste cooking oil as a lubricant at a temperature of 22°C showing: abrasive wear mechanism marked as “A”; plastic deformation marked as “ <i>Pl</i> ” and polishing process marked as “ <i>P</i> ”	70
Figure 5.9: Micrographs of a) aluminium surface before tests and b-d) the worn surface of the aluminium after testing at different applied loads under the condition of waste cooking oil as a lubricant at a temperature of 22°C. 22°C showing: abrasive wear mechanism marked as “A” and polishing process marked as “ <i>P</i> ”	71
Figure 5.10: Micrographs of a) mild steel surface before tests, and b-d) the worn surface of the mild steel after testing under the applied load of 30 N under the condition of waste cooking oil as a lubricant at a temperature of 22°C showing: abrasive wear mechanism marked as “A”; plastic deformation marked as “ <i>Pl</i> ” and polishing process marked as “ <i>P</i> ”.....	72
Figure 5.11: Specific wear rate vs. sliding distance of different materials tested under 40 N applied load using different blends of lubricant.....	74
Figure 5.12: Specific wear rate of different materials tested under 40 N applied load using different blends of lubricant after 10.8 km sliding distance * <i>the left Y-Axis is the scale for the aluminium specific wear rate.</i>	75
Figure 5.13: Correlation between the specific wear rate and the lubricant viscosity for all the materials after 10.8 km sliding distance.....	76
Figure 5.14: Schematic drawing showing the differences in contact mechanisms....	77
Figure 5.15 Friction coefficient vs. sliding distance of different materials tested at 40 N applied load using different blends of lubricant.....	79
Figure 5.16: Ra of the worn surfaces at different blends at 40 N applied load after 10.8 km.....	80

Figure 5.17: Micrographs of worn surface of aluminium after testing using different lubricants at 40 N applied load after 10.8 km sliding distance showing: abrasive wear mechanism marked as “A”; plastic deformation marked as “Pl” and polishing process marked as “P”	82
Figure 5.18: Micrographs of worn surface of brass after testing using different lubricants at 40 N applied load after 10.8 km sliding distance showing: abrasive wear mechanism marked as “A”; plastic deformation marked as “Pl” and polishing process marked as “P”	83
Figure 5.19: Micrographs of worn surface of mild steel after testing using different lubricants at 40 N applied load after 10.8 km sliding distance showing: abrasive wear mechanism marked as “A”; and polishing process marked as “P”	84
Figure 5.20: Specific wear rate of different materials after 10.8 km sliding distance using different lubricants under different environmental temperatures	86
Figure 5.21: Increment percentage in the specific wear rate of different materials after 10.8 km sliding distance using different lubricants under different environmental temperatures compared to the room temperature condition.....	87
Figure 5.22: Friction coefficient vs. sliding distance of different materials tested under 40 N applied load using lubricant (50% WCO + 50% SO) under different temperatures	88
Figure 5.23: Mean values of friction coefficients for all the materials tested under different lubricants and different environmental temperatures	89
Figure 5.24: Sample of the roughness of the worn surfaces under the condition of 50% waste cooking oil and 50% synthetic oil as a lubricant at elevated temperature of 40°C	90
Figure 5.25: Sample of the roughness of the worn surfaces under the condition of 50% waste cooking oil and 50% synthetic oil as a lubricant at elevated temperature of 80°C	91
Figure 5.26: Average roughness of the worn surface of the tested metals under different lubricants and environmental temperature.	92
Figure 5.27: Micrographs of brass using lubricant (50 % WCO + 50% S) under different environmental temperatures under the applied load of 40 N after 10.8 km sliding distance showing: abrasive wear mechanism marked as “A”; and adhesive wear marked as “Ad”	93
Figure 5.28: Micrographs of aluminium using lubricant (50 % WCO + 50% S) under different environmental temperatures under the applied load of 40 N after 10.8 km sliding distance showing: abrasive wear mechanism “marked as “A”; adhesive wear marked as “Ad”, and ploughing marked as “Pl”	93
Figure 5.29: Micrographs of mild steel using lubricant (50% WCO + 50% S) under different environmental temperatures under the applied load of 40 N after 10.8 km sliding distance showing: abrasive wear mechanism “marked as “A”; and pitting marked as “Pt”	94
Figure 5.30: Photo showing a sample of the oil when the mild steel was tested using lubricant (50 % WCO + 50% S) at 40 N after 10.8 km sliding distance with environmental temperature of 80°C	95
Figure 5.31: Micrographs of mild steel debris after testing using lubricant (50% WCO + 50% S) at 40 N after 10.8 km sliding distance with an environmental temperature of 80°C	96

Figure 5.32: Micrographs of aluminium debris after testing using lubricant (50 % WCO + 50% S) at 40 N after 10.8 km sliding distance with environmental temperature of 80°C	97
Figure 6.1: Pressure distribution in journal bearing.....	100
Figure 6.2: Journal bearing setup	102
Figure 6.3 Mechanism of the load applied to the journal bearing in the rig	103
Figure 6.4: Sommerfeld Number of the blends at the operating parameters of 600 rpm and 10 kN load.....	105
Figure 6.5: Pressure distribution around the journal bearing showing the position of the minimum film thickness * <i>all the values of the pressure are in MPa and the vertical arrow represents the load.</i>	107
Figure 6.6: Pressure distribution in journal bearing for different blends.....	108
Figure 6.7: Lubricant temperature (°C) distribution in journal bearing for different blends	109
Figure 6.8: Temperature vs. angle of the blends.....	110
Figure 6.9: Friction coefficient in journal bearings for different blends.....	111
Figure 7.1: ANN configuration for the prediction of A) friction coefficient, and B) specific wear rate (Ws), surface roughness, interface temperature.....	113
Figure 7.2: The method used in the current work for developing the ANN	115
Figure 7.3: Initial ANN Model developed considering two hidden layers of TRAINBFG training function	116
Figure 7.4: Training process for TrainBFG function	117
Figure 7.5: Train output for TrainBFG function.....	118
Figure 7.6: The performance of the ANN model training function to predict the specific wear rate, interface temperature and roughness for different sliding distances, materials and applied loads	121
Figure 7.7: The performance of the feed-forward back propagation network using TRAINRP as training function and a) LEARNGD or b) LEARNGDM as adaption learning function.....	122
Figure 7.8: The performance of the feed-forward back propagation network using TRAINRP as training function, LEARNGD as adaption learning function with different performance functions.....	123
Figure 7.9: The performance of the feed-forward back propagation network using TRAINRP as training function, LEARNGD as adaption learning function and MSEREG as performance function with different numbers of neurons	124
Figure 7.10: The performance of the optimum model to predict the specific wear rate, interface temperature and the roughness under different applied loads and sliding distances	125
Figure 7.11: Required training time for ANN to predict the friction coefficient.....	126
Figure 7.12: Regression of ANN results in predicting the friction coefficient with different numbers of data	127
Figure 7.13: Performance of the ANN to predict the friction coefficient using different training functions and numbers of data	128
Figure 7.14 Performance of the ANN to predict the friction coefficient using different applied loads.....	129
Figure 7.15: Performance of the ANN to predict the friction coefficient using BR training function for different performance functions and different numbers of input data.....	129

Figure 7.16: Performance of the ANN to predict the friction coefficient using BR training function and MSE performance function with different numbers of neurons and input data.....	130
Figure 7.17: Performance of the optimum ANN mode for the friction coefficient prediction.....	131
Figure 7.18: Real experimental data for friction coefficient of aluminium at 30 N applied load in comparing to the predicted data	131
Figure 7.19: Real experimental data and predicted data for brass materials at different operating parameters	133
Figure 7.20: Real experimental data and predicted data for aluminium materials at different operating parameters	135
Figure 7.21: Real experimental data and predicted data for mild steel materials at different operating parameters	136
Figure A.1: Overview of the hybrid tribology machine showing the main dimensions.	160
Figure A.2: Two-dimensional views of the lever for the hybrid tribology machine with the ISO.	161
Figure A.3: Two-dimensional views of the lever holder for the hybrid tribology machine with the ISO.....	162
Figure A.4: Two-dimensional views of the sample holder for the hybrid tribology machine with the ISO.....	163
Figure A.5: The main shaft connecting the counterface and the motor through the coupling.....	164
Figure A.6: Two-dimensional views of the counterface for the hybrid tribology machine with the ISO.....	165
Figure A.7: Two-dimensional views of the lubricant container for the hybrid tribology machine with the ISO.	166
Figure A.8: Two-dimensional views of the machine cover for the hybrid tribology machine with the ISO.....	167
Figure A.9: The seal cup for the hole in which the main shaft enters the lubricant container.....	168
Figure A.10: The balancing weight that is attached to the main lever of the machine.	169
Figure A.11: The main frame of the machine showing the base with the generated slots to attach the components.....	170
Figure A.12: The designed weights for the new machine.....	171
Figure A.13: The weight holder for the new machine.	172
Figure A.14: The pivot for the new machine.	173
Figure B.1: Performance of Trainbfg.....	174
Figure B.2: Performance of Trainbr.....	175
Figure B.3: Performance of Traincgb.....	176
Figure B.4: Performance of Traincgf.....	177
Figure B.5: Performance of Traincgp.....	178
Figure B.6: Performance of Traingd.....	179
Figure B.7: Performance of Traingda.....	180
Figure B.8: Performance of Traingdm.....	181
Figure B.9: Performance of Trainoss.....	182
Figure B.10: Performance of Trainrp.....	183
Figure B.12: Performance of MES.....	185
Figure B.13: Performance of MSEREG.....	186

Figure B.14: Performance of SSE.....	187
Figure B.15: Performance of ANN model with 2 Neurons in the hidden layer.....	188
Figure B.16: Performance of ANN model with 4 Neurons in the hidden layer.....	189
Figure B.17: Performance of ANN model with 6 Neurons in the hidden layer.....	190
Figure B.18: Performance of ANN model with 8 Neurons in the hidden layer.....	191
Figure B.19: Performance of ANN model with 10 Neurons in the hidden layer.....	192
Figure B.20: Performance of ANN model with 12 Neurons in the hidden layer.....	193
Figure B.21: Performance of ANN model with 14 Neurons in the hidden layer.....	194
Figure B.22: Performance of ANN model with 16 Neurons in the hidden layer.....	195
Figure B.23: Performance of ANN model with 18 Neurons in the hidden layer.....	196
Figure B.24: Performance of ANN model with 20 Neurons in the hidden layer.....	197

List of Tables

Table 2.1: Different Types of Vegetable Oil and their Applications	7
Table 2.2: Summary of Recent Studies on Vegetable Oils as Lubricants.....	8
Table 2.3: Main Physical Properties of Vegetable Oils (Quinchia et al. 2012).	10
Table 2.4: Recent Applications of Waste Cooking Oil.....	13
Table 3.1: Fatty Acid Composition of the Collected Waste Cooking Oil.....	20
Table 3.2: Properties of Mild Steel, Aluminium and Brass	21
Table 3.3: Operating Parameters for Adhesive Wear Testing under Lubricant Conditions	32
Table 3.4: Some of the fully synthetic oil specifications	33
Table 3.5: Pour Point and Flash Point of the Blends	34
Table 3.6: ISO Viscosity Grade Requirements ('Mixed-fiber diets and cholesterol metabolism in middle-aged men' 1991; Rudnick 2006; Rudnick 2010).....	37
Table 3.7: Comparison to Previous Works and Standards.....	40
Table 4.1: Recent Works on the Dry Wear Performance of Aluminium, Mild Steel and Brass	58
Table 6.1: Details of the Journal Bearing Rig (Ahmad, Kasolang & Dwyer-Joyce 2013; Ahmad, Kasolang & Dwyer-Joyce 2014; Ahmed et al. 2013; Kasolang et al. 2012).....	104
Table 7.1: Sample of the Input and Output Data for Brass at 50 N Applied Load and Different Sliding Distances	114
Table 7.2: Terms of the Training Function	120

List of Abbreviations

ASTM D97-02	Standard Test Method for Pour Point of Petroleum Products
BOR	block-on-ring
DITA	Di-Isotridecyl Adipate
DSC	differential scanning calorimetry
DSRW	dry sand rubber wheel
EC	ethyl cellulose
EVA	ethylene-vinyl acetate
FE	finite element
POD	pin-on-disc
PUFA	polyunsaturated fatty acid
SEM	scanning electron microscope
SO	synthetic oil
TAG	triacylglycerol
US	United States
USQ	University of Southern Queensland
WCO	waste cooking oil
WSRW	wet sand rubber wheel

Chapter 1: Introduction

1.1 Introduction

The discovery of petroleum in the late 1800s led to the replacement of animal fats, vegetable oils and mineral oils with synthetic oils (SOs). Petroleum oil gradually became the main lubricant base because of its low cost and superior performance. Lubricants are used widely in all fields of the manufacturing and industrial sectors. Lubricants are commonly used to reduce overheating and friction in a variety of engines, machinery, turbines and gears. Studies showed that, in the united states in 2005, more than 38 million metric tons of oils were used in lubrication techniques.

There is growing concern regarding the excessive use of petroleum-based oils, which significantly contributes to environmental pollution (Pop et al. 2008). Furthermore, the demand for fossil fuel and oil products is increasing in numerous areas. It has been predicted that alternative oils will need to increase to about 36 billion gallons by 2022 (Sadaka & Boateng 2009). Thus, there is an urgent need to find alternative resources to meet the great demand for oil in the coming years. The development of alternative fuels and/or oil products from natural resources aiming to replace the fossil products has become the major objective for many researchers and environmental and government bodies, especially in the developed world.

Studies have shown that bio-oils have become the most successful candidate for an alternative fuel source. In the current decade, a few studies have investigated the potential of using sunflower oil, castor oil, soybean oil and pollock oil as bio-fuel for diesel engines. Most of their results have been promising, but many researchers have raised the tribological issue that bio-fuels damage engine components. Since 2010, several bio-lubricants have been under investigation in different countries (Ting & Chen 2011), including soybean oils (the US and South America), rapeseed oil (Europe) and palm oil (Asia) (Cheenkachorn & Fungtammasan 2010; Jayed et al. 2009; Syahrullail, S. et al. 2011). These studies are in their initial stages and many issues need to be addressed before the application of these oils can occur (Kreivaitis et al. 2013; Luo, Yang & Tian 2013). The literature highly recommends thorough research on the performance and potential use of bio-lubricants. Moreover, in using edible bio-oils as fuels, several feed stocks have been proven impractical or infeasible because of their extremely high cost. This high cost is related to their current primary use as food resources, (Yaakob et al. (2013).

The most promising feed stock in the development of a friendly low-cost bio-lubricant is waste cooking oil (WCO), despite the drawbacks of its high free fatty acid (FFA) and water content (Balasubramaniam et al. 2012; Yaakob et al. 2013). Bio-fuels produced from WCO, as reported by many researchers, have numerous advantages such as low pollution (CO₂, CO and NO_x), low costs and acceptable brake-specific fuel consumption. However, to the knowledge of this researcher, no research has yet been attempted on the potential use of WCO as a lubricant.

In the current project, a bio-lubricant is prepared from WCO and applied to metal contact surfaces. The oil was obtained from an Australian restaurant and filtered and prepared locally. A new tribological machine was designed and fabricated locally to perform tribological experiments using the newly developed lubricant at different

environmental temperatures. The experiments were conducted at different operating parameters under dry and lubricant contact conditions for different metal materials (mild steel, brass and aluminium). The artificial neural network (ANN) method was used to predict the friction coefficient under both dry and wet contact conditions.

1.2 Research Question

Replacing synthetic products with bio-friendly products is a vital issue for the environmental regulation sector, researchers and industry. Considering that WCO is free and there is an issue with its disposal, finding a use for it as a bio-friendly lubricant is one potential solution. However, under which conditions and operating parameters can such oil be used? Answering this question requires a comprehensive study that considers the development of a new oil using WCO, the design of a new experimental setup, the preparation of materials, the conduct of experiments under different operating parameters and contact conditions, and finally recommendations for use.

1.3 Objectives of the Project

The main objective of this study is to investigate the possibility of using WCO as a lubricant. To achieve this objective, the following sub-objectives are drawn:

1. To extract bio lubricant oil from WCO and study its effect on the tribological behaviour of different metals
2. To develop a new tribological machine that can to operate under lubricant conditions with various environmental temperatures
3. To study the influence of different operating parameters on the tribological performance of different selected metals against smooth stainless steel (0.1-0.3 $\mu\text{m Ra}$) under dry and lubricant contact conditions
4. To investigate the influence of lubricant temperature on the wear and frictional behaviour of different rubbed metals
5. To categorise the wear mechanism of the worn surfaces using scanning electron microscopy and study the roughness profile of the rubbed surfaces
6. To develop an ANN model considering all the operating parameters and oil temperature to predict the frictional behaviour of selected metals under lubricant contact conditions.

1.4 Significance and Contributions

The success of this project will contribute to many areas including:

- Replacing fossil lubricant with bio-friendly lubricant will assist in reducing the impact of SO on the environment. In addition, using WCO in lubricant applications will be a useful way to dispose of oil
- Producing free bio-oil will contribute to industry since it will save the large amounts of money that is paid for SOs while conforming to current environmental regulations
- The outcomes of this research will be published in related international journals, contributing to the knowledge base

- Developing a new tribology setup will contribute to research in the field of tribology and establish a new research field at the University of Southern Queensland (USQ)

1.5 Organisation of the Thesis

This thesis contains eight chapters which are illustrated and summarised in Figure 1.1. Chapter 1 briefly introduces the importance of lubricants, as well as their benefits to the environment. Chapter 2 reviews the literature on lubricants and their applications. Chapter 3 covers the methodology used for oil preparation and material selection. This chapter also includes the design concept and experimental details. Chapter 4 addresses the dry adhesive wear performance of common metals which establishes the base for this research. Chapter 5 introduces the lubricant characteristics and their effect on the adhesive wear behaviour of the common metals. The results are presented under the condition of room and elevated temperatures. Chapter 6 covers the results and discussion of the bearing tests using different waste cooking oils blends. Chapter 7 presents the results of different artificial neural network (ANN) models and the optimization of the ANN models. Chapter 8 concludes the dissertation and presents the main findings.

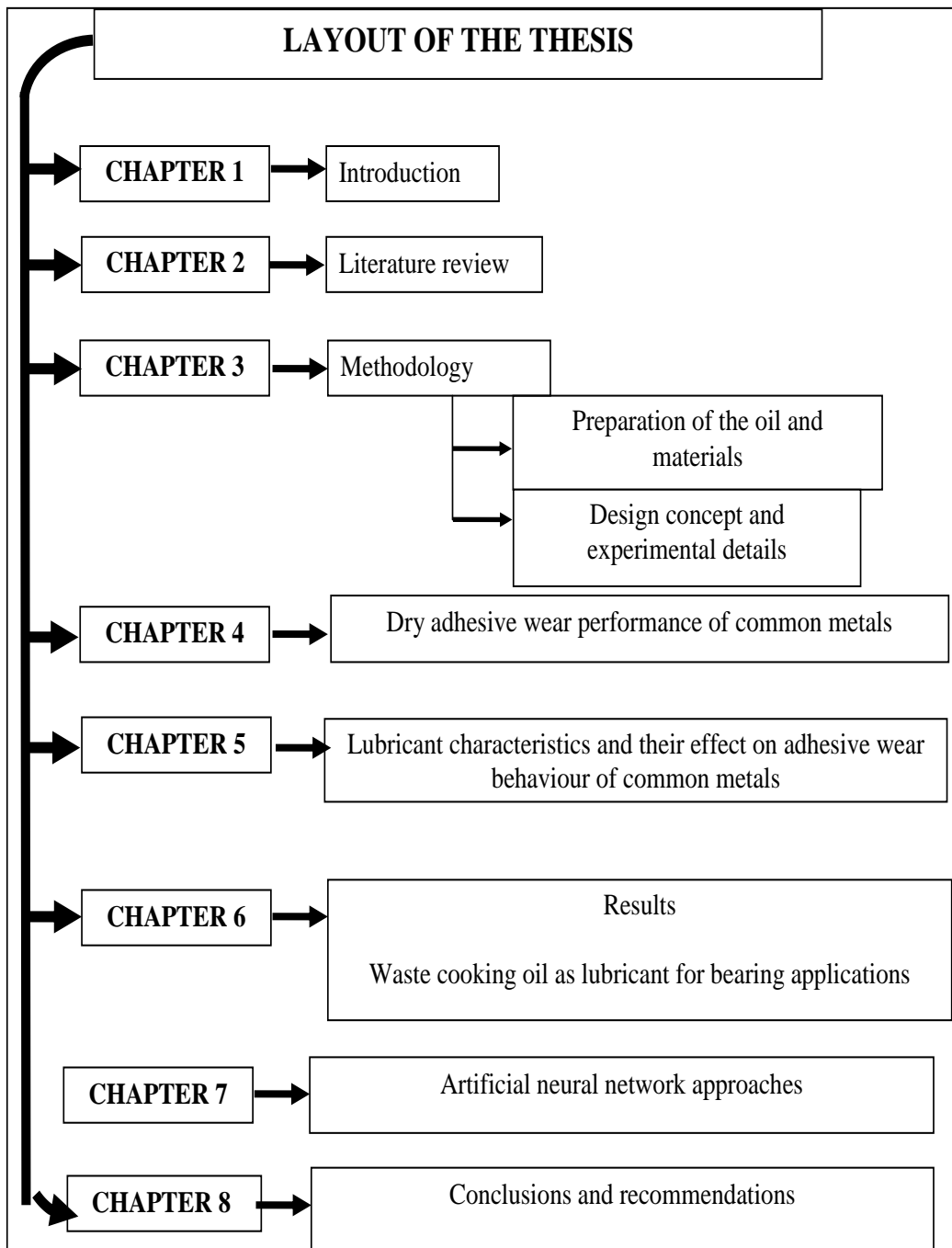


Figure 1.1: Layout of the thesis

Chapter 2: Literature Review

2.1 Introduction

In the current decade, the development of recycled, renewable and sustainable products as replacement for fossil products is vital from industrial, environmental, and academic viewpoints. The excessive usage of petroleum-based oils significantly contributes to the pollution of the environment. The exploration of alternative oils from natural resources to replace fossil oils has become the major focus of many researchers, and environmental and government bodies. In this chapter, a comprehensive literature review of existing research into the use of newly developed lubricants based on plant oils is conducted. However, due to the limited research on the usage of WCO as lubricant, the majority of the literature reviewed in this chapter is related to the biolubricants extracted from vegetable oils.

2.2 Lubricants and Biolubricants

Tribology science is comprised of friction, wear and lubricant branches. It can be traced back to about 4500 BC when the first wheel was developed (Smith et al. 1994). This was followed by the use of animal fat to ease the movement of rocks in the construction of the Egyptian pyramids.

When two objects are in contact with each other, contact pressure is created between them; causing surface damage if there is no protector between them. A lubricant is used as a protector between mechanical devices to reduce the wear between their components (Yousif & El-Tayeb 2008). One hundred years ago, water was mainly used to cool cutting tools its use was due to its high availability and thermal capacity. Lubrication and cooling in machines are vital to reducing the effect of any cutting process at the interface of a cutting tool and work piece. The main drawbacks of the coolant are poor lubrication and the corrosion of machines. Mineral oils were also used at that time due to their higher lubricity, but the high costs and low cooling ability of mineral oils led to their use only in “low cutting speed machining operations” (Lawal, Choudhury & Nukman 2012). Any lubricant can be used to remove and reduce the heat from a device during its operation. Lubricants are commonly used to reduce overheating and friction in a variety of engines, machinery, turbines, and gears ('Chapter 3 - Lubricants and Their Composition' 2014; Geitner & Bloch 2012).

New areas of research were developed in tribology with the discovery of fossil oils and synthetic lubricants for various tribological applications. Lubricants are being used widely in all fields of manufacturing for materials and machines. In the current era, petroleum-based lubricants are mostly used by industries. However, the excessive usage of fossil oil lubricants is affecting the environment; causing problems such as groundwater, surface water and soil contamination and air pollution (Chapman 2014; Kim 2014; Pop et al. 2008). Specifically, synthetic lubricants can be emitted into the environment through cleaning activities and accidental leakage. Further to this, wastewater lubricants include free oil and emulsified oil, and are created from a mixture of oil with a wastewater and washing agent. Several techniques have been developed to overcome these problems, such as

corrugated plate interception (Khondee et al. 2012) and gravitational oil separation (Panpanit & Visvanathan 2001).

Recently, the excessive world consumption of crude oil has had a severe economic impact, as it has led to a huge increase in the price of fuel products worldwide. Moreover, there is also a huge environmental impact. This has motivated researchers in the area of oils and fuel products to find an alternative friendly product to replace the synthetic product for several applications (Yusaf, Yousif & Elawad 2011). In addition, the use of environmentally friendly lubricants with renewable properties and sources, like inedible vegetable oils, are being reconsidered (Shashidhara, Y. & Jayaram, S. 2010). The high interest in the field of biolubricants is evidenced by the increasing number of relevant publications (Figure 2.1). The following sections will discuss the recent issues raised by such publications regarding potential biolubricants and their required characteristics.

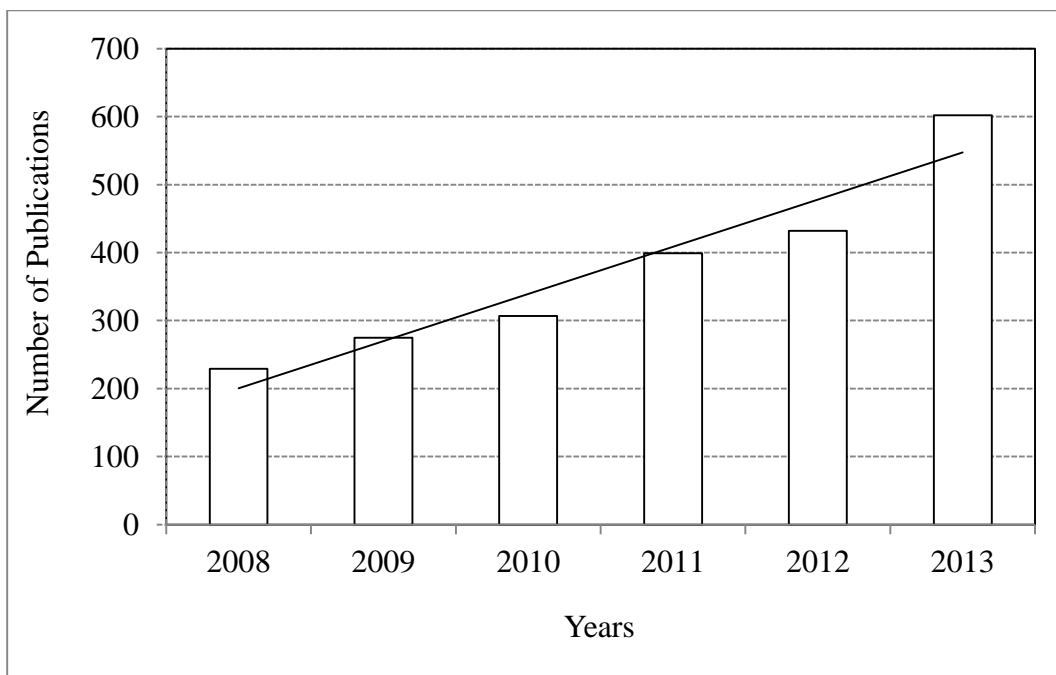


Figure 2.1: Data extracted from an international database (www.sciencedirect.com) showing the number of publications in the area of biolubricants.

2.2.1 Biolubricants in the Recent Era

Most of the lubricants used in rotary machine elements are based on mineral oils and SOs combined with different additives to meet the requirements of the intended application (Li et al. 2008). The main disadvantages and limitations of mineral oils are the poor biodegradability, high cost and limited supply (Delgado-Zamarreño et al. 2007). There is a need for environmentally friendly lubricants (Quinchia et al. 2014) due to strict government and environmental regulations as reported by recent studies (Atabani et al. 2013; Mobarak et al. 2014). Petroleum-based lubricants are toxic to the environment and difficult to dispose of. Many lubricant manufacturers have reconsidered vegetable oils over synthetic fluids due to a combination of renewability, biodegradability, excellent lubrication performance and low cost (Nagendramma & Kaul 2012; Quinchia et al. 2012).

Bio-oil can be divided into vegetable and animal, based on its main ingredient. Vegetable oil is more popular than animal oil due to its availability, ease of extraction and low cost (Shashidhara, Y. M. & Jayaram, S. R. 2010; Suarez et al. 2009). Vegetable oils are promising candidates as they provide a base fluid for eco-friendly lubricants. As lubricants, they have numerous advantages such as good contact (Lawal, Choudhury & Nukman 2013), excellent lubricity (Suarez et al. 2009), biodegradability (Franco & Nguyen 2011; Yilmaz 2011), very low volatility and high viscosity indices (VI) (i.e. minimum changes in viscosity with temperature) (Quinchia et al. 2010), and a high flash point due to the high molecular weight of the triglyceride molecule and excellent temperature–viscosity properties (Mejía, Salgado & Orrego 2013). Conversely, in their natural form, vegetable oils cannot fully meet the performance criteria for most lubricants due to drawbacks including poor low-temperature properties, opacity, precipitation and poor flow at a relatively moderate temperature. Table 2.1 outlines the possible applications for different vegetable oils.

Table 2.1: Different Types of Vegetable Oil and their Applications

Vegetable oils	Applications
Canola oil (Mortier, Fox & Orszulik 2010)	Hydraulic oils, metalworking fluids, food grade lubes, penetrating oils, chain bar lubes, tractor transmission fluids
Castor oil (Shashidhara, Y. & Jayaram, S. 2010)	Grease, gear lubricants
Coconut oil (Chatra, Jayadas & Kailas 2012)	Gas engine oils
Crambe oil (Kazmi 2011)	Intermediate chemicals, grease, surfactants
Cuphea oil(Kazmi 2011)	Motor and cosmetics oil
Jjoba oil(Kazmi 2011)	Cosmetic industry, grease, lubricant applications
Linseed oil(Kazmi 2011)	Paints, coating, lacquers, stains, varnishes
Olive oil (Mortier, Fox & Orszulik 2010)	Automotive lubricants
Palm oil (Syahrullail, S et al. 2011)	Grease, steel industry, rolling lubricant,
Rapeseed oil (Shashidhara, Y. & Jayaram, S. 2010)	Air compressor, chain saw bar lubricants, biodegradable grease

Vegetable oils can be edible or nonedible. Edible oils are more commonly available than inedible oils. However, since most vegetable oils are edible, a limitation can be found in using such oil in tribological applications, i.e. human consumption of edible oils limits the usage of such oils. Therefore, edible oil is not highly recommended for use as a lubricant and/or fuel (Atabani et al. 2013; Haldar, Ghosh & Nag 2009; Rizwanul Fattah et al. 2013). Thus, two points should be considered in developing a new oil: the oil should have less impact on the environment and be inedible. The researcher finds WCO to be a potential alternative to synthetic and edible oils. From a fuel point of view, there are several recent studies aiming to convert WCO into bio-fuels using different techniques (Talebian-Kiakalaieh, Amin & Mazaheri 2013; Yaakob et al. 2013).

With regard to vegetable oils, most research has addressed the wear and frictional performance of the oil without any chemical additives, as reported recently by Madankar, Pradhan and Naik (2013) who worked with castor seed oil. Castro et al.

(2006) studied the wear properties of different modified neat soybean oils without any additives using a tribological setup at a fixed speed of 700 rpm. No remarkable effect of the different oils was found on the wear and frictional performance of the soybean oil. Table 2.2 summaries recent works on vegetable oil as a lubricant and their findings. Despite the growing research interest in this new field, there is no clear direction on the application of vegetable oil as a lubricant.

Table 2.2: Summary of Recent Studies on Vegetable Oils as Lubricants

Oil Type	Main remarks
Soybean Oil	This work used mixtures of soybean oil original, epoxidised and hydrogenated as the base oils, focusing on their application as engine biolubricants. The results show that the epoxidised soybean oil has extremely high viscosity in comparison with engine lubricants and the original soybean oil, whereas the hydrogenated soybean oil is clearly opposite,(Ting & Chen 2011).
Castor Oil	There is excellent potential for a castor oil-based biodegradable 2T-lubricant in two-stroke engines to reduce smoke pollution (Singh 2011).
Rapeseed Oil	The results show that sage and thyme extracts have good oxidation stabilisation properties. Therefore, the modification of rapeseed oil with these extracts can improve the oxidation stability of rapeseed oil both in storage and in use (Kreivaitis et al. 2013).
Sunflower Oil	A comparative life cycle assessment analysis for the sunflower oil production line from conventional farming with organic farming showed environmental advantages (Spinelli, Jez & Basosi 2012).
Jatropha Oil	Jatropha oil in the base lubricant acted as a very good additive that reduced the friction and wear scar diameter by maximum 34% and 29%, respectively during the tribo test (Shahabuddin et al. 2013).
Palm Oil	Compared to mineral-based commercial oil, the palm oil-based lubricant exhibits superior tribological properties, but offer no clear advantage on engine and emission performance (Cheenkachorn & Fungtammasan 2010).

2.2.2 Characteristics of Biolubricant Oils

Low resistance to oxidative degradation and poor low temperature properties are the main performance issues associated with the use of vegetable oils as a lubricant. Different methods for solving these problems include reformulation of additives, chemical modification to enhance thermal stability, and genetic modification of the seed oil crop.

Triethanolamineoleate, triethanolmine and oleic acid are the main additives to the base oils that are used as lubricant oils. These affect the thermal stability of rapeseed and the tribological behaviour of base oils; demonstrating significantly better thermal stability and tribological behaviour.

Modifications of the carboxyl group (including esterification/trans esterification techniques) and of the fatty acid chain (including selective hydrogenation—dimerisation/oligomerisation—formation of C–C and C–O bonds, metathesis and oxidation techniques) are the two main chemical modification techniques in use.

Different methods of genetic engineering and new vegetable oil types are used. Sunflower and high oleic soyabean oils are good examples having higher thermo-oxidative stability and higher load transportation capacity. They need less adjustment to be used as base oil lubricants, compared to conformist plant-based oils as reported by Shashidhara, Y. and Jayaram, S. (2010).

Quinchia et al. (2014) studied the low temperature behaviours of different types of vegetable oils used in lubricating applications. Quinchia et al. (2010) and Quinchia et al. (2012) also studied these behaviours after blending vegetable oils with pour point additives. Blends were prepared by rotating the samples at 300 rpm at 100 °C –150 °C for 5–10 hrs, depending on the concentration and types of additive, and then cooled at room temperature. This thermal process was required to ensure that the additives were completely soluble in the vegetable oils. Different vegetable oils were used as base stocks: castor (from Spain), sunflower (from the local supermarket), soybean, rapeseed and high-oleic sunflower (from Germany and Spain). Their main physical properties are listed in Table 2.3. From the work reported by Quinchia et al. (2012); it can be found that unsaturated fatty acids is the key element influencing the low-temperature properties of vegetable oil-based lubricants. Furthermore, the presence of the fatty acids shows greater potential in using such oils due to the fact that the fatty acids present a high level of biodegradability and low toxicity compared to the conventional oils (Adhvaryu & Erhan 2002). Fatty acids in oil play a role in delaying nucleation and reducing crystallization of the lubricants. However, this depends on their chemical structure and composition. From the data presented in this table, it can be seen that castor oil exhibited good lubricant characteristics at low-temperature compared to the others which was due to its low content in saturated fatty acid content (3.66%) and the presence of hydroxyl groups in the fatty acid chain (ricinoleic acid, 82.48%). This in turn hampered the crystal packing process of the molecules, (Quinchia et al. 2012).

Table 2.3: Main Physical Properties of Vegetable Oils (Quinchia et al. 2012).

Oils	Palmitic (16:0)	Stearic (18:0)	Oleic (18:1)	Linoleic (18:2)	Linolenic (18:3)	Linolenic (18:3)	Unsaturated /saturated ratio
Castor oil	2.63	1.51	4.74	8.36	–	82.80	23.20
Soybean oil	11.28	2.70	24.39	56.28	5.34	–	6.15
Rapeseed oil	4.56	–	65.99	21.13	8.16	–	20.90
Sunflower oil	6.18	2.16	26.13	65.52	–	–	11.00
High oleic sunflower oil	3.84	4.42	83.66	8.08	–	–	11.10

Thermal analysis by differential scanning calorimetry (DSC), pour point temperature measurement, viscosity measurements at low temperature and statistical analysis are the main methods used to study the behaviour of vegetable oils.

Thermal analysis by DSC can be defined as the analysis of cooling curves (heat flow (W/g) vs. temperature) of the blends with cold flow and viscosity improver additives, which are obtained by using a scanning calorimeter (Q-100). Samples are heated in hermetic aluminium tubes at 25°C, and directly cooled with a cooling rate of 5°C/min to -80°C. The samples are then cleaned with nitrogen, which has a flow rate of 50mL/min, and the cooling curve for each sample is analysed to determine freezing temperature and wax appearance.

The pour point can be defined as the lowest temperature at which the vegetable oil can flow when it is cooled. The pour point of vegetable oils and their blends with additives are determined by the Standard Test Method for Pour Point of Petroleum Products (ASTM D97-02). In the viscosity measurements at low temperature method, the dynamic viscosities for vegetable oils are measured by using a coaxial cylinder in a rotational controlled-strain rheometer (Quinchia et al. 2012).

DSC is a method used to determine the crystallisation for vegetable-based lubricants. It is more accurate and faster than viscosity measurements and pour point temperature at low temperature methods. In all tests, castor oil demonstrate a better wear and frictional performance at low temperature because it has a low of saturated fatty acid content and it has hydroxyl groups in the fatty acid chain; which can obstruct the crystal packing system of triacylglycerol (TAG) molecules. Vegetable oils have a lower ratio of unsaturated/saturated fatty acids and crystallise at higher temperatures. Additionally, the concentrations of polyunsaturated fatty acids (PUFAs) have more impact on low temperature properties than the concentration of saturated fatty acids. Therefore, rapeseed oil has better behaviour at low temperatures compared with other oils that have a similar molecular structure such as soybean and high oleic sunflower oils. Pour point depressant (PPD) additives are used to improve the low-temperature behaviours of vegetable oils. PPD additives increase the low-temperature performance and decrease the pour point for vegetable oils which depend on their fatty acid composition. A blend of sunflower and pour point depressant was found to have a lower pour point than neat oil (Quinchia et al. 2012).

The biodegradability of lubricants investigated by standardised tests have provided valuable information for regulation assessment and how the chemical structure of lubricants influences biodegradability. Poor solubility of lubricating base oils in water is the major problem obstructing the biodegradability. Ultimate and primary biodegradability are the two phases of biodegradability used for analysing oils of different chemical structure such as synthetic polyolester, rapeseed, conventional mineral, and poly (a-olefin) oils.

The Co-coordinating European Council for the development of performance tests for lubricants and engine fuels (CEC L-33-A-93) test is used to evaluate primary biodegradability of lubricants by using triplicate flasks containing Di-Isotridecyl Adipate (DITA) as the reference material, and duplicate neutral and poisoned flasks, which are prepared for various duration of times (0, 7, 14 and 21 days) during the test period (Beran 2008).

The Organisation for Economic Cooperation and Development Guidelines for Testing of Chemicals 301B ready biodegradability (OECD 301B and OECD 310 tests) are used to evaluate the ultimate biodegradability of lubricants.

Despite the fact that vegetable oil-based lubricants have low oxidative stability compared to petroleum based lubricants, they are becoming commonly used in many countries. For example, corn and soybean oil are used in the US, and rapeseed oil is used in Europe and North America (Cheenkachorn & Fungtammasan 2010).

2.3.1 Edible and Inedible Oils

Recently, great concern has been raised about using edible vegetable oil, because it may cause starvation in poor and developing countries. Another problem arise the utilisation of available arable land, as ecological imbalances can be created when countries begin clearing forests. Hence, these feed-stock cause deforestation and wildlife damage. Therefore, inedible vegetable oils will be attractive as sustainable biodiesel. Examples of inedible seed crops oils include *Jatropha curcas* (tobacco), Deccan hemp (castor, jojoba, sea mango), Coriander, Salmon oil, Desert date, Cardoon (Milkweed) and Tung (Lucky Bean Tree). Microalgae oils are considered to be an inexhaustible source of biodiesel. They are very economical compared to edible oils. Microalgae give the highest oil yield, 25 times higher than that of traditional biodiesel crops. The waste of cooked vegetable oils is another relatively cheap biodiesel feedstock. Since the expiry of one source will have harmful effects in the long term, the consumption of biodiesel feedstock should be as diversified as possible, relying on multiple sources across the globe (Atabani et al. 2013).

Using inedible vegetable oils will not compete with countries' demands for food. Vegetable oil lubricants cover a small market segment and are increasing slowly and steadily in open applications such as chainsaws, forestry and two-stroke engines. More efforts have been made to change global laws and policies to ensure the environmental safety. In all cases, the environmental compatibility of lubricants must be checked. Inedible vegetable oils have the potential to divert agricultural practices and strengthen the economies (Shashidhara, Y. & Jayaram, S. 2010).

Biomass like edible crops, inedible crops, microorganisms, algae, recycled cooking greases, wood (lignocelluloses) and animal waste are used to create bio-oils. The most popular crops used for the production of bio-oil are canola, corn, soybean, rapeseed, mahua, mustard, jatropha, safflower, sunflower and palm. For bio-ethanol production, sweet sorghum, straw, sugar cane/beet, rice, wheat and corn can be used. The fuel vs. food debate and the environmental impacts of conversion and cultivation will limit the use of food crops to produce fuel. Converting residues from lignocellulose material or wood into biofuels is difficult as it is only in the coming decades technology is expected to reach the commercial stage. However, large-scale production of oil from microorganisms and microalgae can be a challenge (Jayasinghe & Hawboldt 2012).

2.3 Waste Cooking Oil

In using edible bio-oils as fuels, several feedstock have been proven impractical or unfeasible because of their extremely high cost and their usage primarily as food resources (Yaakob et al., 2013). WCO can be considered the most promising bio-oil feedstock despite its drawbacks, such as its high FFA and water content (Balasubramaniam et al. 2012; Yaakob et al. 2013). WCO can be produced from different sources and its base materials are plant-based lipids (sunflower, corn, margarine, coconut, palm, olive, soybean, oil and canola) or animal-based lipids (butter, ghee). It can be freely collected from food production industries, restaurants and houses using a special recycling bin; but this requires building public awareness (Yaakob et al. 2013). WCO and fats cause significant disposal problems in many parts of the world affecting the daily lives of millions of people. (Dovì et al. 2009) and (Iglesias et al. 2012) reported that the estimated amount of WCO collected in Europe is about 100,000–700,000 tons/year. In the US, about 11 billion litres (2.9 billion gallons) of recycled vegetable oil is produced yearly, mainly from deep fryers, snack food and fast food (Mendelsohn & Neumann 2004). Several recent studies have aimed to convert such waste oil into bio-fuels (Talebian-Kiakalaieh, Amin & Mazaheri 2013; Zhang, Wang & Mortimer 2012). Table 2.4 lists recent WCO applications. As reported by many researchers, bio-fuels produced from WCOs have numerous advantages such as low pollution (CO₂, CO and NO_x), low cost and acceptable brake-specific fuel consumption. Moreover, biodiesel produced from WCO may improve the pump plunger lubrication conditions (Pehan et al. 2009). However, it has been reported that bio-diesel produced from WCO highly damages engine components (Galle et al. 2012). In general, biodiesels have significant effects on the engine from a tribological point of view. Some biodiesel properties such as higher viscosity, lower volatility and the reactivity of unsaturated hydrocarbon chains cause injector coking and trumpet formation on the injectors, more carbon deposits, oil ring sticking and thickening and gelling of the engine lubricant oil (Pehan et al. 2009). Many biodiesel investigations have revealed the wear of engine components such the piston, piston ring, cylinder liner, bearing, crankshaft, cam tappet, valves, and injectors (Demirbas 2006; Giannelos et al. 2005).

Table 2.4: Recent Applications of Waste Cooking Oil

Oil Type	Applications	Finding
Palm kernel shell		The study indicates that it was similar to palm fatty acid distillate from palm oil and could be used as alternative feedstock for biodiesel production using a hydro treating process (Kim et al. 2013)
Sago waste		The bio-oils have potential as a valuable source for fuel or chemical feedstock (Abdul Aziz et al. 2013).
Waste cooking oil methyl ester	As fuel for single-cylinder four-stroke engine	The blends result in the reduction of carbon monoxide and hydrocarbon and an increase in nitrogen oxide emission (Muralidharan, Vasudevan & Sheeba 2011).
Waste cooking oil (sunflower oil)	As fuel for diesel engine	Promising results were indicated (Balasubramaniam et al. 2012).
Oil collected from fish restaurant	As fuel for diesel engine	In this comparative study, conversion of waste cooking oil to methyl esters was carried out using the ferric sulfate and the supercritical methanol processes. This resulted in a feedstock-to-biodiesel conversion yield of about 85–96% using a ferric sulfate catalyst (Patil et al. 2010).

To the researcher’s knowledge, no research has been attempted on the use of WCO as a lubricant. However, several articles have reported on vegetable oil as lubricants in industrial applications. The edibility of vegetable oil is its main limitation as a lubricant. Therefore, WCO may be a better alternative as a lubricant compared to bio-oils and/or virgin vegetable oil.

2.4 Tribological Test Rig

Test rigs are applicable to multiple or repetitive tests and a wide range of operation. They can perform extreme value tests safely, use accurately adjusted loads, study different variables separately and perform demanding measurements (Yousif & El-Tayeb 2010). The optimal way to obtain sufficient understanding of the tribological behaviour of two metals under dry or lubricant contact conditions is to carry out a number of experiments (El-Tayeb, Yousif & Yap 2008). Various tribological rigs have been developed for this purpose.

In the case of the dry contact condition, experiments are usually conducted at an atmospheric temperature of the air surrounding the rubbing zone. However, under lubricant contact conditions, different techniques have been attempted to perform the experiments. In most cases, the lubricant is tested at room temperature (Luna et al. 2011; Madankar, Pradhan & Naik 2013; Syahrullail, S. et al. 2011). Oil viscosity is, however, tested under different temperatures (Agach et al. 2012; Blum & Ovaert 2012). In this case, the tribological experiments do not reflect the real application of the oil especially when the contact temperature is much higher than the room temperature. To avoid contradictory or misleading results, experiments should be

conducted at the same temperature at which the viscosity is tested. Thus, there is a need to develop a new rig configuration in which the test can be conducted under lubricant conditions considering different lubricant temperatures.

2.4.1 Operating Parameters Effects

Several studies have examined the frictional and wear behaviour of metals under neat biolubricant conditions. Most work has focused on specific applications in which the sliding speed, sliding distance, environmental temperature and applied load is fixed (e.g. Luo, Yang & Tian (2009)). However, it is well known that the operating parameters have a significant influence on the wear and frictional behaviour of metal contact under dry and/or lubricant conditions, as reported by works (Kumar & Bijwe 2011; Prasad 2011; Tewari 2012). For example, Prasad (2011) investigated the frictional and wear behaviour of grey cast iron under different test parameters (applied load, sliding speed and test environment) and found that the wear loss increased with increasing sliding speed and load. However, the presence of oil lubricant caused a reduction in wear loss. Temperature near the specimen surface increased with test duration. The rate of increase was high initially followed by a reduction in the rate of increase. The friction coefficient also followed an identical trend. Increasing applied load and sliding speed brought about higher frictional heating while the severity of heating was reduced in the presence of the oil lubricant. The friction coefficient decreased with increasing load wherein the rate of reduction was high initially, followed by the attainment of a steady state value. Also, increasing sliding speed caused the friction coefficient to decrease during dry sliding, while it produced a mixed effect on the property in the presence of the oil lubricant. Thus, the operating parameters should be considered in testing a new lubricant. This motivates the current study to focus on the influence of the operating parameters on the newly developed bio-oil from WCO.

2.4.2 Effect of Lubricant Temperature on the Wear and Frictional Behaviour of Metals

With regard to biolubricants, several studies have examined the influence of oil temperature on the viscosity of the bio-oil in which it was heated. For instance, Ting and Chen (2011) studied the viscosity of soybean oil-based biolubricants at different temperatures and found that increasing the temperature reduced the viscosity of the oil, which in turn affected the friction and wear characteristics of the rubbed surfaces. Variation in the viscosity value significantly controls the interaction between the two rubbed surfaces. In that work, the increased in the temperature reduced the viscosity of all the selected oils which in turn influences the oil film characteristics in the interface. In the case of low viscosity with high bearing loads, interaction between the surfaces increase which resulted in material removal from the soft part. In addition, resistance to the material removal exhibited high friction coefficient. On the other hand, with the presence of a high viscosity of the oil film in the interface, separation of the interacted surfaces was highly possible with the coating lubricant as described by Velkavrh and Kalin (2012). In this situation, low wear and friction were expected since there was less interaction between the asperities in contact.

Although vegetable oils have some excellent properties as lubricants, some limitations should be technologically overcome, such as their limited range of viscosities. Quinchia et al. (2010) used an ethylene-vinyl acetate (EVA) copolymer as a viscosity modifier for sunflower oil, high-oleic sunflower oil and soybean oil. The viscosity experiments were conducted at moderate temperature (below 40°C) and EVA was found to be very effective since it highly improves the viscosity of the oil. Similar works have been reported (Erhan, Sharma & Perez 2006; Madankar, Pradhan & Naik 2013; Nagendramma & Kaul 2012), focusing on the influence of temperature on oil viscosity only in practical application. The interface temperature associated with the environmental temperature may have a combined effect on the friction and the wear behaviour of the rubbed surfaces. In this thesis, the focus is on the combination of both the environmental and interface temperatures and a new tribology machine will be developed to conduct such experiments (see the new tribology machine section).

2.4.3 Influence of additives on characteristics of lubricants

Biolubricants such as vegetable oils have strong interactions with lubricated surfaces ('Mixed-fiber diets and cholesterol metabolism in middle-aged men' 1991) and the amphiphilic nature of the biolubricant introduces a good film/force relationship because of the long fatty acid chains and the presence of polar groups in the vegetable oil structure (Adhvaryu, Erhan & Perez 2004); i.e. vegetable oil-based lubricants are effective as both boundary and hydrodynamic lubricants, (Fox & Stachowiak 2007). Due to the high demand for friendly bio-lubricants there is recent interest in studying the influence of different types of additives on the biolubricant characteristic. These studies attempted to improve the biolubricant properties and identifying the industrial applications. Recently, Tang and Li (2014) comprehensively addressed the issues associated with the additives and their impact on properties of the biolubricant covering the works from 2007 to 2014 in a review article. Fox and Stachowiak (2007) reported a review work on the vegetable biolubricants and the importance of the additives. In all the reported works, the main aim of including additives in the biolubricants is to improve the lubricity of the oil owing to reduce the friction, material removal in the rubbing zone, (De Barros et al. 2003; Neville et al. 2007) and/or generate a film on the rubbed surfaces, (Vengudusamy et al. 2012). Minami et al. (2008) suggested that there are two different mechanisms for the lubricant behaviour in the interface which are either the lubricant film will be stable on both rubbed surfaces or on one of them only. If the lubricant film generated on both surfaces, significant reduction in the friction and material removal will be noticed. However, if the lubricant film stabilised on one surface only, there will be less reduction in both wear and friction compared to the first scenario. From the recent works, there is a great correlation between the viscosity and the lubricant performance of biolubricants, (Binu et al. 2014; Jacobs et al. 2014; Quinchia et al. 2014), and this in turn influences the film generated in the interface. Furthermore, the amount of additive significantly controls the viscosity of the lubricant, Quinchia et al. (2009).

For the vegetable oil (biolubricant), ethylene vinyl acetate (EVA) is commonly used as an additive to improve the viscosity of lubricant. This was been proven when sunflower oil blends exhibited higher viscosity values which are needed for applications such as the lubrication of bearings and four-stroke engines ('Mixed-fiber diets and cholesterol metabolism in middle-aged men' 1991; Martín-Alfonso & Franco 2014; Quinchia et al. 2009). 3 wt % - 5 wt % of EVA has been recommended (in these works) for the very light vegetable oils (sunflower, castrol) since 5% of the EVA thickened the oil to a suitable thickness at elevated temperature, (Quinchia et al. 2012; Quinchia et al. 2010), giving very good film-forming properties and excellent friction and wear behaviour. Quinchia et al. (2014) reported that the hydroxyl functional group, that increases both the viscosity and polarity of this vegetable oil were the main contributors to the achieved improvement associated with the addition of the EVA. On the hand, the EVA addition to vegetable oils impacted on the onset freezing temperature during a cooling temperature sweep test (Quinchia et al. 2010).

Another important modifier is the ethyl cellulose (EC) which is commonly used as thin film coaterial. Ethyl cellulose (EC) is a kind of water insoluble that having favourable mechanical properties, low cost and good film formation (Yang et al. 2014). Ethyl cellulose has been proven to be a good additives (thickener) for vegetable oil in lubrication applications, e.g. castor oil (Núñez et al. 2012; Sánchez et al. 2011; Singh 2011), and soybean (Quinchia et al. 2012; Quinchia et al. 2014). From these reported works, ethyl cellulose (EC) was found to be a good potential additive in the formulation of environmentally-friendly lubricants containing high oleic oil, i.e. it significantly improved lubricant viscosity, viscosity index, and low-temperature behaviour, (Quinchia et al. 2012; Quinchia et al. 2014).

2.4.4 Dry Adhesive Wear Behaviour of Common Metals

Despite several studies on the frictional and wear behaviour of metals, there is still a need for a better understanding of metal behaviour under different tribological applications. Recent studies have reported on the tribological performance of different metals such as aluminium (Birol 2013; Kumaran & Uthayakumar 2013; Rao et al. 2013), steel (Felder et al. 2012; Leiro et al. 2013; Máscia et al. 2013) and brass (Feser et al. 2013; Gava et al. 2013). Most of these studies focused on the application of the metals and experiments were conducted to accommodate specific operating conditions (i.e. specific sliding speed, sliding distance, environmental temperature and applied load) (Alvarez-Vera, Ortega-Saenz & Hernandez-Rodríguez 2013; 2009; Umanath, Palanikumar & Selvamani 2013). Consequently, understanding of the wear and frictional behaviour of the metals is limited as operating parameters have a significant influence on this behaviour under both dry and wet (lubricant) contact conditions (Berglund, Marklund & Larsson 2010; Kumar & Bijwe 2011; Prasad 2011; Tewari 2012; Yousif 2013b).

In addition, various studies have presented the wear results in different formats. For example, the wear performance of a metal has been presented in wear rate (Slavkovic et al. 2013), weight loss (Forati Rad, Amadeh & Moradi 2011); volume loss (Vasheghani Farahani et al. 2014), specific wear rate and/or wear resistance (Cassar

et al. 2012; Jahangiri et al. 2012). Each form introduced a different understanding and trend, which makes the results misleading and the data unable to be compared. Therefore, it is recommended that the wear performance of materials be presented in terms of specific wear rate, which represents the volume loss per applied load and sliding distance. This motivates the current study to evaluate the wear and frictional behaviour of aluminium, steel and brass materials sliding against a stainless steel counterface considering different operating parameters to gain the value of the specific wear rate at the steady state condition and identify the wear mechanism.

2.5 Artificial Neural Networks

The wear and frictional behaviour of materials can be described as a response of materials rubbed onto one another. This can involve different parameters and elements making the prediction of the frictional and/or wear behaviour of materials very complex and unpredictable at some stages. There recently have been several attempts to use finite element (FE) methods (Dai, Zhang & Tang 2013; Leonard et al. 2014; Martínez et al. 2012; Xin, Gaoliang & Zhe 2014), but they were all based on several assumptions that limited the developed model. Martínez et al. (2012) stated that ‘to numerically implement the wear model, it is necessary to set up a procedure for determining the relationship between the friction coefficient and the contact pressure for the material and counter material contact pair’. In other words, the development of the FE models for tribological application is limited and requires a great deal of experimental data for each material and condition.

Nevertheless, new researchers have considered new approach to the prediction of tribological characteristics. Both fuzzy logic and ANNs are similar in approach can be described as a black box in which there are inputs, hidden layers of logic arguments, and outputs (Nasir, T et al. 2010).

Comparison and/or combined of FE and ANNs for nonlinear behaviour of crack propagation, spring back of materials and safe sea-state have been investigated (Gajewski & Sadowski 2014; Jamli, Ariffin & Wahab 2014; Yasseri et al. 2010). The studies concluded that FE and ANN exhibited very comparable results under very limited conditions. When different parameters and conditions are involved in the prediction, ANN produced better prediction outcomes than FE.

From a tribological perspective, there are several recent studies on the possibility of using ANN to predict the wear and frictional values of different materials (Abdelbary et al. 2012; Busse & Schlarb 2013; He et al. 2014; LiuJie, Davim & Cardoso 2007). The most important factor impacting on an ANN model’s performance is the amount of data, the more data in the input and output, the better the performance that can be archived. It should be mentioned here that some studies combined the prediction of the friction coefficient with the specific wear rate (Gyurova & Friedrich 2011), as outputs under certain operating parameters in which the wear data is less than the friction coefficient and interface temperature led to poor prediction in wear outputs. This has been noticed in some studies pertaining to the prediction of the friction and wear performance of some composite materials considering different volume fractions (Gyurova, Miniño-Justel & Schlarb 2010) and/or the orientations of the fibres (Nasir, T. et al. 2010).

2.6 Summary of the Literature

This chapter reviewed the recent literature on biolubricants, WCOs, tribology machines and ANN approaches. The chapter can be summarised as follows:

1. There is a growing demand for alternative lubricants to replace synthetic lubricants from both economic and environmental perspectives. The researcher identifies the potential use of WCO as a lubricant to address this issue since WCO is a deposit substance (low cost), and environmentally friendly (i.e. filtered from waste oils extracted from either vegetable or animal oils)
2. WCOs are available everywhere in large quantities and disposal is currently a problem. Some recent studies have attempted to convert WCOs into biofuels for diesel engines, but WCO biofuels have been shown to degrade engine life. In this thesis, an attempt is made to use WCO as a lubricant using different blend ratios with SOs, and to identify its applications
3. The dry adhesive wear behaviour of metals is comprehensively reported in the literature. However, there is confusion and contradiction in presenting the wear data in terms of wear rate, weight or volume loss, specific wear rate, and wear resistance. In the current study, the dry adhesive wear behaviour of different metals is presented in different forms
4. Different tribological setups have been developed and reported in the literature. However, no machine was able to test the tribological behaviour of metals under different operating parameters. In this study, a new tribological machine is developed to test the wear and frictional performance of different metals under dry/lubricant conditions at different lubricant temperatures
5. An ANN approach is a promising tool in predicting the tribological behaviour of materials. However, there are arguments (in the literature) about the number of inputs required to gain good prediction outputs. In this work, a new ANN model is developed to predict the frictional performance of metal/metal contacts at different input parameters, considering individual inputs and/or combined inputs.

Chapter 3: Methodology and Newly Designed Machine

3.1 Introduction

This chapter discusses the preparation and extraction of WCO and its blending procedure with SO. The metal selections and their fundamental characteristics, the experimental setup and procedure for the dry adhesive wear testings, and the new concept of the new tribology machine associated with this experimental procedure are also introduced.

3.2 Preparation of Materials

3.2.1 Waste Cooking Oil Preparations

WCO can be obtained from different sources such as restaurants and fast-food outlets. For this study, WCO was collected from fish and chips restaurants in Toowoomba city, Queensland, Australia. Based on information obtained from the restaurant owners, fish and chips are cooked in cotton seeds oil at a temperature of 180 °C. The oil is used for seven days and it heated up for seven hours a day (from 10 am to 5 pm), i.e. the oil is used for 49 hours. For one restaurant, about 10 litres of oil need to be disposed of daily. The collected oil was placed in a 200-litre tank. The steps involved in cleaning and preparing the oil are described in Figure 3.1. The collected oil was dirty and full of undesirous substances (e.g. small burnt chips or leftover fish). In order to purify it, different-sized sieves were used to extract the debris. The oil was then heated to 90–100°C in order to remove the moisture from it. The oil was kept at this temperature for about one hour. While the oil was cooling down, it was filtered using a micro-filter (woven mesh fabrics) supplied by Sefar Filter, Australia. This type of filter is recommended for filtering chemicals as it is able to resist high temperatures. The fabrics used in designing the filter have thread diameters < 250 µm and mesh openings < 500 µm and can be ultrasonically welded. The main characteristics of the fabric used in the filter are high dimensional stability and tensile strength, constant fabric stiffness and thickness, repeatable pore size and filtration performance, low pressure drop and high flow rate.

Before blending the waste cooking oil with the synthetic oil, 5% (wt) of EVA copolymer and 2% (wt) of EC were used as additives. Their impact will be discussed later in this chapter. Different blend ratios were used in preparing the blends of the waste cooking oil (WCO) and fully synthetic oil (SO) as lubricants: 0, 25 vol. %, 50 vol. %, 75 vol. % and 100 vol. % of WCO in SO. 5w-30 fully synthetic oil is used in this work which was supplied by Shell Helix. The technical data for each oil grade is provided by the company via <http://www.shell.com/global/products-services/on-the-road/oils-lubricants>. Some of the fully synthetic oil specification are MRV, ASTM D4684 (17000), Density, ASTM D4052 (852), Flash point, ASTM D92 (240), Pour point, ASTM D97 (-48).

The WCO was heated up to 80°C and the SO was gently added in about 5% increments to reach the required percentage. An electrical mixer was used to mix the blends at 80°C for about 30 mins. The blends were cooled down to room temperature

and kept in glass containers to prevent any chemical reaction or moisture absorption. In the last stage of this work, different blends were used for journal bearing tests.

The fatty acids composition of the pure WCO has been tested with the GC-FID technique under the operating condition of an oven: 150 °C (75.0 min) isothermal, Carrier: helium, 21 cm/sec at 150 °C, and Detector: FID, 250 °C. The results of the fatty acids composites of the WCO are presented in Table 3.1.

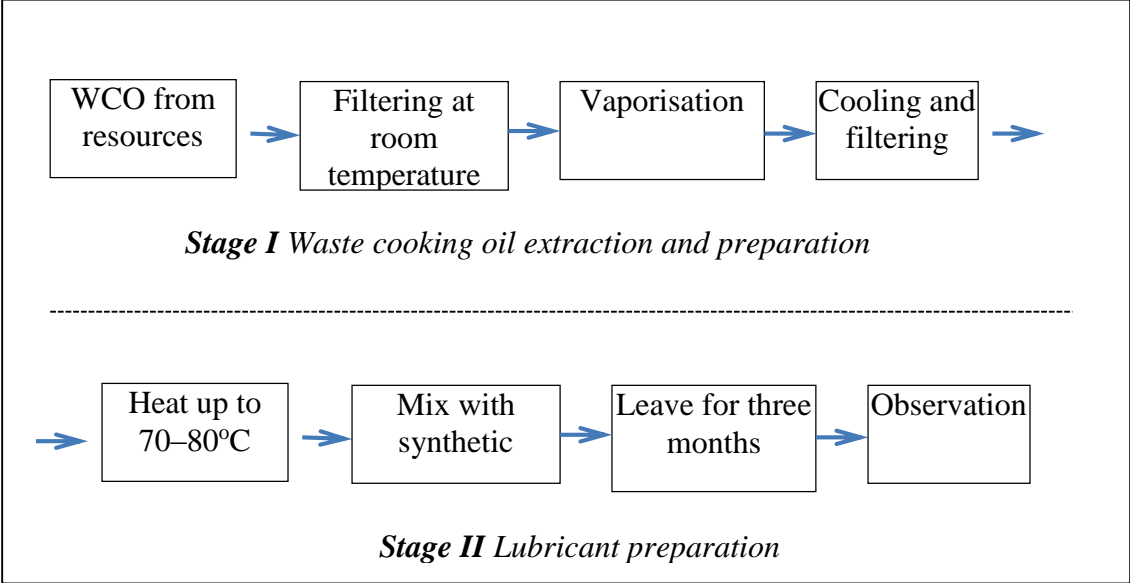


Figure 3.1: Waste cooking oil extraction, preparation and blending

Table 3.1: Fatty Acid Composition of the Collected Waste Cooking Oil

Fatty Acid Composition	%
Myristic (14:0)	0.9
Palmitic (16:0)	21.9
Palmitoleic (16:1)	0.1
Stearic (18:0)	5.2
Oleic (18:1)	41.0
Linoleic (18:2)	29.3
Linolenic (18:3)	0.7
Additives (unknown)	0.9

There is little research on the influence of the chemical compositions of WCO on the tribological behaviour of metals. However, Majdoub et al. (2014) recently reported that oleic and linoleic have been used as additives for PAO4 oil to reduce the friction coefficient. Their results showed that the addition of about 1% of those fatty acids assisted in reducing the energy loss due to the adhesive rubbing process, reducing the friction coefficient. Ikeda, Tomohiro and Ito (2014) investigated the influence of palmitic, stearic, oleic and linoleic acids on palm oil as a lubricant and found that stearic gained optimum results in terms of the wear and frictional performance of the palm oil.

3.2.2 Metals Selection

In the literature there are several materials are selected for tribological applications in such things as bearings and bushes. Among the most common and recent materials used under dry and lubricant contact conditions are mild steel (Liu, Zhu & Liang 2005; Wang, Dohda & Haruyama 2006), brass (Amirat et al. 2009; Panagopoulos, Georgiou & Simeonidis 2012) and aluminium (Erarslan 2013; Wang et al. 2012). Mild steel (SAE 1020, chemical composition: C=0.20%, Mn=0.45%, P=0.04% max, S=0.05% max), aluminium (6060) and commercial brass (58 Cu, 4% Pb and 38% Zn) have been selected for the current study. Samples were prepared from 50 mm x 20 mm x 25 mm blocks of the material using the milling machine at the University of Southern Queensland. Some of the supplied properties of the materials are given in Table 3.2. For the counterface materials, the experiments were conducted against a stainless steel ring (AISI 304).

Table 3.2: Properties of Mild Steel, Aluminium and Brass

Materials	σ_y MPa	σ_u MPa	E GPa	Elongation, %	Hardness HB
Mild steel	380	480	200	15	73
Aluminium alloy	180	220	69.5	13	45
Brass	310	430	96	27	62
Stainless steel (AISI 304)	621	290	28	55	82

3.3 Hybrid Tribological Machine

As was mentioned in Chapter 2, most the experiments in the literature were conducted to study the viscosity of the oil at different temperature and/or the tribological performance of metal contacts under lubricant conditions at room temperature. Because oil may be used at elevated temperatures, the combination of interface and environmental temperatures may affect the interaction behaviour of the asperities in contact, and so affect the real application of the oil. This factor is considered in the design of the project's new machine.

3.3.1 The Block-on-ring Concept

Tribological testing can be done by various laboratory tribo-machines such as pin-on-disc (POD), ASTM G99, block-on-ring (BOR), ASTM G77 or G137-953, dry sand rubber wheel (DSRW), ASTM G655, wet sand rubber wheel (WSRW), ASTM G105, as well as the sand/steel wheel test under wet/dry conditions (ASTM B611; (Yousif 2013a). For the current study, a BOR configuration was selected due to its popularity amongst researchers in the field of lubricants. In this configuration (Figure 3.2), a block of the material was pressed using a dead weight onto a rotating ring (counterface). The rubbing process began with line/line contact and increased to area/area contact, thereby varying the contact area at the running-in stage. This assisted in understanding the integration of the asperities in contact at the initial stages of the sliding process.

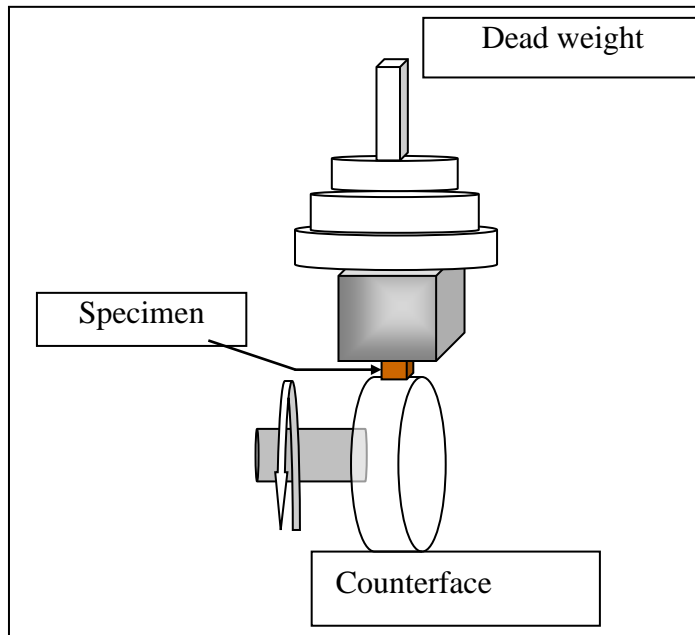


Figure 3.2: Block-on-ring technique

3.3.2 Integration of Lubricant Temperature in the New Machine

The addition of the lubricant container can be implemented in the technique associated with the lubricant heater to heat up the lubricant temperature during the test. CATIA software was used to design the new components for the machine. Figure 3.3 presents a three-dimensional drawing of the newly designed machine and lists its main components. The main purpose of the machine is to provide tribological environments under lubricant condition. A detailed drawing of all the main parts of the machine is provided in appendix A.

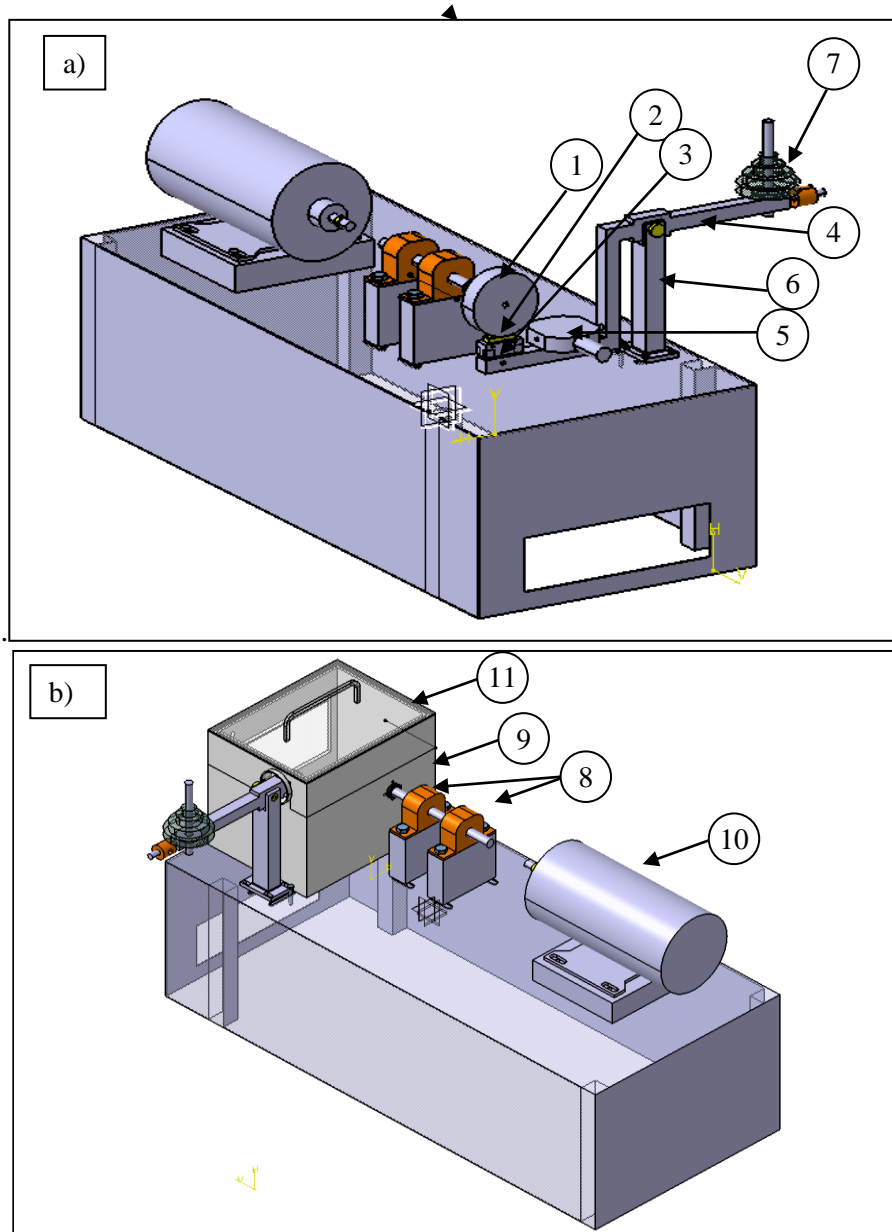


Figure 3.3: Three-dimensional view of the hybrid tribology machine

Notes. 1. Counterface stainless steel (AISI 304), 2 Sample, 3. Sample holder, 4. Lever, 5. Load cell, 6. Lever holder, 7. Weight (applied load), 8. Bearings, 9. Container cover, 10. 0.5 hp motor, 11. Oil container.

The frictional force was captured by a custom-made load cell immersed in the lubricant. The load cell was designed especially to work under this condition. It is able to work under temperatures up to 150°C and any lubricant condition. A special load cell provided by Bestech Australia Pty Ltd was used in the machine, where it was fixed in a position that enable the measurement of the frictional force (Figure 3.4). It was specially designed to be operated at high temperature and lubricant conditions, and it was directly connected to a computer to capture the frictional force. The machine operated using a DC 0.5 hp motor working with 24 V power. This helped to control the sliding speeds using the data requisition system. The container was filled with new oil for each set of data.

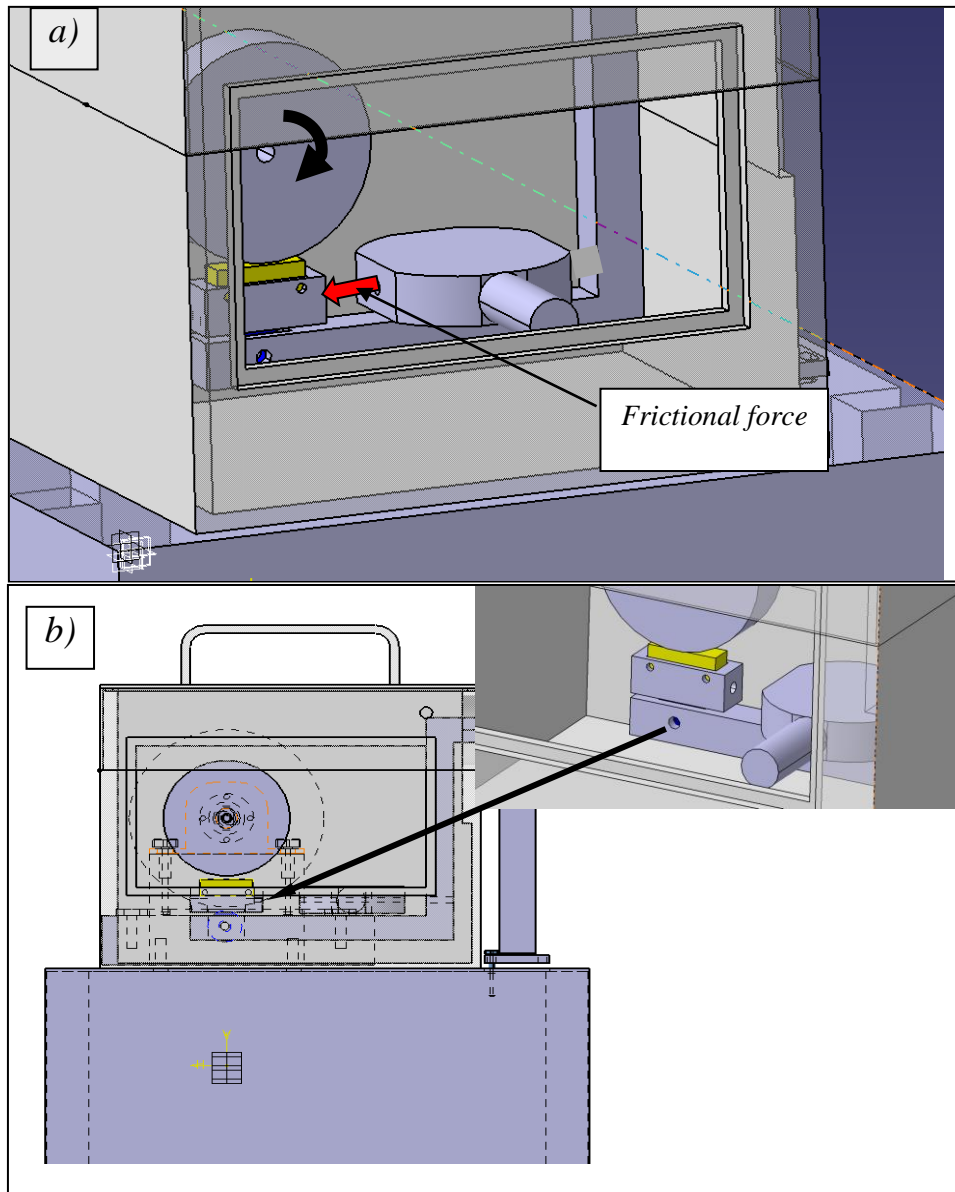


Figure 3.4: The custom-made load cell sensing frictional force

In the current design, the specimen was fully immersed in a lubricant container which represented the real implementation of the lubricant. In other studies, in which the main application of vegetable lubricants seems to be for ball bearings, the oil was applied through a pump onto the counterface (Shahabuddin et al. 2013; Xiao et al. 2014). Those works may assist in understanding the tribological behaviour of the rubbed pair under lubricant condition but not the performance of the lubricant itself. In the current study, the sample was fully covered by the lubricant and the lubricant was allowed to penetrate in the interface freely, to represent its real application. To achieve such complicated environments, a sealing problem may occur. A heater was placed in the container to heat up the oil. In addition, a special window glass was designed to monitor the temperature distribution inside the container to observe the correlated interface temperature with the wear and frictional results.

In light of this, a few leakage interactions were considered in the design and sealed well (Figure 3.5): the entrance of the lever, rotated shaft (coming from the motor), load cell wire, glass window, and cover of the container. A special sealing silicon

(high-temperature RTV silicone, Loctite) was used to seal of the load cell wire and the glass window associated with some bracket and screws to prevent any leakage of lubricant during the high speed of the counterface. For the cover of the container, a groove was machined at the top of the container and filled with a hydronic O-Ring seal (Fluorocarbon Elastomer O-Ring with a diameter of 4mm), which has high resistance to elevated temperature. To seal the hole of the shaft in the container, a hydraulic seal was used and a cup was designed to hold the seal firmly on the container wall (Figure 3.5b). For the entrance of the lever, a flexible rubber cover (Joint Boot Dust Shield Cover) was used to prevent any leakage of the oil from that entrance (Figure 3.5c).

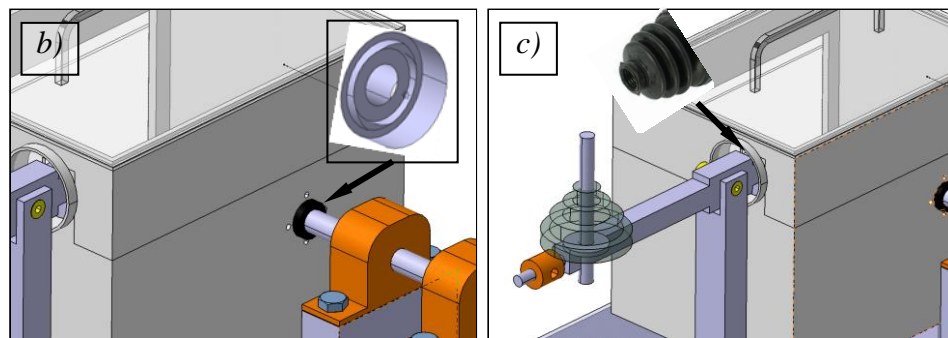
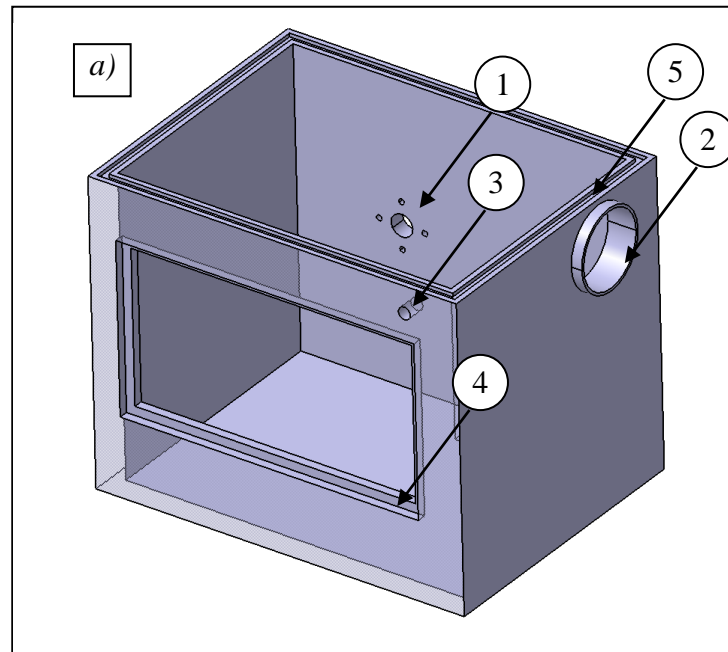


Figure 3.5: Leakage and sealing sections in the lubricant container

The machine was fabricated locally at the USQ workshop with the use of different CNC machines (Figure 3.6). Optimisation and reconsideration processes were undertaken after the fabrication. Some safety regulation standards were included in the design for authorisation purposes. First, a cover was needed for the coupling and shaft from the motor to the counterface in the container in case the operator mistakenly placed his or her finger on the shaft (Figure 3.6a). Moreover, emergency stop was required and placed above the power supplier. At this position, the emergency stop is easy to find, and close to the operator in case of emergencies

(Figure 3.6 b). To avoid any leakage during the operating process, all the seals were placed and then checked (Figure 3.6c).

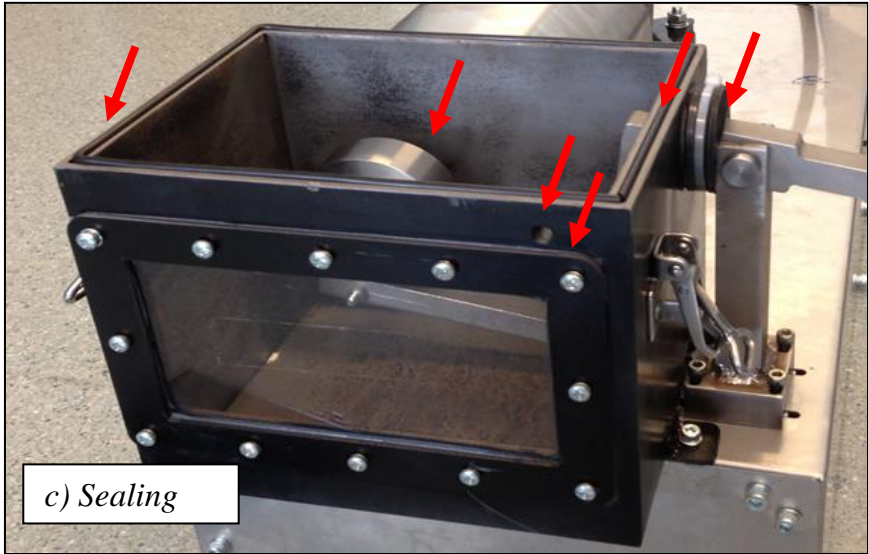
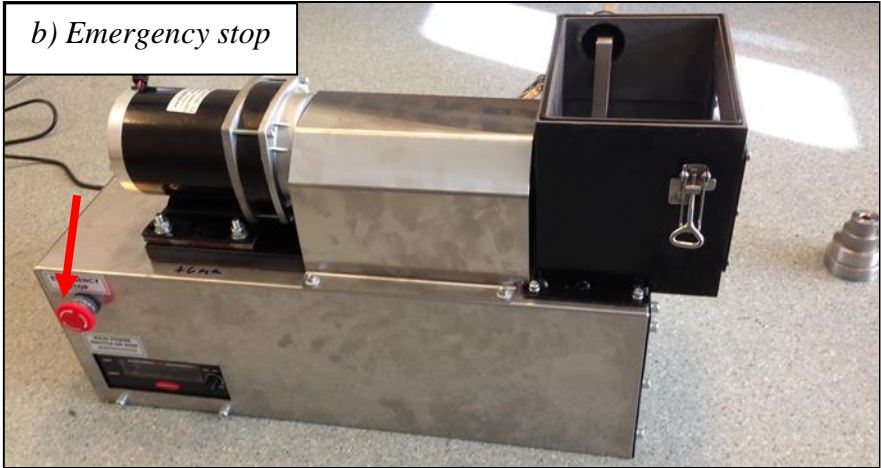
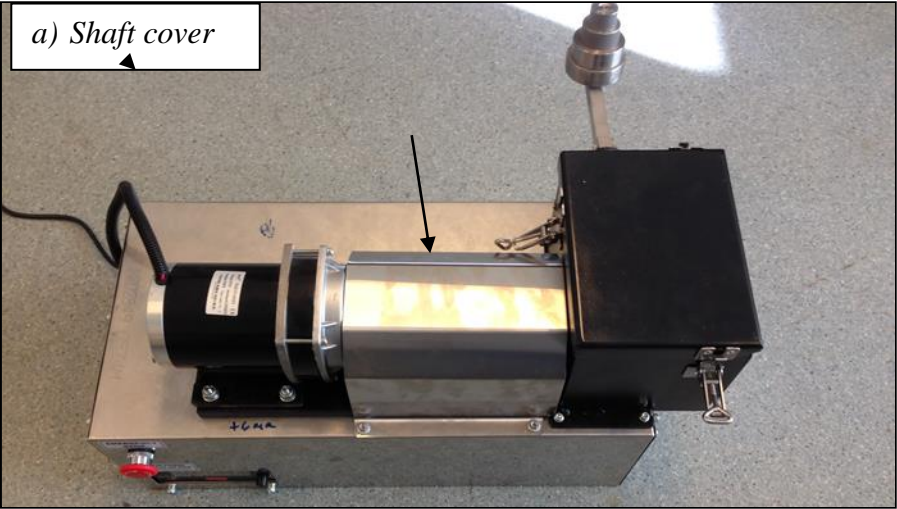


Figure 3.6: Assessment stage of the hybrid tribology machine before operation

Figure 3.7 displays the machine under the operating condition of the lubricant, showing the capture of the frictional force with the presence of the lubricant in the container and monitoring the heat distribution in the container using the thermo-imager.

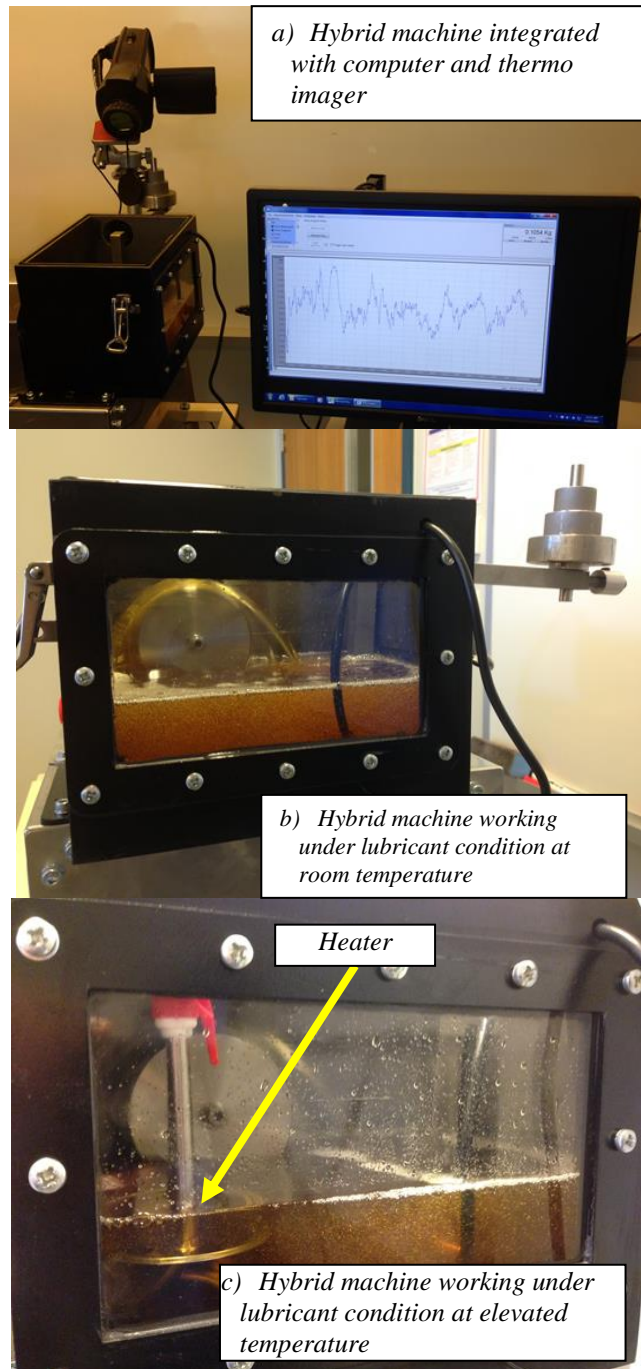


Figure 3.7: Photos of the hybrid tribological machine integrated with the computer

3.3.3 Verification of the New Hybrid Tribological Machine

For verification of the new hybrid machine and establishing datum data, dry tests were conducted using the newly designed machine under the same pressure and sliding speed as those used with the laboratory machine (Chapter 4 and Section 3.4.1). The pressures used for the laboratory machine were 38 kPa, 90kPa and 113.7kPa at a sliding speed of 2.8m/s. The pressure was determined based on the applied load divided by the worn surface after the tests. 113.7 kPa was used for the verification, which was equivalent to the applied load of 1.13 kg at similar speed of 2.8m/s of the laboratory machine.

The specific wear rate (*SWR*) of the selected metals was determined using equation (3.1):

$$SWR = \frac{\Delta w / \rho}{L \times D} \tag{3.1}$$

where the Δw is weight difference (before and after the test) which will be determined using a very high precision weight scale, ρ is the density of the materials, L is the applied load, and D is the sliding distance.

The results of the specific wear rate of three tests for each condition are predicted in Figure 3.8 for all the materials using both the laboratory and new hybrid machine. Both results were close and the error percentage was less than 5%, which could be due to the complexity of the experiments.

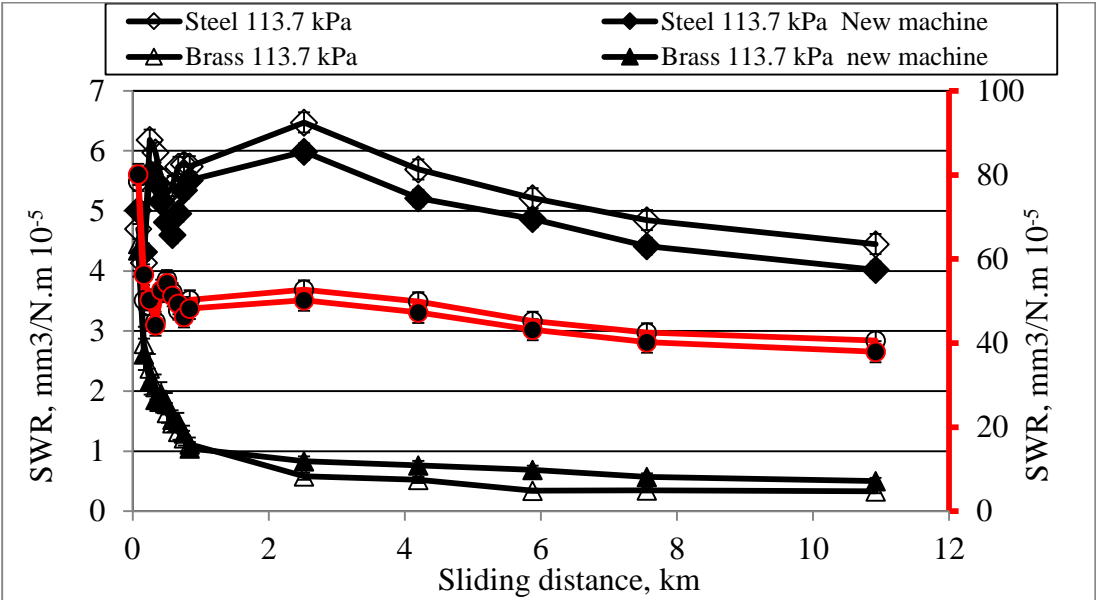


Figure 3.8: Specific wear rate of the selected materials at 113.7 kPa applied stress using the new hybrid and laboratory machines at 2.8m/s sliding distance

3.4 Experimental Procedure

The experiments were divided into two categories. At the initial stage, dry adhesive wear testings were performed using the available tribology machine at USQ (Yousif (2013a)). The machine is able to conduct several tribological tests. With this machine, the first category of the testing was conducted (i.e. comprehensive evaluation of the dry adhesive wear behaviour of common metals). But, the machine is not capable of using lubricants at elevated temperatures. Therefore, in the second category, the adhesive wear testing under lubricant conditions was conducted using the newly designed tribological machine (hybrid machine). In the following sections, both dry and lubricant testings are explained.

3.4.1 Dry Adhesive Wear Testing

For the experiments, adhesive wear tests were conducted against a stainless steel ring (AISI 304) using the BOR technique according to the ASTM G77-98 (ASTM G77-98 Standard Test Method for Ranking Resistance of Materials to Sliding Wear Using Block-on-Ring Wear Test) (Figure 3.9). The machine was equipped with a load cell to capture the frictional force during sliding. The sample (3) was fixed to the holder, which was placed on a ball bearing to gain the minimum frictional contact. Calibration was made for each set of testing and the average of the results reported. Further information about the machine can be found in Yousif (2013a).

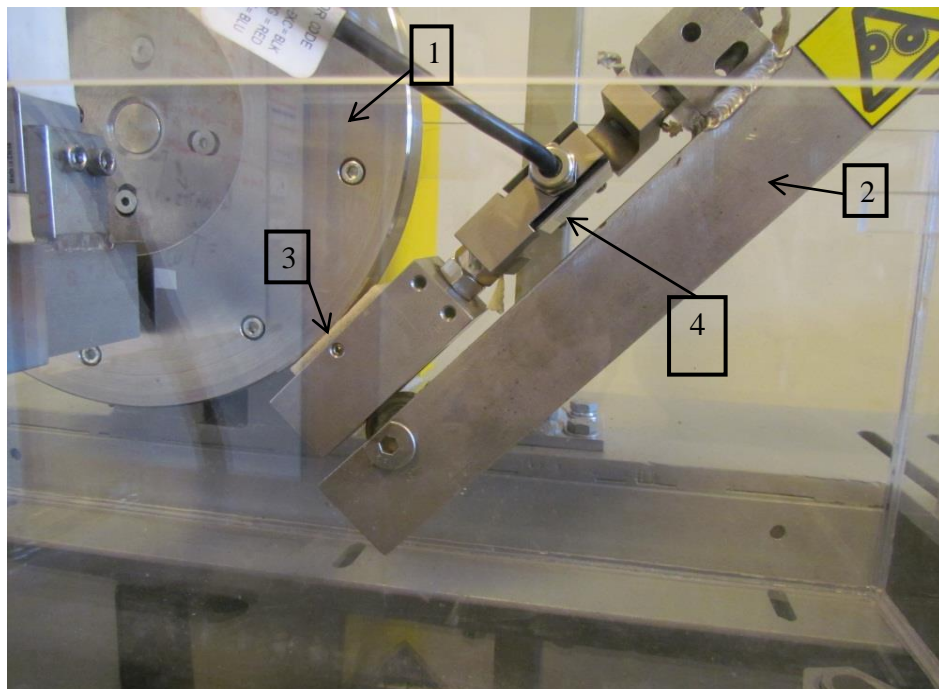


Figure 3.9: Tribological machine with block-on-ring configuration (Yousif (2013a))

Notes. 1. Counterface, 2. BOR load lever, 3. Specimen, 4. Load cell.

To ensure intimate contact between the sample and the counterface, before each test the disc was polished with abrasive SiC paper (G1500) to a surface roughness of 0.1-0.3 μm Ra. Acetone was used to clean the surface before each test, followed by wet cotton to remove the acetone and clean the surface. The samples were polished

before each test and the roughness of their surfaces was measured. The roughness of the samples were about 0.075 μm Ra, 0.4 μm Ra, and 0.25 μm Ra for mild steel, aluminium and brass, respectively (Figure 3.10).

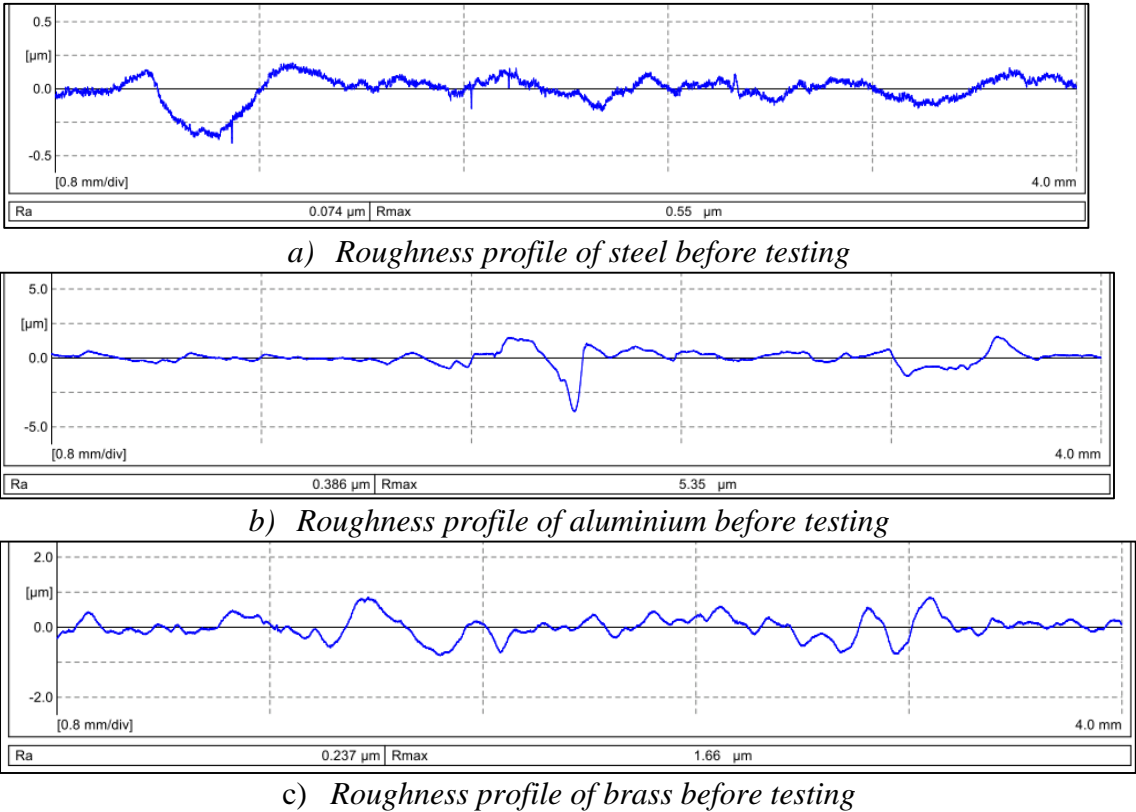


Figure 3.10: Roughness profiles of sections on the polished samples before testing * the scale of the figures are different since they are auto-generated by Mahr roughness machine.

Sliding tests were conducted at ambient temperature and humidity conditions with various normal loads (30 N, 40 N and 50 N), and sliding distances (0–10.8 km) and sliding speed of 2.8 m/s. It is known that each material has its own pressure x velocity limit. For the current study, preliminary experiments were conducted to determine the PV limits of the selected metals and gain the optimum velocity, with a constant applied load of 50 N. 2.8 m/s sliding velocity was found to be the optimum for the three selected metals considering different applied loads. The normal applied loads were equivalent to 38 kPa, 90kPa and 113.7kPa which were calculated after the test by dividing the applied load by measuring the worn surface area. Surface morphology and collected debris were examined after each test using a scanning electron microscopy. A Mahr roughness profile machine was used to determine the roughness of the rubbed surfaces after each test. The roughness was measured against the sliding direction for both the metal surfaces and the counterface. The sample, counterface, interface and environmental temperatures were monitored using a thermo-imager device.

Friction coefficient μ is calculated using equation (3.2) where F_f is the frictional force which is captured via the load cell and L is the applied load:

$$\mu = \frac{F_f}{L} \quad (3.2)$$

3.4.2 Adhesive Wear Testing Under Lubricant Condition

The newly designed machine was used to conduct wear testing under the lubricant condition. The first step in the experiments was to prepare the sample and counterface similar to the preparation process explained in Section 3.4.1.

WCO blends, WCO:SO of 0 vol. %, 25 vol. %, 50 vol. %, 75 vol. % and 100 vol. % were used in the current study. Several steps had to be considered in conducting the experiments. At the initial stage, the specimens were polished, weighed and then fixed in the holder of the hybrid machine. The lever of the machine was loaded with the required dead weight. The lubricant container was filled with the lubricant to a level of about 30 mm above the specimen to ensure that the specimen was fully immersed in the lubricant during the test. To avoid lubricant splash during the experiments, the container was firmly covered. Then the heater was switched on to the required temperature. The panel controller was set to the required rotational speed and the load cell reader and timer was set to zero. The machine was then switched on and, when the required time was reached, it was switched off.

At the end of each test, it was important to wait for the lubricant to cool down and then clean the lubricant container by vacuuming it using the oil pump and then filter the oil and extract the debris. The specimen was removed and cleaned with acetone. Weight and surface roughness of the specimens were determined after the test was completed. The direction of the roughness measurement was perpendicular to the sliding direction. The lubricant container was cleaned with acetone to remove any residual oil after each set of tests. Frictional force was saved on the computer during the experiments.

Different sliding distances were used in the study to differentiate between the running-in and steady state regions (0 - 10.8 km). The operating conditions and parameters are given in Table 3.3. For each test, at least three repetitions were conducted and the average of the results was determined. Since the dry tests were conducted at the speed of 2.8 m/s, the lubricant tests were conducted at the same speed for comparison purposes.

Lubricant tests were conducted against a stainless steel ring (AISI 304) and, to ensure intimate contact between the sample and the counterface, before each test the disc was polished with abrasive SiC paper (G1500) to a surface roughness of 0.1-0.3 $\mu\text{m Ra}$, i.e. the three metals were tested on an identical surface characteristic. This ensured that the wear and frictional data of the three different metals were comparable under the same contact and operating conditions. Acetone was used to clean the surface before each test, followed by wiping wet cotton to remove the acetone and clean the surface. The specimens were machined from a block of the metals, and before the tests the specimens were polished. The roughness of the samples were about 0.075 $\mu\text{m Ra}$, 0.4 $\mu\text{m Ra}$, and 0.25 $\mu\text{m Ra}$ for mild steel,

aluminium and brass, respectively (Figure 3.10). A Mahr roughness profile machine was used to determine the roughness of the rubbed surfaces before and after each test. The roughness was measured against the sliding direction for both the metal surfaces and the counterface.

Table 3.3: Operating Parameters for Adhesive Wear Testing under Lubricant Conditions

Duration, min	Applied load, N	Oil temperature, °C
15	5	30
30	10	40
45	15	60
60	20	80
15	5	30
30	10	40
45	15	60
60	20	80
15	5	30
30	10	40
45	15	60
60	20	80
15	5	30
30	10	40
45	15	60
60	20	80

At the end of the lubricant tests, the debris was collected and extracted for scanning electron microscope (SEM) observation. In the extraction, the debris was immersed in the oil and then collected in small tubes (Figure 3.11). A centrifuge machine was used to extract the debris at the first stage of oil separation. The lubricated debris was washed more than five times with acetone and then centrifuged. A hot air dryer was used to dry the debris. The collected debris was attached to a conducted carbon tap for the SEM observation.

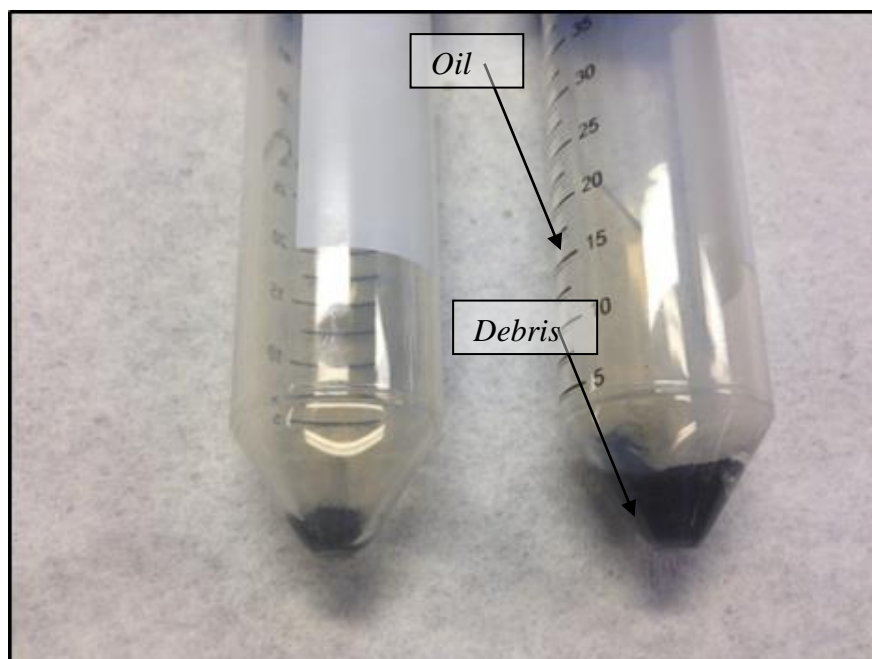


Figure 3.11: Extraction of the debris from the lubricant

Different oils were used in this work, and these were supplied by Shell Helix. The technical data for each oil grade is provided by the company via <http://www.shell.com/global/products-services/on-the-road/oils-lubricants>. Some specific details of the selected oil are given in Table 3.4. The main conventional oil used in the work is 5W-30 which is fully synthetic (as determined by Shell Helix).

Table 3.4: Some of the fully synthetic oil specifications

	MRV, ASTM D4684	Density, ASTM D4052	Flash point, ASTM D92	Pour point, ASTM D97	Remarks
5w-30	17000	852	240	-48	fully synthetic
5w-40	19300	840.3	242	-45	fully synthetic
10w-50	21500	862.3	235	-41	fully synthetic
15w-40	26100	882	230	-33	multi-grade

3.5 Properties of Waste Cooking Oil

3.5.1 Pour Point and Flash Points

Pour point is one of the important properties of oil since it represents the characteristics of the oil at the condition in which it becomes semi solid and not able to flow. The ASTM D 97 standard is used in this study and has been adopted by many researchers (Rahman et al. 2014). In the test, a pour point tester was adopted with a cooling system working with methanol as the cooling agent. 45 ml of the blend was placed in a test jar and the level of the liquid marked. The jar of the blend then began cooling to about -40°C using the pour testing apparatus. While the blend was cooling, the movement of the blend and pour point was observed. Once the blend solidified, it was placed on the apparatus horizontally to heat up at atmospheric condition, the temperature was taken with each 3°C drop, and the flow of the blend

was observed until the first droplet fell. This process was repeated three times for each blend. The results are presented in Table 3. 5. It is clear that the pour point of the WCO is greater than the SO and WCO blends. This has also been reported for rapeseed oil (Quinchia et al. 2012). Quinchia et al. (2012) recommended that vegetable oil-based lubricants may need lower their pour point temperatures for some applications such as hydraulic fluids, chain saw oils and saw mill oils. Similarly, for such applications, it is recommended that PPD additives are considered to assist in delaying the nucleation and crystal growth stages of the oil (Asadauskas & Erhan 1999).

The flash point can be defined as the lowest temperature at which the oil forms an explosive vapour under normal atmospheric conditions. A Cleveland open cap tester was used to determine the flashpoint according to ASTM D92. The average of the flash point of the blends is given in Table 3.4. In general, the higher the flash point the better. In comparing the WCO and the SO, the flash point of the WCO is greater, which can be an advantage. All the research related to WCO aimed to investigate the performance of the biofuel extracted from the WCO (Bezergianni, Dimitriadis & Chrysikou 2014; Cao et al. 2014). In these works, it was highly recommended to reduce the flash point to about 150°C by using ferric sulfate and potassium hydroxide as catalysts in a two-step reaction.

Table 3.5: Pour Point and Flash Point of the Blends

Blend	Pour point	Flash point
0% SO	-16 °C ± 1.25	285 °C ± 8
25% SO	-22 °C ± 1.5	275 °C ± 6
50% SO	-26 °C ± 1.7	243 °C ± 6
75% SO	-30 °C ± 1.9	236 °C ± 5
100% SO	-36 °C ± 0.75	225 °C ± 5

3.5.2 Viscosity of the Waste Cooking Oil and its Blends

The dynamic viscosity of the used oil and its blends against different temperatures is plotted, in two forms, in Figure 3.12. It has been mentioned here that the results in the figures are presented for unused waste cooking oil (before cooking), after filtering (cooked and filtered), and prepared blends of waste cooking oil with the 5% (wt) of EVA copolymer and 2% (wt) of EC and the synthetic oils. The figures show that there is a dramatic increase in the viscosity of the waste cooking oil with the addition of the additives and further increase achieved with the addition of synthetic oil. In other words, the unused waste cooking oil (cotton seeds) exhibits very low viscosity and cooking it with fish and chips slightly increase the viscosity. The addition of the 5% (wt) of EVA copolymer and 2% (wt) of EC significantly impacts the viscosity behaviour of the oil as the waste oil becomes competitive especially at higher temperature. Such improvement will dramatically impact the tribological performance of the oil.

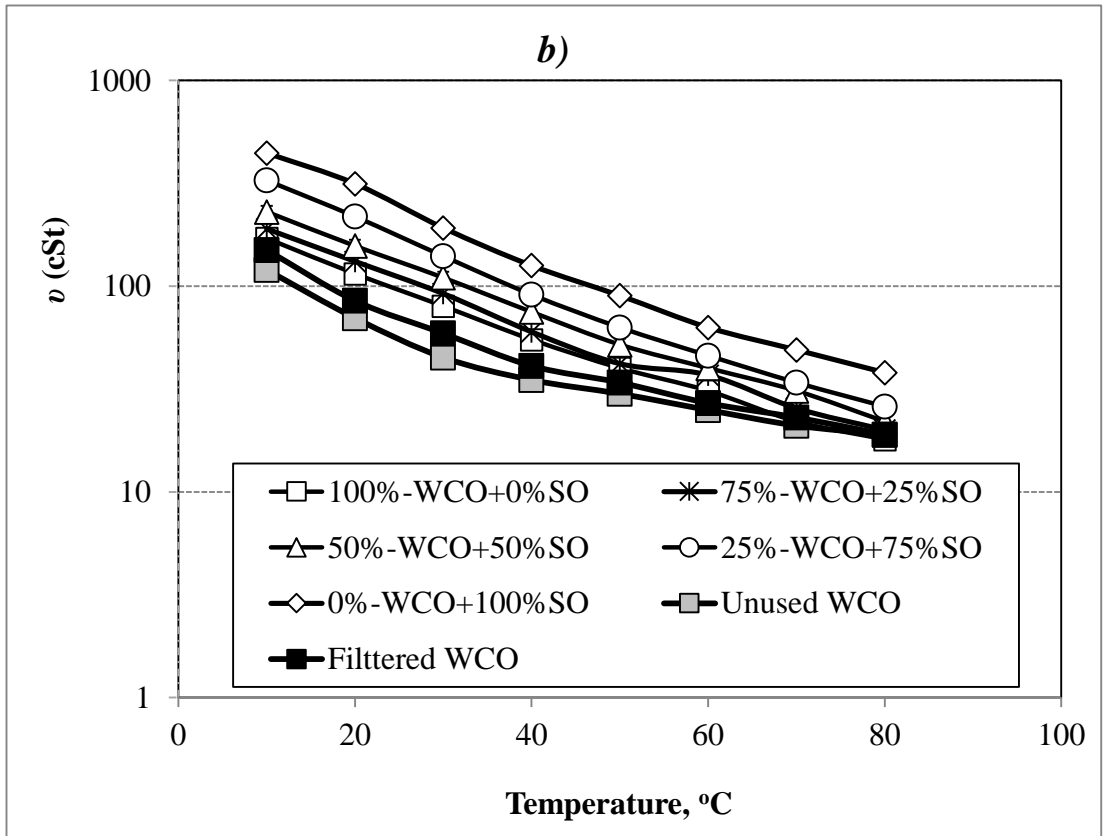
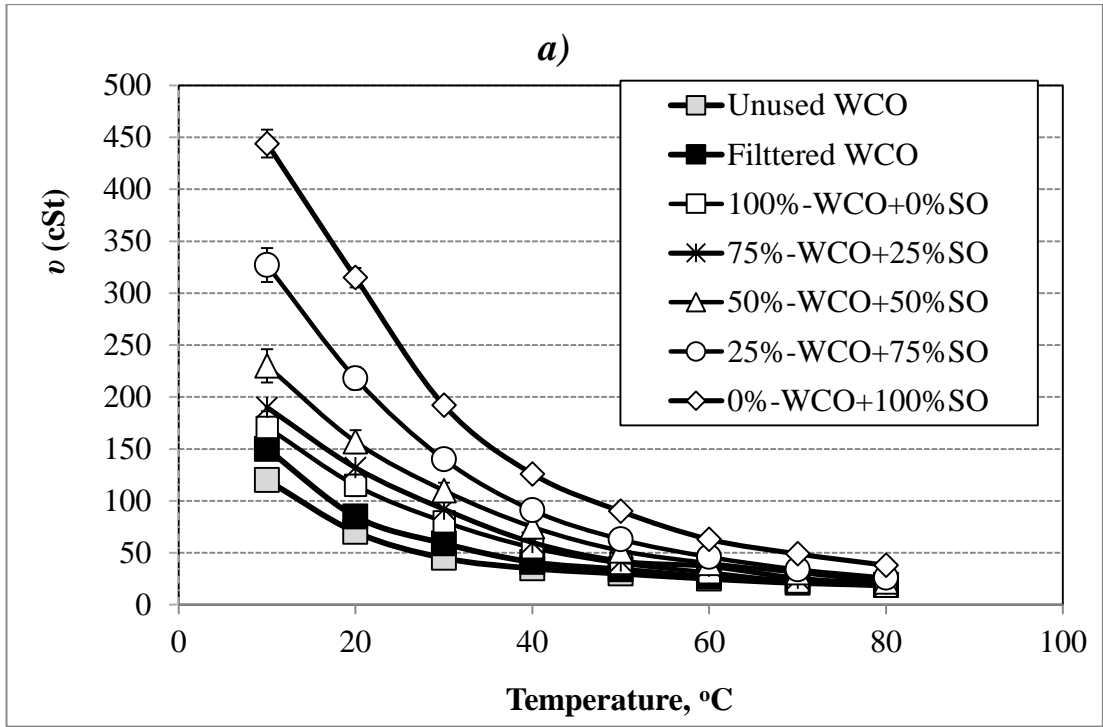


Figure 3.12: Viscosity vs. temperature of different blends of waste cooking and synthetic oils

Some of the data in the literature is presented in log form (Ting & Chen 2011) and for comparison purposes the current values are presented in these two forms. The general trend of the viscosity decreases with increases in the temperature as this is expected for all the types of oil. For the 0% blend of WCO (fully synthetic) there was

approximately 900% drop in viscosity when the temperature was increased from 10°C to 80°C. Meanwhile, the drop in viscosity of the pure WCO was about 600%. These results are promising for WCO in terms of stability and less sensitivity to temperatures compared to synthetic oil. A similar trend can be seen in Figure 3.12b.

It is well known that the determination of oil application and performance is based on viscosity at 40°C and 80°C. Therefore, the viscosities of the blends at those temperatures are extracted from Figure 3.12 and presented in Figure 3.13. It is obvious that SO has higher viscosity values compared to its blends. Moreover, the increased addition of WCO reduces the viscosity of the blends for both selected temperatures (Figure 3.13).

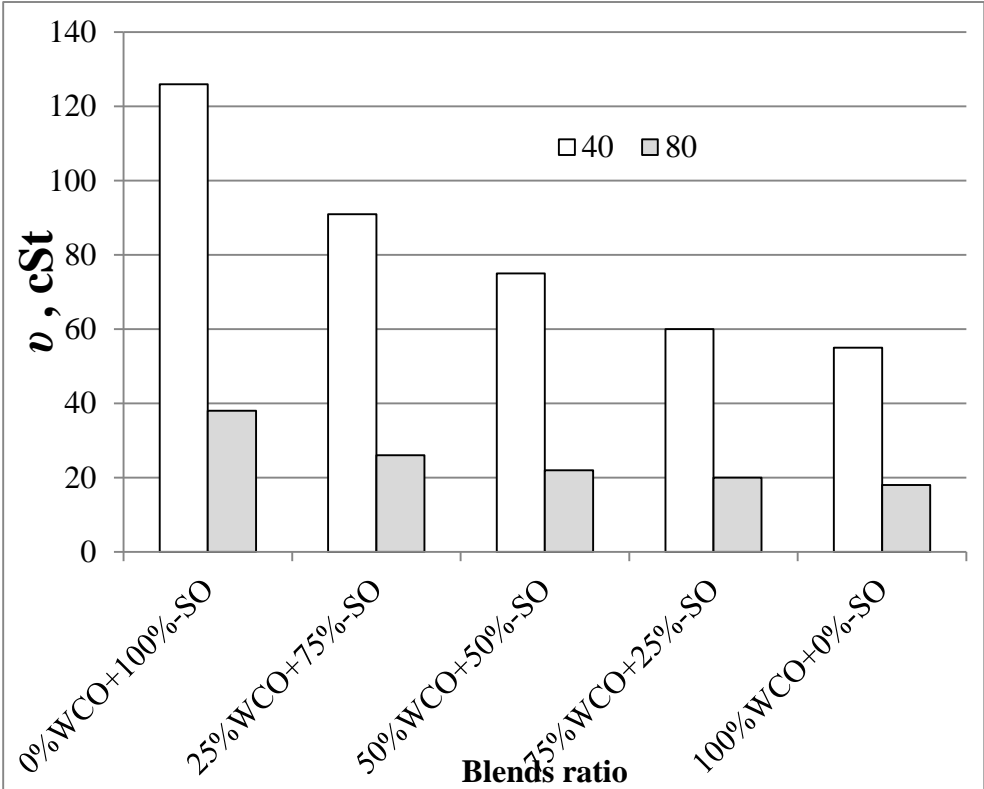


Figure 3.13: Viscosity of the blends at 40°C and 80°C

The ISO viscosity grade requirements are listed in Table 3.6. For the current blends it can be seen that pure WCO can fit with the ISO VG 68, which can be used for crankcase oil grades 20 W (Brockwell, Dmochowski & Decamillo 2004; Stachowiak & Batchelor 2013). However, further study is required to determine the degradability of the oil and the tribological performance of the components under this lubrication condition.

Table 3.6: ISO Viscosity Grade Requirements ('Mixed-fiber diets and cholesterol metabolism in middle-aged men' 1991; Rudnick 2006; Rudnick 2010).

Kinematic viscosity	ISO VG32	ISO VG46	ISO VG68	ISO VG100	Pure waste cooking oil
@40 °C	>28.8	>41.4	>61.4	>90	65.5
@100 °C	>4.1	>4.1	>4.1	>4.1	9.5

Further to the above and since there are few studies on the WCO as a lubricant, the viscosity of different grades of oils were tested and compared with those of WCO (Figure 3.14). In general, WCO exhibits the lowest viscosity compared to other SOs. This can be both an advantage and disadvantage since low viscosity means less resistance to the shear (low friction) and less film thickness in the interface when two bodies are under sliding condition. Nevertheless, one can see that the pure WCO is close to the W5-30 oil. The W5-30 fully synthetic oil is recommended for both gasoline and diesel engines. However, the viscosity index must also be considered to determine the application of the oil.

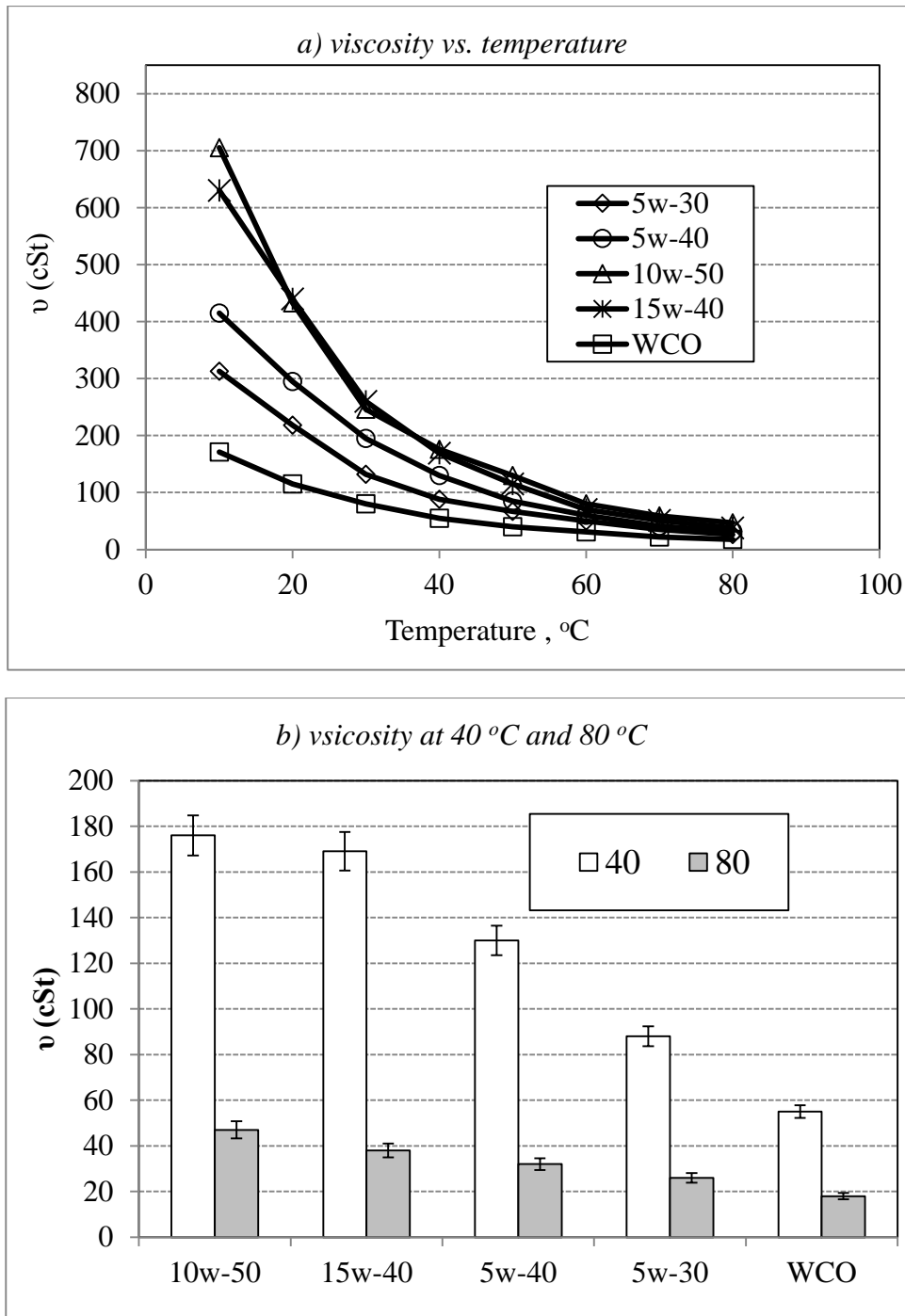


Figure 3.14: Waste cooking oil viscosity with industrial lubricant

The viscosity index of WCO and its blends were determined by measuring the viscosity of the lubricant at an elevated temperature of 100°C. The results are presented in Figure 3.15. It seems there is a significant deterioration in the viscosity of the WCO. In this work, 5% (wt) of EVA copolymer (density, at 23 °C, 0.956 g cm⁻³; molecular weight, 60250 g mol⁻¹; melting temperature, 59 °C) and 2% (wt) of EC (density, at 25°C, 1.14 g cm⁻³; molecular weight, 68960 g mol⁻¹; melting temperature, 155°C) were used as additives to enhance viscosity at high temperature. The advantages of the EVA are that it is an inert, non-toxic and stable material, not expected to be biodegradable and not hazardous (Quinchia et al. 2010). EC is a kind of water-insoluble cellulose ether having good mechanical properties, relatively low

cost and good film-forming performance (Yang et al. 2014). The addition of the additives significantly improved the viscosity index of all the WCO blends, making it comparable to the fully synthetic oil of 5W-30 (≈ 155). The blends with the additives were used in the journal bearing tests presented in Chapter 6.

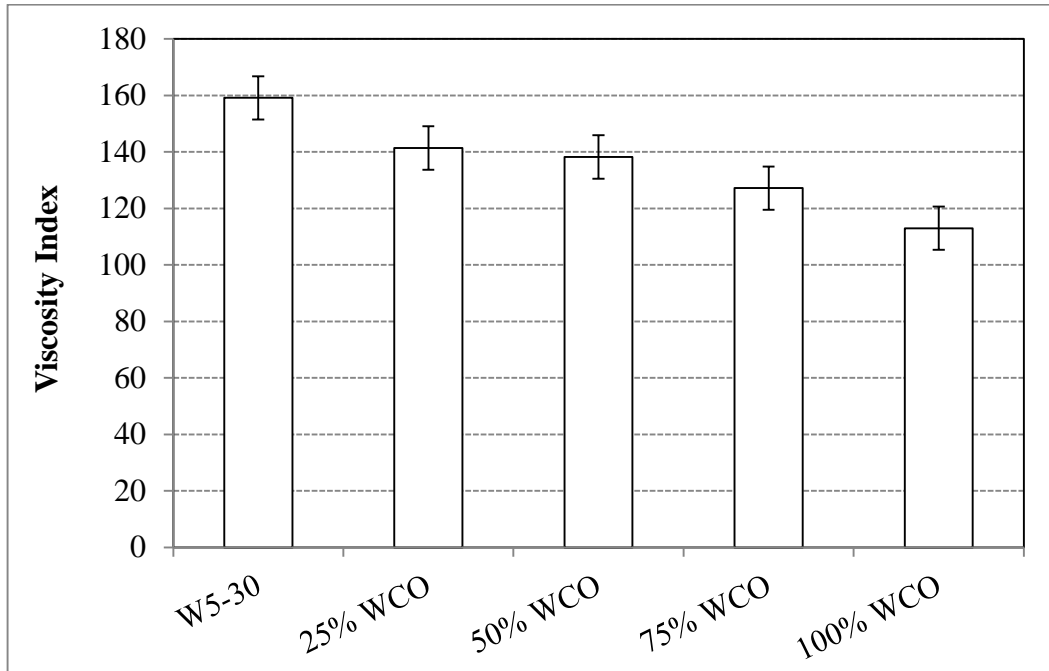


Figure 3.15: Viscosity index of waste cooking oil and its blend with W 5-30

The use of some vegetable oils as a potential lubricant has been investigated in previous studies, the most recent of which are summarised in Table 3.7. These show the viscosity of vegetable oils at 40°C and 80°C. There are different ranges of viscosity for the oil and there could be comparable values for the pure WCO with soybean and sunflower oil (Quinchia et al. 2014), even though WCO exhibits a better viscosity value. In (Paredes et al. 2014), a modifier was used to improve the viscosity performance of the vegetable oil, and this can be considered for future work on WCO.

Some important points can be drawn from this literature as follows:

- There is a growing environmental need to find alternative lubricants, and a great deal of research has focused on the possibility of using vegetable oils. Inedible rather than edible oils is highly recommended.
- The disposal of WCO is an issue. WCO's potential as an alternative fuel for diesel engines has been explored, but it is limited as a fuel; because it impacts substantially on engine performance from a tribological perspective.
- The potential of using WCO as an alternative lubricant was investigated in the current study. From a viscosity point of view, there are promising results regarding its use as a lubricant, but further study is recommended.

Table 3.7: Comparison to Previous Works and Standards

	ν (cSt) at 40 °C	ν (cSt) 80 °C
0	126	38
25	94	26
50	75	22
75	60	20
100	55	18
Original soybean (Ting & Chen 2011)	≈ 175	≈ 29
Jatropha oil (Shahabuddin et al. 2013)	≈ 172	≈ 23
Soybean oil (Quinchia et al. 2014; Quinchia et al. 2010)	33.6 ± 0.9	12.3 ± 0.5
Sunflower oil (Quinchia et al. 2010), (Quinchia et al. 2014)	32.9 ± 2.3	12.7 ± 0.8
Castor oil (Quinchia et al. 2014; Quinchia et al. 2010)	242.5 ± 21.7	37.1 ± 1.7
Castor seeds (Madankar, Pradhan & Naik 2013)	248.8	NA
Iluent (polyalphaolefin), and high-oleic vegetable oils (Erhan, Sharma & Perez 2006).	42.33	
BIO-H01 is a mixture of 83.5% high oleic sunflower oil and 13.5% ditridecyl adipate (Paredes et al. 2014)	37.41	11.42
BIO-H02 blend of high oleic sunflower oil at 73% and 24% of disooctyl adipate (Paredes et al. 2014)	27.67	9.08

Chapter 4: Wear Behaviour and Mechanism of Different Metals Sliding Against Stainless Steel Counterface

4.1 Introduction

Understanding the wear mechanism significantly contributes to the body knowledge associated with the tribology of common metals, and helps to predict, overcome and prevent the failure of designed components. In the current study, the wear and frictional performances of brass, aluminium and mild steel metals are investigated at different operating parameters: sliding durations (0–10.8 km) and applied loads (0–50 N) against a stainless steel counterface under dry contact conditions. The experiments were performed using a BOR machine. To categorise the wear mechanism and the damage features on the worn surfaces and the collected debris, scanning electron microscopy was used. A thermal imager was used to understand the heat distribution in the contacted bodies and the interface regions. The results revealed that the operating parameters influence the wear and frictional behaviour of all three metals. Brass metal exhibited better wear and frictional behaviour compared to aluminium and mild steel. Three different wear mechanisms were observed: two-body abrasion (brass), three-body abrasion (aluminium) and adhesion (mild steel).

4.2 Background

Several works have been reported on the frictional and wear behaviour of metals. However, there is still a demand to understanding the metal behaviour under different tribological applications. Recently, there are publications have reported on the tribological performance of different type of metals such as aluminium (Birol 2013; Kumaran & Uthayakumar 2013; Rao et al. 2013), steel (Felder et al. 2012; Leiro et al. 2013; Máscia et al. 2013) and brass (Feser et al. 2013; Gava et al. 2013). From these works, it is found that most of the previous attempts have been focusing on the application of the metals which in turn influences the experiments have been conducted to accommodate specific operating conditions, i.e. specific sliding speed, sliding distance, environmental temperature and applied load (Alvarez-Vera, Ortega-Saenz & Hernandez-Rodríguez 2013; 2009; Umanath, Palanikumar & Selvamani 2013). As a result, understanding the wear and frictional behaviour of metals is confusing with studies being incomparable as operating parameters have significant influence on the wear and frictional behaviour of metals under either dry or wet (lubricant) contact conditions (Berglund, Marklund & Larsson 2010; Kumar & Bijwe 2011; Prasad 2011; Tewari 2012; Yousif 2013b). In (Prasad 2011), friction and wear behaviour of grey cast iron has been investigated under different test parameters, i.e. applied load, sliding speed and test environment and the results revealed that the wear loss increases with the sliding velocity and/or applied load increase.

Furthermore, high applied load and sliding speed introduces high frictional heating. Beside the above, the current results revealed that the reported works in the literature have presented the wear results in different formats. For example, the wear performance of a metal have been presented as wear rate (Slavkovic et al. 2013), weight loss (Forati Rad, Amadeh & Moradi 2011), volume loss (Morris et al. 2011)

specific wear rate and/or wear resistance (Cassar et al. 2012; Jahangiri et al. 2012). The current study to evaluate the wear and the frictional behaviour of aluminium, steel and brass materials sliding against stainless steel counterface considering different operating parameters to gain the value of specific wear rate at the steady state condition and identify the wear mechanism.

4.3 Dry Wear Behaviour of Selected Metals

The specific wear rate of the selected materials against sliding distance under different applied load was obtained. The specific wear rate at the steady state and the friction coefficient are reported for all the materials under different applied loads in Figures 4.1 - 4.6. The temperature distribution in the contact zone is presented in Figure 4.7. Roughness and SEM observations are presented in Figures 4.8 - 4.13.

4.3.1 Specific Wear Rate against Sliding Distance

The specific wear rate of the selected materials against sliding distance is presented in Figure 4.1 for different applied loads: a) brass, b) aluminium, c) mild steel. The specific wear rates of the three materials are presented in Figure 4.2 under 50 N applied load. Due to the high value of the specific wear rate of the aluminium material, its results are presented in the second Y-Axis. However, there are no remarkable differences in trends among the materials.

The behaviour of all the materials can be divided into two stages as running in, which is the initial stage of the sliding, and the steady state. At the running in stage, interaction between the asperities is initiated and continued for about 2 km–5 km, and there is less integration between the asperities in contact. In the steady state where the asperities are adopted and the surfaces are in intimate contact. The fluctuation in the specific wear rate at the running-in period is mainly due to the modifications taking place during the sliding. In other words, some of the asperities transfer from the sample surface onto the counterface surface or the opposite depending on the hardness of the materials (Krishnaveni, Sankara Narayanan & Seshadri 2005; Wieleba 2002), contact conditions (Yousif & Chin 2012) and operating parameters (Bonny et al. 2010; Yousif 2013a). For the current results, the wear data is presented as specific wear rate, which is the volume loss per the applied load times the sliding distance. This reflects the real situation of the contact between the bodies.

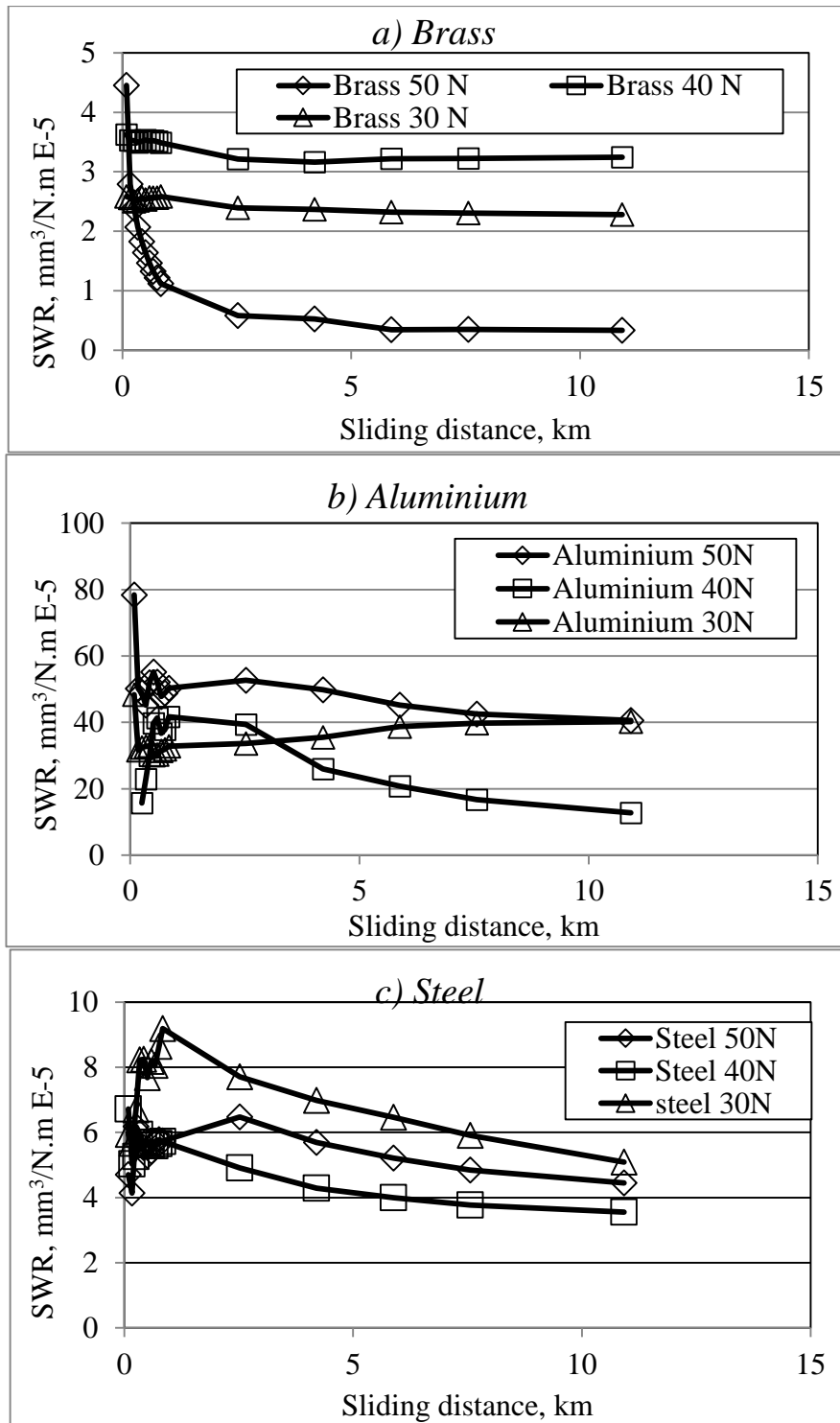


Figure 4.1: Specific wear rate vs. sliding distance of brass, aluminium and mild steel materials under dry contact conditions

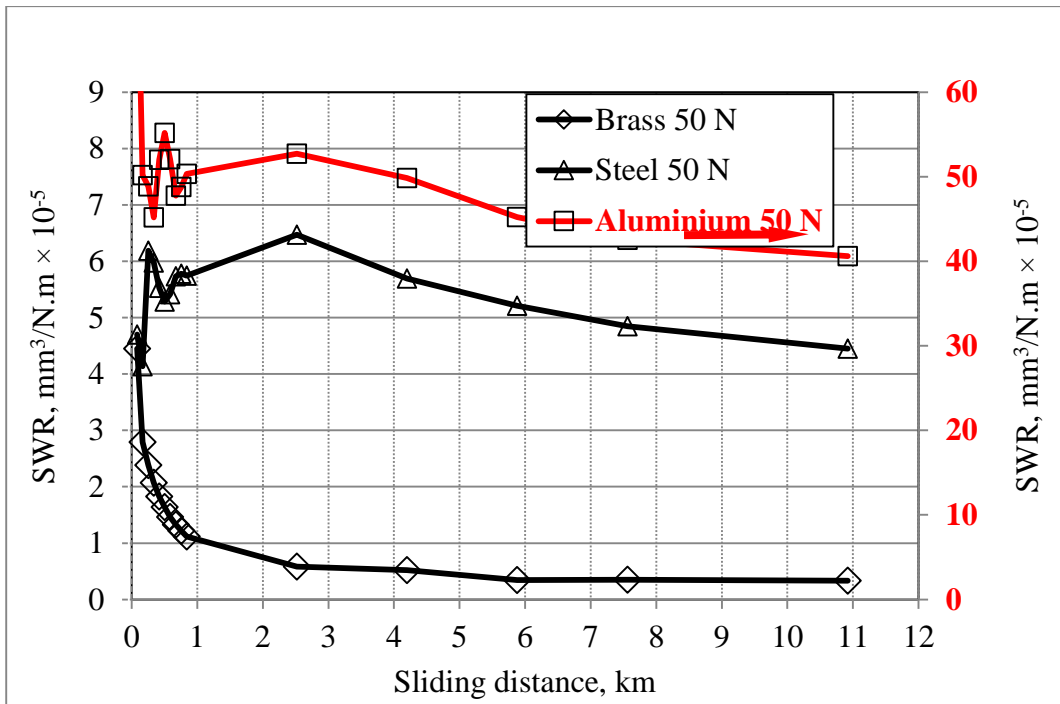


Figure 4.2: Specific wear rate vs. sliding distance of brass, aluminium and mild steel materials under dry contact conditions

In some reported works, steady state is a proportional relation between the weight loss (Bateni et al. 2005; Prasad, Modi & Yegneswaran 2008), volume loss or wear depth (Páczelt, Kucharski & Mróz 2012) with the sliding distances. Figure 4. 1 is represented in terms of weight loss in Figure 4.3 under the applied load of 50 N. The figure indicates that the weight loss increases with the longer sliding distances which is in agreement with previously published works, (Bateni et al. 2005; Prasad, Modi & Yegneswaran 2008). In other words, it can say that the steady state in the specific wear rate versus sliding distance (Fig. 4.2) reflects the slop of the weight loss versus distance (Fig. 4.3).

For the current results, the steady state of each material at different applied loads are determined and displayed in Figure 4.4. The maximum and minimum values of the specific wear rate at steady state are introduced with the error bars on the figure for the set of tests at each load. In Figure 4.3, it is clear that the aluminium material has very poor wear performance compared to the mild steel and the brass under the 50 N applied load. Similarly, Figure 4.4 shows that aluminium exhibits a very high specific wear rate representing very poor wear performance (i.e. weak wear resistance). For mild steel and brass, comparable specific wear rate values can be found particularly under 40 N applied load. With applied loads higher or lower than 40 N, brass displays better wear resistance compared to mild steel even though mild steel is harder. This can be due to modification occurring on the counterface surfaces or the debris generated in the interface. It is suggested that the removed material from the mild steel is very hard and may roll or slide on rubbed surfaces when they are on their way out of the interface zone. This results in three-body abrasion, which always leads to high material removal as reported by many researchers (Birol & Isler 2011; Máscia et al. 2013). In the case of the brass material, a coating process can occur during the sliding which helps to cover the stainless steel counterface and results in very low material removal as reported by (Elleuch et al. 2006). Another

reason could be that the brass debris is not as hard as the mild steel debris, which results in low material removal from the sample surface. This point is further elaborated upon in the surface observation section.

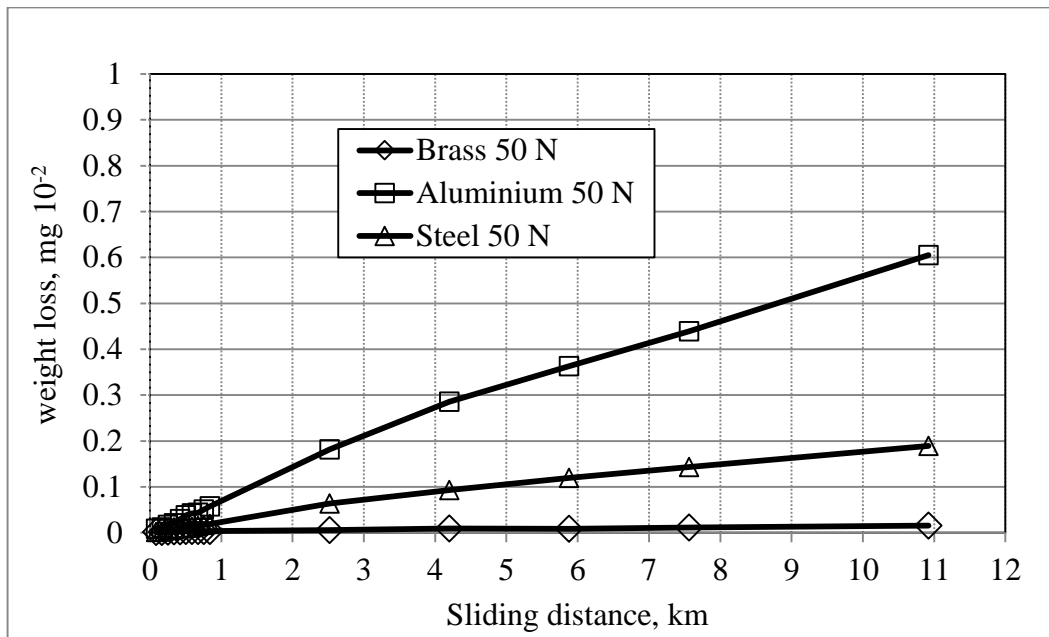


Figure 4.3: Weight loss vs. sliding distance of brass, aluminium and mild steel materials under dry contact conditions

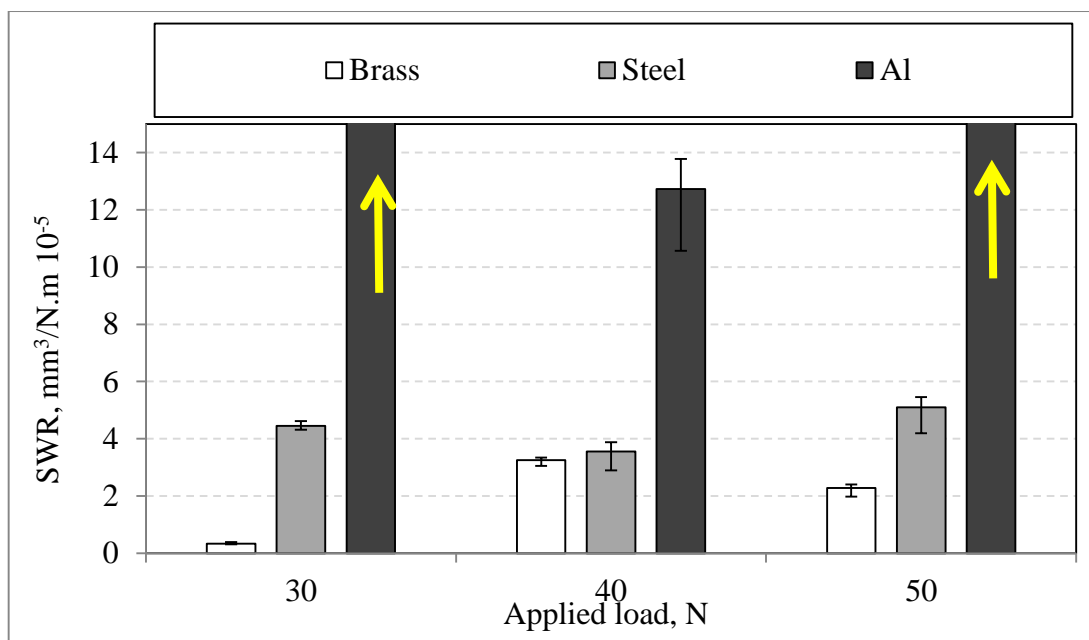


Figure 4.4: Summary of specific wear rate at steady state of brass, aluminium and mild steel materials under dry contact conditions at different applied loads after 10.8 km sliding distance

4.3.2 Dry Frictional Behaviour of Selected Metals

The friction coefficient of the selected three materials against sliding distance is displayed in Figure 4.5 under various applied loads. For the other applied load, the trend of the frictional data is the same as the 50 N applied load, but the values are different. Therefore, the 50N applied load was selected to show the trends in Figure 4.5, and the average of the friction coefficient with the maximum and minimum values are summarised in Figure 4.6.

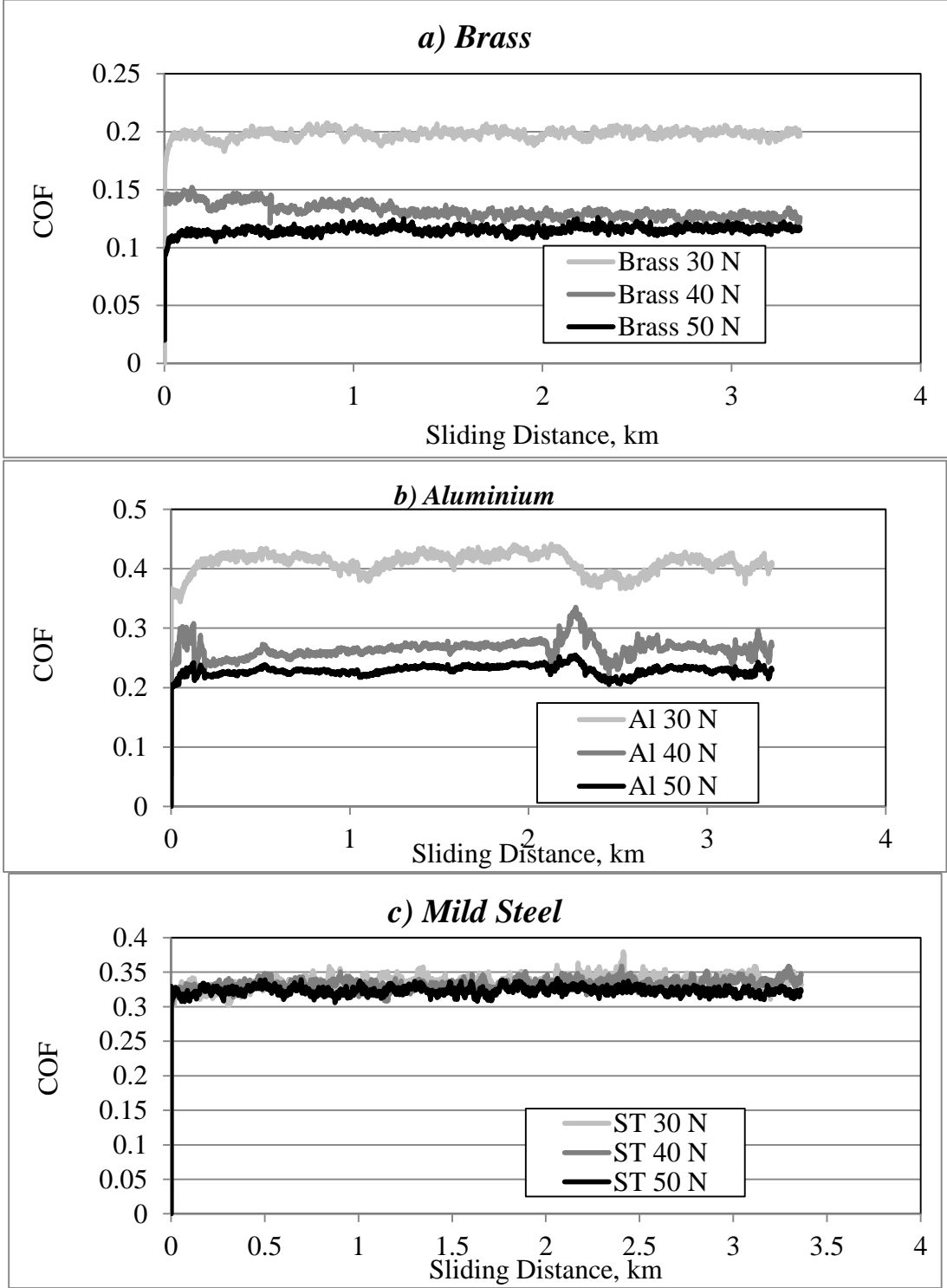


Figure 4.5: Friction coefficient vs. sliding distance of brass, aluminium and mild steel materials under dry contact conditions

The frictional behaviour for all the materials seems to be steady, especially with brass and mild steel. Aluminium exhibits a slight fluctuation in the value, which represents a modification on the surface during the sliding. Such behaviour has been reported previously reported by Alidokht et al. (2012), to be caused when materials transfer from surface to another and detachments occur leading to such fluctuation in the friction coefficient (Behnagh, Besharati Givi & Akbari 2012; Sahin, Çetinarlan & Akata 2007).

With regard to the influence of the applied load on the frictional behaviour of the materials, Figure 4.6 shows that increasing the applied load reduces the friction coefficient especially for the brass and aluminium materials. Mild steel shows no significant effect of the applied load on its frictional behaviour. Brass exhibits the lowest friction coefficient of the three materials.

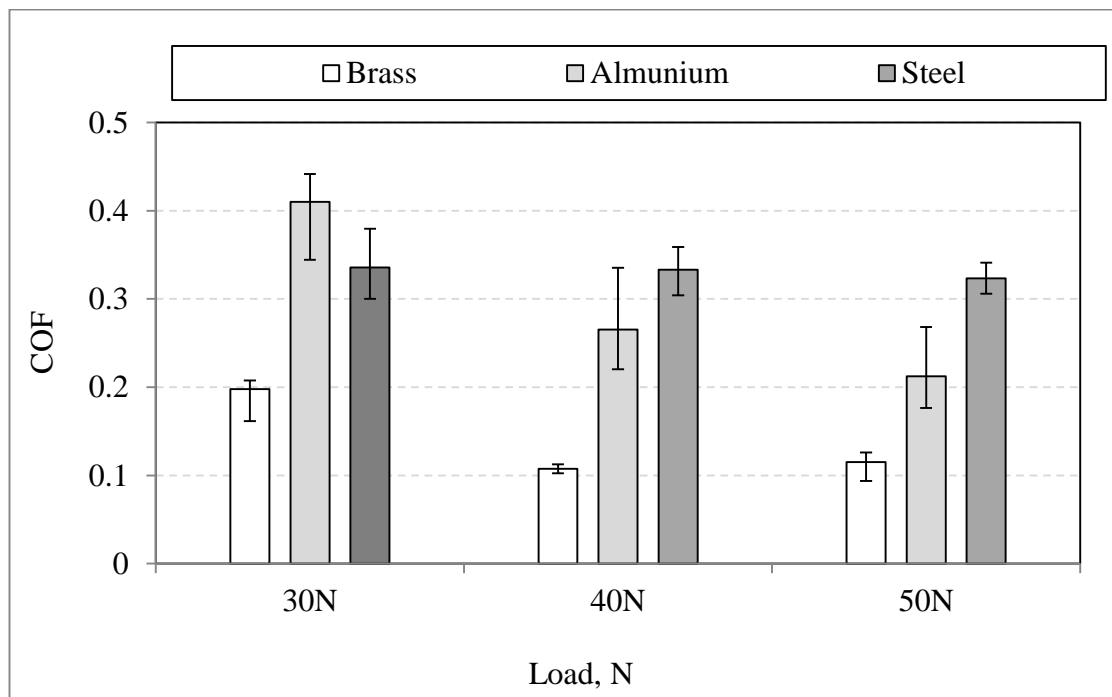


Figure 4.6: Summary of friction coefficient at steady state of brass, aluminium and mild steel materials under dry contact conditions at different applied loads after 10.8 km sliding distance

Differences in the wear and frictional behaviour of those materials are due to the interaction between the surfaces during sliding. Several studies have attempted to correlate the friction and wear behaviour of materials (Kato 2000; P. Suh 1973). In general, there are very few researchers who agree that there is a correlation between the frictional and wear performance of materials (that is, the high friction coefficients represent high resistance in the interface which results in good wear performance). The majority agree that wear is a response to the rubbing process, which is independent of the frictional behaviour. In the current study, the high friction coefficient seems to be when the mild steel was rubbed against the stainless steel counterface. At the same operating condition and parameters, mild steel exhibited intermediate wear performance compared to brass, which has a very low friction coefficient. Thus, there is no correlation between the friction and wear performance of the currently selected materials which is in agreement with (Kato 2000; P. Suh 1973). However, there could be another output of the rubbing, interface temperature, which may contribute to the wear performance of the materials. In the current study,

a thermo-imager device was used to monitor the rubbed bodies during sliding to record temperatures at different sliding distances.

Figure 4.7 shows the maximum temperature on the rubbed surfaces (interface) after 2.5 km sliding distance for the applied load of 30 N. It indicates that a high interface temperature can be found when the mild steel material rubbed against the stainless steel. This should represent the high friction in the interface since the relationship between the friction and the heat is proportional. Based on this, it seems that the high interface temperature with the high shear force in the interface (frictional force) contributes to the intermediate wear performance of the mild steel compared to the brass. For the aluminium, despite the low interface temperature and intermediate friction coefficient, the wear performance was the poorest compared to the mild steel or brass. This could be due to the high removal of material from the aluminium surface which results in very low resistance in the interface and generates low heat compared to the mild steel. For further discussion of this wear mechanism, SEM observations will be presented in the section on worn surfaces and collected debris.

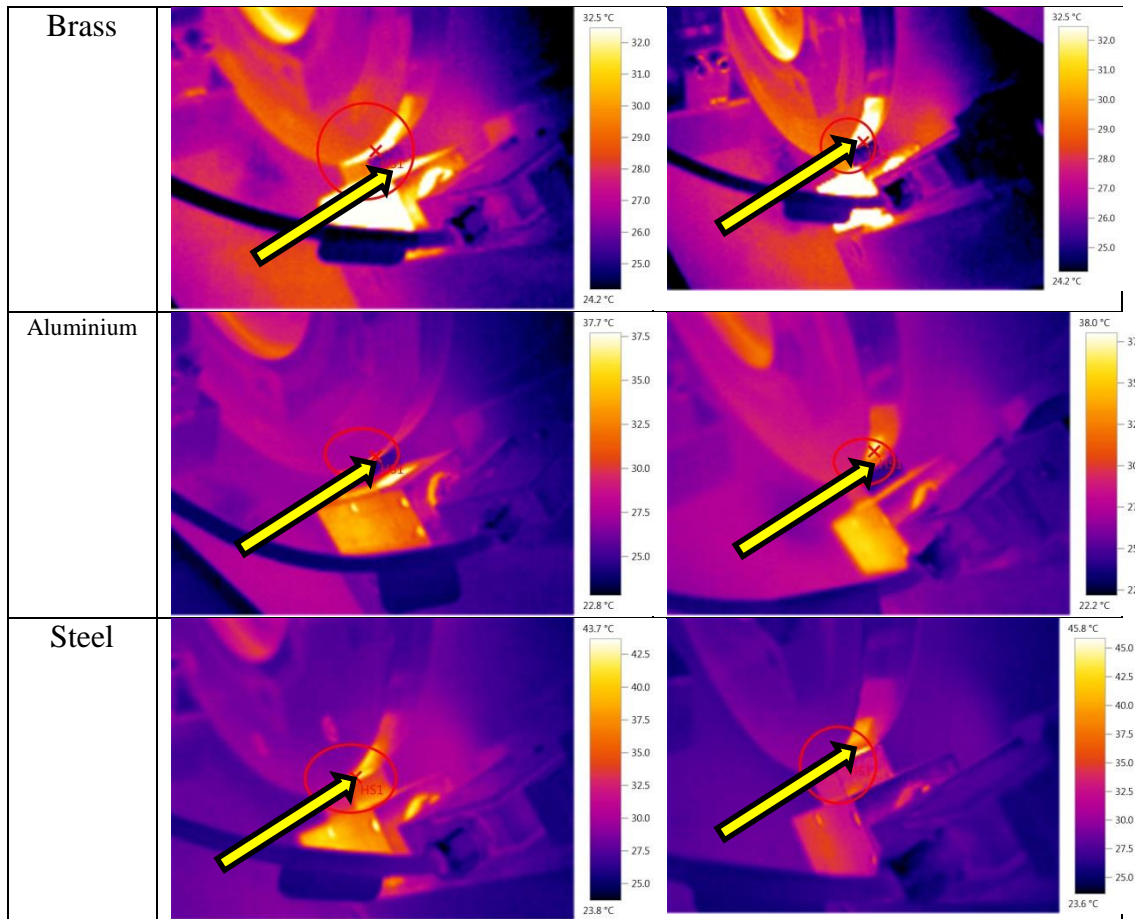
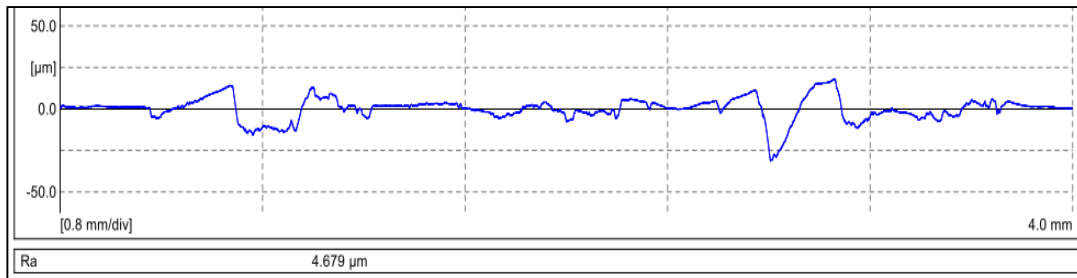


Figure 4.7: Heat distribution in the rubbing area of the metals with the counterface after 2.5 km sliding distance under 30 N applied load * The arrow points out the main measurement spot.

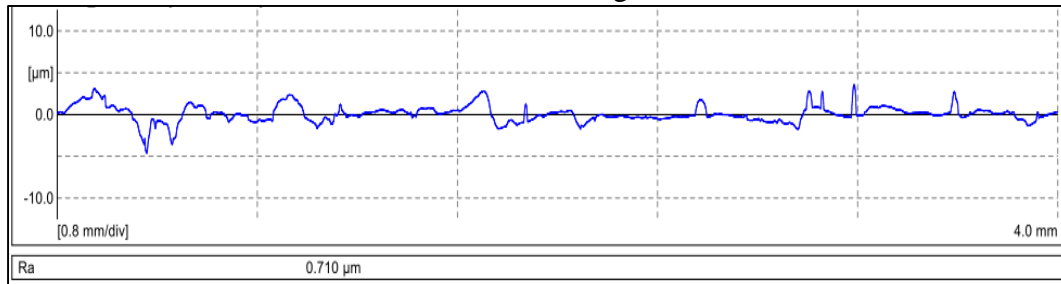
4.3.3 Worn Surface Observation on Selected Metals Subjected to Dry Sliding

4.3.3.1 Roughness modification on the surface

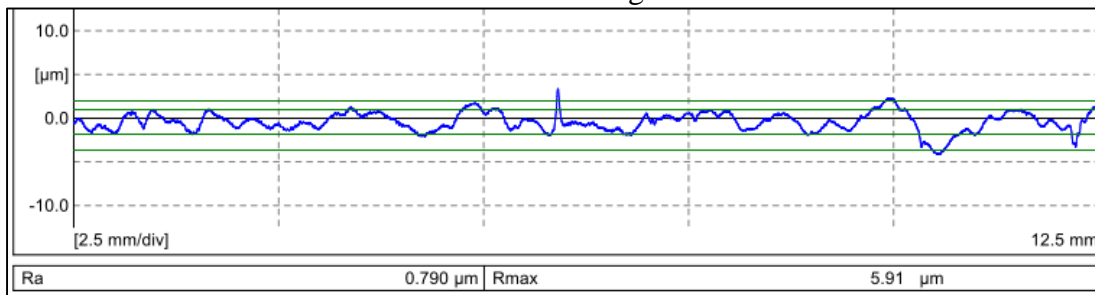
It was mentioned in the presentation of the results that, the modification on the surface characteristics during sliding may influence the wear and frictional behaviour of the materials. One of the characteristics that may assist in understanding the wear and frictional behaviour is the roughness of the contacted bodies. Figure 4.8 displays samples of the collected roughness profiles for the worn surfaces. It should be mentioned here that, before each test, the stainless steel counterface roughness was about $0.1 \mu\text{m Ra}$ – $0.3 \mu\text{m Ra}$ and the roughness of the samples were about $0.075 \mu\text{m Ra}$, $0.4 \mu\text{m Ra}$ and $0.25 \mu\text{m Ra}$ for mild steel, aluminium and brass, respectively. The roughness value was measured with the direction of the sliding.



a) Maximum roughness of the steel after testing under 30 N applied load and 10.8 km sliding distance



b) Maximum roughness of the brass after testing under 30 N applied load and 10.8 km sliding distance



c) Maximum roughness of the aluminium after testing under 30 N applied load and 10.8 km sliding distance

Figure 4.8: Samples of the roughness profile of the specimens after the tests showing the maximum reading at different applied loads after 10.8 km sliding distance

The average roughness of the five reading a associated with the maximum and minimum values for the worn surface of the materials at different applied loads after 10.8 km sliding distance are presented in Figure 4.9. It can be seen that the roughness of the mild steel is much increased after the test, followed by the aluminium, and then the brass. It seems the lowest roughness value of the brass is the main reason of its high wear performance compared to others. For the mild steel, the high increase in the roughness seems unrelated to its wear and frictional behaviour. Conversely, debris was collected after each test. The lowest amount of debris collected was in the case of the mild steel, while aluminium introduced too much debris.

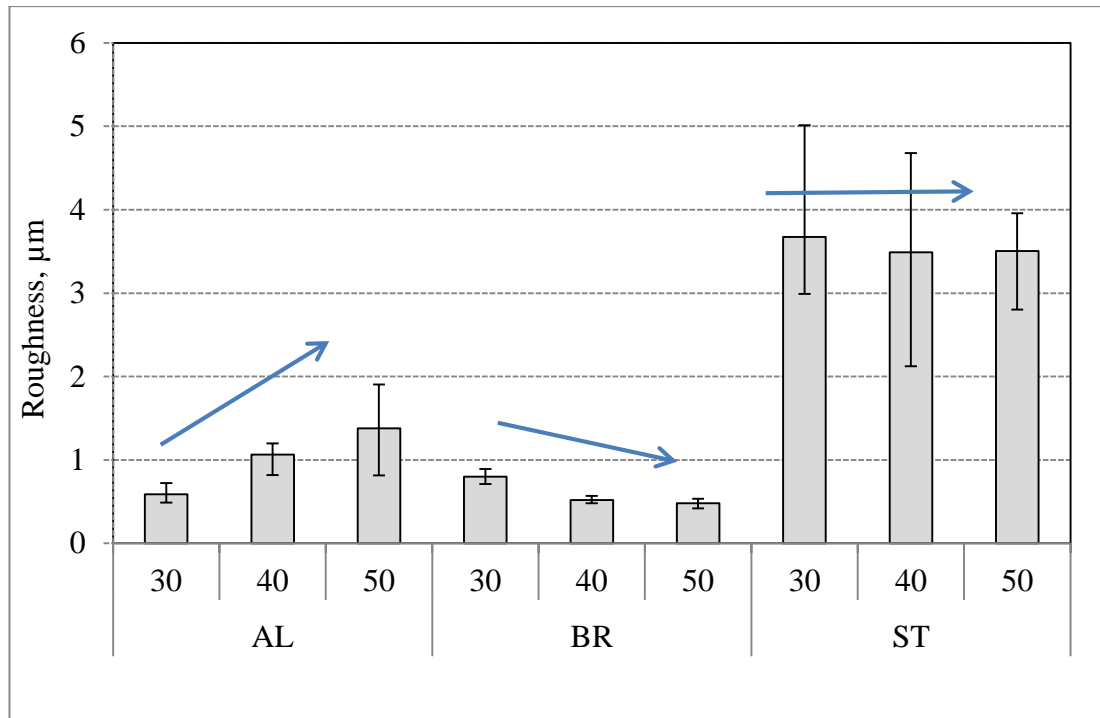


Figure 4.9: Average worn surface roughness after the test at different applied loads after 10.8 km sliding distance

The roughness of the counterface could not be measure since the experiments were conducted on a thin ring (Block on Ring machine). In addition, since the counterface is stainless steel and the samples are softer than the stainless steel, the modification on the stainless steel surface would be due to the transfer of the soft part onto the stainless steel counterface. In this case, measuring the roughness of the stainless steel will not reflect the influence of the rubbing on the real surface of the stainless steel counterface. Furthermore, before each test the stainless steel counterface was polished to remove any attached debris or film. To comprehensively study the impact of the rubbing of metals on the stainless steel counterface, it is recommended to use a block on disk machine with which measuring the roughness of the track, hardness and optical microscopy will be possible.

4.3.3.2 Observed Wear types and comparison with previous reported works

It is important to describe the different type of wear before observing the worn surfaces of the metals. It should be mentioned here that defining the wear type is very difficult due to the fact that there is a great different between the contact mechanism and the damage feature on the worn surfaces. Bhushan (2000) stated that *“three are many terms used of describe wear, and they are not always well differentiated. This sometimes makes understanding wear mechanism confusing and difficult”*. Fundamentally, wear modes are classified into four categories as adhesive, abrasive, fatigue and corrosive, (Burwell Jr 1957). Such classification was used recently by many researchers such as (Bhushan 2013b, 2013a; D'Annibale & Luongo 2013; Li et al. 2013; Stachowiak & Batchelor 2013).

Adhesive wear is the most common type of wear resulting from two flat solid bodies which are in sliding contact under either lubricated or dry contact conditions. It arises from the strong adhesive forces that are generated at the interface of two solid materials where intimate contact is made over a number of junctions or patches. The most crucial part of adhesive wear is the formation of an interfacial transfer film on the hard counterface and plastic deformation (Bhushan 2013b; Myshkin, Petrokovets & Kovalev 2006). At the asperity contact, contacts are sheared by sliding, which may cause fragments to detach from one surface and adhere to the other surface. In other words, the junctions or patches continue to be made or broken as sliding continues. Those particles which do not transfer off or back to the original surface form loose wear particles. The adhesive process occurs due to high local pressure. Asperities deform to increase the real area of contact to support the pressure. Without surface films, the surfaces would adhere, but small amounts of contaminant would minimize or prevent adhesion under purely normal loading. When tangential forces are applied, contaminants are dispersed at the point of contact and cold welding at junctions can take place. With a continual sliding motion, new junctions are formed and sheared.

On the other hand, abrasive wear occurs whenever a hard surface slides over and cuts grooves away from the other surface (Tylczak & Oregon 1992). There are two categories of abrasive wear: two-body abrasion and three-body abrasion, (Trezona, Allsopp & Hutchings 1999). In Two-body abrasion occurs when one surface is harder and rougher than the corresponding surface. The asperities of the rough surface dig into and remove material from the softer surface. In a three-body abrasion, the three bodies correspond to two surfaces and the small particles caught between these surfaces. These particles, such as hard debris or foreign particles, which are sandwiched between both bodies, are sufficiently hard that they are able to abrade one or both of the surrounding surfaces. The third body is able to change the nature of the interface drastically if it forms strong stubborn films on either of the two rubbed surfaces (Zmitrowicz 2005).

Beside the adhesive and abrasive wears, fatigue wear can be one wear type that can be observed occurring when the repeated sliding or rolling (adhesive wear) takes place over a track, (Szolwinski & Farris 1996). Under dry or lubricated contact conditions, rubbed metals surfaces may be initiated with an adhesive wear mechanism and with the repetition of the sliding, crack is initiated on the surface showing aggressive deterioration (Choi, Lee & Lee 2013). Moreover, in many cases, the adhesive wear can be transferred into either abrasive or fatigue due to the repetition of the stress in the contact area and modification on the roughness of the surfaces (Trezona, Allsopp & Hutchings 1999). Amamoto and Goto (2006) referred to the initial adhesive wear as mild wear and the transition into another wear mode (fatigue or abrasive) as severe wear.

Micrographs of the worn surface of the materials under different applied loads are presented in Figures 4.10–4.12. For the mild steel, Figure 4.10 shows that the worn surface of the materials indicates a different wear mechanism. At a low applied load of 10 N, Figures 4.10a and b show plastic deformation indicating high resistance in the interface, which could explain the good wear performance of the mild steel at a 30 N applied load (Figure 4.4). At the high applied load of 50 N, it seems there is abrasion on the surface, which could indicate the presence of third bodies in the

interface. Further to this, micro-cracks can be seen, especially at the edge of the worn surface (Figure 4.10c). Some of the debris was able to adhere to the mild steel surface and generate a weak layer of macro-cracks and voids.

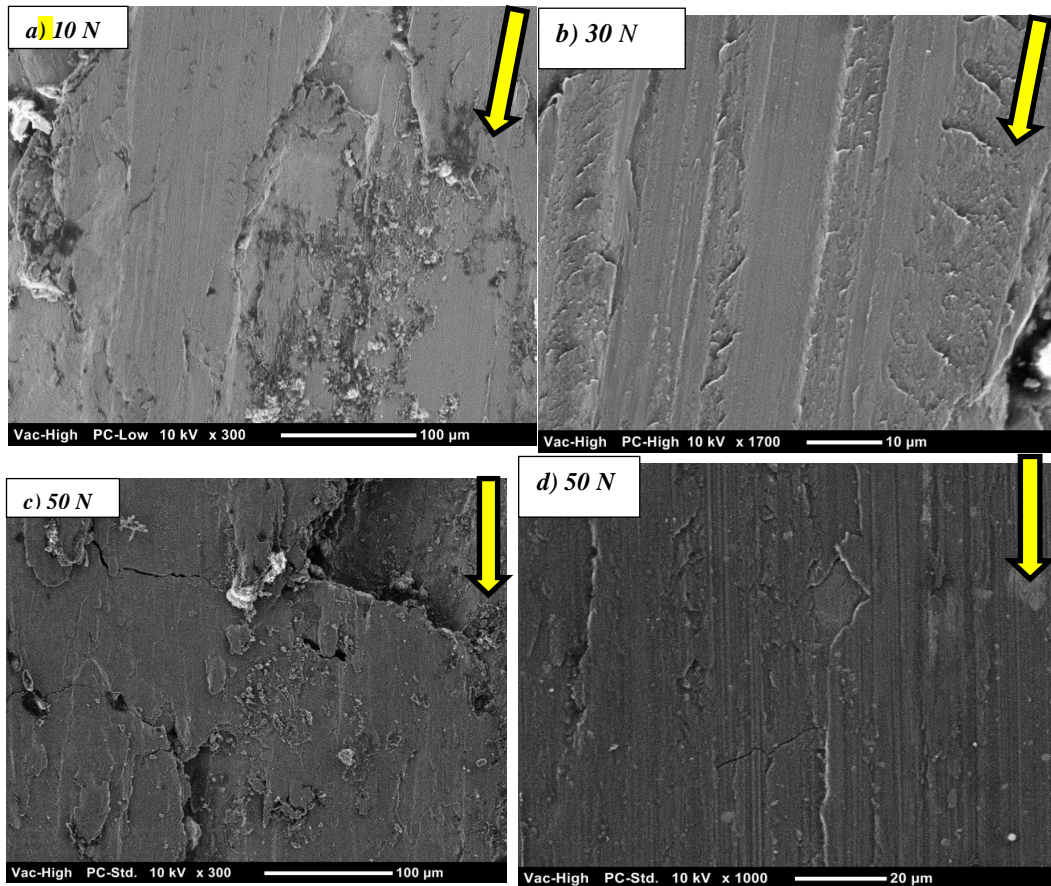


Figure 4.10: Micrographs of the steel surface after the sliding showing different wear mechanisms

For the aluminium, the micrographs of the worn surfaces are presented in Figure 4.11. The wear mechanism seems to be a pure adhesive wear associated with the ploughing process in some regions. In addition, there is an abrasion nature on the surface (Figure 4.11d). The wear results show that the aluminium has higher material removal from the surface. However, the micrographs showed that the surfaces were subjected to pure adhesive wear. It seems that high plastic deformation occurred in the interface, which led to higher material removal and smoothed the surface at the same time. This can be further clarified with the micrographs of the debris.

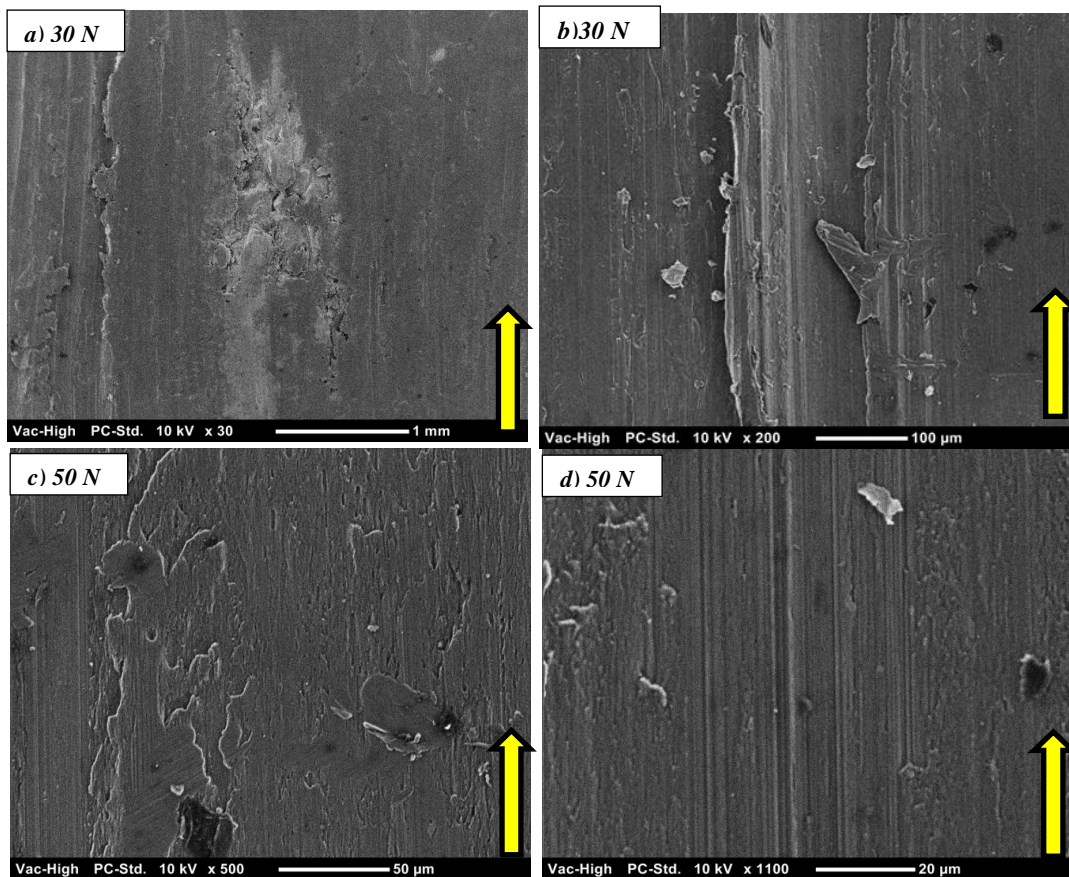


Figure 4.11: Micrographs of the aluminium surface after the sliding showing adhesive, abrasive and ploughing wear mechanisms

For the brass, the worn surface clearly shows plastic deformation even though there is a rough area (Figures 4.12a and b). It seems that the high applied load assists in adhering the debris to the worn surface, which stabilises the surface and results in good wear performance of the brass at high applied load.

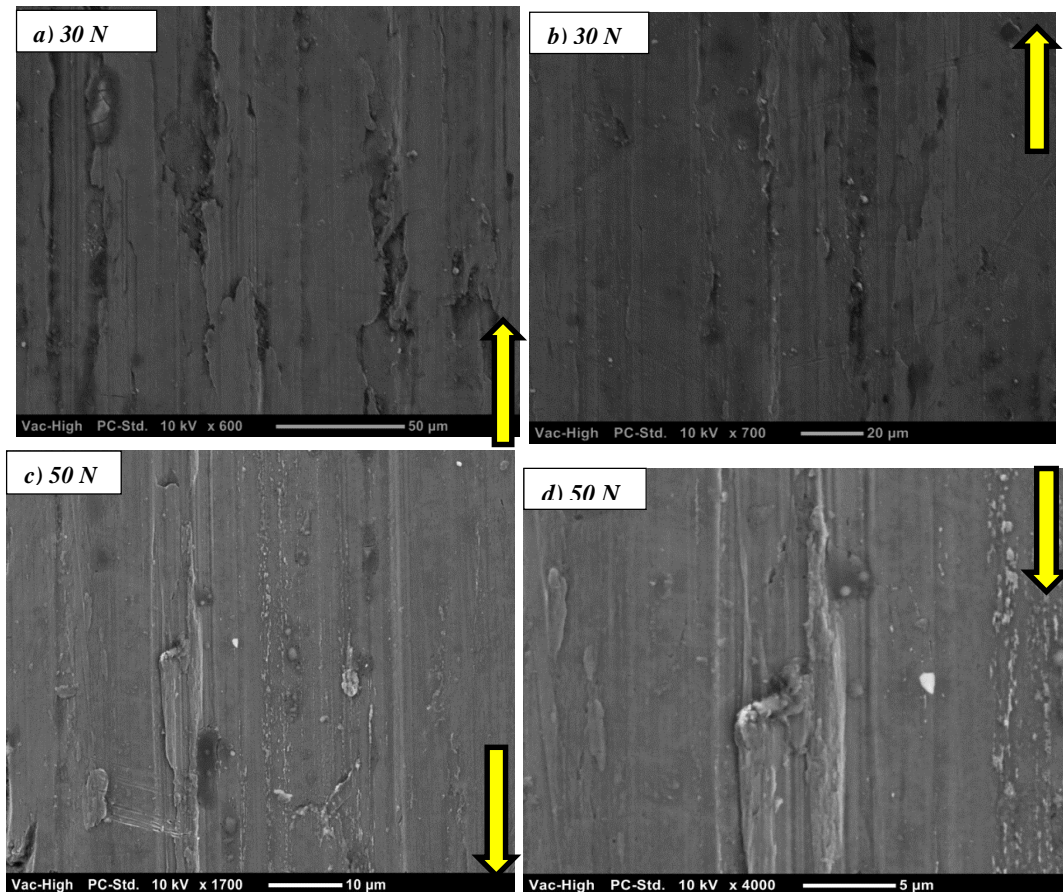


Figure 4.12: Micrographs of the brass surface after the sliding showing purely adhesive associate with small area of abrasive wear mechanisms

For further understanding, the collected debris is presented in Figure 4.13 for the three materials after the tests under a 50 N applied load. All the micrographs were taken at the same magnification ($\times 60$). The Figure clearly shows a clear distinction between the debris sizes of the materials. Mild steel introduces very small debris, which could indicate good resistance in the interface. However, the small size of the debris may give them the opportunity to act (roll or slide) in the interface, which results in high friction and wear in the case of sliding or high wear, and low friction in case of rolling. In the current study, mild steel exhibited intermediate wear and frictional performance which may indicate that the debris was rolling and sliding at the same time in the rubbing area. This could explain the abrasion nature of the mild steel worn surface on the micrographs in Figures 4.10a and c. Aluminium introduces very large debris sizes which could result from the high plastic deformation in the interface, resulting in high material removal. This can explain the poor wear performance of the aluminium (Figure 4.4). The ease of material removal of the aluminium leads to its low friction coefficient (Figure 4.6).

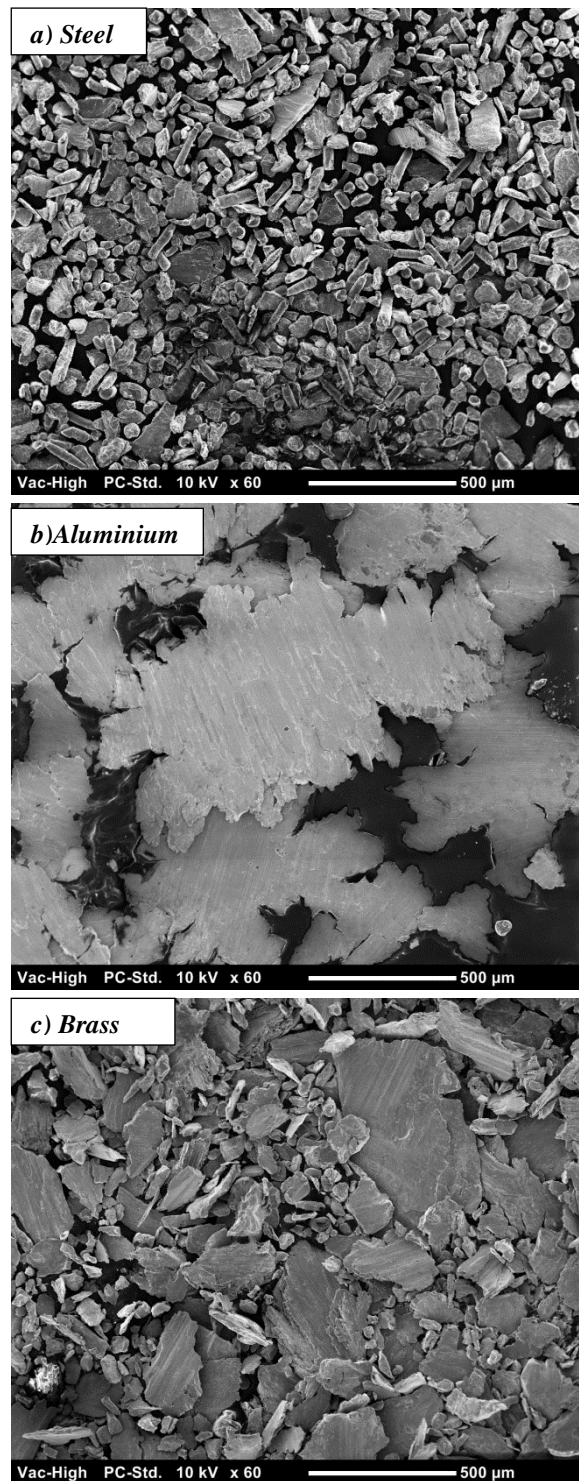


Figure 4.13 Micrographs of the collected debris after stainless steel sliding against mild steel, aluminium and brass under the applied load of 50 N for 10.8 km sliding distance

In light of the above and the summary of the results, three different wear mechanisms can be found: two-body abrasion nature in the case of brass, since it has better wear performance than the others but shows a rough surface with less debris (Figure 4.14a), and three-body abrasion nature in the case of aluminium, since there is too much of debris associated with the very rough surface (Figure 4.14b); and pure adhesive in the case of mild steel since it has the lowest amount of debris and the micrographs of the worn surface showed clear plastic deformation (Figure 4.14c).

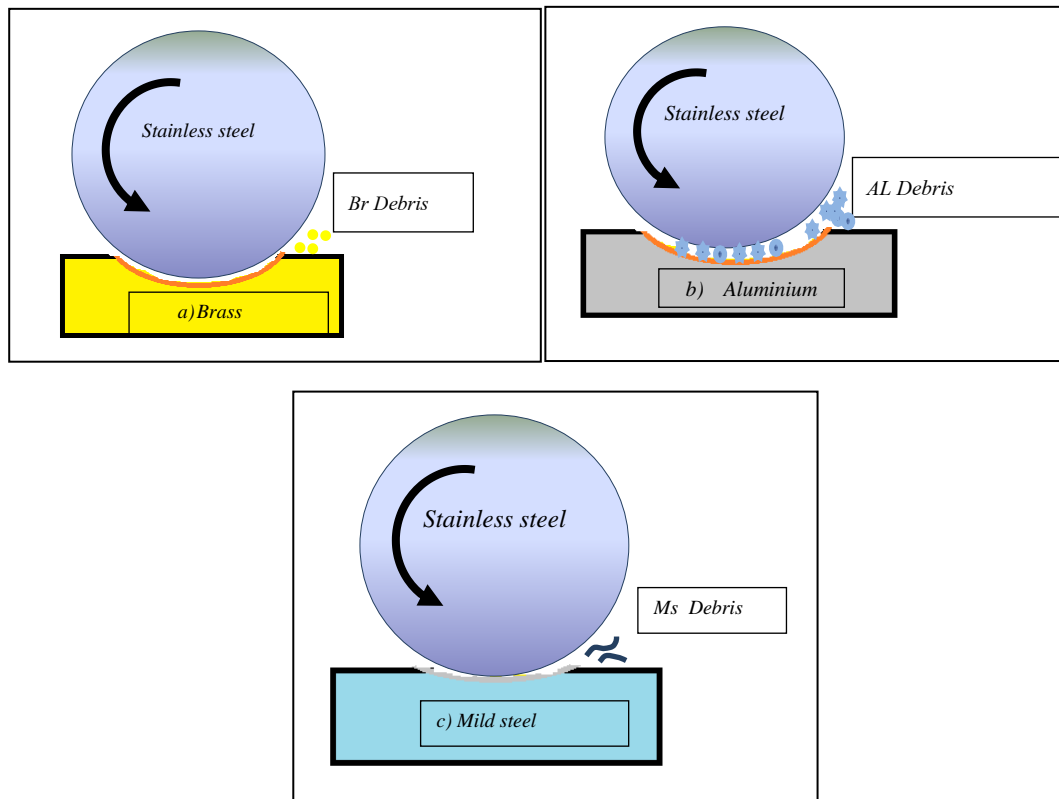


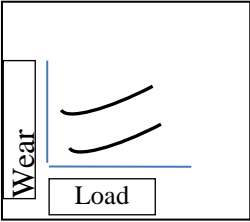
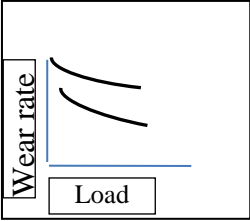
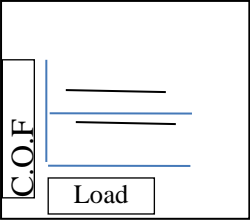
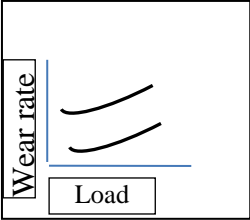
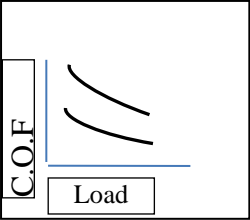
Figure 4.14: Schematic drawing showing different wear mechanisms exhibited when stainless steel rubbed against a) brass, b) aluminium and c) mild steel

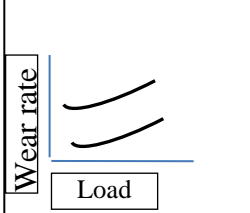
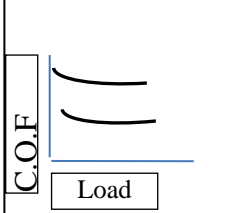
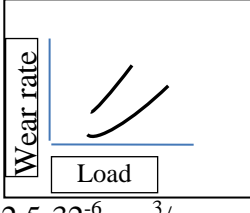
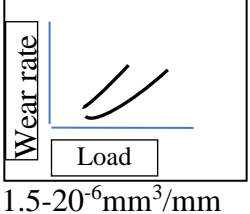
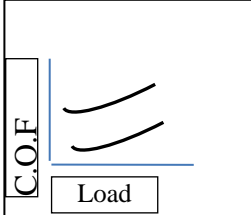
It should be mentioned here that the presence of the 4% of Pb in the brass can significantly contribute to the good performance of the brass compared to the mild steel and aluminium. It is well known that the Pb is one of the solid lubricant additives which assists in generating a lubricant film on the counterface, (Shi et al. 2014). This is mainly due to the fact that Pb has a low melting point and high flash temperature observed in some reported works such as (Moshkovich et al. 2014; Turhan 2005).

In the current study, brass exhibited a low specific wear rate (Figure 4.4), low friction coefficient (4.6), and patches of debris (Figure 4.13 c). Such behaviour of the brass compared to the aluminium and mild steel, is attributed to the presence of 4% of Pb. In other words, the Pb managed to generate the film on the counterface, however, it was weak to adhere to the counterface which resulted in low friction and the observed patches of debris. Despite of this, the brass did not exhibit an abrasion nature compared to the mild steel and the aluminium which is due to the low melting temperature of the debris of brass (Pb content). This can help with further clarification of the better friction and wear performance of the brass compared to the aluminium and mild steel. A summary of relevant studies is presented in Table 4.1. One can see that there are some differences in the wear behaviour in terms of the trends and values of the specific wear rate of the materials. It seems the different presentation of the data displays different trends and even values of the wear. At this stage, it is not possible to compare the current results with the literature in terms of wear value and/or trend unless they are presented in the similar unit of wear. However, the wear damage on the worn surface of the materials can be discussed with the literature.

(Bermúdez et al. 2001) tested aluminium against a steel ball and high plastic deformation associated with the ploughing process took place, resulting in high wear. Due to the high concentrated load of the steel against relatively soft aluminium in the interface (ball/flat), the dominant wear was ploughing. In this work, there was no observation of debris. (Zhu et al. 2012) reported a similar wear mechanism and damage feature of the selected aluminium sliding against mild steel, despite the tests being conducted at an elevated environmental temperature of 200 °C (the sample and the counterface were heated to that temperature). In (Wei et al. 2011), the mild steel suffered from an oxidation process at an elevated temperature of 200 °C and above. Conversely, at room temperature, similar damage was observed to that of the current study. However, it was reported that wear predominates as pure adhesion despite the fact that the work reported a large size of debris removal. The current SEM observations and those of (Wei et al. 2011) agree upon the point that there is significant damage to the surface of the mild steel due to the presence of debris in the interface. Similar reported observations are given by Wang, Wei and Zhao (2010). With regards to the brass material, there is not much research to date (Amirat et al. 2009). In (Amirat et al. 2009), the wear data is not available, but observations of the worn surfaces, show a clear abrasion nature on the surface, which is in high agreement with the current study.

Table 4.1: Recent Works on the Dry Wear Performance of Aluminium, Mild Steel and Brass

Reference	Against	Operating parameters	Wear	Friction
(Bermúdez et al. 2001), pin-on-disk	Aluminium/ mild Steel	400m, sliding distance speed 0.02 m/s	 0-900 10^{-5} mm ³ /m	Not available
(Zhu et al. 2012) , pin-on-disk	Aluminium/ mild Steel	200m, sliding distance speed 0.4-1 m/s	 7-9 10^{-6} g/N.m For 20 N -50N	 0.3 - 0.5 For 20 N -50N
(Vasheghani Farahani et al. 2014) , pin-on-disk	Aluminium/ mild Steel	1000m, sliding distance speed 1 m/s	 1.7-3.3 10^{-3} mm ³ /m For 20 N -50 N	 0.3 - 0.9 For 20 N -50 N

(Wei et al. 2011) , pin-on-disk	Mild steel/steel pin	1200m, sliding distance speed 1 m/s	 <p>Wear rate vs Load graph showing two upward-sloping curves. The y-axis is labeled 'Wear rate' and the x-axis is labeled 'Load'.</p>	 <p>C.O.F vs Load graph showing two upward-sloping curves. The y-axis is labeled 'C.O.F' and the x-axis is labeled 'Load'.</p>
			1.0-9.0 10^{-6} mm ³ /mm For 50-200 N	0.55-1.25 For 50-200 N
(Wang et al.) , pin-on-disk	Mild steel/Steel pin	1200m, sliding distance speed 0.1 m/s	 <p>Wear rate vs Load graph showing two upward-sloping curves. The y-axis is labeled 'Wear rate' and the x-axis is labeled 'Load'.</p>	Not available
			2.5-32 10^{-6} mm ³ /mm For 50-200 N	
(Wang, Wei & Zhao 2010) , pin-on-disk	Mild steel/Steel pin	1200m, sliding distance speed 0.1 m/s	 <p>Wear rate vs Load graph showing two upward-sloping curves. The y-axis is labeled 'Wear rate' and the x-axis is labeled 'Load'.</p>	Not available
			1.5-20 10^{-6} mm ³ /mm For 50-300 N	
(Amirat et al. 2009) , pin-on-disk	Brass/ Steel pin	1000m, sliding distance speed 0.5 m/s	Not available	 <p>C.O.F vs Load graph showing two upward-sloping curves. The y-axis is labeled 'C.O.F' and the x-axis is labeled 'Load'.</p>
				0.2-0.25 For 25 N - 37 N

4.4 Chapter Summary

After conducting the experimental work and discussing the results, the following conclusions and recommendations can be drawn:

- The trend of the specific wear rate vs. sliding distance is almost the same for all the selected metals sliding against stainless steel. The curve is divided into two regions: running in and steady state. In the latter, the specific wear rate is almost steady with increases in the sliding distance
- The friction coefficient was almost steady for all the materials except the aluminium/stainless steel, which introduced slight fluctuations due to the modifications on the surfaces during the sliding
- The wear mechanism varies for each type of material. Mild steel rubbed against stainless steel exhibited an abrasive wear mechanism due to the presence of hard debris in the interface. Meanwhile, aluminium showed a purely adhesive nature when it was rubbed against a stainless steel counterface. Brass exhibited abrasive wear associated with plastic deformation.

Chapter 5: The Potential Use of Waste Cooking Oil as a Lubricant

5.1 Introduction

The experimental data collected from the newly designed hybrid tribology machine is presented in this chapter. The influence of different blends of lubricant, lubricant temperature and operating parameters on the adhesive wear and frictional behaviour of brass, aluminium and mild steel sliding against a stainless steel counterface are addressed. The worn surfaces are also examined to categorise damage features and assist in the analysis of the data.

5.2 Influence of Waste Cooking Oil on the Tribological Performance of the Metals

In this section, the influence of WCO at room temperature, 20°C, on the adhesive wear and frictional behaviour of the metals sliding against stainless steel counterface is discussed.

5.2.1 Wear Behaviour of Metals Under Waste Cooking Oil Lubricant Conditions

The specific wear rate of brass, aluminium and mild steel materials against the sliding distance for different applied loads are presented in Figure 5.1, including the specific wear rate under the dry condition and applied load of 10 N. The dry wear data are presented in the second Y-axis (right) as the values of the dry wear are greater than the lubricant condition data. Figure 5.1a displays the specific wear rate for the brass, indicating that there is a decrease in the specific wear rate with an increase of the sliding distance for all the applied loads and conditions. This decrease indicates the establishment of integration between the asperities in contact. For the influence of the WCO on the adhesive wear behaviour of brass, Figure 5.1a shows that the presence of the WCO in the interface significantly reduces the specific wear rate since the values fall by about five times compared to the dry contact conditions. There could be many reasons for the fall in the specific wear rate in the case of WCO presence compared to the dry. First, in dry contact conditions, surface modification takes place on the counterface, which increases the roughness of the counterface and leads to a high level of material removal, which in turn increases the roughness of the samples (Section 4.3.3). In contrast, the presence of the WCO acts as a cleaner of the interface, which prevents the formation of film on the counterface, that is, less modification to the roughness of the counterface as reported in the literature (Ronkainen, Varjus & Holmberg 1998; Wang et al. 2010). Conversely, it has been reported that the presence of a liquid in the interface helps to reduce the interface temperature, which in turn reduces the material removal from soft surfaces (Yousif, Devadas & Yusaf 2009). Furthermore, Louaisil et al. (2009) analysed the interface temperature on friction and wear in cold rolling with the presence of the oil, concluding that “*a great influence of temperature and lubricant on friction and wear has been put forward*”. In the current study, interface temperature dramatically increases under the dry contact condition, which could damage the surface characteristics of the material. However, the presence of the WCO in the interface played the role of cooling agent in the interface. In light of this, the WCO helped to

cool down and clean up the interface, which improved the adhesive wear performance of the metals.

With regard to the influence of the WCO on the adhesive wear behaviour of aluminium and mild steel materials sliding against the stainless steel counterface, Figures 5.1b and c display similar trends and findings to the brass material in Figure 5.1a. Both materials exhibit better wear performance under WCO lubricant condition compared to the dry and there is a decrease in the specific wear rate with the increase in sliding distance.

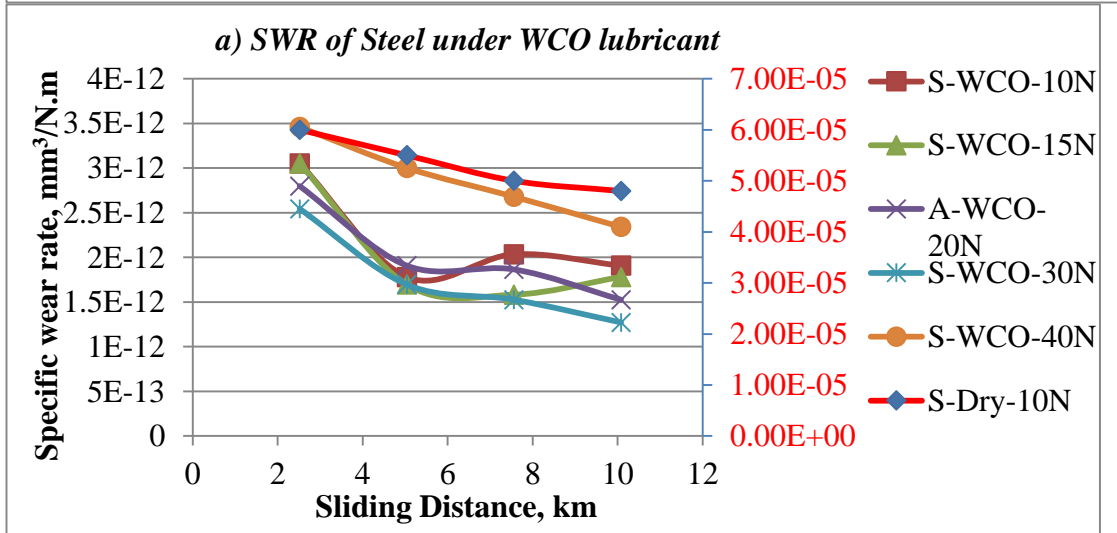
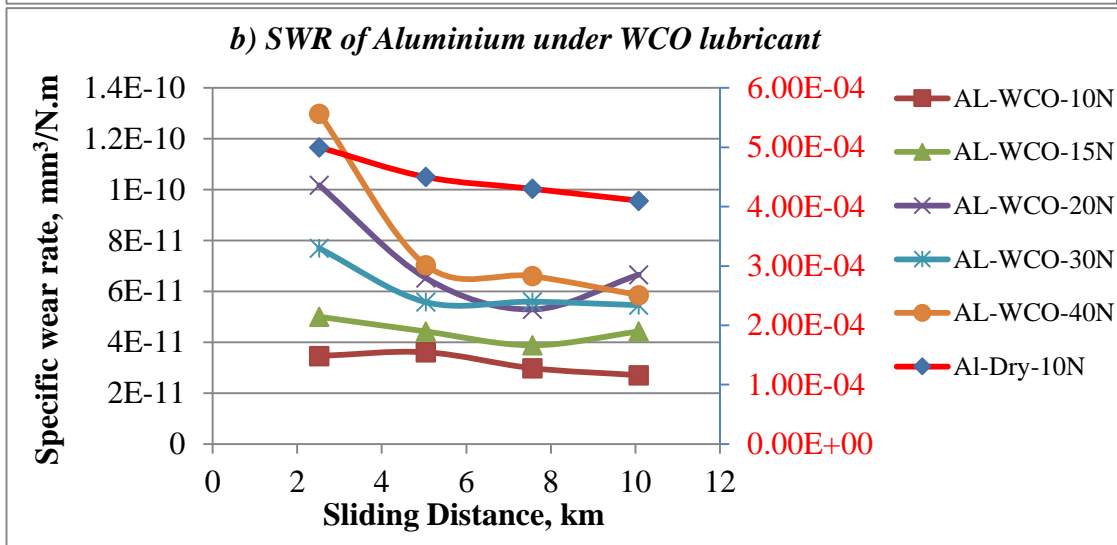
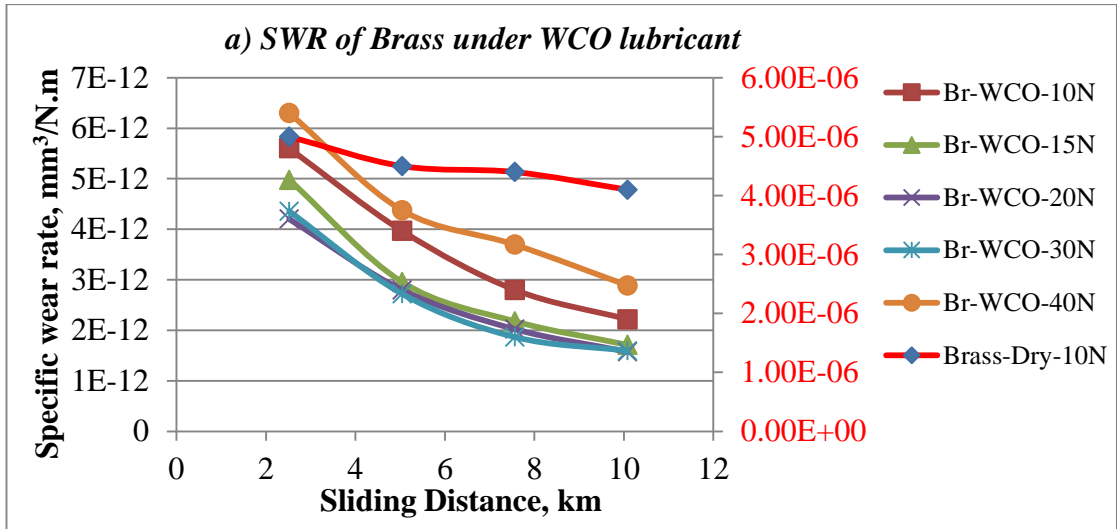


Figure 5.1: Specific wear rate of the metals against sliding distance under different applied loads using waste cooking oil as a lubricant at 22°C

To understand the influence of the applied load and the differences in the wear behaviour of the metals, the specific wear rate value at the maximum sliding distance (10.8 km) was extracted from Figure 5.1 and presented in Figure 5.2. For each material there is a different trend in the influence of the applied load on the wear performance. For the brass materials, there is a decrease in the specific wear rate

with the increase of the applied load, that is, there is relatively less removal of the material at a higher applied load compared to a low load. After each test, the roughness of the worn surface was measured and a very minor change was found in the roughness of the brass surface with the increase of the applied load. As there is a weight loss and modification on roughens of the samples, the generation of lubricant film in the interface is not possible. This will be explained further with the aid of the SEM in Section 5.2.3.

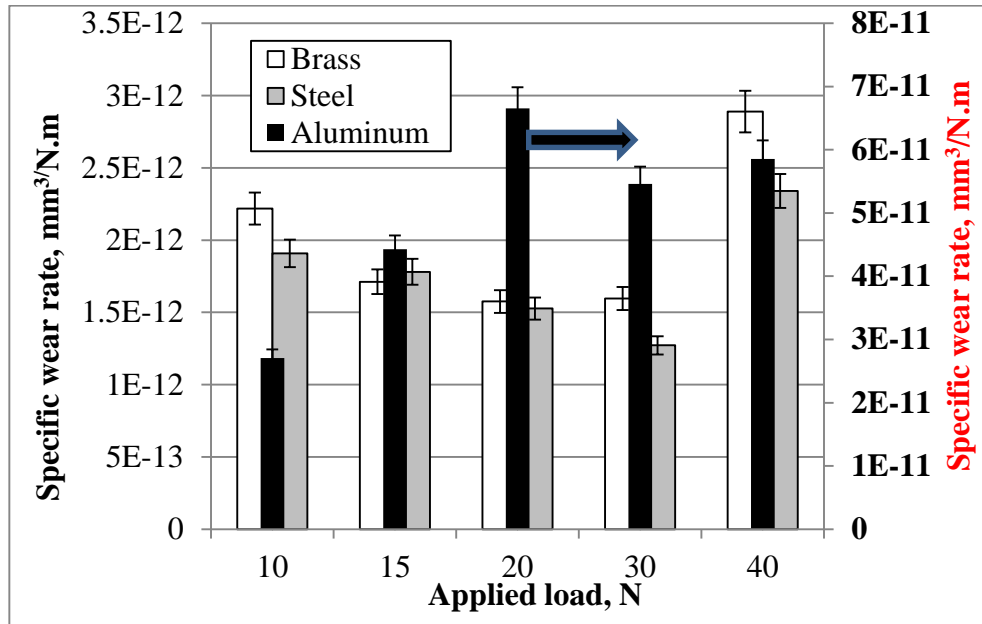


Figure 5.2: Specific wear rate of the metals against applied load using waste cooking oil as a lubricant at 22°C after 10.8 km sliding distance. Left Y axis shows the SWR for brass and steel metals, and right Y axis show the SWR for the aluminium metal.

At this stage, it seems at high applied loads and the presence of the oil, a polishing process took place. This polishing process prevented greater removal of material from the surface. This was not the case with the aluminium materials, as there was an increase in roughness, which indicates attack from the counterface on the aluminium surface and could explain the increase in the specific wear rate with the increase of the applied loads. For the mild steel, there was a drop in the specific wear rate with the increase of the applied loads which could be similar to that of the brass. In comparing the three materials, it is obvious that the aluminium exhibits the poorest performance compared to the brass and the mild steel materials. Confusion over the influence of the mechanical properties on the adhesive wear performance of materials is reported by many scholars. (Shipway & Ngao 2003) reported that there is a poor relationship between the mechanical properties with the abrasive wear performance of 20 polymeric materials. However, Budinski and Ives (2005) and Larsen et al. (2008) claim otherwise. From the mechanical properties of the three materials in Table 3.2, one can see that aluminium has relatively poorer mechanical properties compared to mild steel and brass, which could indicate the correlation between their mechanical properties and their adhesive wear performance.

Tang and Li (2014) addressed the roles of additives on the lubricant performances covering three models of lubricant behaviour in the interface, i.e. there is physical or chemical absorption on rubbing metal surfaces to form monolayers (Beltzer & Jahanmir 1988), thick film action model due to the high viscous films (Anghel,

Bovington & Spikes 1999), and a lack of adhesion of the liquid with the adsorbed monolayer might lead to the liquid slip (Choo, Forrest & Spikes 2007). The current results have been discussed with the aim of the second model. In some works on the vegetable oils, (Biresaw & Bantchev 2008), it was found that the film thickness in the thin film region can be influenced by physico-chemical properties and chemical composition (degree of unsaturation, functional groups and chain length) rather than viscosity. Fatty acids have a wide-ranging chain length, unsaturation and functionality, and the effect of such variability on tribological properties of new vegetable oils is not yet understood.

The chemical composites of the current used waste cooking oil contains a high fatty acid content as mentioned in Table 3.1, and the acids are mainly Oleic and Linoleic. Majdoub et al. (2014) found that oleic and linoleic can be used as additives for PAO4 oil to reduce the friction coefficient which is due to the improvement in reducing the energy loss. Ikeda, Tomohiro and Ito (2014) investigated the influence of palmitic, stearic, oleic and linoleic acids on palm oil as a lubricant and found that stearic gained optimum results in terms of the wear and frictional performance of the palm oil. From previous researches by Salimon, Salih and Yousif (2012) and Salih, Salimon and Yousif (2011), it has been reported that the oleic acid significantly improved the physicochemical and tribological properties of the synthetic product oils. Moreover, stearic acid has been reported to be a good coater candidate for different applications, (Nampi et al. 2011; Tseng, Liu & Hsu 1999; Yao et al. 2013). In the current study, 5.2 % of the waste cooking oil is stearic which significantly supports the second mode of the lubricant (Beltzer & Jahanmir 1988).

5.2.2 Frictional Performance of Metals Wear under Waste Cooking Oil Lubricant Conditions

Figure 4.5 presented the friction coefficients of brass (0.11-0.2), aluminium (0.2-0.42) and mild steel (0.33) sliding against stainless steel counterface under dry contact conditions. In this section, the friction coefficient of the materials against the stainless steel under lubricant conditions at different applied load is presented. Figure 5.3 displays a sample of the friction coefficient against the sliding distance for the materials at the applied load of 30 N. The trends of the friction coefficient against the sliding distance for all the applied loads are the same. Therefore, the friction coefficient values of the materials at the steady state are presented in Figure 5.4 at different applied loads. The Figure shows that the friction coefficient for all the materials have very low values ($\ll 0.05$) compared to the values under dry contact conditions. Regarding the friction coefficients of the materials and their performance, mild steel exhibited lower friction coefficient value at the low range of applied loads (10 N -20N). On the other hand, at the higher range of applied load (30 N and 50 N), aluminium introduces a relatively low friction coefficient compared to the others. Despite of this, the differences in the friction coefficient values among the materials is about 0.01. It is well known that the presence of the lubricant in the interface will reduce the interaction between asperities, which will reduce the resistance to the shear (i.e. low friction). However, it can be seen from Figure 5.4 that the increase in the applied load increases the friction coefficient due to increase in the applied force to enforce the interaction between the asperities.

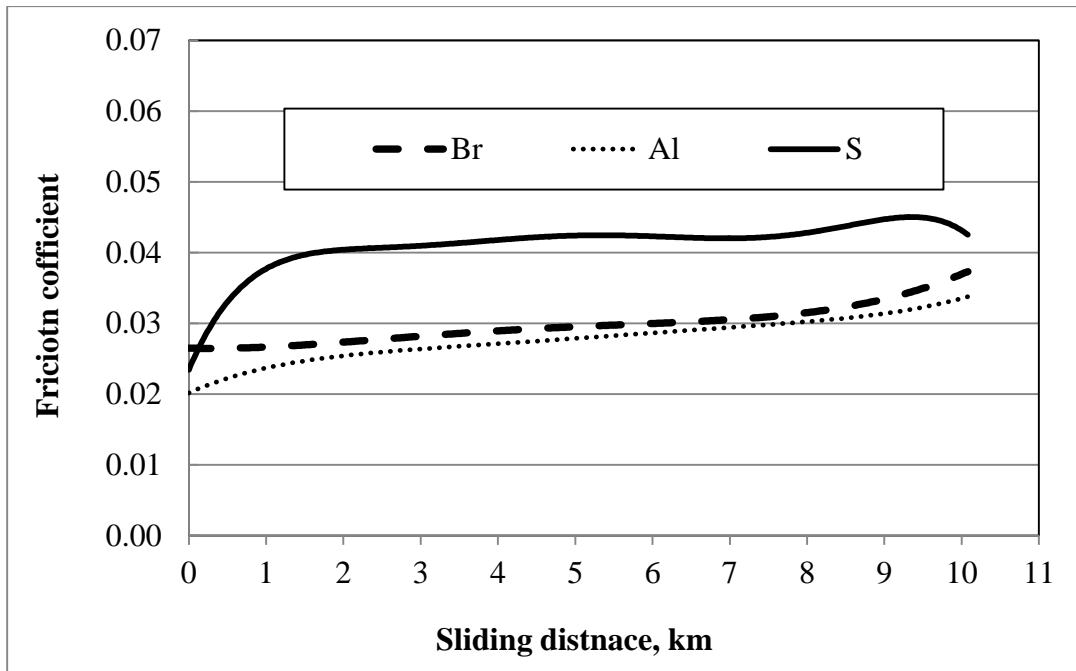


Figure 5.3: Friction coefficients of the metals against sliding distance using waste cooking oil as a lubricant at 22°C under the applied load of 30 N

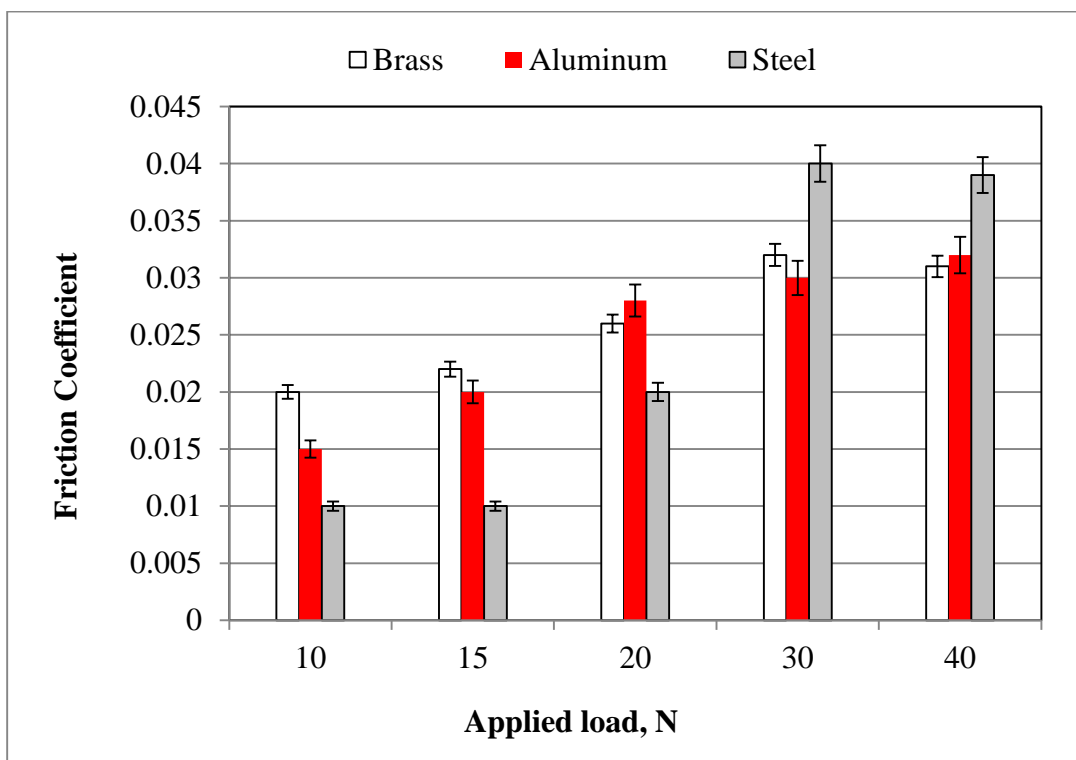


Figure 5.4: Mean friction coefficients of the metals against applied load using waste cooking oil as a lubricant at 22°C

Many scholars have indicated that the increase in the friction coefficient represents the resistance to wear, leading to less removal of the materials (Fischer & Tomizawa 1985; Wang & Rack 1991), especially when the materials are used for brake applications. However, for low friction-coefficient applications (e.g. bearings, sliding components), designers are always exploring the possibility of reducing the friction

and wear at the same time (e.g. knee joint, crank shaft, journal bearings). In the current study, it seems there is a promising result for the selected materials under WCO lubricant conditions since the specific wear rate and friction coefficient are low. Y. Wang et al. (2010) also reached the same conclusions when the Al₂O₃/SiCp/Al hybrid metal matrix composites was tested under dry/lubricant contact conditions. Zhao et al. (1997) studied the influence of contact conditions (dry, water and oil) on the wear and frictional behaviour of titanium, sliding against stainless steel, and found that the presence of the oil in the interface significantly improved the surface characteristics of the titanium and low friction and specific wear rate were exhibited. Prasad (2007) discovered the same when he investigated the sliding wear performance of a zinc-based alloy reinforced with SiC particles in dry and lubricated conditions.

In addition to the roles played by the presence of the oil in the interface in terms of clearing and polishing, it absorbed the frictional heat. Under dry contact conditions, the interface temperature reached up to 70°C in some cases for the aluminium materials. Under lubricant conditions, the counterface temperatures for all the materials under different applied loads are presented in Figure 5.5. The increase in temperature is not remarkable and can be neglected in terms of its influence on the wear behaviour of the metals.

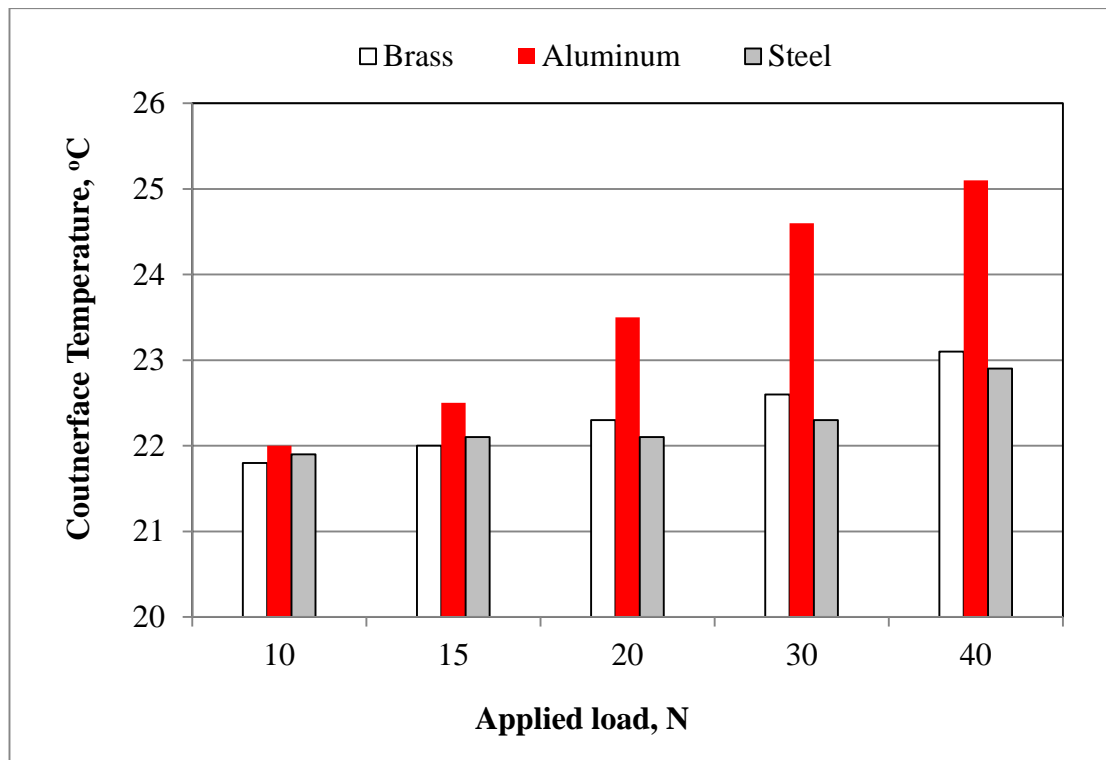


Figure 5.5: Counterface temperature against applied load using waste cooking oil as a lubricant at starting temperature of 22°C

5.2.3 Observations of Worn Surface Tested Under Waste Cooking Oil

5.2.3.1 Roughness of the Worn Surface

The roughness and the micrographs of the worn surfaces of the materials are discussed in this section. A sample of the roughness profile for the worn surfaces is presented in Figure 5.6. The average roughness of the surfaces for all the materials at

different applied loads is presented in Figure 5.7. The roughness of the aluminium surfaces is greater than the brass and the mild steel for all the applied loads, which could explain the greater specific wear rate of the aluminium compared to those of the brass and the mild steel. Further discussion will be given with the aid of the SEM observation. From Figure 5.7, the roughness of the brass reduces with the increase in the applied load which indicates that a polishing process occurred. Such polishing process results in low specific wear rates (Figure 5.2), is reported by many researchers (Hung et al. 2011; Miller 1980; Preis et al. 2012).

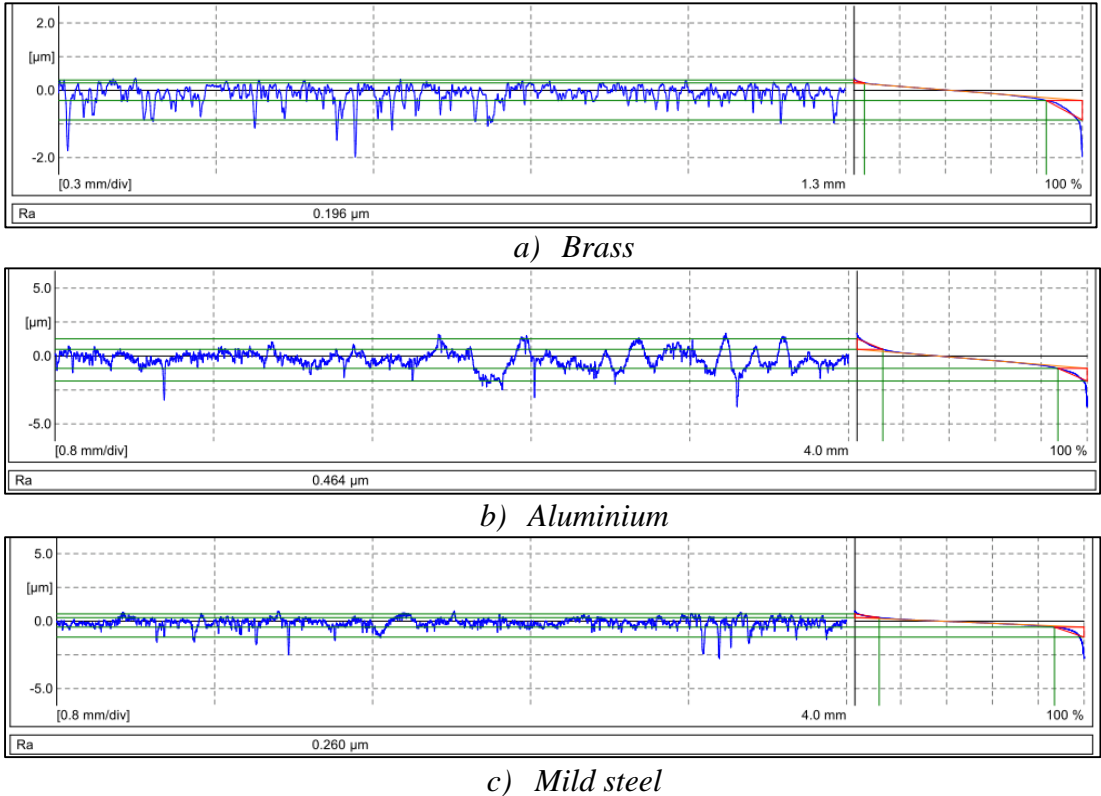


Figure 5.6: Sample of the roughness of the worn surfaces under the condition of waste cooking oil as a lubricant at a temperature of 22°C

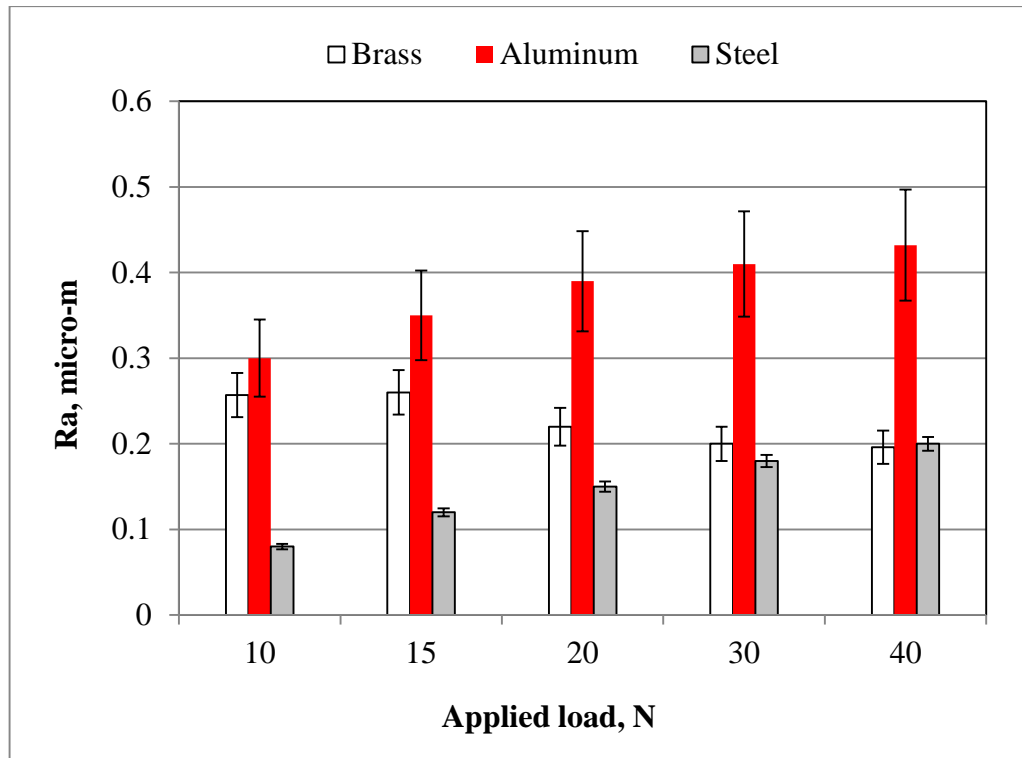


Figure 5.7: Ra of the worn surfaces at different applied loads under the condition of waste cooking oil as a lubricant at a temperature of 22°C at the applied load of 30N.

5.2.3.2 SEM Observation

The micrographs of the worn surface for the three materials are presented in Figures 5.8–5.10. Figure 5.8 shows the worn surface of the brass before the test and after the test at different applied load with the presence of the WCO at a room temperature of 20°C. At the low applied load of 10 N, Figures 5.8b and c show signs of plastic deformation (marked as Pl), abrasion nature (marked as A) and polishing process (marked as P). Since there is an abrasive nature, high material removal from the surface at the low load of 10 N is expected as presented previously in Figure 5.2.

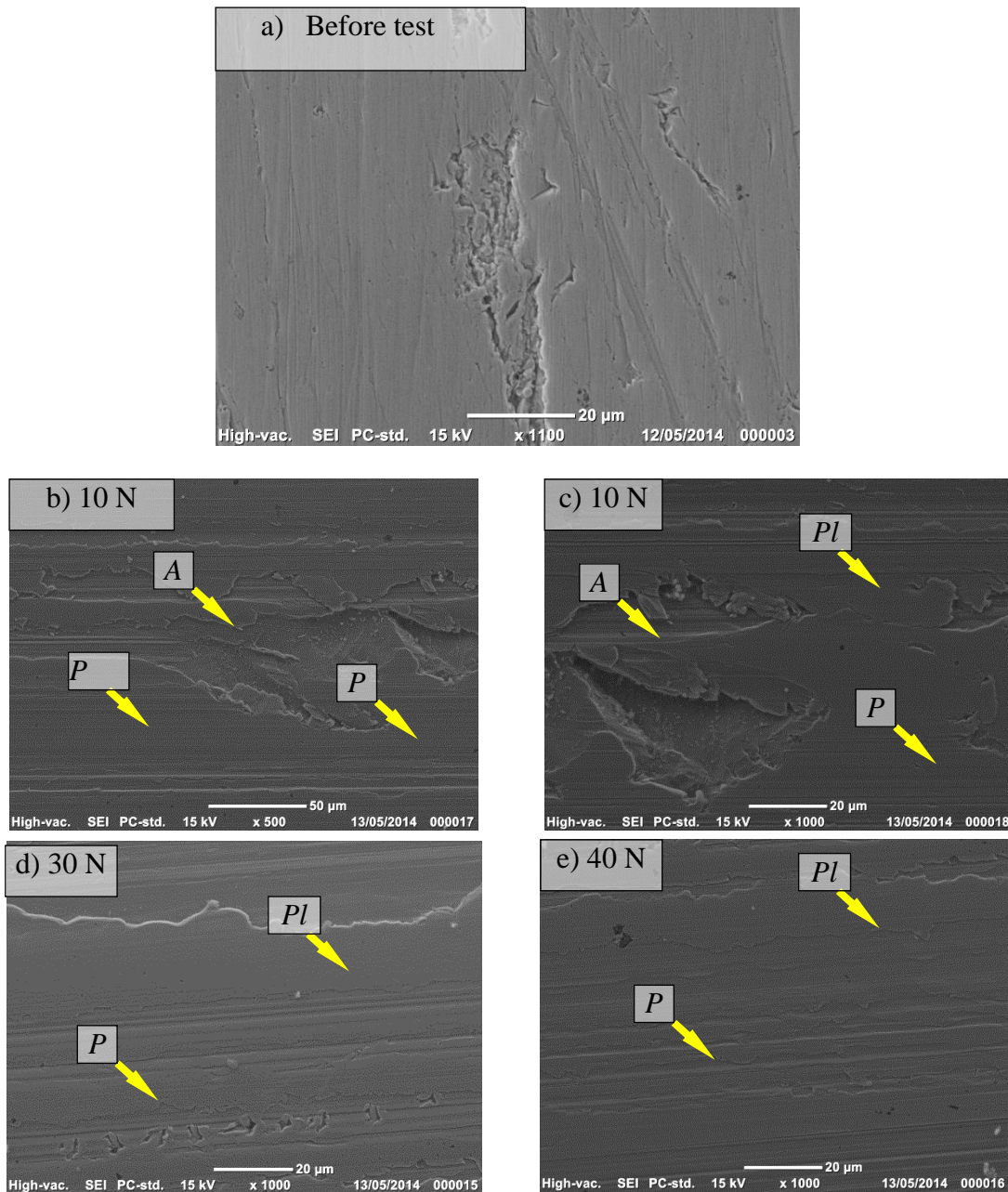


Figure 5.8: Micrographs of a) brass surface before tests b-e) the worn surface of the brass after testing at different applied loads under the condition of waste cooking oil as a lubricant at a temperature of 22°C showing: abrasive wear mechanism marked as “A”; plastic deformation marked as “P” and polishing process marked as “Pl”

There are two possibilities for the presence of the abrasion on the brass surface at low load. The low load could not plastically deform the surface of the brass, which generated weak film and may be detached (Figures 5.8b and c). The association of the low load with the presence of the WCO in the interface reduces the interaction between the asperities, leading to low friction as shown in Figure 5.4.

Figure 5.9 displays the micrographs of the worn surface of the aluminium after the test at different applied loads. At the entire applied loads, an abrasion nature can be observed, indicating high material removal from the surface, that is, a high specific wear rate (Figure 5.2). This abrasive nature and pitting-like processes could be due to

the fact that the aluminium is considered to be relatively soft compared to the stainless steel counterface. In other words, it is suggested that the tips of the counterface plough the surface of the aluminium, which in turn generates the abrasion nature and leads to high material removal. In light of this, it is confirmed that an abrasion process occurs on the aluminium surface despite the WCO presence.

For the worn surface of the mild steel material, Figure 5.10 shows the micrographs at different applied loads. One can see that a polishing process took place at all the applied loads during the rubbing process. In other words, the adhesive wear was like the steel polishing process that was confirmed in Figure 5.7 when the roughness of the worn surface slightly increased with the applied load. Such a smooth surface maintains a low specific wear rate (Figure 5.2) and low friction coefficient (Figure 5.4). Despite the fact that the friction of the mild steel was relatively high compared to those of the aluminium and the brass, the value of the friction coefficient of the mild steel was very low (below 0.05, c.f. Figure 5.4). In comparisons between the micrographs of the worn surface under dry (Figures 4.10– 4.12) and lubricant contact conditions (Figures 5.8–5.10), the severe abrasion nature on the worn surface in the dry conditions disappeared with the presence of the WCO. This is mainly due to the fact that the WCO largely cleaned the interface of the removed debris, which had acted as a third body in some cases under the dry contact conditions.

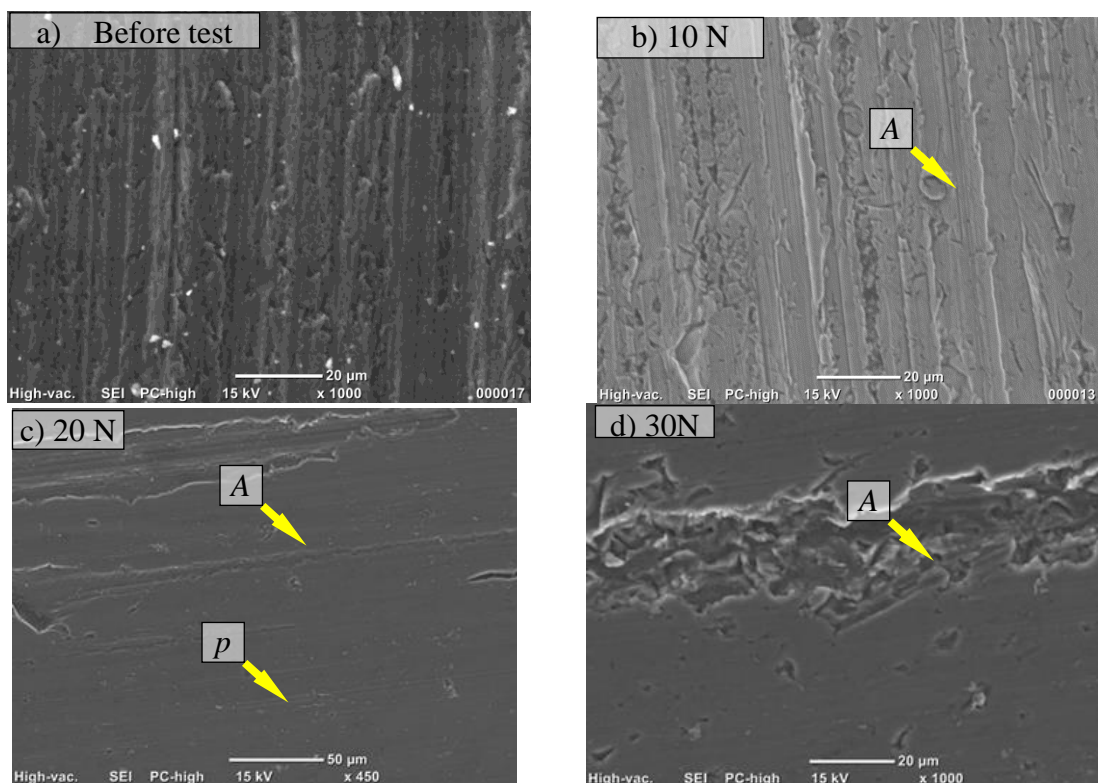


Figure 5.9: Micrographs of a) aluminium surface before tests and b-d) the worn surface of the aluminium after testing at different applied loads under the condition of waste cooking oil as a lubricant at a temperature of 22°C. 22°C showing: abrasive wear mechanism marked as “A” and polishing process marked as “P”

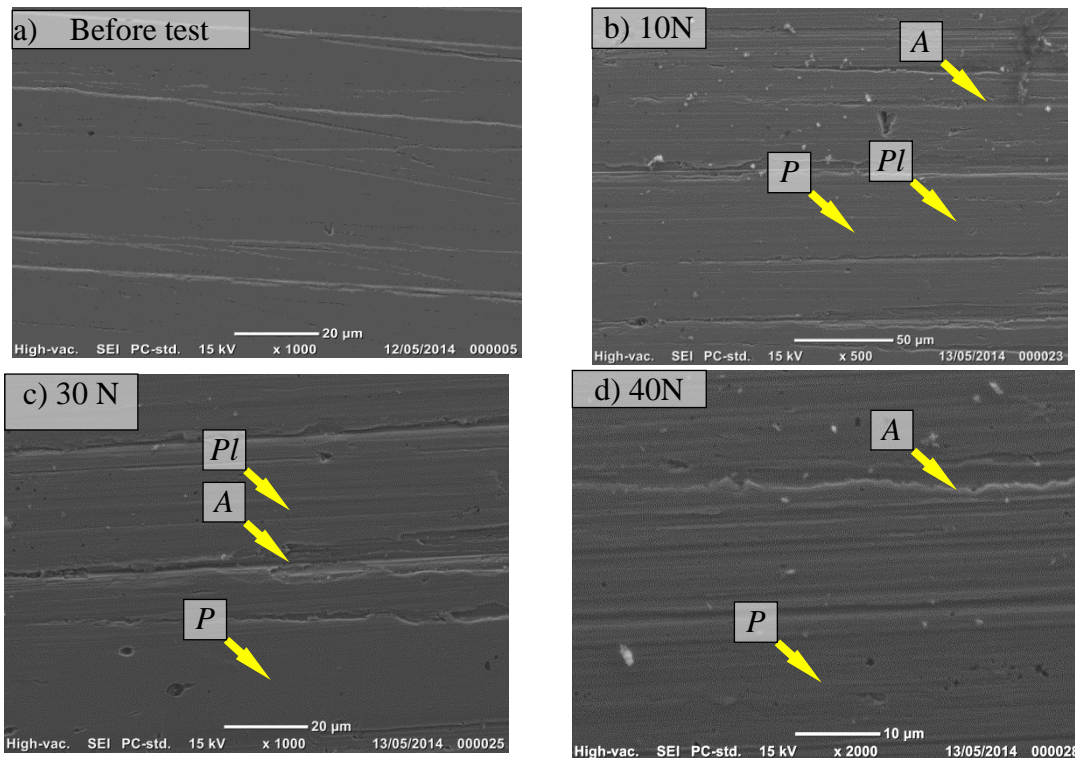


Figure 5.10: Micrographs of a) mild steel surface before tests, and b-d) the worn surface of the mild steel after testing under the applied load of 30 N under the condition of waste cooking oil as a lubricant at a temperature of 22°C showing: abrasive wear mechanism marked as “A”; plastic deformation marked as “P” and polishing process marked as “P”

Based on the micrographs and roughness profiles of the worn surfaces, the thought of the lubricant film generation in the rubbing area with the presence of the applied load is not that possible. The SEM observation showed different damage feature on all the worn surfaces of the metals which reflects the interaction between the asperities. Moreover, the roughness modifications on the metals’ surfaces indicate the interlocking and engagement of the asperities on contact. In the light of this, it can come to conclusion that the presence of complete lubricant film in the interface is not possible.

5.3 Wear and Frictional Behaviour of Metals Using Different Blends of Lubricant

In this section, the wear and frictional results collected under different blends of WCO with the fully synthetic oil are presented. It should be mentioned that 5% (wt) of EVA copolymer and 2% (wt) of EC were used as additives to enhance the viscosity for all the blends.

5.3.1 Wear Behaviour of Selected Metals using Different Blends of Lubricant

The specific wear rate of brass, aluminium and mild steel against sliding distance tested under different blends of lubricants are presented in Figure 5.11. In general, with the increase of the sliding distance there is a reduction in the specific wear rate for all the materials and blends of lubricants. This is expected for the running-in

stage and integration between the asperities at the first stage of the rubbing process. With respect to the impact of blend ratio on the wear behaviour of the metals, brass and aluminium exhibited relatively better wear behaviour when fully synthetic oil is used compared to the pure WCO. Meanwhile, mild steel experiences no remarkable influence from the blends on its wear performance.

Blending the SO with the WCO reduces the specific wear rate by $2 \cdot 10^{-12} \text{ mm}^3/\text{N.m}$ for the brass and by $4 \cdot 10^{-12} \text{ mm}^3/\text{N.m}$ for the aluminium. It seems the synthetic oil has a better influence on the wear performance of the metals compared to the waste cooking oil. With the addition of the synthetic oil (SO) to the WCO, a reduction in the specific wear rate can be seen depending on the blend ratio. With the increase of the amount of SO, an increase in the reduction of the specific wear rate can be seen. The main difference in the blends that may impact on the interface their viscosity at room temperature (about 22°C). From the data presented in Figures 3.12 and 3.13, it can be seen that the viscosity of the WCO is less than that of the synthetics and the blends.

From Figures 3.12 and 3.13, one can see that the synthetic oil has the highest viscosity value compared to the WCO blends. At the operating temperature (about 22°C), Figure 3.12a showed that the viscosity of the 100% synthetic oil was about 320 cSt, while the 100% WCO was about 120 cSt. Such a drop in the viscosity significantly impacts on the wear results. When there is relatively high viscosity oil present in the interface, the ability to separate the two rubbed bodies is greater than when less viscous oil used in the interface.

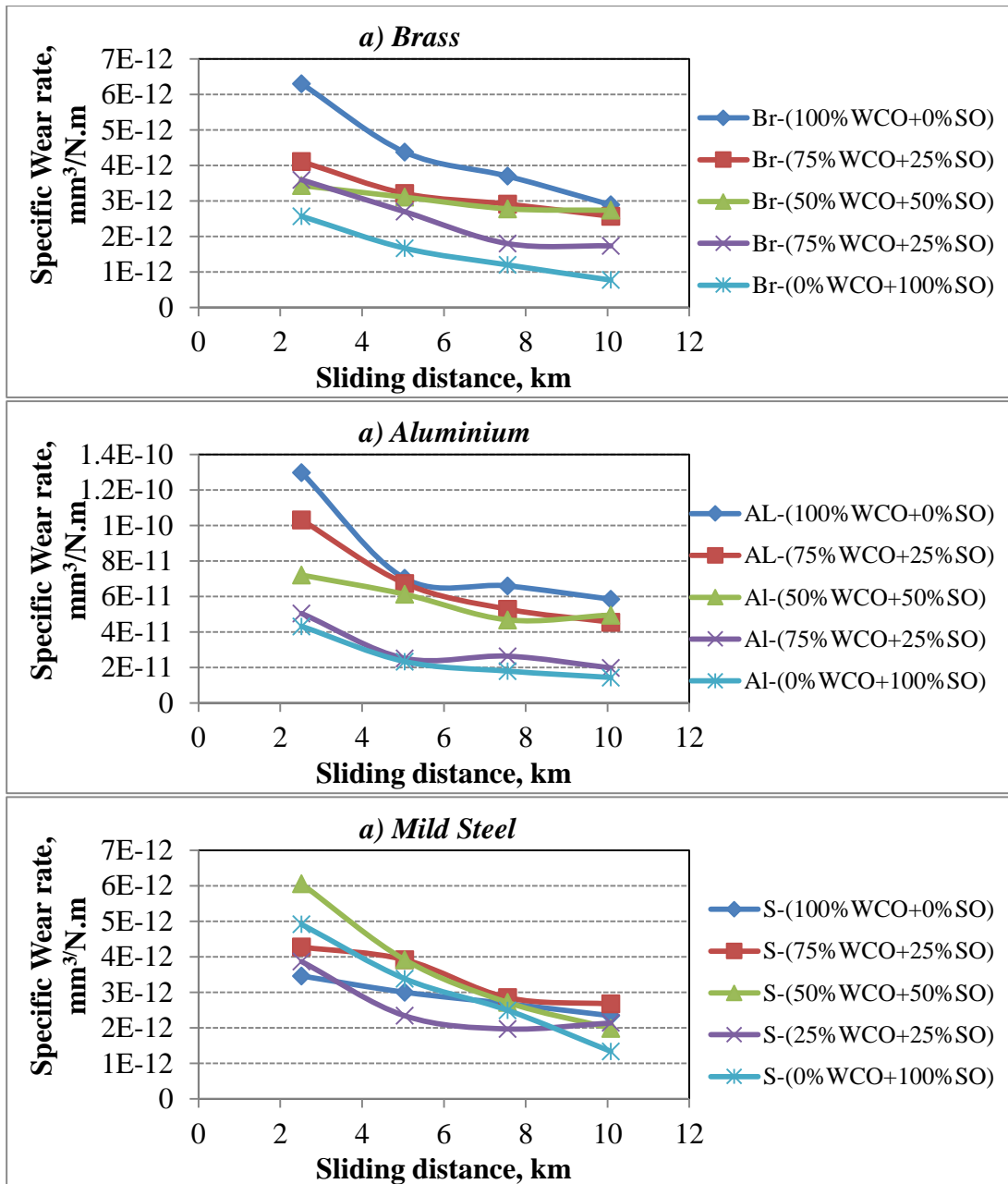


Figure 5.11: Specific wear rate vs. sliding distance of different materials tested under 40 N applied load using different blends of lubricant

In lubricant science, viscosity can be defined as the fluid's ability to resist motion. Furthermore, ASTM International stated that a higher viscosity fluid will typically make a thicker film between the moving surfaces and support greater loads, (*Fuels and Lubricants Handbook* ; Gohar & Safa 2010; Spikes & Olver 2002). The film thickness has a proportional relation with the oil viscosity and speed. However, increase the applied load reduces the film thickness. In other words, the high viscosity of lubricant in the interface helps to separate the two rubbed parts or at least reduce the contact between the asperities. However, with low viscosity, there is less resistance to the shear of the oil, and the contact between the asperities is more integrated than that expected with the high-viscosity lubricant. Ciantar et al. (1999) reported that the viscosity of the lubricant combination was seen to play a major role, that is, low-viscosity oils resulted in severe wear, material transfer and friction. In

addition, it was recently reported that wear decreases with higher viscosity of the oil when the steel rubbed against steel contact (Velkavrh & Kalin 2012). In another work, aluminium was tested against steel with the presence of Jatropa Blended Lube Oil (Imran et al. 2013), showing that blending the Jatropa oil with SAE 40 by more than 10% exhibited relatively deeper scars on the surface of the aluminium due to the fact that Jatropa has a lower viscosity than the selected SAE 40 lubricant. In light of the above, it can be summarised that a reduction in viscosity increases the material removal for all the materials. Figure 5.12 displays the specific wear rate of all the materials under different blends of lubricant after 10.8 km sliding distance.

For further exploration, the specific wear rate of the materials is plotted against the viscosity of the lubricants in Figure 5.13. Despite the fact that some of the points do not fit with the fitted line of the data, a good correlation can be seen in the values of the error mean square (R^2). This can clearly be seen with the brass materials since $R^2=0.9656$. In other words, with the presence of a high-viscosity lubricant in the interface, there is a relatively low wear rate. Figure 5.14 displays the expected wear mechanism in three cases: a) dry contact conditions, b) high-viscosity-lubricant in the interface and c) low viscosity-lubricant in the interface. In the case of dry contact conditions, it is expected that a high interaction between the asperities in contact will be shown.

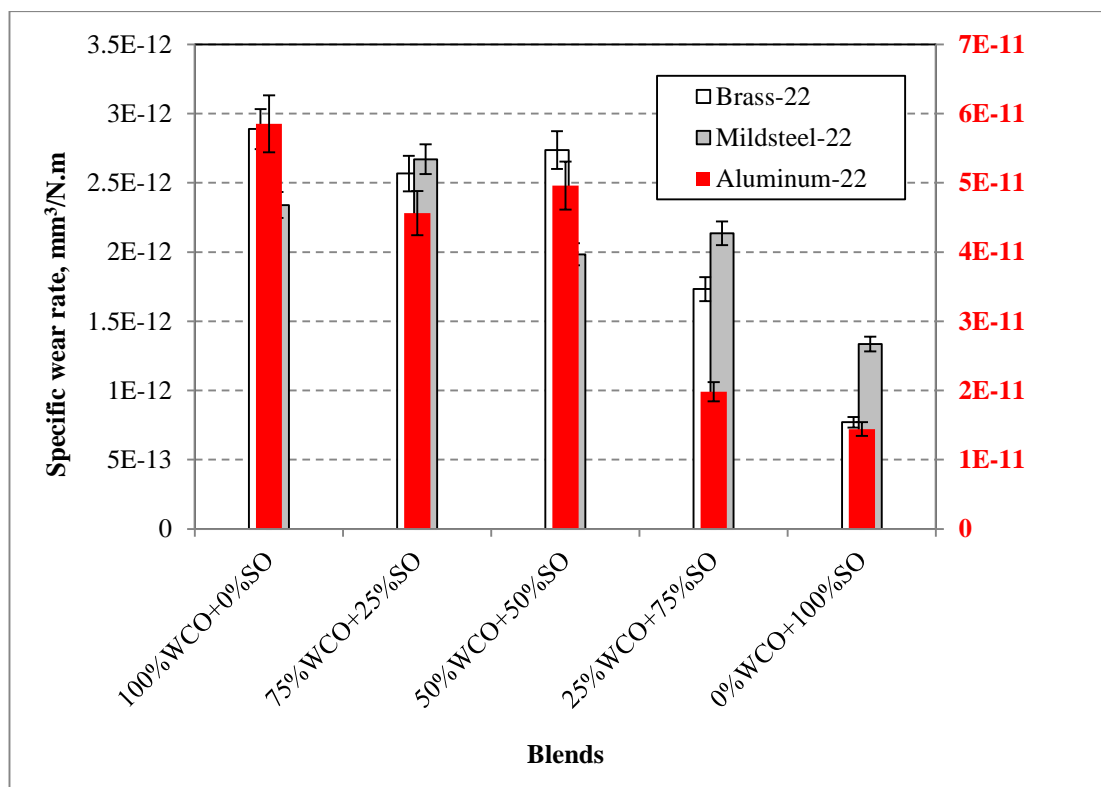


Figure 5.12: Specific wear rate of different materials tested under 40 N applied load using different blends of lubricant after 10.8 km sliding distance * the left Y-Axis is the scale for the aluminium specific wear rate.

With the presence of the shear stress (frictional force) in the interface under the dry contact conditions, significant removal of material can be expected (as seen in the wear results under the dry contact conditions, Figure 5.1). Conversely, it is suggested that the presence of the high-viscosity lubricant in the interface will separate the rubbed parts (Figure 5.14b), which results in a reduction in the interaction between

the surfaces and less removal of material is expected. Further to this, the shear force is carried by the lubricant rather than transferred to the tips of the materials. Under this condition, it is expected to gain low friction as well, which will be elaborated in the next section. The intermediate condition is when a low-viscosity lubricant is present in the interface (Figure 5.14c). In this condition, there was intermediate separation to the two rubbed surfaces, but there was still an interlocking mechanism in the interface, which could be removed with the rubbing process (i.e. described as a polishing process). Micrographs and roughness of the worn surfaces may assist in further understanding this phenomenon and these are presented in the next section.

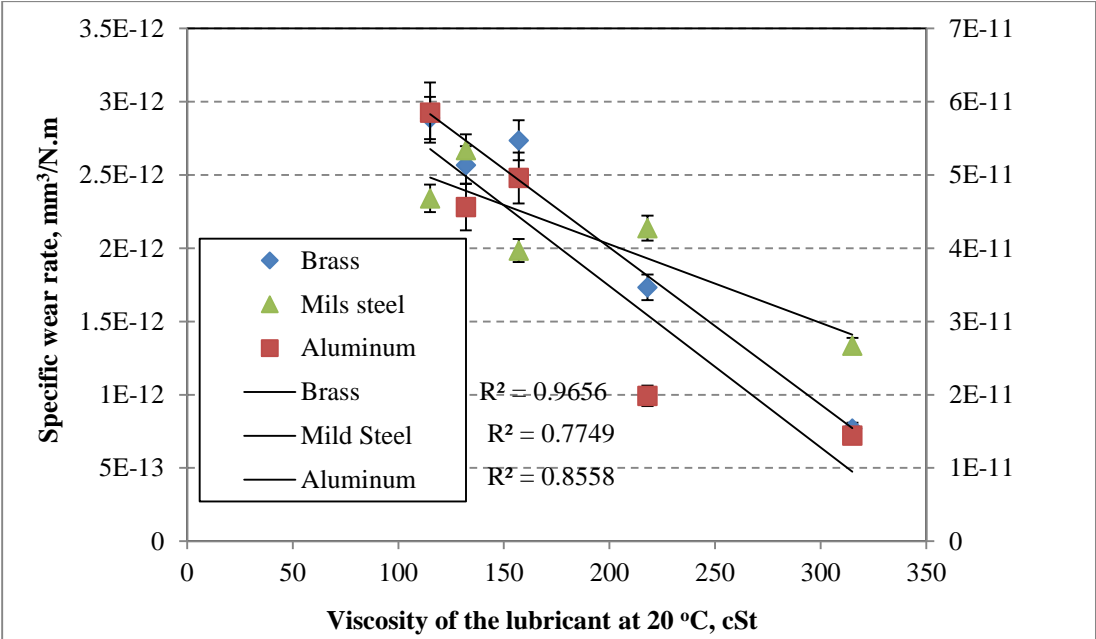


Figure 5.13: Correlation between the specific wear rate and the lubricant viscosity for all the materials after 10.8 km sliding distance

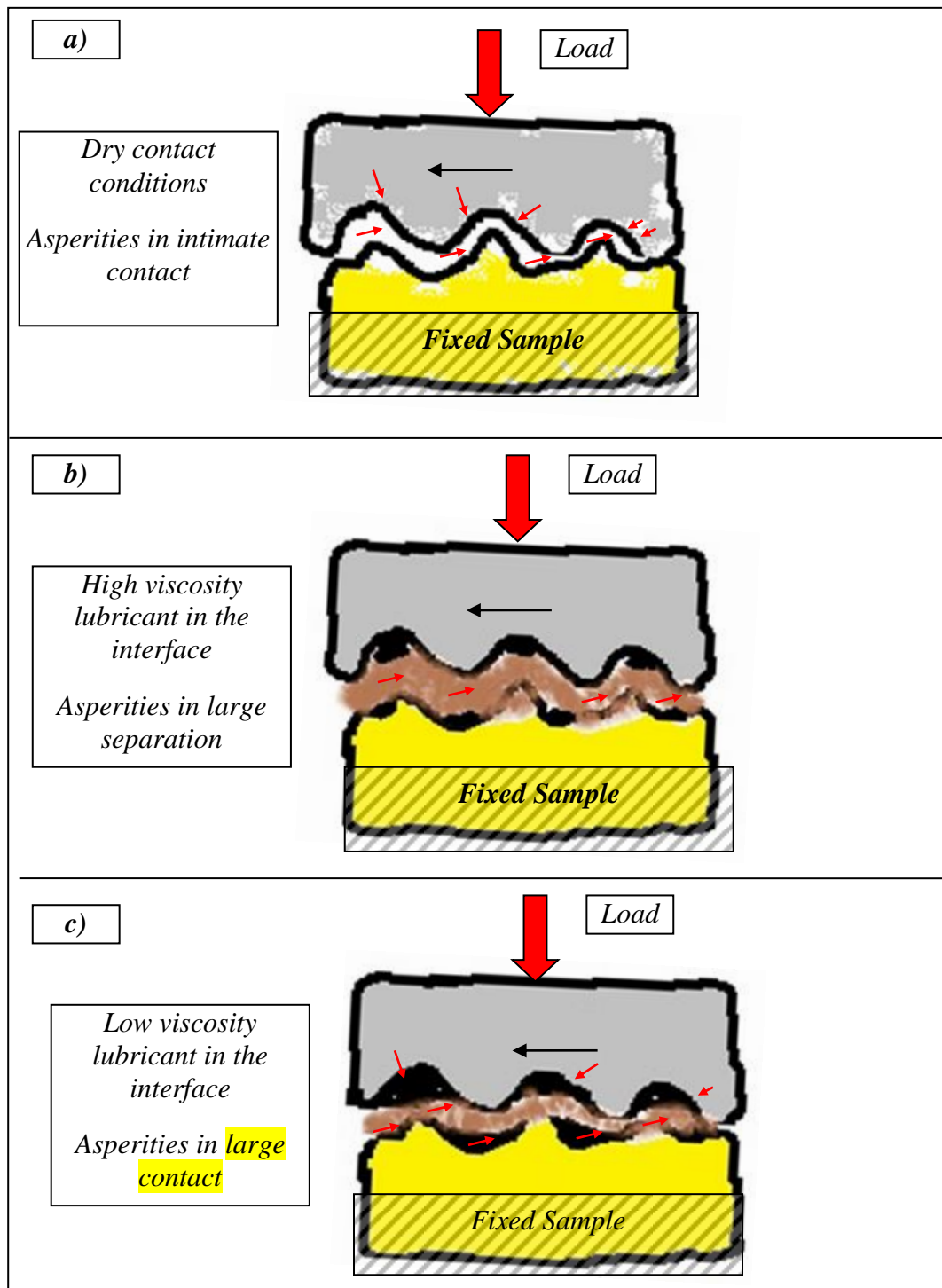


Figure 5.14: Schematic drawing showing the differences in contact mechanisms

5.3.2 Frictional Wear Behaviour

The friction coefficient vs. sliding distance for all the materials under different blends of lubricant is presented in Figure 5.15. In general, one can see that there is a fluctuation in the friction coefficient, which can be ignored since the value above and below the mean is about 0.002. Thus, one can say that there are not many differences in terms of values for the friction coefficient for all the blends and the materials. The minor differences in the value of the friction coefficient can be due to the viscosity of the blends, the lubricant behaviour in the interface, and the interaction between the

asperities during the sliding. Obviously, the blend of the 100% WCO generated relatively high friction compared to others especially for the aluminium and the mild steel materials. Fully synthetic oil showed the lowest friction coefficient compared to others, which could be expected since its viscosity is greater. McQueen et al. (2005) reported that friction is more sensitive to film formation ability, while Velkavrh, Kalin and Vižintin (2009) reported that high rotational velocity tends to reduce the friction between steel/steel contact regions. For the current study, the influence of the viscosity associated with the modification occurred on the rubbed surfaces during the rubbing process influence the friction. It is suggested that the presence of the lubricant in the interface washes the rubbed surface (cleaning the debris) and separates the rubbed parts (Figure 5.14b and c).

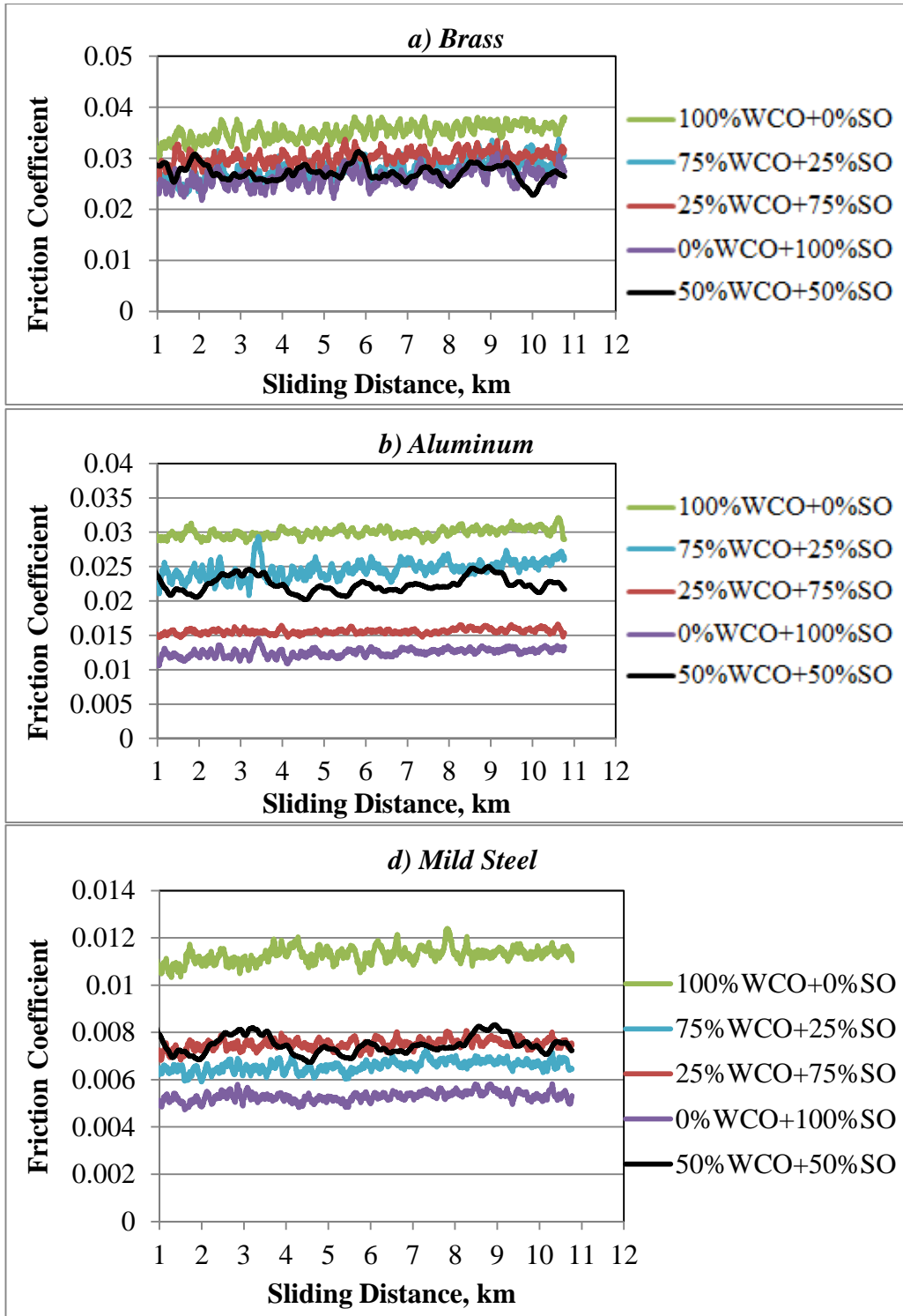


Figure 5.15 Friction coefficient vs. sliding distance of different materials tested at 40 N applied load using different blends of lubricant

5.3.3 Surface Observations

In this section, the roughness of the worn surface with the micrographs will be discussed. Figure 5.16 shows the roughness of the worn surface for different materials after testing under different blends of lubricant. In general, there is no remarkable influence of the type of blend on the roughness of the materials. The aluminium worn surface exhibited greater roughness compared to the mild steel and the brass. This may be because its surface provided less resistance during the rubbing process as indicated in Figure 5.12, showing that aluminium has a relatively high material removal rate compared to the brass and the mild steel.

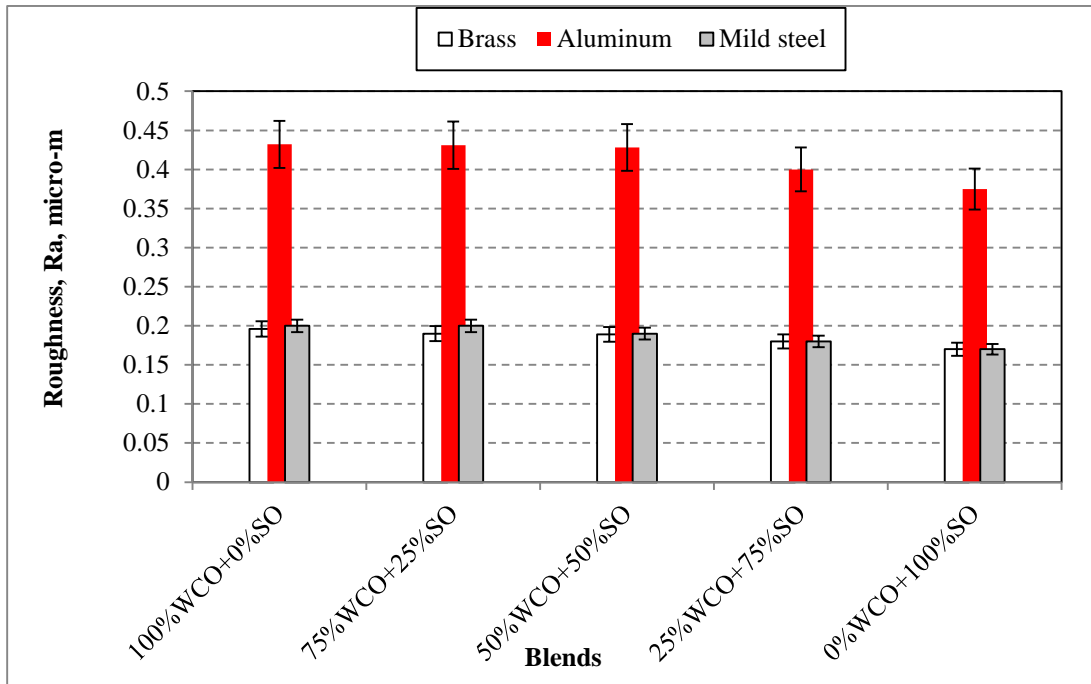


Figure 5.16: Ra of the worn surfaces at different blends at 40 N applied load after 10.8 km

In Figure 5.15 aluminium materials introduce a relatively higher friction coefficient compared to the brass and the mild steel when 100 %WCO and 100% SO oils were used, which is due to the greater roughness of the surface during the rubbing. This obstructs the movement and causes high resistance and removal of materials from the surface. This may be explained further with micrographs of the worn surface.

Commonly, the wear and frictional data have been interpreted and discussed with the aid of the viscosity modification due to the additives and/or environmental temperature, (Borugadda & Goud 2014; Delgado, García-Rico & Franco 2014; Quinchia et al. 2014; Shahabuddin, Masjuki & Kalam 2013; Shahabuddin et al. 2013; Sharma & Dalai 2013; Syahrullail, Kamitani & Shakirin 2013). On the other hand, recent work by Tang and Li (2014) comprehensively covered the topic of the roles of additives on lubricant performances addressing three models on the role of additives as:

- 1 Friction modifiers physically or chemically adsorbed on rubbing metal surfaces to form monolayers (Beltzer & Jahanmir 1988),
- 2 Thick film action model, where friction modifiers formed viscous films (Anghel, Bovington & Spikes 1999),

- 3 Lack of adhesion of the liquid with the adsorbed monolayer might lead to liquid slip (Choo, Forrest & Spikes 2007).

Since there is still debate about on those models and there is no standard testing to confirm, the current results are discussed according to the viscosity changes, micrographs of the worn surfaces, and roughness modifications on the selected metals. Future study is recommended to study those models for the waste cooking oil performance.

Also, the synthetic oil may have chemisorbed and EP additives. Such additives greatly impact on the ability of establishing the good adhered film on the rubbed surfaces. This significantly reduces the interaction between the two rubbed surfaces and results in low specific wear rate and the friction coefficient. Further comprehensively study to cover this area is recommended

Figure 5.17 displays the micrographs of the worn surface of the aluminium tested under different blends of lubricants. One can see that there is a clear trend of roughness increase in the surface with the WCO in the interface compared to the fully synthetic oil. Nevertheless, an abrasion nature can be seen with all the lubricants used, which indicates that the aluminium has poor resistance to the wear against stainless steel under the lubricant conditions. This explains the poor wear behaviour of the aluminium compared to the brass and mild steel given in Figure 5.12.

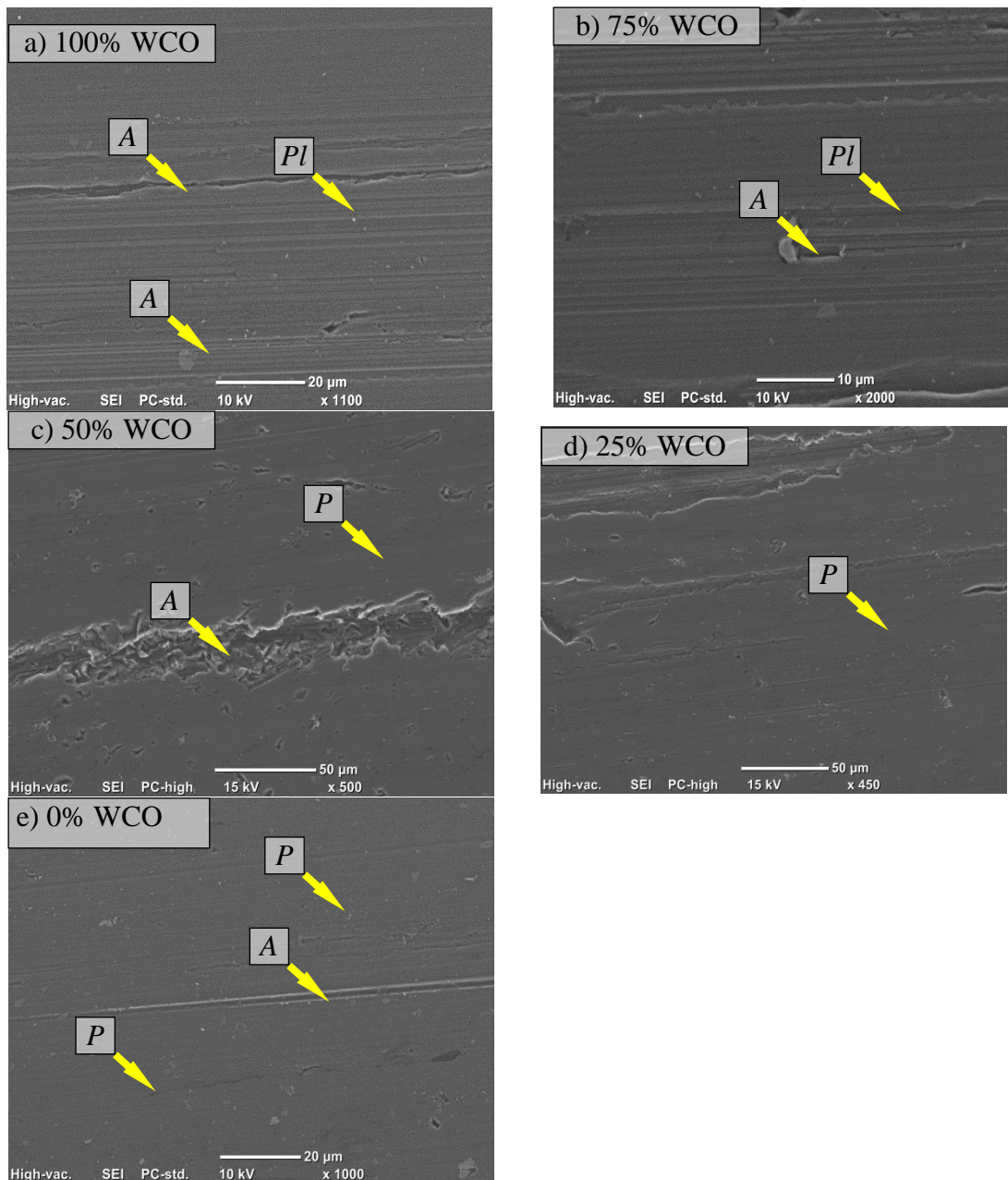


Figure 5.17: Micrographs of worn surface of aluminium after testing using different lubricants at 40 N applied load after 10.8 km sliding distance showing: abrasive wear mechanism marked as “A”; plastic deformation marked as “Pl” and polishing process marked as “P”

For the brass worn surface, Figure 5.18 displays the micrographs of the surfaces after the test under different blends of lubricant. There appears to be no remarkable influence of the blends on the wear mechanism despite some abrasion nature that can be seen when pure WCO used and 50% blends. However, during the SEM observation, such features were not common on the surface. The wear mechanism is purely adhesive wear and polishing. This assisted in reducing the material removal, which in turn resulted in good wear performance of the brass compared to the aluminium (Figure 5.14). Furthermore, such a smooth surface with the presence of the lubricant in the interface exhibited a low friction coefficient (Figure 5.15a).

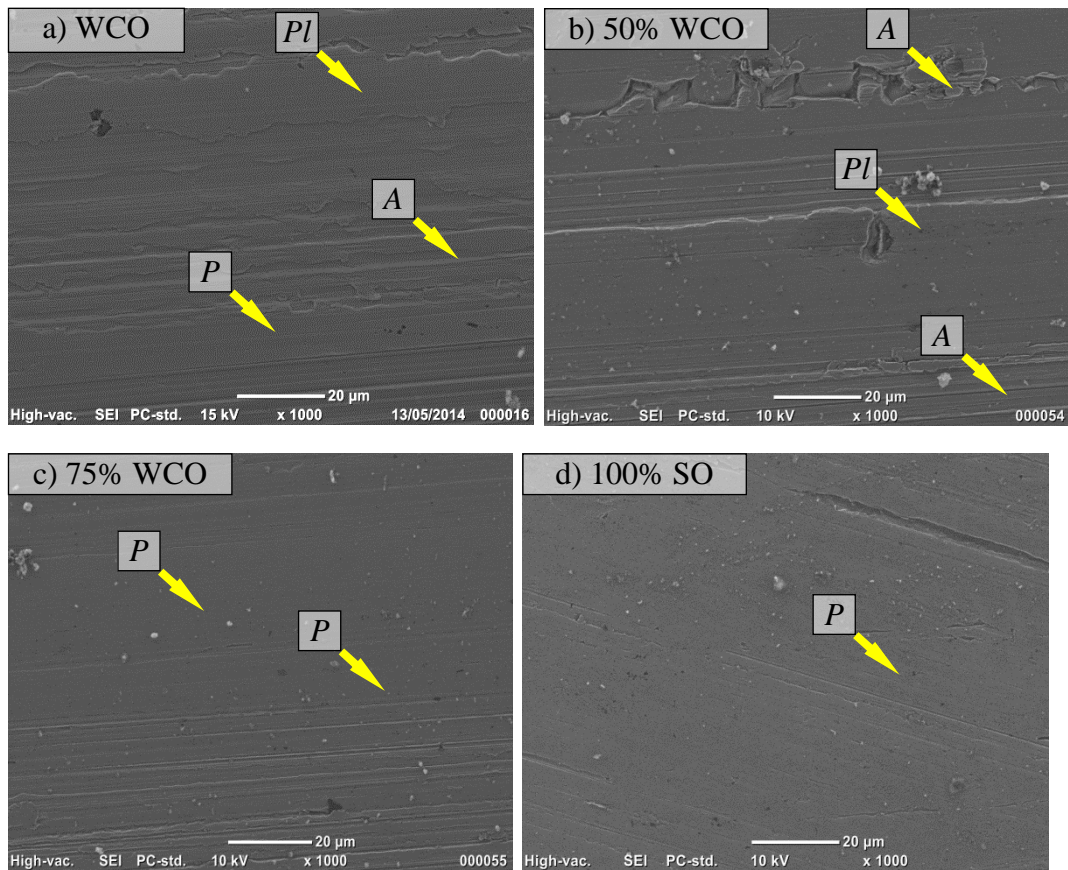


Figure 5.18: Micrographs of worn surface of brass after testing using different lubricants at 40 N applied load after 10.8 km sliding distance showing: abrasive wear mechanism marked as “A”; plastic deformation marked as “P” and polishing process marked as “P”

For the mild steel worn surface, the micrographs are presented in Figure 5.19 after the experiments under different blends of lubricant. There is clear abrasion nature for almost all the blends used especially with the less synthetic oil. This is mainly due to less viscosity of the blends with the less synthetic oil. Moreover, a mild steel surface is considered to be stronger than other materials (aluminium and brass) which make it difficult to deform the tips of the mild steel surface. The stainless steel counterface scratches the mild steel surface which results in such an abrasion nature. However, the wear results showed that mild steel exhibited good wear resistance compared to the aluminium because it is harder than the aluminium, which results in high material removal resistance (Figure 5.12). The high resistance in the interface of the mild steel associated with relatively high friction (especially with the 100%WCO, Figure 5.15) could be explained by the abrasive wear mechanism in the case of the mild steel.

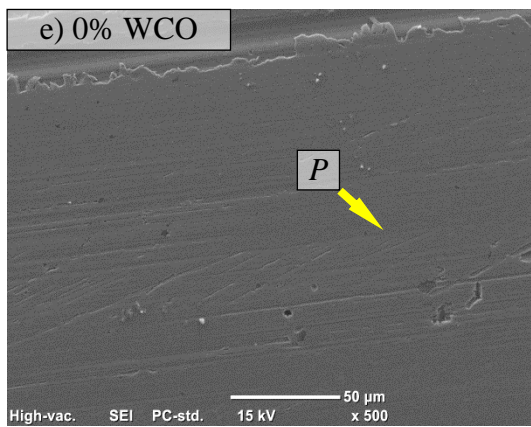
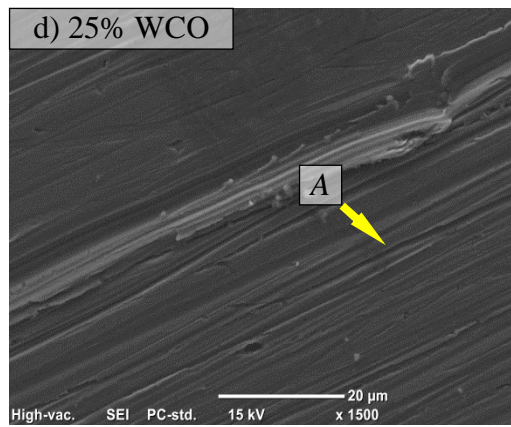
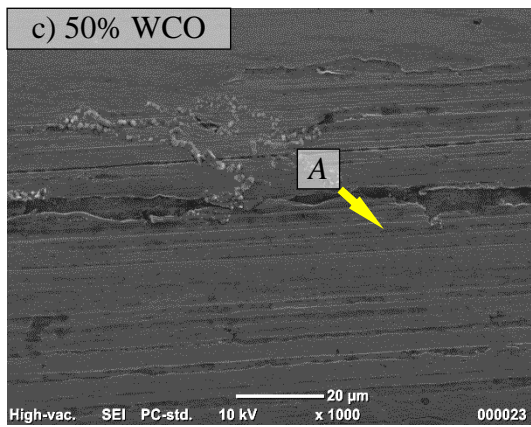
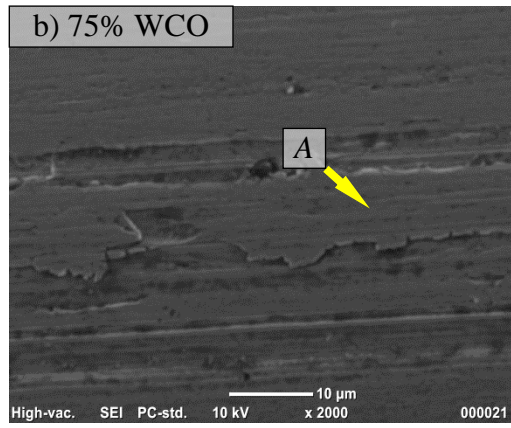
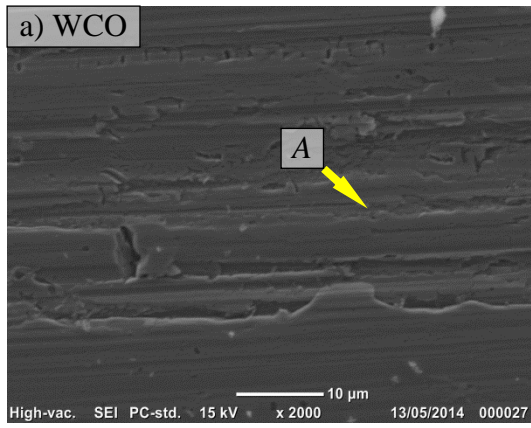


Figure 5.19: Micrographs of worn surface of mild steel after testing using different lubricants at 40 N applied load after 10.8 km sliding distance showing: abrasive wear mechanism marked as "A"; and polishing process marked as "P"

5.4 Influence of the Lubricant Temperature on the Wear and Friction Behaviour of the Metals

In this section, the specific wear rate, frictional coefficient, micrographs of the worn surfaces, roughness of the worn surface and debris morphology are presented when the experiments were performed under different lubricant temperatures. It should be mentioned here that these tests were conducted with a sliding distance of 10.8 km only under the applied load of 40 N, which can be considered to be a steady state.

5.4.1 Wear Behaviour

The influence of the different lubricant temperatures on the specific wear rate of the brass, aluminium and mild steel are presented in Figure 5.20 considering three different temperatures: 22°C (room temperature), 40°C and 80°C. In general, one can see that the increase in the lubricant temperature increased the specific wear rate for all the materials. The main reason for the increase in the specific wear rate with the increase of the temperature is the reduction in the viscosity of the lubricant with the temperature increase (see Figure 3.13). The presence of the low-viscosity lubricant in the interface may help to clean the interface area but not separate the rubbed bodies completely, as seen in Figure 5.14. Ciantar et al. (1999) reported that low-viscosity oils resulted in severe wear since there is material transfer between the asperities and worn materials increase. This has also been concluded by Velkavrh and Kalin (2012) and Imran et al. (2013) when the tests were conducted at different lubricant viscosity. The current study highlights that the temperature of the same lubricant impacts the wear performance. In addition to the viscosity modification due to the environmental temperature leading to an increase in the interaction between the asperities, the low viscosity of the oil helps to clean the interface from the worn debris. This could have advantages or disadvantages since washing out the debris will prevent the presence of the third body reported in Figure 4.13. Conversely, the washing out of the debris from the interface prevents film formation (plastic deformation on the rubbed surface), which in turn increases the removal of the material and decreases the stability of the surface characteristics. In other words, there are two occurrences that may assist in understanding the increase of the specific wear rate with the increase of the environmental temperature (reducing the viscosity): the continuation of modifications on the rubbed surfaces and the low separation of the two rubbed bodies. Observations of the SEM and the roughness of the worn surface will assist further and is discussed in the next sections.

Figure 5.21 displays the percentage increments in the specific wear rate due to an increase in the environmental temperature. It seems that the material most sensitive to the changes in the lubricant temperature is the aluminium compared to the brass and the mild steel. However, from Figure 4.4, the specific wear rate of the aluminium was much higher than the $14 \cdot 10^{-5} \text{ mm}^3/\text{N.m}$ under dry contact conditions, i.e. the presence of any type of the oil at high temperature of 80°C reduces the specific wear rate by more than four times. Under dry contact conditions, the high heat in the interface associated with the third body (Figure 4.14) significantly damaged the surface of the aluminium. Despite the environmental temperature being at 80°C, the specific wear rate is much lower than in the dry contact conditions. It can be said that

the presence of the oil in the interface significantly reduces the specific wear rate due to the reduction in the interaction between the asperities and cleaning the rubbing area rather than cooling the interface only.

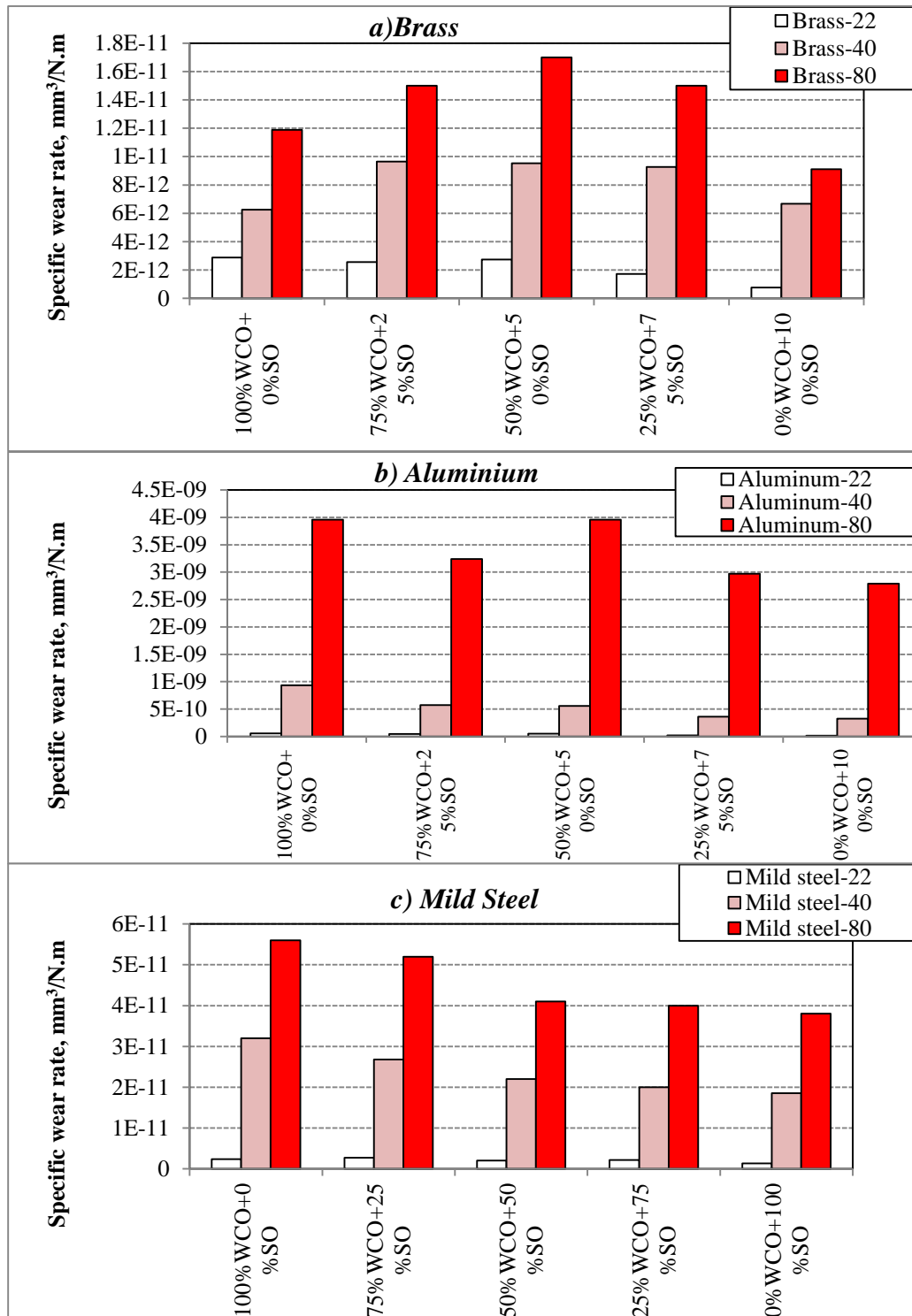


Figure 5.20: Specific wear rate of different materials after 10.8 km sliding distance using different lubricants under different environmental temperatures

Figure 5.21 shows that the mild steel and the brass materials seem to be less sensitive to the changes in viscosity of the lubricant due to the changes in the temperature. This could be due to the greater hardness of those materials compared to the aluminium. Although there is low a possibility of separation between the asperities, with the usage of the low viscosity of lubricant, the mild steel and the brass had higher resistance to material removal compared to the aluminium. However, mild steel exhibited slightly higher material removal compared to the brass especially at higher lubricant temperatures, which could be due to the differences in the interaction between the asperities in contact. Since the mild steel has greater strength and hardness, there is high shear in the interface which may lead to an aggressive rubbing process, i.e. high material removal. For the brass, the intermediate properties compared to aluminium and mild steel may mean the contacted asperities have the ability to adapt to each other and the polishing process may have taken place during the rubbing process. Micrographs of the worn surfaces, roughness, and debris micrographs may aid further understanding of this issue.

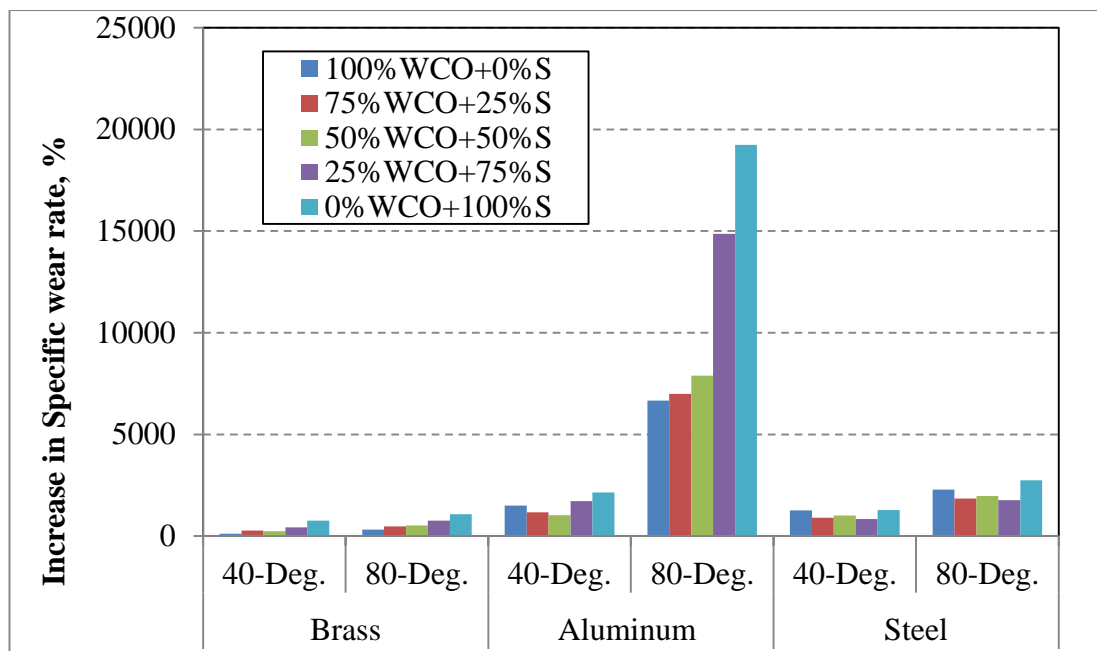


Figure 5.21: Increment percentage in the specific wear rate of different materials after 10.8 km sliding distance using different lubricants under different environmental temperatures compared to the room temperature condition

5.4.2 Frictional Behaviour

Samples of the friction coefficient against sliding distances for the materials tested at different lubricant temperature with a blend of 50% WCO + 50% SO are introduced in Figure 5.22. At the steady state after about 4 km sliding distance, there is a dramatic increase in the friction coefficient of all the materials when the lubricant temperature increases representing the high interaction between the asperities.

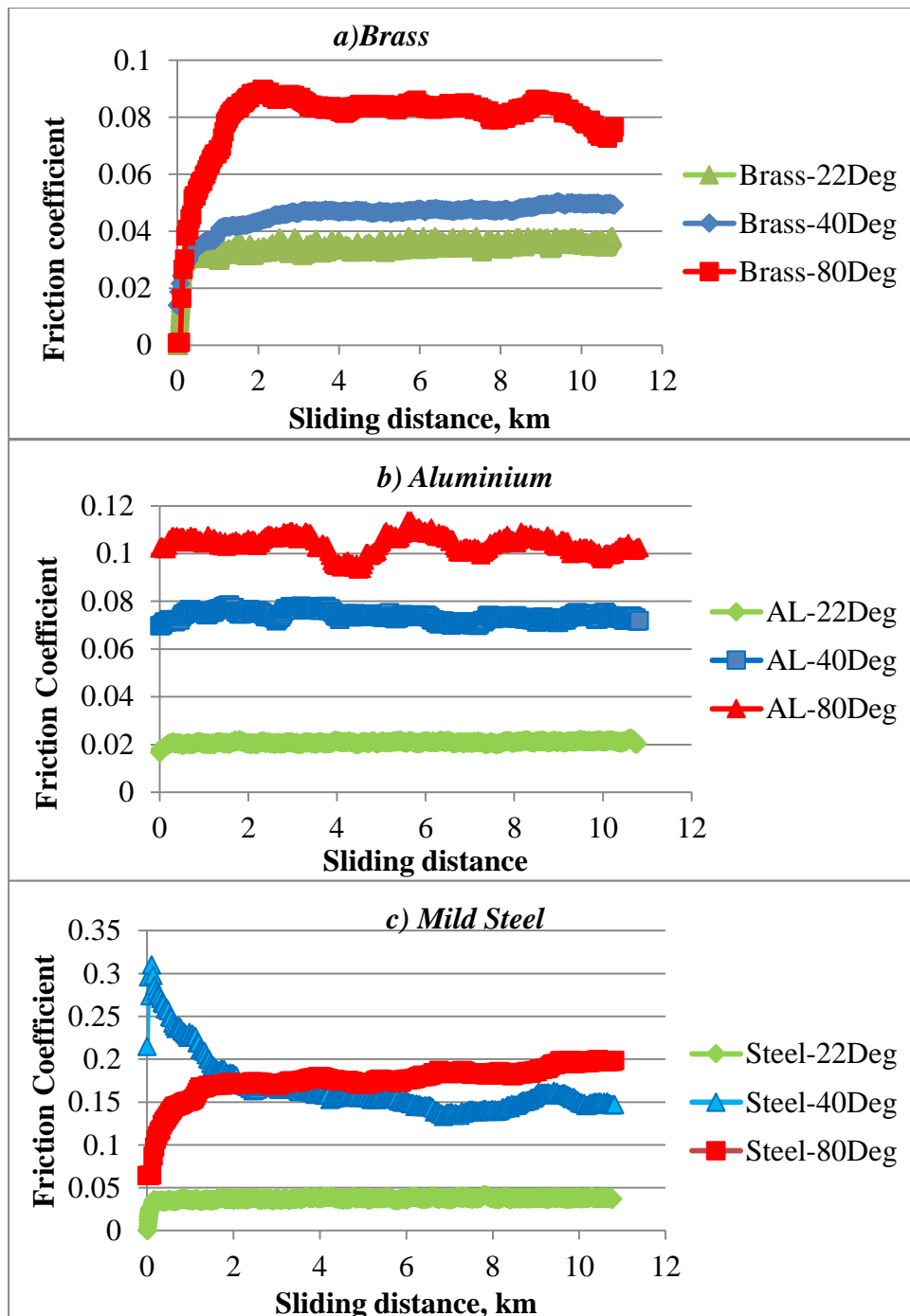


Figure 5.22: Friction coefficient vs. sliding distance of different materials tested under 40 N applied load using lubricant (50%WCO + 50%SO) under different temperatures

The mean friction coefficients of brass, aluminium and mild steel under different lubricant conditions and temperatures are presented in Figure 5.23. One can see that the increase in the temperature increased the friction coefficients for all the materials with all the types of blends. The maximum friction coefficient can be seen with high temperature and the usage of the pure WCO. This is mainly due to the fact that the lowest viscosity of all the blends used is the pure WCO at the high temperature. The highest friction coefficient can be seen when the mild steel was rubbed with the presence of the WCO at a temperature of 80°C.

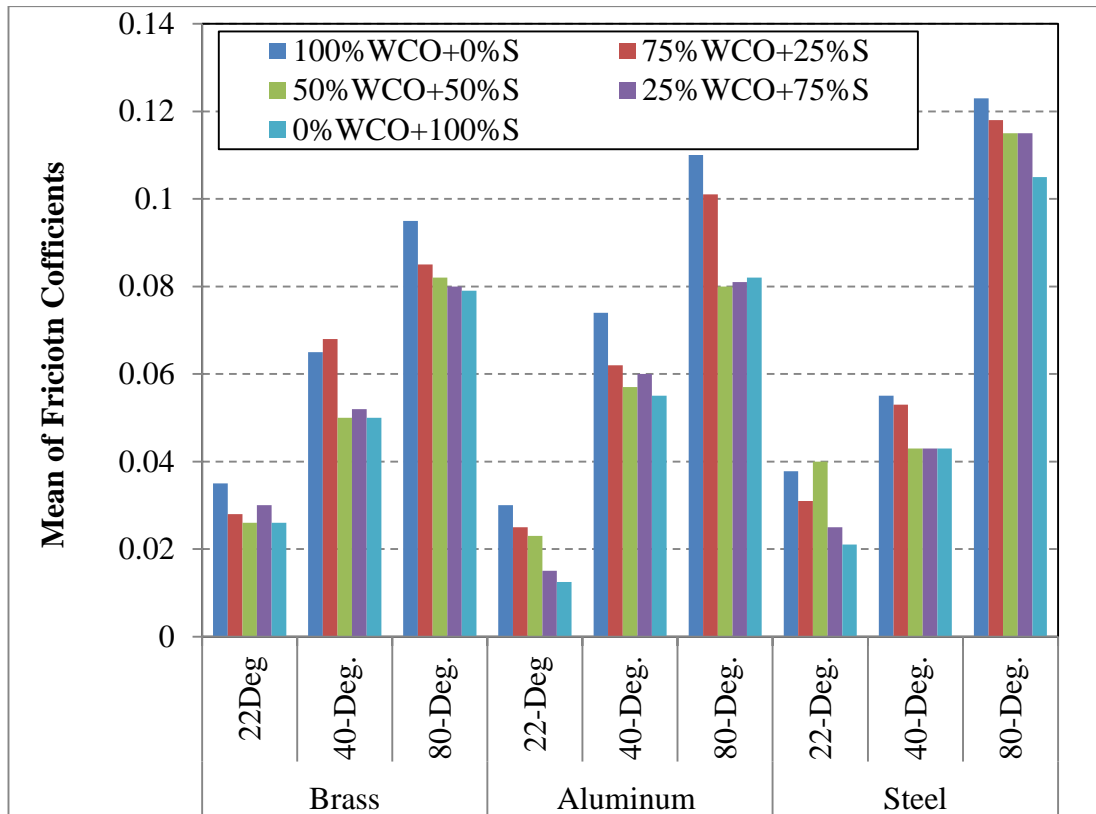
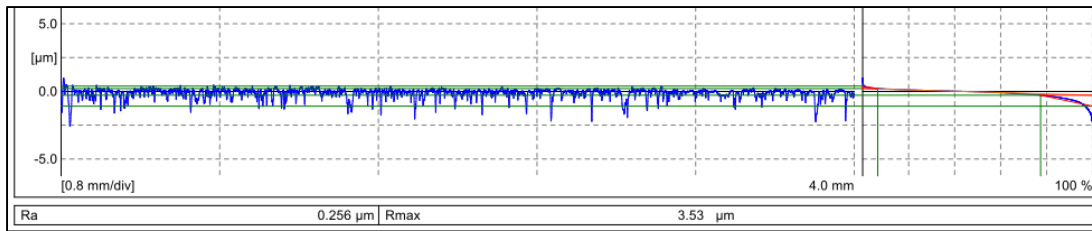


Figure 5.23: Mean values of friction coefficients for all the materials tested under different lubricants and different environmental temperatures

It should be mentioned here that the friction coefficients of aluminium, brass and mild steel were in the ranges of 0.1–0.2, 0.2–0.4 and 0.3–0.35, respectively. Despite the low viscosity of the lubricant at high temperature, there is a comparable reduction in the friction coefficients compared to dry contact conditions. It is known that the presence of the oil in the interface washes the interface and reduces the interaction between the asperities, which in turn reduces the friction coefficient compared to dry conditions. However, the low viscosity of the oil may assist in cleaning the interface but not completely prevent the interaction between the asperities. Therefore, one can say that the reduction in the friction coefficient when the lubricant is introduced is due to the washing the debris and slightly preventing the interaction between the rubbed surfaces (i.e. mixed lubrication region). Similar findings have been reported when sunflower, soybean and castor oils, blended with 4% (w/w) of EVA and 1% (w/w) were tested recently by (Quinchia et al. 2014). The increase in the temperature of (especially) the soybean oil reduced the viscosity, which in turn increased the wear and friction of the steel/steel contact. Velkavrh and Kalin (2012) suggested the same regarding the influence of the lubricant viscosity on the friction coefficient of diamond-like carbon coatings and steel.

5.4.3 Surface Observation

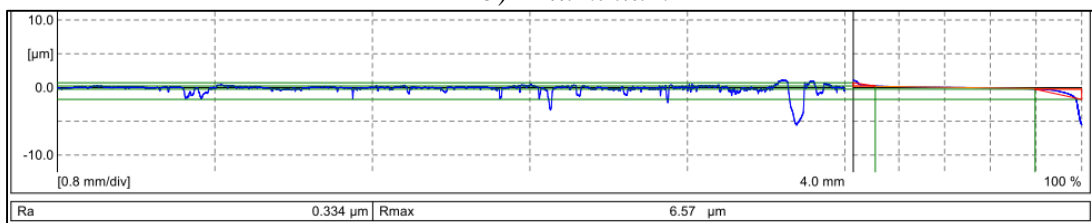
This section covers the roughness of the worn surfaces, micrographs of the worn surfaces and the debris analysis. Samples of the roughness of the metals are given in Figures 5.24 and 5.25 for the worn surfaces of the selected metals under the conditions of 50% WCO and 50% SO as lubricant at elevated temperatures of 40 °C and 80°C.



a) Brass



b) Aluminium



c) Mild steel

Figure 5.24: Sample of the roughness of the worn surfaces under the condition of 50% waste cooking oil and 50% synthetic oil as a lubricant at elevated temperature of 40°C

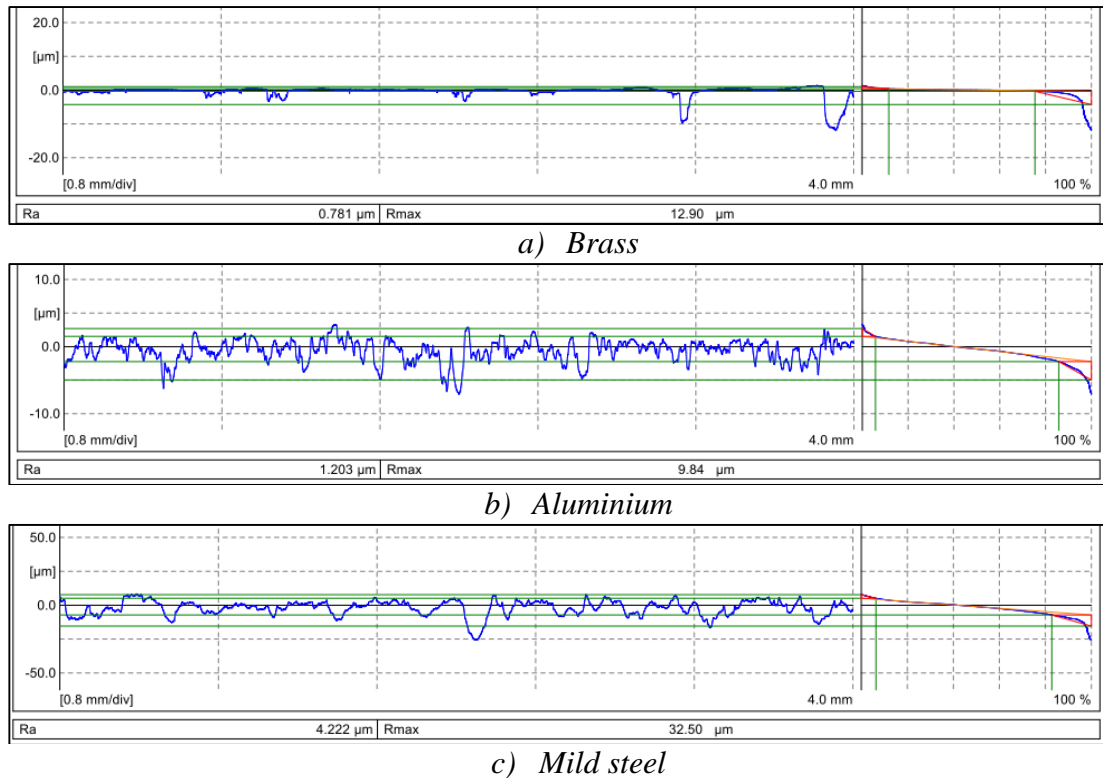


Figure 5.25: Sample of the roughness of the worn surfaces under the condition of 50% waste cooking oil and 50% synthetic oil as a lubricant at elevated temperature of 80°C

A summary of five readings for the same sample of worn surface is presented in Figure 5.26 for all the materials tested under different lubricants and their temperatures. It seems that the increase in the temperature increases the roughness of the surface especially for the mild steel and the aluminium when lubricant at 80°C is used. The increase in the roughness of the metals indicates the severity of the counterface attack on those materials despite the lubricant presence. This is highly pronounced on the mild steel worn surface and aluminium. This may help to understand the significant increase in the specific wear rate of those materials when the lubricant temperature increased (Figure 5.21). Further, the increase in the friction coefficient of the materials with the increase of the lubricant temperature (Figure 5.22) represented resistance in the interface, which can be explained with the increase of the roughness of the worn surfaces. Referring to Figure 4.9, the roughness of the worn surfaces for the steel and aluminium was above 3 μm and about 1 μm, respectively. In other words, the presence of the lubricant at high temperature managed to reduce the interaction between the asperities and somehow achieved less roughness on the worn surface compared to dry contact.

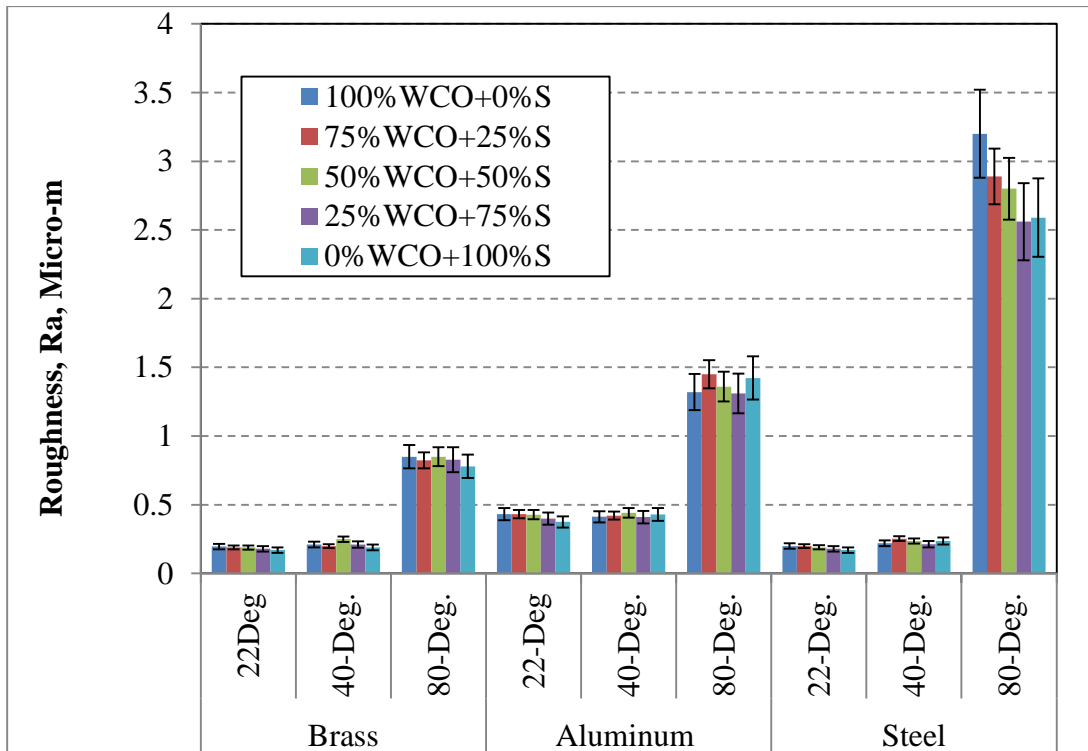


Figure 5.26: Average roughness of the worn surface of the tested metals under different lubricants and environmental temperature.

For the brass materials, there are not many changes in the roughness of the worn material despite the increase in roughness when the temperature was increased to 80°C. Figure 5.27 displays the micrographs of the worn surface of the brass showing a relatively smooth surface compared to the aluminium (Figure 5.28) and the mild steel (Figure 5.29). Figure 5.27 displays the micrographs of brass using lubricant (50% WCO + 50% S) under different environmental temperatures under the applied load of 40 N after 10.8 km sliding distance. In general, the increase in the temperature had an impact on the wear mechanism of the brass, i.e. at high temperature, an increase in the abrasiveness on the surface of the brass can be observed. In comparing Figure 5.27a with Figures 5.27c and d, there is an abrasion nature which can explain the greater roughness of the brass at the higher temperature (Figure 5.26), increase in the friction (Figure 5.23) and significant removal of materials (Figure 5.21). The modification on the worn surface after testing due to the usage of different temperature for the same blends (50% WCO + 50% S) are more pronounced when the aluminium was tested (Figure 5.28). Figures 5.28c and d represent a very rough surface compared to the one tested at low temperature (Figure 5.28a), which indicates the weakness of the surface at these conditions. At the low temperature, the worn surface of the aluminium shows that some of the worn material is still adhered on the surface. In other words, the aggressive abrasion process on the surface of the aluminium could explain the high material removal from the surface, especially at high temperatures (Figure 5.21).

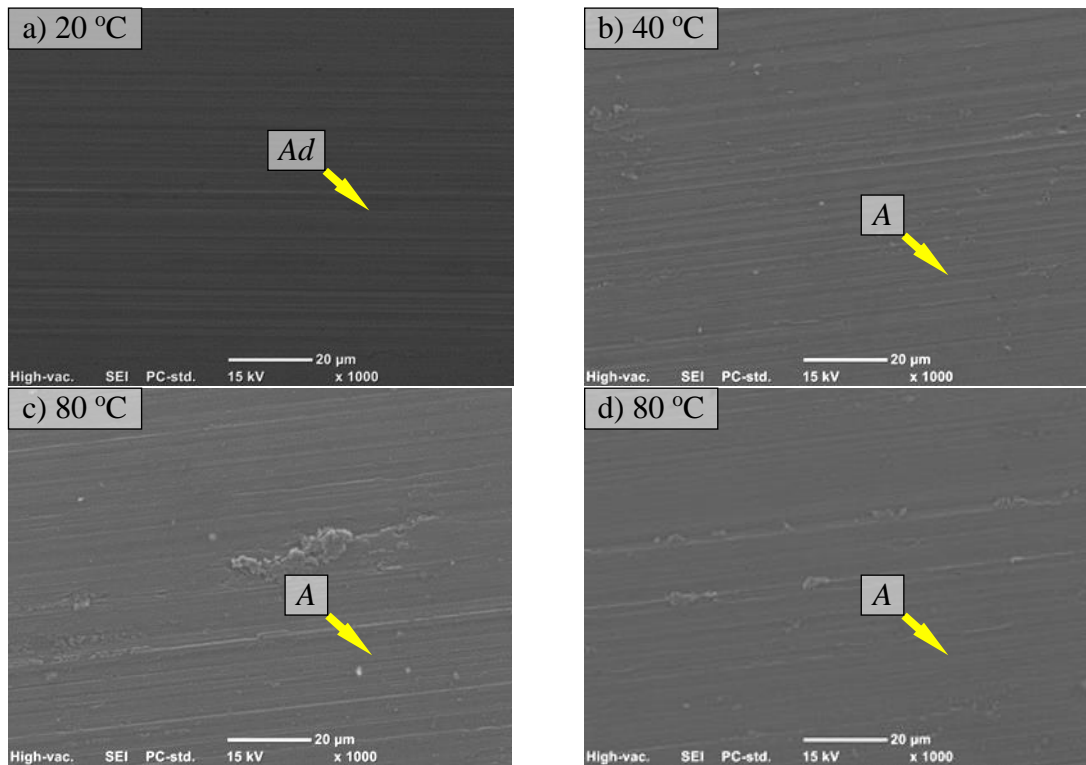


Figure 5.27: Micrographs of brass using lubricant (50 % WCO + 50% S) under different environmental temperatures under the applied load of 40 N after 10.8 km sliding distance showing: abrasive wear mechanism marked as “A”; and adhesive wear marked as “Ad”

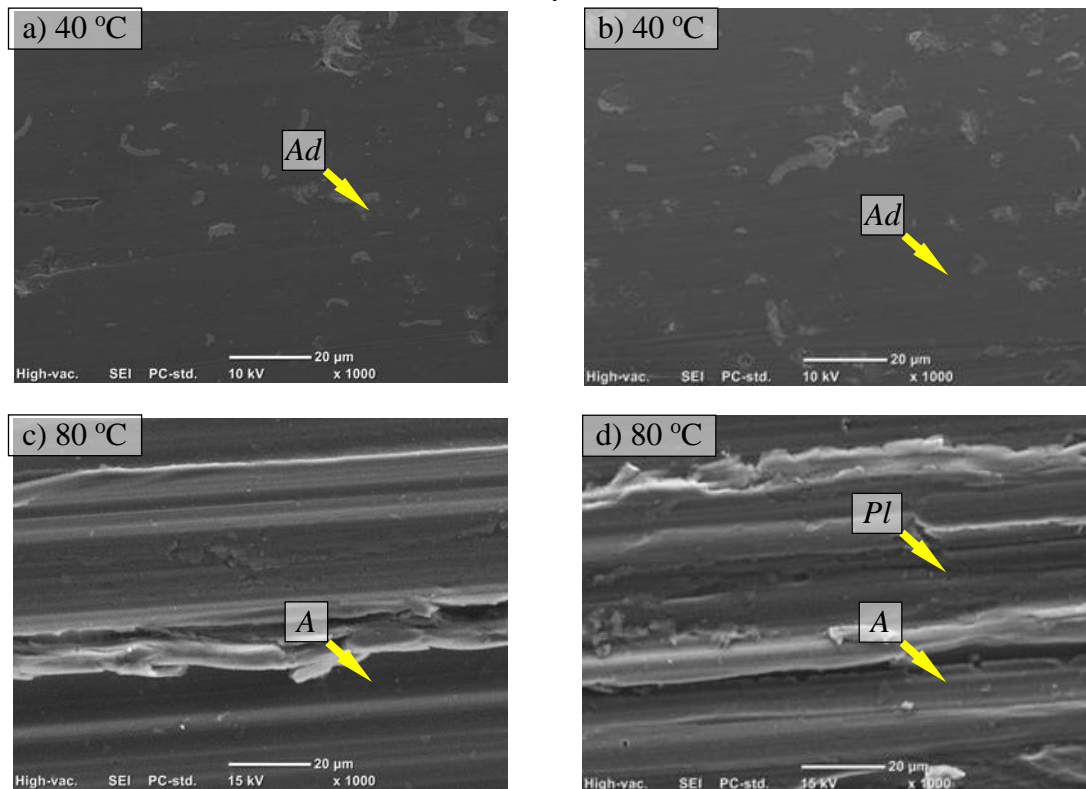


Figure 5.28: Micrographs of aluminium using lubricant (50 % WCO + 50% S) under different environmental temperatures under the applied load of 40 N after 10.8 km sliding distance showing: abrasive wear mechanism “marked as “A”; adhesive wear marked as “Ad”, and ploughing marked as “Pl”

Figure 5.29 displays micrographs of mild steel using lubricant (50 % WCO + 50% S) under different environmental temperatures at the applied load of 40 N after 10.8 km sliding distance. From this figure, one can see that the increase of the temperature from 40°C to 80°C allows the counterface to significantly attack the mild steel surface compared to the low temperature environment. The reason for this is similar to that for the previous example; the increase in the temperature reduced the viscosity, which increased the interaction between the asperities in contact. When the stainless steel counterface rotates against the mild steel sample, an abrasion nature can be seen (Figure 5.26), which leads to a higher friction coefficient (Figure 5.22 c) and higher specific wear rate (Figure 5.20 c) compared to the values at low environmental temperature.

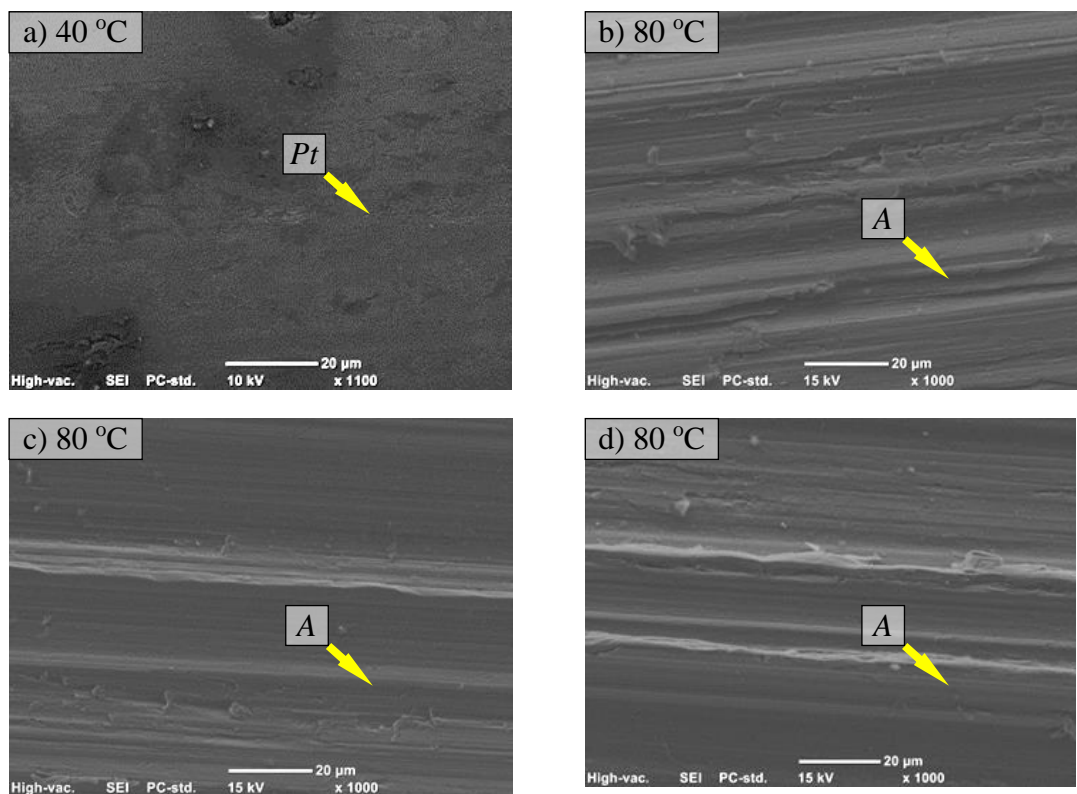


Figure 5.29: Micrographs of mild steel using lubricant (50% WCO + 50% S) under different environmental temperatures under the applied load of 40 N after 10.8 km sliding distance showing: abrasive wear mechanism “marked as “A””; and pitting marked as “Pt”

The abrasion nature of the worn surface of the mild steel may be due to the presence of the removed debris in the interface, which acted as a third body in the hot lubricant. At the temperature of 80°C, it should be mentioned that the colour of the oil changed during the rubbing process (Figure 5.30). The collected debris was extracted from the oil and then observed using the SEM. Figure 5.31 displays the micrographs of the debris when the mild steel was tested at an elevated temperature. One can see, from Figure 5.29 and Figure 5.31, that there is abrasive two body process occurring during the sliding which is predominant as ploughing.

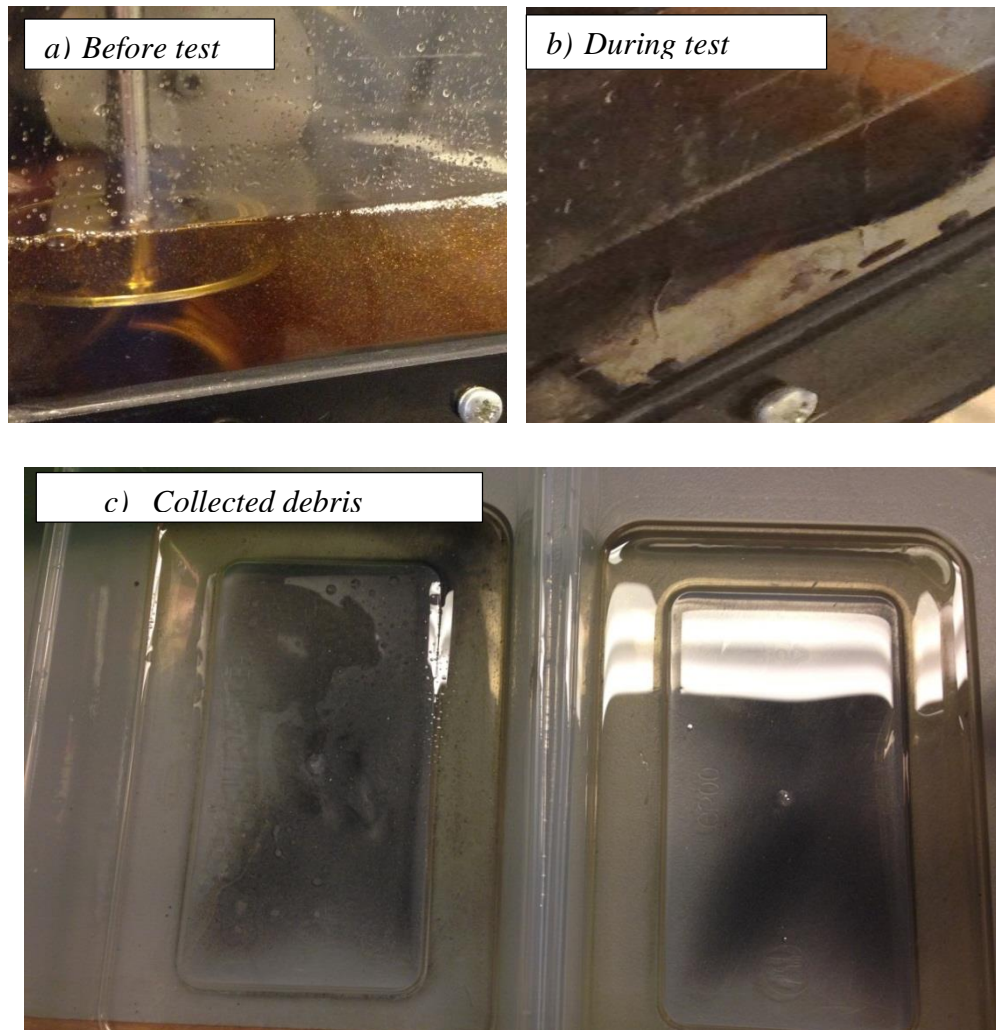


Figure 5.30: Photo showing a sample of the oil when the mild steel was tested using lubricant (50 % WCO + 50% S) at 40 N after 10.8 km sliding distance with environmental temperature of 80°C

The mild steel debris looks like metal fibres, which indicates the large amount of material removed from the mild steel surface. That debris was in the lubricant and rotated and entered the rubbing interface. The naked eyes saw that the colour of all types of lubricant changed dramatically with time. One could see through the side window of the container (Figure 5.30 a, b) the changes in the oil colour. In addition to this, a centrifuge setup was used to extract the debris from the oil as described in Chapter 3, Figure 3.11. This confirms that the debris floated in the lubricant and had the ability to enter the interface. This increased its attachment to both rubbed surfaces leading to high friction and high material removal. It is important to note here that the roughness of the counterface was measured and a pronounced increase in the roughness of the stainless steel counterface was recorded, i.e. $\approx 0.1 \mu\text{m Ra}$ before testing, and $\approx 1.3 \mu\text{m Ra}$ after testing. This confirms that the wear mechanism for the mild steel against the stainless steel at elevated lubricant temperature was abrasive wear, which can be categorised as third-body abrasion or two-body abrasion. Under dry contact conditions (Figure 4.12) this abrasion nature was not witnessed. It seems that the presence of the low viscosity oil in the interface of the mild steel/stainless steel contact area prevented the adaption of the two surfaces (no plastic deformation and formation of film) and brought the hard debris (mild steel) to the interface, which attacked both surfaces. For the brass, it was difficult to extract

the debris from the oil since it was in very small amounts and difficult to filter. With more than 10 times washing using the acetone and the centrifuge machine to clean the debris from the oil, it was not able to collect the debris and perform the SEM observation.

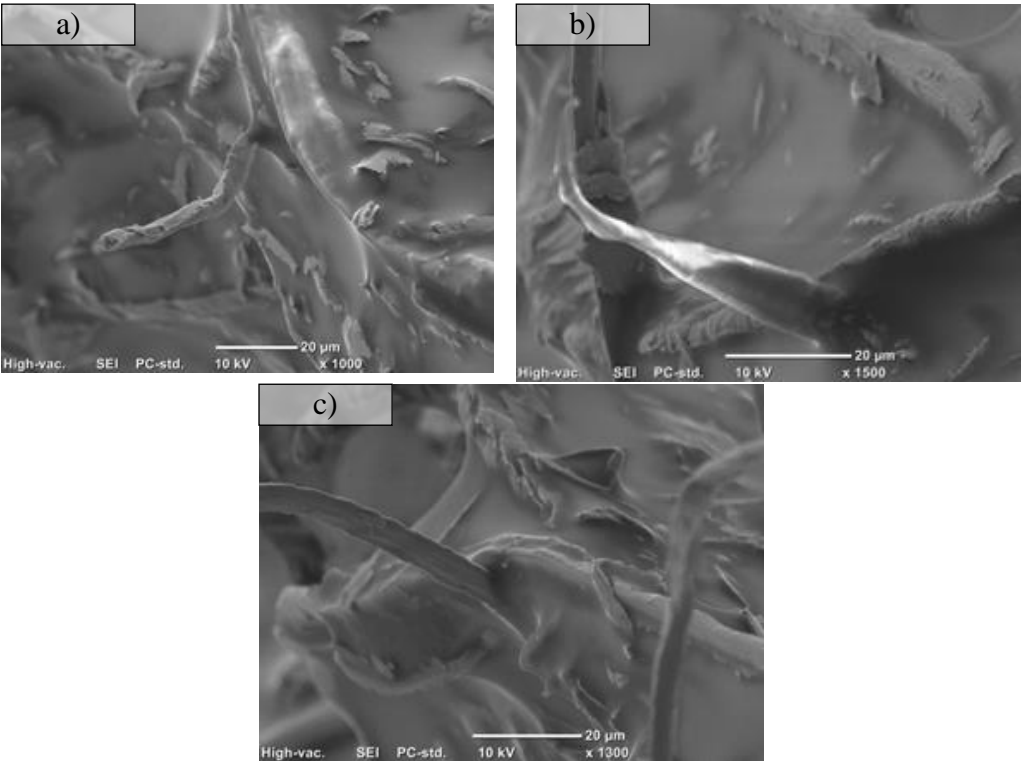


Figure 5.31: Micrographs of mild steel debris after testing using lubricant (50% WCO + 50% S) at 40 N after 10.8 km sliding distance with an environmental temperature of 80°C

Figure 5.32 displays aluminium debris after testing using lubricant (50% WCO + 50% S) at 40 N after 10.8 km sliding distance with an environmental temperature of 80°C. The micrographs of the debris show patches of debris that are different from the one seen in the case of the mild steel (Figure 5.31). It seems that the weakness of the aluminium generated such forms of debris and the presence of such debris in the interface attacked the weak surface (aluminium) more than the stainless steel counterface since it is much harder than the aluminium. The roughness of the counterface increased slightly after testing the aluminium, i.e. from $\approx 0.1 \mu\text{m Ra}$ before testing to $\approx 0.5 \mu\text{m Ra}$ after testing.

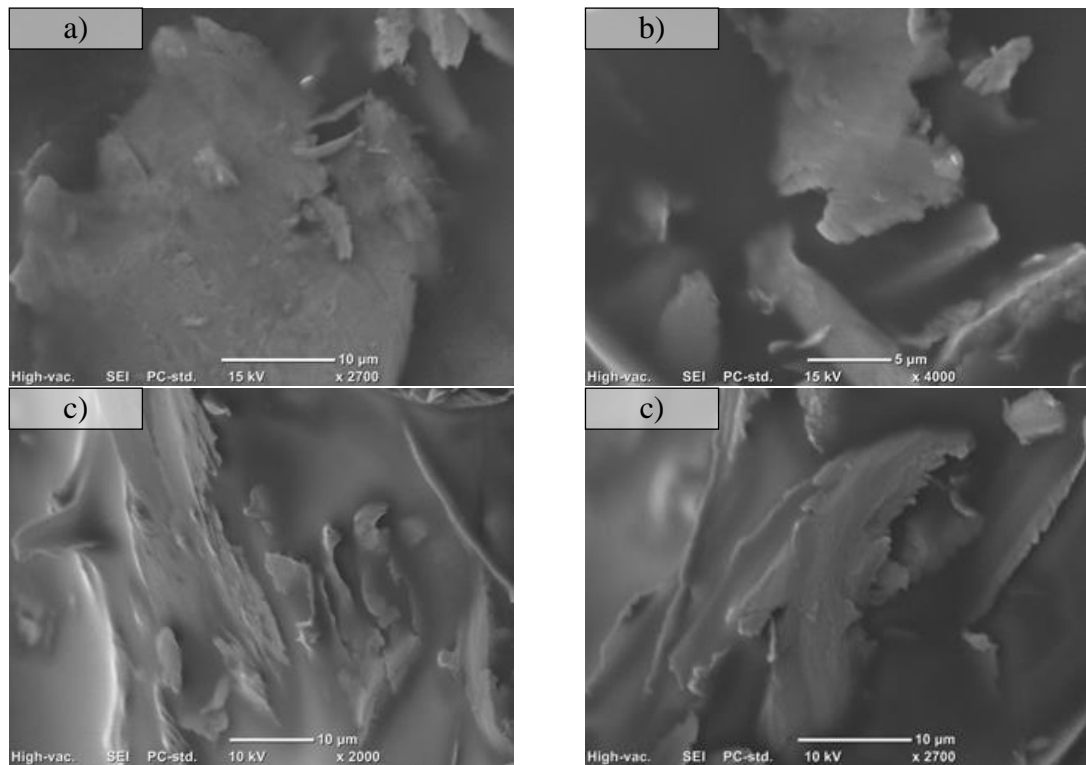


Figure 5.32: Micrographs of aluminium debris after testing using lubricant (50 % WCO + 50% S) at 40 N after 10.8 km sliding distance with environmental temperature of 80°C

The most relevant works have been conducted by (Abdullah et al. 2013; Imran et al. 2013; Louaisil et al. 2009; Quinchia et al. 2014; Shahabuddin et al. 2013; Tang & Li ; Velkavrh & Kalin 2012). All these works are recent and agreed that a reduction in the viscosity for any reason (e.g. type of oil, environmental effect, additives, blend ratio) leads to a high wear rate and friction coefficient for any type of rubbing metals.

5.5 Chapter Summary

This chapter discussed the influence of WCO on the wear and frictional behaviour of brass, aluminium and mild steel considering different operating parameters, WCO/SO blend ratios and lubricant temperatures. In general, operating parameters applied load, sliding distance, type of metal, type of lubricant blend and temperature blend have equal effects on the wear and frictional behaviour of the selected materials. The main points can be summarised as follows:

1. WCO with its blends has a significant influence on the wear and frictional performance of brass, aluminium and mild steel metals. At room temperature, presence of the lubricant in the interface significantly reduced the specific wear rate and friction coefficients for all the materials
2. The blend ratio of the WCO with the SO controlled in the wear and friction coefficients of the selected materials, especially at room temperature as viscosity varied with the blend ratio. Thus, viscosity of the lubricant is the key to determining the wear behaviour of the materials. High viscosity reduced the specific wear rate and decreased the friction coefficient. Correlation between wear performance and the viscosity was established with the available data confirming the above findings. In addition, the presence of

the fatty acids in the waste cooking oil significantly impacted on the wear and frictional results especially the 5.2% stearic

3. At room temperature, the general wear mechanism was predominant by a polishing process in the case of brass. An abrasion nature was observed in the cases of the aluminium and the mild steel. Aluminium exhibited the poorest wear and frictional performance compared to brass and mild steel at all the operating parameters and blend ratios
4. The temperature of the lubricant was the most influential element determining wear and the frictional performance of the selected materials. Increasing the temperature reduced the viscosity of all blends, which were dramatically reduced at the elevated temperature of 80°C. The increase in the temperature increased the interaction between the rubbed surfaces (reducing the separation), which led to high friction associated with high material removal especially for the mild steel and aluminium
5. A three-body abrasion wear mechanism was observed when the mild steel was tested under lubricant at elevated temperature, due to the presence of the hard debris in the lubricant, which acted as a third body in the interface. Aluminium also exhibited an abrasion nature at the elevated temperature due to the weakness of its surface. Brass showed relatively good wear and frictional performance at all lubricant temperatures as a polishing process took place during the rubbing.

Chapter 6: The Performance of Waste Cooking Oil in Journal Bearings

6.1 Introduction

In this chapter an attempt is made to use the prepared and modified WCO as a lubricant for journal bearings. Since this is the last stage of the work, it can be regarded as the main outcome of the research. The chapter introduces the background of the research in using bio-oils in lubricants for journal bearings, the experimental procedure, and finally, the results and discussion.

6.2 Working Mechanism of Journal Bearings

The two general classes of bearings are journal bearings, also known as sliding or plain surface bearings, and rolling element bearings. In the current study, WCO was used as lubricant for journal bearings. There have been many studies on the parameters (e.g. inlet pressure, inlet position, geometry) and the performance of journal bearings (Ahmad, Kasolang & Dwyer-Joyce 2014; Du et al. 2014). A few works have also recently attempted to study the pressure temperature and friction in the journal bearings (Ahmad, Kasolang & Dwyer-Joyce 2013; Ahmad, Kasolang & Dwyer-Joyce 2014; Chauhan, Sehgal & Sharma 2010). The most common plain journal bearing is the single groove journal bearing used in several industrial applications (Childs 2014). Journal bearings consist of a journal rotating freely in a supporting metal sleeve. The pressure, temperature and film thickness are the main output parameters that indicate the lubricant performance for the journal bearing application (Ahmad et al. 2013; Chauhan, Sehgal & Sharma 2010; Deligant, Podevin & Descombes 2011; Solghar, Brito & Claro 2014).

Since the viscosity of the lubricant is highly dependent on the temperature (as explained in Chapter 2), monitoring of the temperature in the journal bearing, i.e. the oil behaviour has been recommended by Bang, Kim and Cho (2010). Chauhan, Sehgal and Sharma (2011) reported that the lubricant temperature highly controlled the capacity of the journal bearings, i.e. the applied load. Thus, oil temperature is an important parameter to be considered in evaluating journal performance.

Most of the old and recent studies have developed a prediction equation to calculate the temperature inside the journal bearings (Allmaier et al. 2013; Majumdar & Saha 1974). A recent study by Cerda Varela, Bjerregaard Nielsen and Santos (2013) attempted to correlate the theoretical and experimental data of journal-bearing parameters. The prediction of the steady-state behaviour of the tilting-pad bearing with controllable lubrication exhibited good agreement with the experimental works. Several assumptions have been made to close the theoretical results to the experimental. Brito et al. (2014) reported that “*the complexity of the problem frequently led to the use of oversimplified models*”, that is, the incorporation of lubricant feeding conditions is usually oversimplified which in turn ignores the effect of lubricant feeding pressure, feeding temperature or the actual geometry of grooves. Therefore, experimental results are more reliable than the theoretical, especially for journal bearings. In the current study, the lubricant temperature in the journal bearing is captured at different rotational angles for different selected blends.

The pressure distribution in the journal bearings is an essential parameter to be investigated as it controls the load capacity of the journal bearing. Figure 6.1 shows the classic pressure distribution in a journal bearing, showing the lifting pressure that determines the capacity of the journal. A number of studies have modelled the pressure distribution in the journal bearing using commercial CFD software (Nishio, Somaya & Yoshimoto 2011) and/or an experimental procedure (Ahmad, Kasolang & Dwyer-Joyce 2014).

Kasolang et al. (2012) investigated the pressure conditions of the lubricant to ensure the good performance of journal bearings. Experimental work was conducted to determine the pressure distribution around the circumference of a journal bearing. Pressure sensors were located around the journal bearings. The captured pressure values were compared to the theoretical values and good agreements have been achieved. In the current study, the same journal bearing setup is used.

Ahmad, Kasolang and Dwyer-Joyce (2014) examined the influence of different oil groove locations on the pressure distribution revealing that the location of groove significantly influenced the pressure profile. Furthermore, the pressure profile in the converging region (before the minimum film thickness) was the lowest when the groove position was at an angle of 30°. In light of the above, the new prepared lubricants were tested to study the temperature, pressure and frictional distribution in the journal bearing.

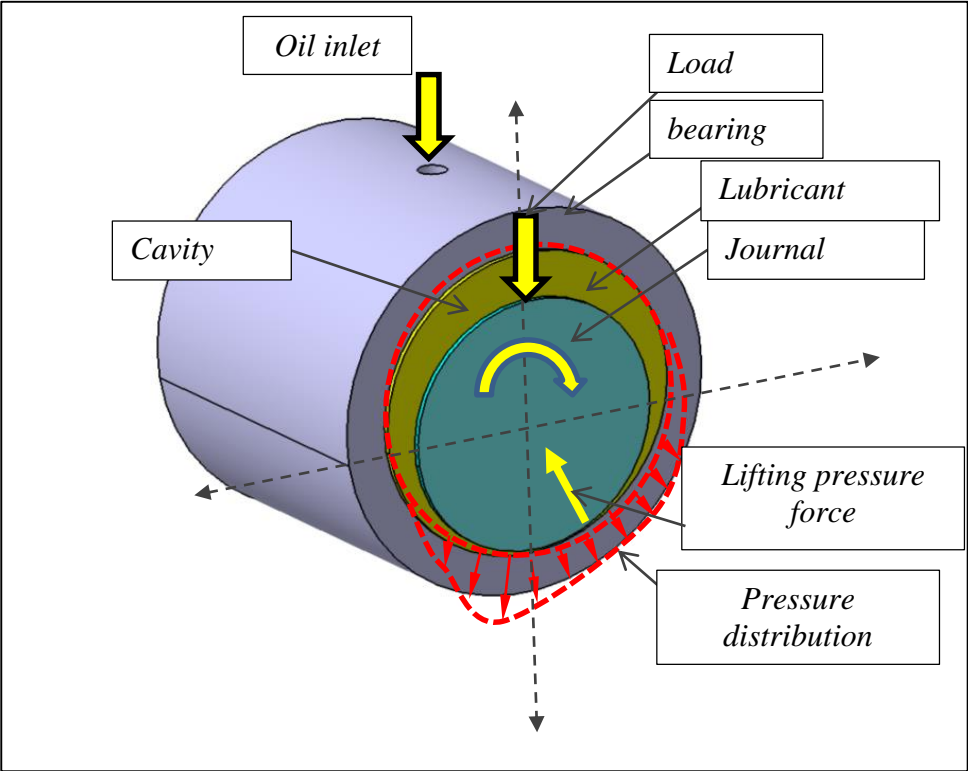


Figure 6.1: Pressure distribution in journal bearing.

6.3 Lubricant Preparation and Experimental Procedure

6.3.1 Lubricant Selection and Preparation for Journal Bearing Tests

For the journal bearing tests, the lubricant was prepared six months before the experiments as the stability of the lubricant must be considered before testing. 20 litres of four WCO blends were used; the ratios of the SO to the WCO were 0 vol. %, 25%, 50 vol.%, and 100 vol.%, and marked as oil A, B, C and D, respectively. After six months, the viscosity of the blends were checked before conducting the tests. 5% (wt) of EVA copolymer (density, at 23 °C, 0.956 g cm⁻³; molecular weight, 60250 g mol⁻¹; melting temperature, 59 °C) and 2% (wt) of EC (density, at 25°C, 1.14 g cm⁻³; molecular weight, 68960 g mol⁻¹; melting temperature, 155°C) were used as additives to improve the viscosity of the oil.

6.3.2 Journal Bearing Setup

A robust versatile journal bearing (CM-9064) rig was used in this study. Figure 6.2 shows the bearing rig. The main components of the rig are the frame, bearing unit, loading, drive, lubrication unit, control, and measuring and control unit. The rig has the facility to capture the temperature and pressure around the journal bearing and the friction coefficients. Figure 6.2 shows that the journal is mounted horizontally. Calibration is completed annually by the supplier company. However, before conducting the experiments, the rig was checked using a computer integrated with the rig. The rig was connected to the computer using a data acquisition system to capture the temperature, pressure and friction during the test. The shaft of the journal was fixed on self-affiliated bearings in a horizontal manner and then powered by a motor. In generating the hydrodynamic bearing, it would be active when the centrifugally casted faultless bearing glides when the journal reaches a clearance of 100 µm.

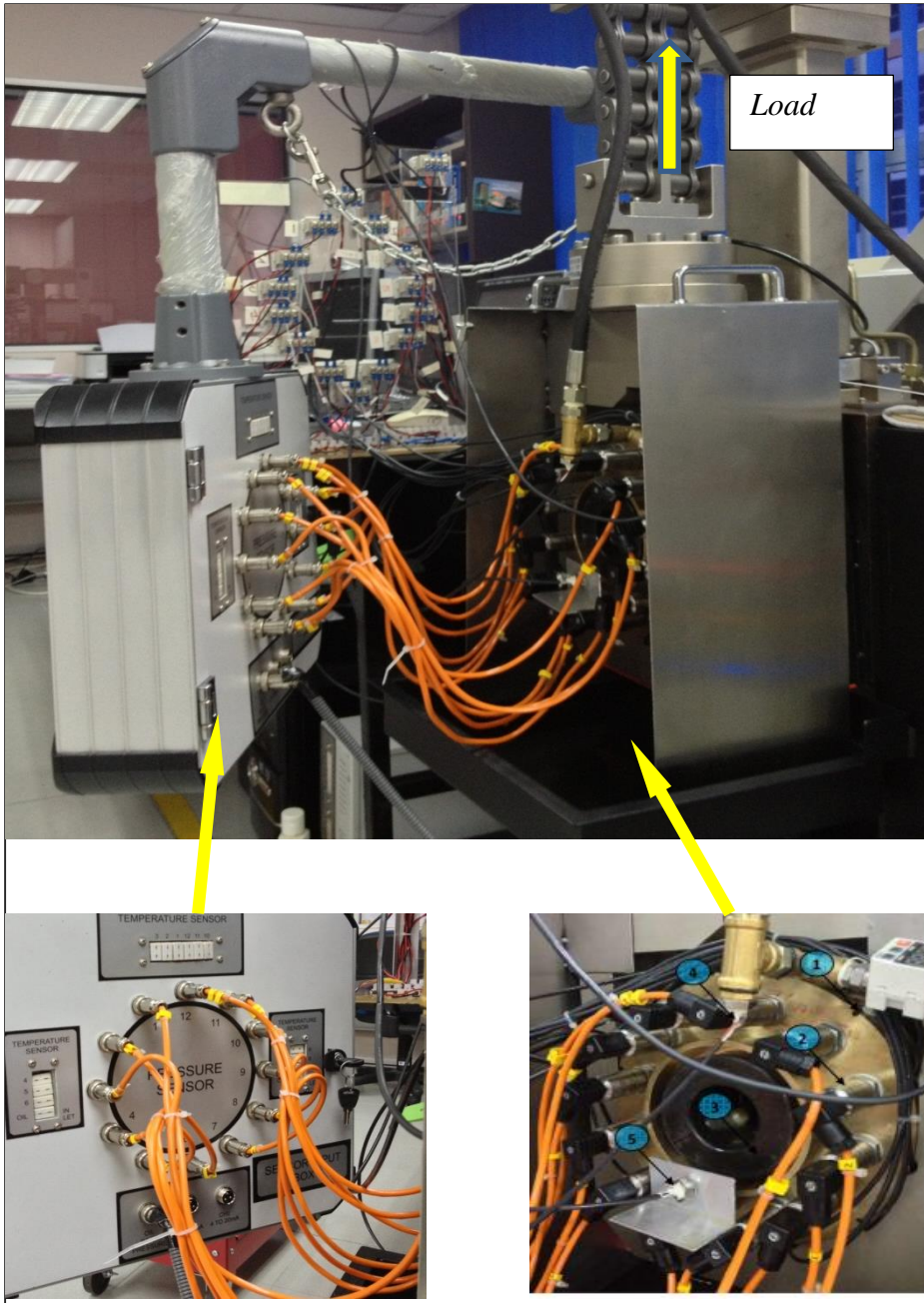


Figure 6.2: Journal bearing setup

Notes. 1. Temperature sensors, 2. pressure sensors, 3. shaft, 4. temperature thermocouple of inlet oil, 5. temperature outlet.

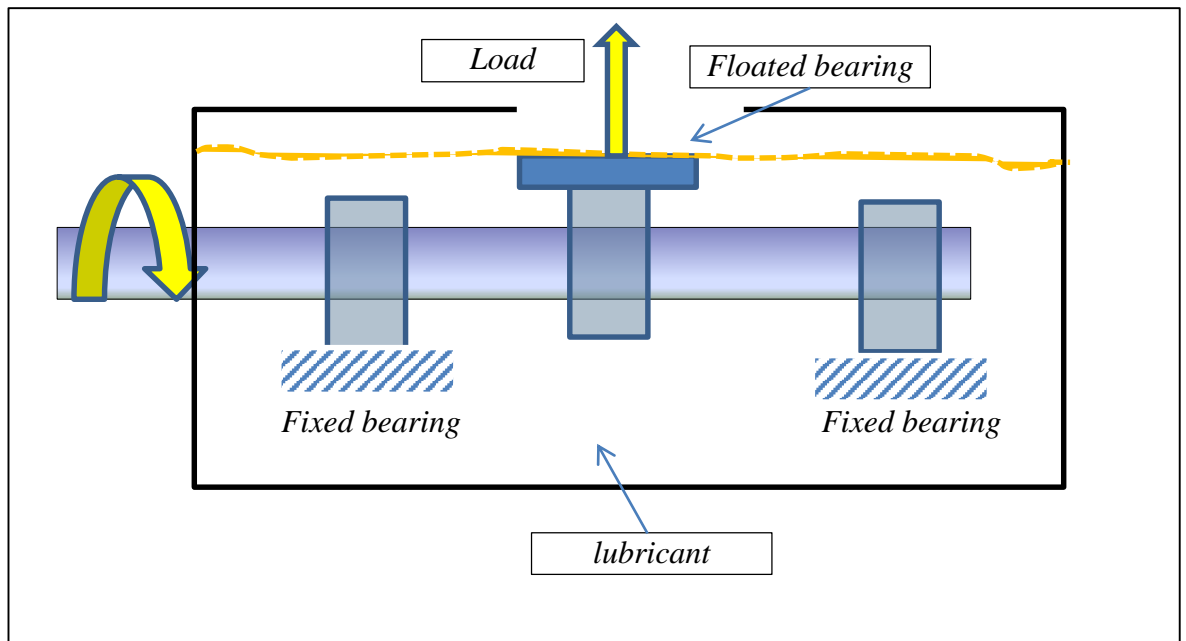


Figure 6.3 Mechanism of the load applied to the journal bearing in the rig

During the experiments, the bearing could be pulled upward to apply radial force by a loading lever (Figure 6.3). The radial clearance can be 0.05 mm with L/D ratio of 0.5. The surface of the journal bearing has a roughness of about 1.6 μm Ra. The inner diameter of the bearing is 100 mm. Further details are given in Table 6.1.

In the experiments, the journal was fixed to self-affiliated bearings in a horizontal manner, twisted by using a servo-moto. The hydrodynamic bearing could be generated. A lube tank having a volume of 20 litres of lubricant adjoined the journal bearing to deliver the oil. A gear pump was used to flow the oil into a sieve of 50 microns and then into three points of the uppermost region of the journal bearing. The outlet of the lubricant came from the bottom of the housing of the bearing. The oil flow was at a constant of 6 litres per minute.

Table 6.1: Details of the Journal Bearing Rig (Ahmad, Kasolang & Dwyer-Joyce 2013; Ahmad, Kasolang & Dwyer-Joyce 2014; Ahmed et al. 2013; Kasolang et al. 2012)

Part detail	Range
Bearing material	Phosphorous bronze
Inner bearing diameter, D	100.1 mm
Bearing length, L	50 mm
Surface roughness	0.8Ra on ID ground & polished
Journal material	EN-353 steel
Outer journal diameter, D	100 mm
Surface roughness	0.8 Ra ground & polished
Radial clearance, c	52 μm (0.05mm)
c/r ratio	0.001
Load range, W	5-100 kN
Journal speed	100 – 1000 RPM
Lubricant viscosity	68 cSt @ 40°C 8.8 cSt @ 100°C
Lubricant	ISO VG 68
Pressure sensor	
Model	MEAS (M 5156)
Range	10 MPa
Accuracy	(0.001 \pm 1% measured value) MPa
Temperature sensor	
Model	PT 100, make: Ajay sensor
Range	Max 200 °C
Accuracy	(1 \pm 1% measured temp.) °C
Frictional torque sensor	
Model	Beam type load cell (Sensortronic)
Range	30 kg
Accuracy	(0.01 \pm 1% measured value) Nm

6.3.3 Experimental Procedure

The experimental procedure for the journal bearing was not complicated as the rig operated with the assistance of the control system integrated with a computer. In this work, the applied load was set to be 10 kN as recommended by the literature (Ahmad, Kasolang & Dwyer-Joyce 2013; Ahmad, Kasolang & Dwyer-Joyce 2014; Ahmed et al. 2013; Kasolang et al. 2012) and the experts in the laboratory, despite the fact that the rig can take a further load. The speed was selected to 600 rpm, which is considered the maximum for such a lubricants in terms of viscosity, following the guidelines of the manufacturer. Once the bearing was placed and the tank was filled with the lubricant (selected blend), the rig began operation. The test continued for 30 minutes and then the temperature and the pressure were captured by the computer. The steady state of the friction coefficient was captured at the end of the test.

6.4 Results and Discussion

The pressure and temperature distributions with the friction coefficient around the journal bearing are presented in this section. Before presenting the results, it is important to determine the Sommerfeld Number, which is calculated using Equation 6.1:

$$S = \left(\frac{r}{c}\right)^2 \frac{\mu N}{P} \quad (6.1)$$

where:

S is the Sommerfeld Number

r is the shaft radius = 50 mm

c is the radial clearance = 52 μ m

μ ; is the absolute viscosity of the lubricant, Pa.s which is obtained from chapter 3

N is the speed of the rotating shaft in rev/s = 600 rpm x 60 = 36000 rev/s

P is the pressure = applied load/ dl = 10 kN / (50 x 100) = 2 MPa

The variable parameter influencing the Sommerfeld Number is the viscosity at the mean temperature of the lubricant in the journal bearing. The viscosity of the blends at different temperatures was presented in Chapter 3. The temperature in the journal bearing was determined from the data acquisition system from the journal bearing rig. In this work, the absolute viscosity of the lubricant was determined based on the leaking temperature which was approximated by measuring the outlet oil temperature of the bearing as suggested by (Kasolang et al. 2013; Khonsari & Booser 2008).

Accordingly, the Sommerfeld Number was determined for each blend of lubricant and is presented in Figure 6.4.

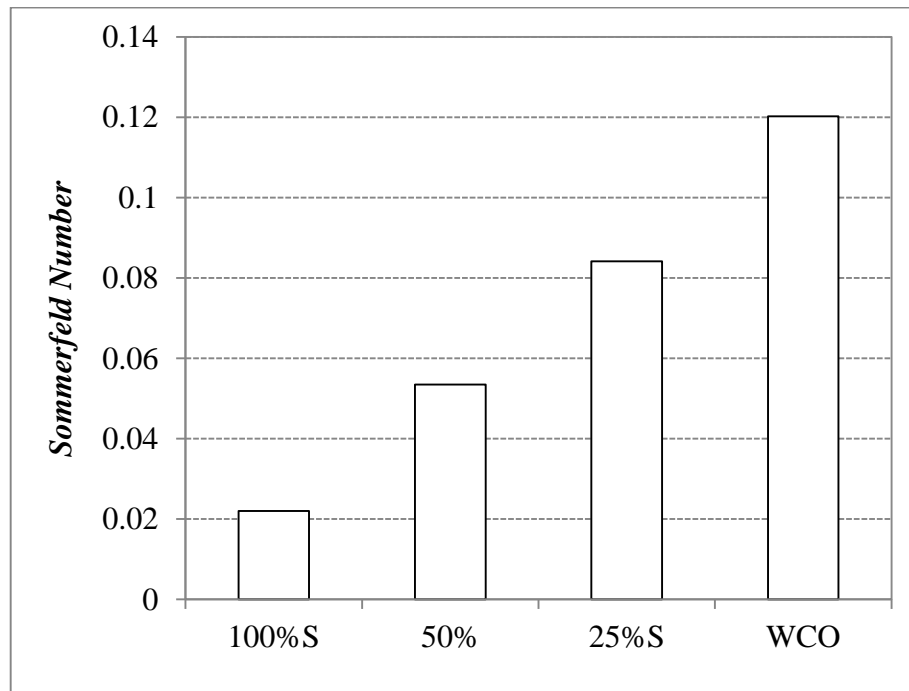


Figure 6.4: Sommerfeld Number of the blends at the operating parameters of 600 rpm and 10 kN load

The predicted lubricant film thickness was determined using the minimum film thickness against the Sommerfield number chart provided by Seireg (1998). The Sommerfield numbers in Figure 6.4 were used to determine the minimum film thickness for all types of oils. h_0/c (minimum film thickness/ clearance (0.05mm)) was determined using the minimum film thickness against the Sommerfield number chart, (Seireg 1998), and then the film thickness was calculated. It should be mentioned here that L/D (bearing length/ bearing diameter) is equal to $\frac{1}{2}$. The minimum film thickness for all types of oils were determined, i.e. 100 %SO $\approx 4 \mu\text{m}$, 50 %SO $\approx 7.5 \mu\text{m}$, 25 %SO $\approx 9.5 \mu\text{m}$, 0 %SO $\approx 13 \mu\text{m}$. As the film thickness is greater than the roughness of the composite, there was sufficient fluid film in the bearing.

6.4.1 Pressure Distribution

Twelve pressure sensors were located around the journal bearing (each 30° had a sensor around the 360°) to capture the pressure value at each angle. The captured data for each blend of lubricant is presented in Figure 6.5. In general, there is a classic trend for the pressure value around the journal bearing since it showed an atmospheric pressure value at the angle of 360° which represents the inlet of the oil (Hamrock, Schmid & Jacobson 2004). When the oil began to enter the journal bearing, an increase in the pressure could be seen with the increase of the angle, until the maximum pressure area reached an angle of about 210° . The increase in the pressure indicates the closeness of the bearing to the journal. Similar trends have been reported in all the literature and were recently mentioned by Brito et al. (2014) and Ahmad, Kasolang and Dwyer-Joyce (2014). It should be mentioned here that the decrease in the bearing clearance increased the average oil temperature and thus reducing viscosity and viscous drag. This may reflect the performance or the quality of the lubricants.

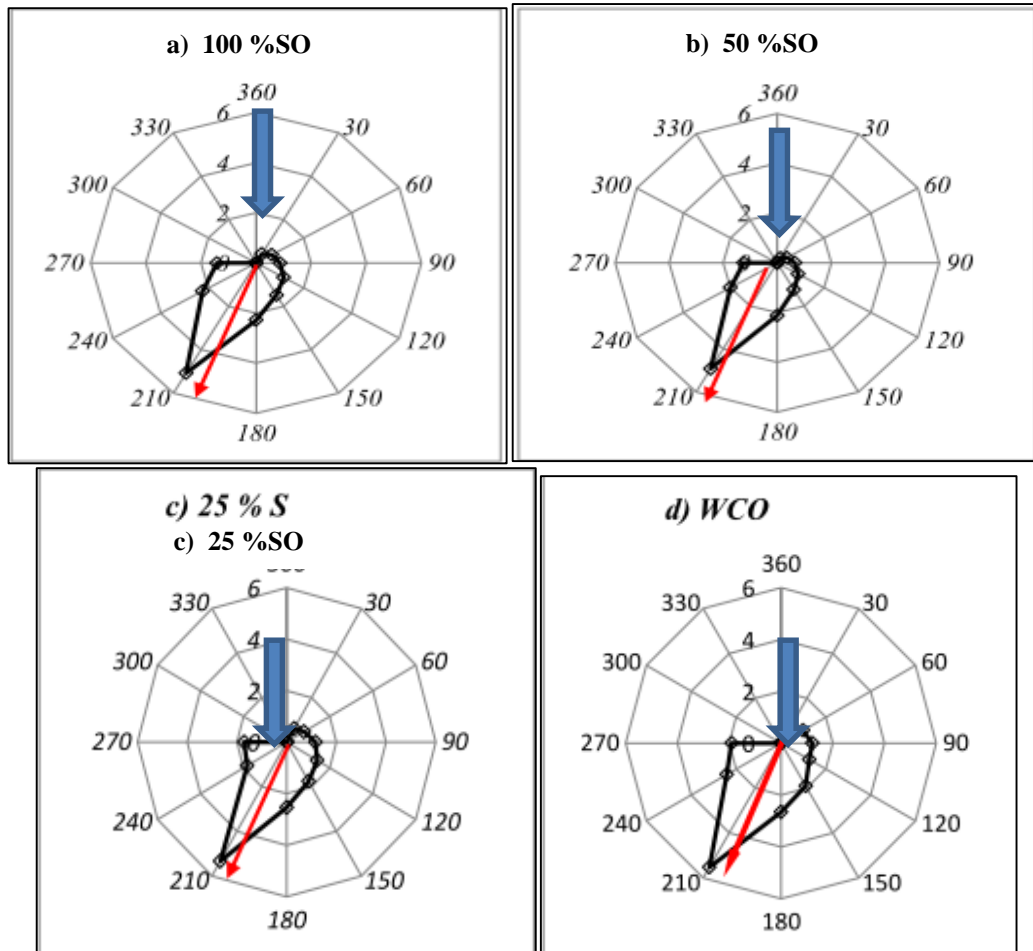


Figure 6.5: Pressure distribution around the journal bearing showing the position of the minimum film thickness * all the values of the pressure are in MPa and the vertical arrow represents the load.

For comparison purposes, the pressure distribution in the journal bearings for all the lubricants is represented in Figure 6.6, showing the values of the pressure around the journal bearing at a load of 10 kN and a speed of 600 rpm. The figure shows that the modified WCO without the addition of the SO exhibits the maximum pressure compared to the others, followed by the 25% S, 100% SO and then 50% S. Conversely, the differences in the values of the pressure are not significant and could be due to different reasons such as the chemical modification of the lubricants, or the increased temperature in the interface. The current pressure values were competitive with the Shell Tellus S2 M (Ahmad, Kasolang & Dwyer-Joyce 2014), which showed a maximum pressure of 4 MPa -5 MPa at the 500 rpm and 10kN load. A similar range of pressure has been reported by Chauhan, Sehgal and Sharma (2010), who used an ellipse journal bearing at a high speed of 2000 rpm for different grades of oil. In other words, WCO can be considered a good alternative oil in terms of pressure generation in the journal bearing, which can produce good lift to the bearing at the operated conditions. However, there are different consideration should be taken in selecting the lubricants for different applications, i.e. degradation, stability of the viscosity, and homogeneity of the blends at elevated temperatures. For further confirmation of the possibility of using this new lubricant and understanding of the degradation of the lubricants. It should be mentioned that, different blends have been prepared for the tests and kept for three months to ensure the homogeneity of the blends.

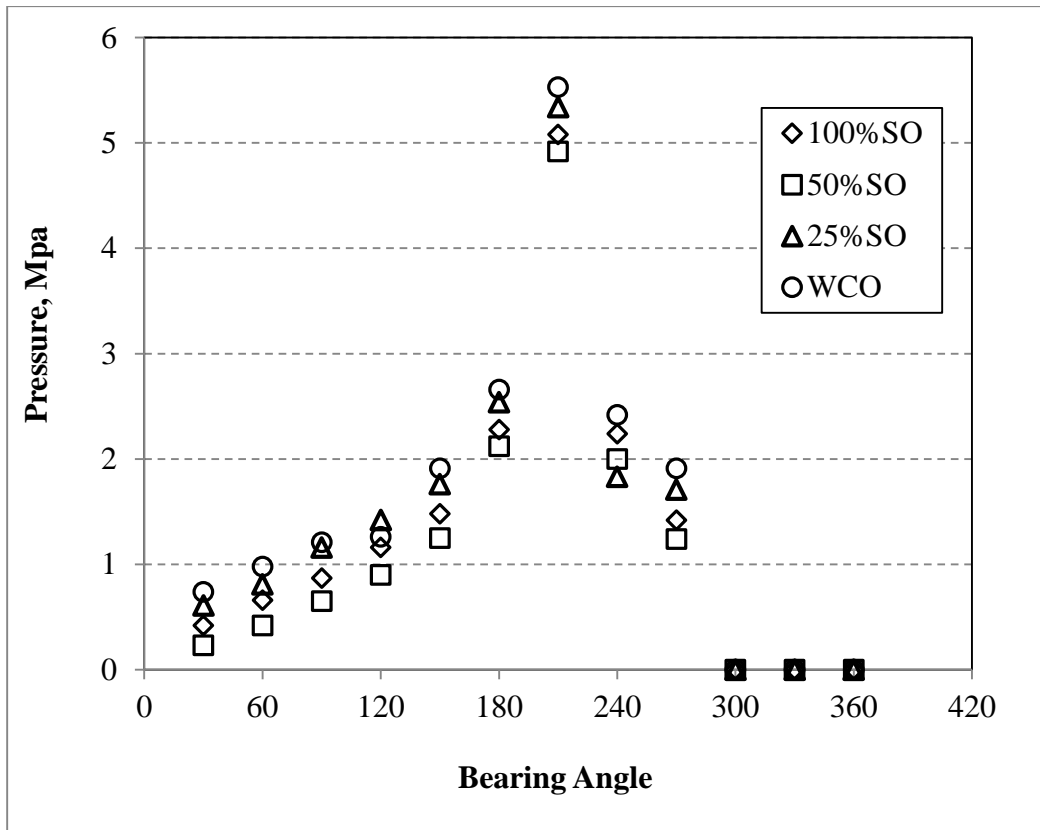


Figure 6.6: Pressure distribution in journal bearing for different blends

6.4.2 Lubricant Temperature in Journal Bearing

Similar to the pressure distribution around the journal bearing, the temperatures were captured by 12 sensors around the journal bearing. For each type of blend, the temperature distribution is presented in Figure 6.7 showing the value of the temperature at each angle. In general, the trend of the temperature seems to be same for all the tested lubricants since the maximum temperature can be located at about 210°C. There was an increase in the temperature of the oil towards the minimum film thickness and the higher pressure, as seen in the previous section. It was noted in Chapter 3 and in the reported works, that an increase in the temperature reduces the viscosity of the oil, and high reduction in the viscosity is not recommended at the minimum film thickness as there will be less lifting to the journal and failure may result (Muzakkir et al. 2011; Muzakkir, Lijesh & Hirani 2014).

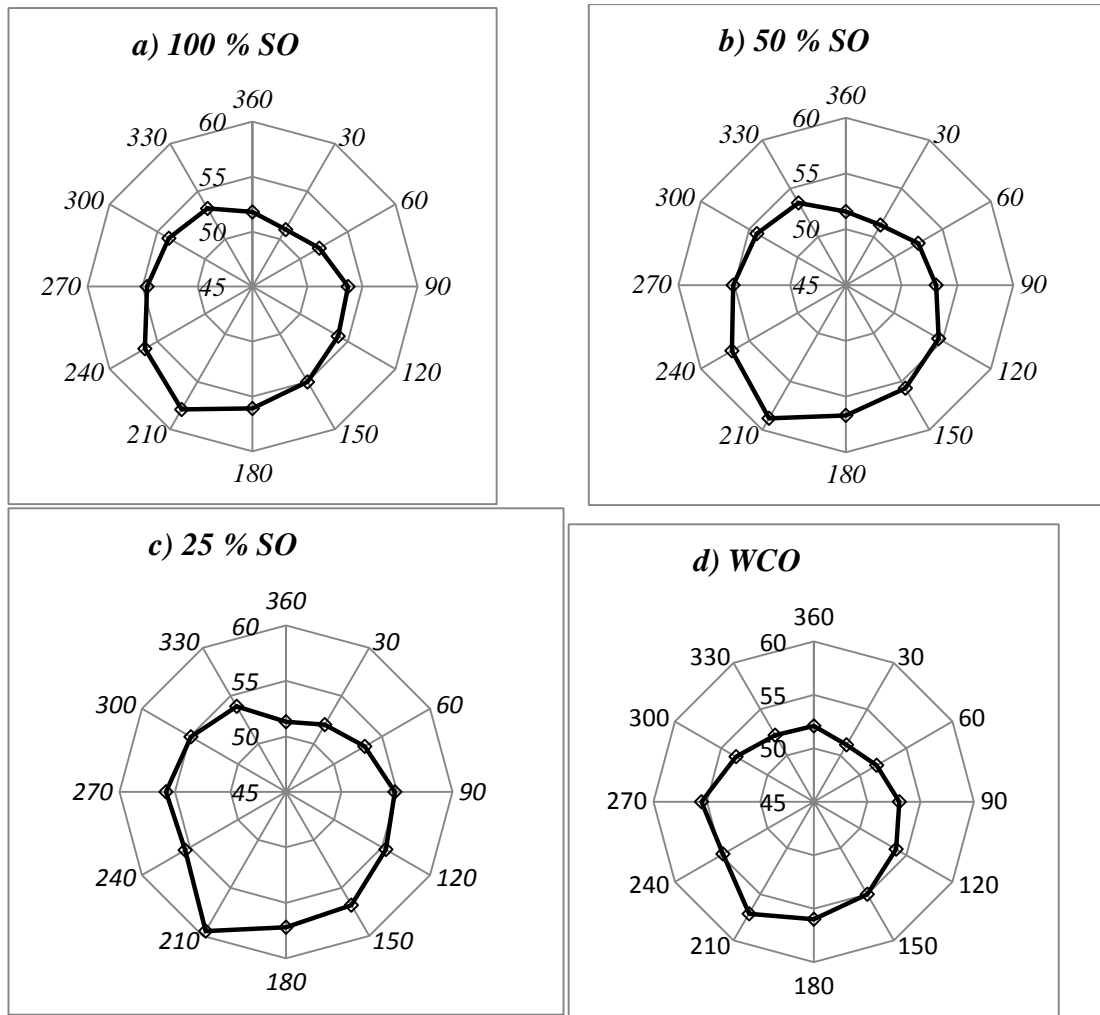


Figure 6.7: Lubricant temperature (°C) distribution in journal bearing for different blends

Figure 6.7 is represented in Figure 6.8, which shows the differences in the temperature distribution of the tested lubricants against the angle. Basically, one can see that the lowest temperature could be seen when the WCO was tested as the maximum temperature that can be seen is about 57°C. The fully synthetic oil gains a temperature of about 58°C, which is slightly higher than the SO, that is, WCO is very competitive to the fully synthetic oil. However, blending the two oils achieved a higher temperature compared to the pure SO or WCO, which indicates that there could be an issue related to the blending process of the oil. García-Zapateiro et al. (2013) reported that oleic and ricinoleic acids-derived estolides and their blends with vegetable oils significantly influence the viscosity and thermal flow of vegetable oil. In term of values, Shell Tellus S2 M (Ahmad, Kasolang & Dwyer-Joyce 2014) exhibited a maximum temperature of about 44°C at a slightly lower speed of 500 rpm compared to the current speed of 600 rpm.

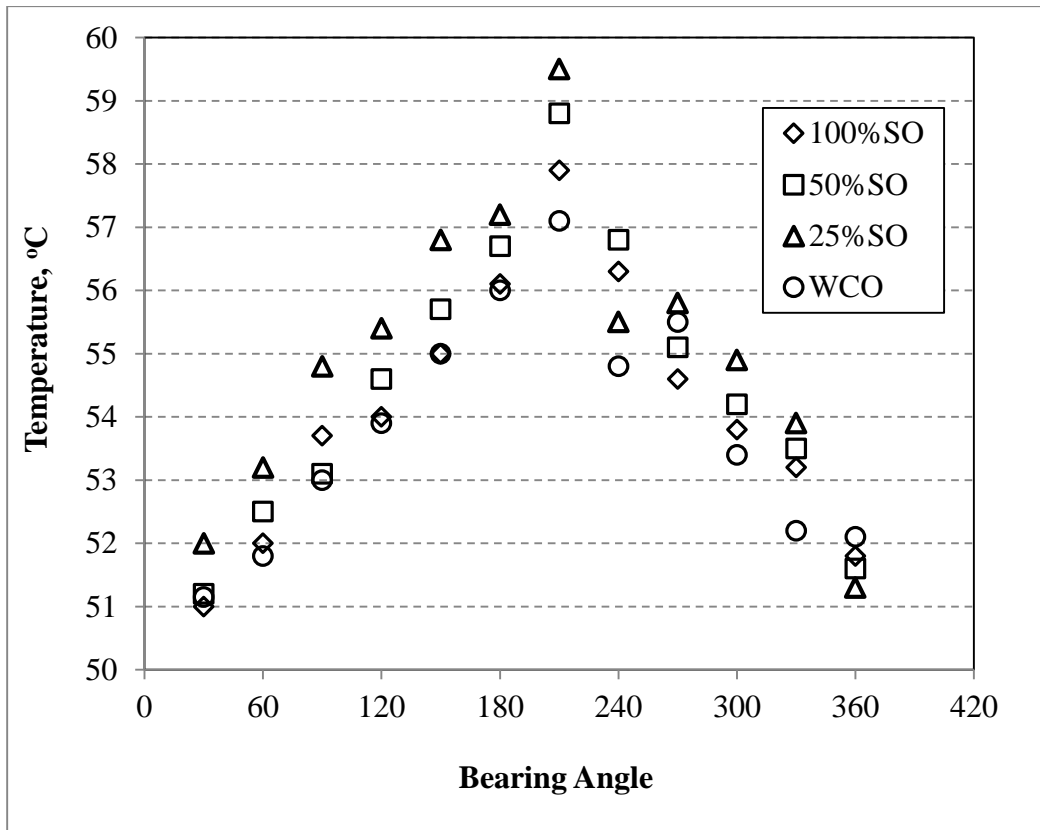


Figure 6.8: Temperature vs. angle of the blends

6.4.3 Friction Coefficient

The main concept of using the journal bearing is to carry the load of the rotating shaft with a very low friction coefficient to reduce power loss. The friction coefficient obtained from the experimental work for the current lubricants are presented in Figure 6.9. The figure shows very low friction coefficient values for all the lubricants. However, SO exhibits the lowest friction coefficient of about 0.028, while the WCO shows about 0.016. In the literature, ISO VG 32 showed similar values of friction coefficient (Bouyer & Fillon 2011) when the speed was increased to 1000 rpm. Furthermore, SAE 90 gear oil showed an 0.05 friction coefficient at a speed of 750 rpm (Ünlü & Atik 2007). This shows that the prepared oil is very competitive with industrial oil in terms of the friction coefficient.

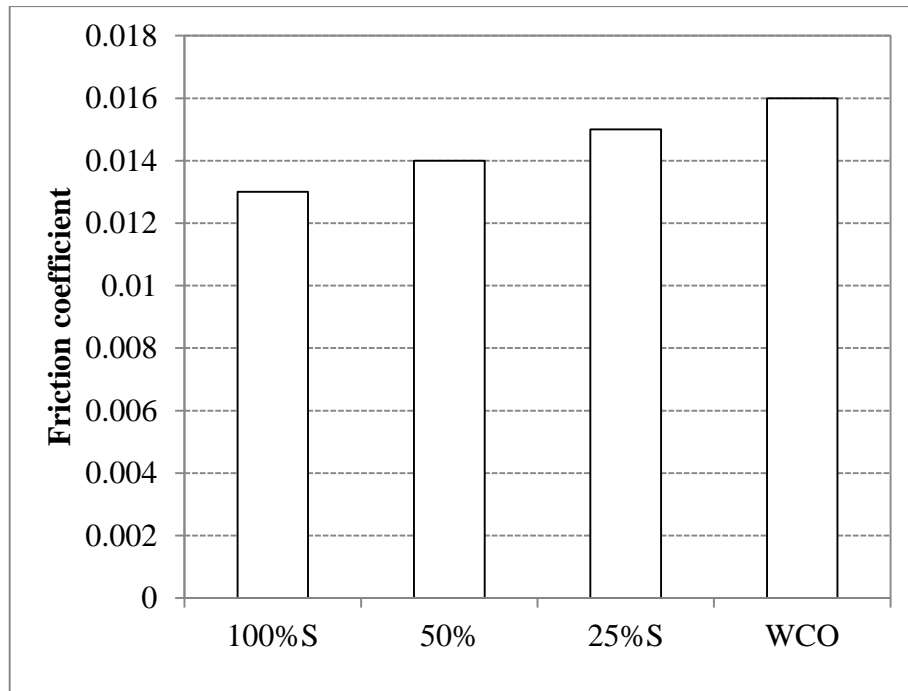


Figure 6.9: Friction coefficient in journal bearings for different blends

6.5 Chapter Summary

This chapter introduced the potential of WCO and its blends for journal bearing applications. The experiment results concluded that WCO and its blends are a very competitive candidate compared to industrial oils. Pressure and temperature distributions showed comparable results across all the selected blends of lubricants. In comparing the current results to those of some industrial oils in the available literature, WCO was found to have the ability to be used as a lubricant for journal bearings. Further study on the chemical modifications and the oil degradation is recommended for future work.

Chapter 7: Prediction of Dry Wear Performance Using Artificial Neural Networks

7.1 Introduction

This chapter comprehensively examines the accuracy and prediction performance of artificial neural networks (ANNs) for friction, wear, interface temperature and roughness of metal/metal adhesive wear. The methodology and development of the model are also described. The study is divided into two groups focusing on the friction coefficient prediction and on the wear, interface temperature and roughness.

7.2 Development of the ANN Model

7.2.1 Selection of the Model

In developing the model, the feed-forward neural network approach was used in prediction with different training functions and numbers of input data used to study the optimum performance of the model. Matlab R2012B was used for the simulation. The Feed-forward neural network approach has recently been used by many researchers for tribological parameter prediction due to the non-linearity of the problems investigated (Abdelbary et al. 2012; Busse & Schlarb 2013; Li, Zhu & Xiao). In this approach, after training the model, the input moves in only one direction, forward, through the hidden layer and then to the output layer, i.e. there are no loops (Meireles, Almeida & Simões 2003). In developing the feed-forward, one and two hidden layers are used to gain the optimum model in terms of the number of hidden layers.

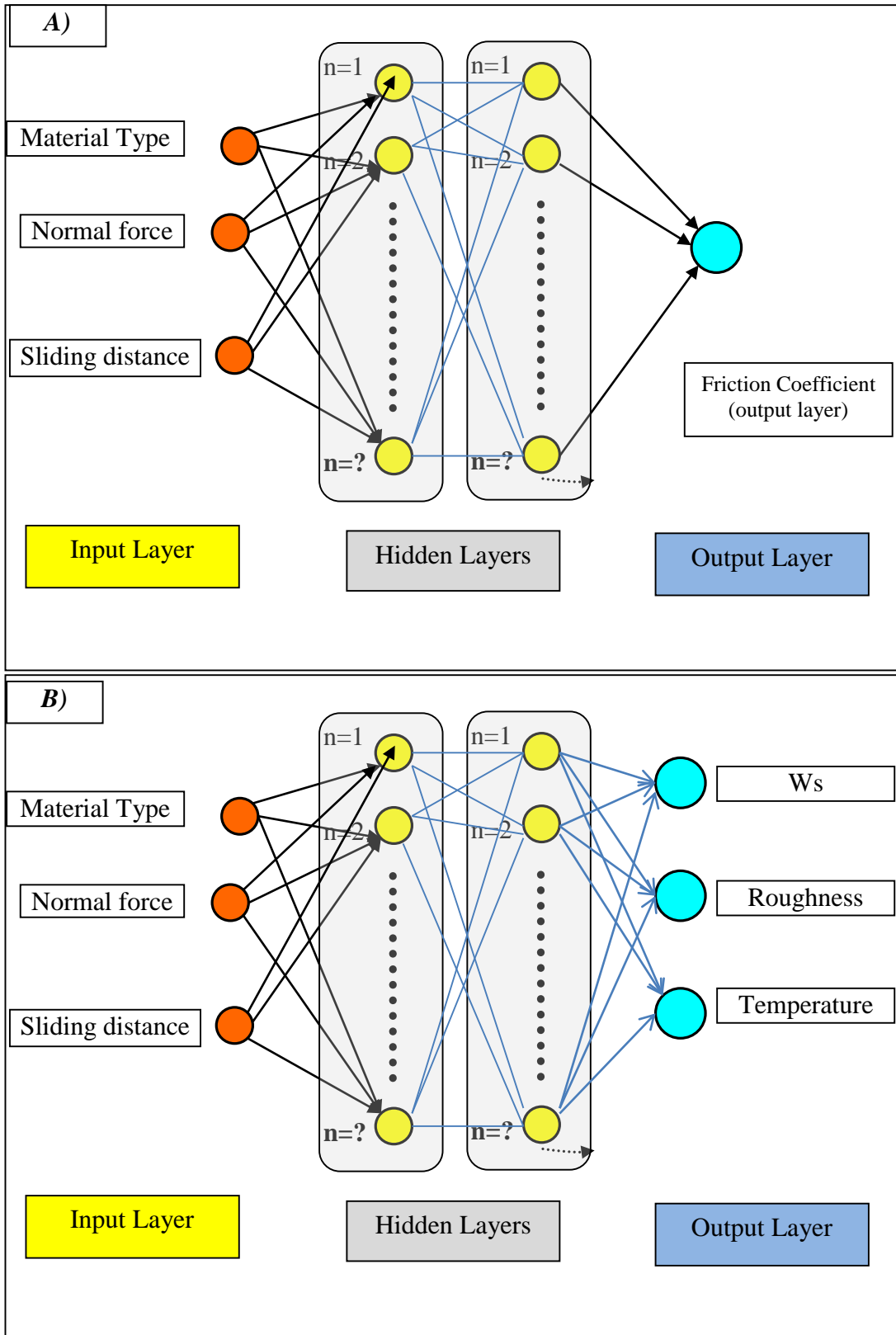


Figure 7.1: ANN configuration for the prediction of A) friction coefficient, and B) specific wear rate (W_s), surface roughness, interface temperature

7.2.2 Experimental Data and ANN Development Method

The input data for the model was obtained experimentally (Chapter 4) and the average of the three tests was used as the input for each parameters. A sample of the organised data is given in Table 7.1. The rest of the data was presented in Chapter 4. As there were many parameters to be considered in the prediction to identify the optimum approach, “nntool” was used to generate different networks using the same input data (Figure 7.2). Once the data was arranged in an Excel file, the input and output data was imported to the window and the network developed there.

Table 7.1: Sample of the Input and Output Data for Brass at 50 N Applied Load and Different Sliding Distances

Sliding distance, km	Specific wear rate, $10^{-5}\text{mm}^3/\text{N.m}$,	Temperature, °C	Roughness, Ra, μm
0	0	24	0.23
0.084	4.450113	26	0.24
0.168	2.79195	27	0.27
0.252	2.380952	28	0.25
0.336	2.069161	29	0.29
0.42	1.825397	30	0.34
0.504	1.639267	31	0.32
0.588	1.465824	32	0.31
0.672	1.325113	33	0.29
0.756	1.218821	35	0.32
0.84	1.11678	37	0.37
2.52	0.582955	38	0.42
4.2	0.522676	39	0.39
5.88	0.343375	40	0.4
7.56	0.350844	41	0.41
10.92	0.335121	42	0.48

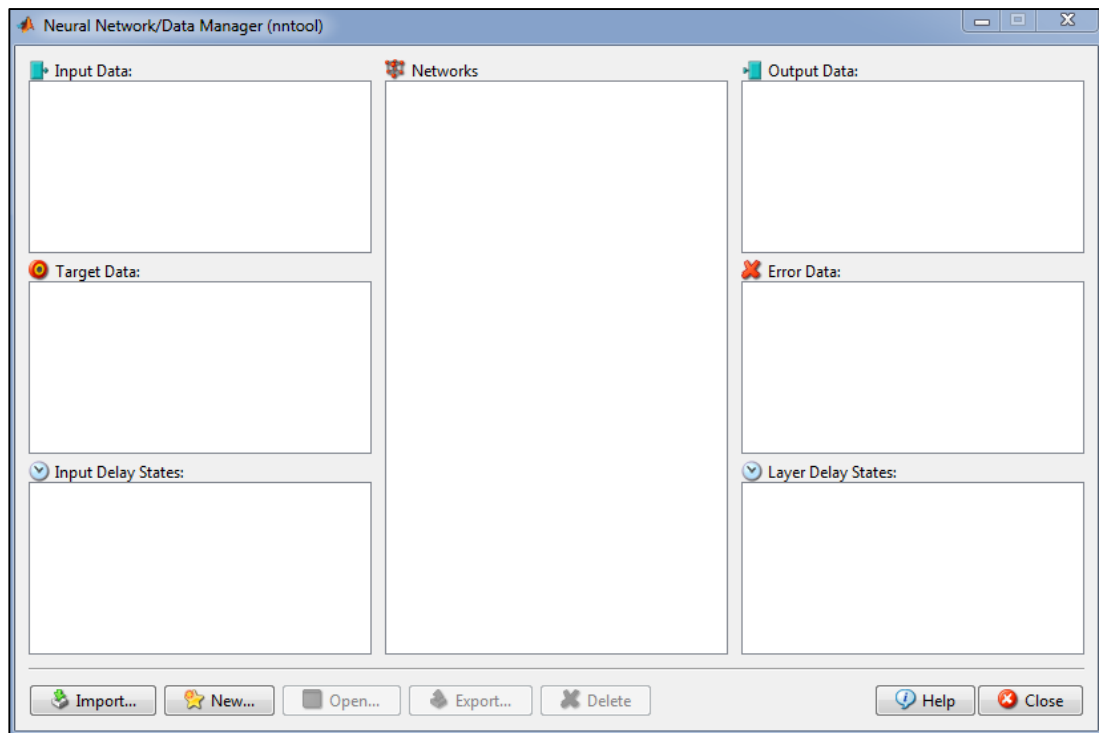


Figure 7.2: The method used in the current work for developing the ANN

7.2.3 Selection of the ANN Parameters

In developing and selecting of the ANN parameters (training function, adaption learning function, performance function, number of layers, transfer function and number of neuron), the ANN tool box is a user-friendly way to set up those elements. Figure 7.3 shows an example of an ANN that contains two inputs and four outputs with 10 neurons in the first hidden layer and four neurons in the second hidden layer. The Transing function was used for both layers. In the current study, all types of functions were tested with a different numbers of neurons for one and two hidden layer models.

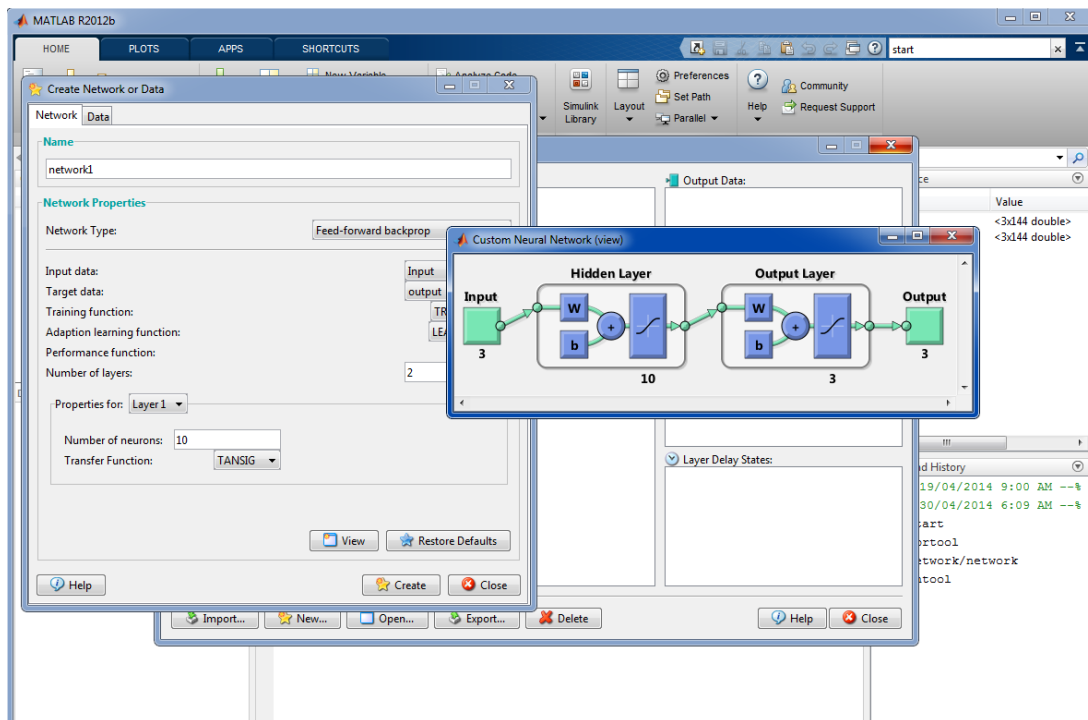


Figure 7.3: Initial ANN Model developed considering two hidden layers of TRAINBFG training function

7.2.4 Training the ANN Model

Figure 7.4 shows an example of the training procedure for an ANN model. In the training several parameters were provided as outputs to indicate the performance of the ANN. For example, Figure 7.5 shows the output of the training indicating time, the performance of the model in terms of training, validation, test, and the combination of all via the regression function. Furthermore, performance can be determined through best validation performance via mean squared error (MSE), and training status in terms of the number of checking, learning rate and epochs. However, due to the fact that the output of the model has different parameters, MSE was not recommended. The current study focused on the training, validation, testing, and the combination of all via regression and the MSE as recommended by many published works (Cheng et al. 2013; Elangasinghe et al. ; Zerrouki, Aifa & Baddari 2014).

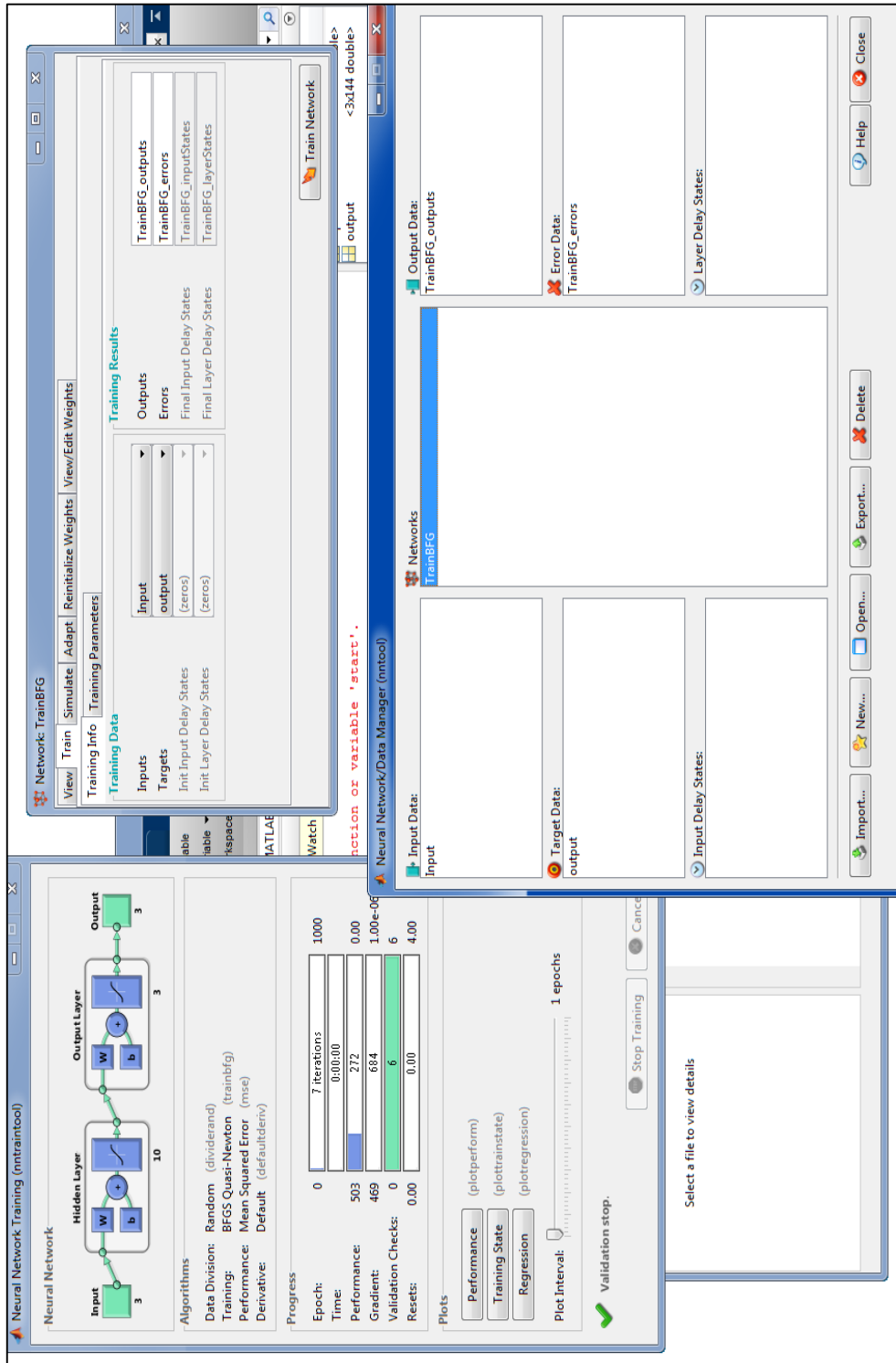


Figure 7.4: Training process for TrainBFG function

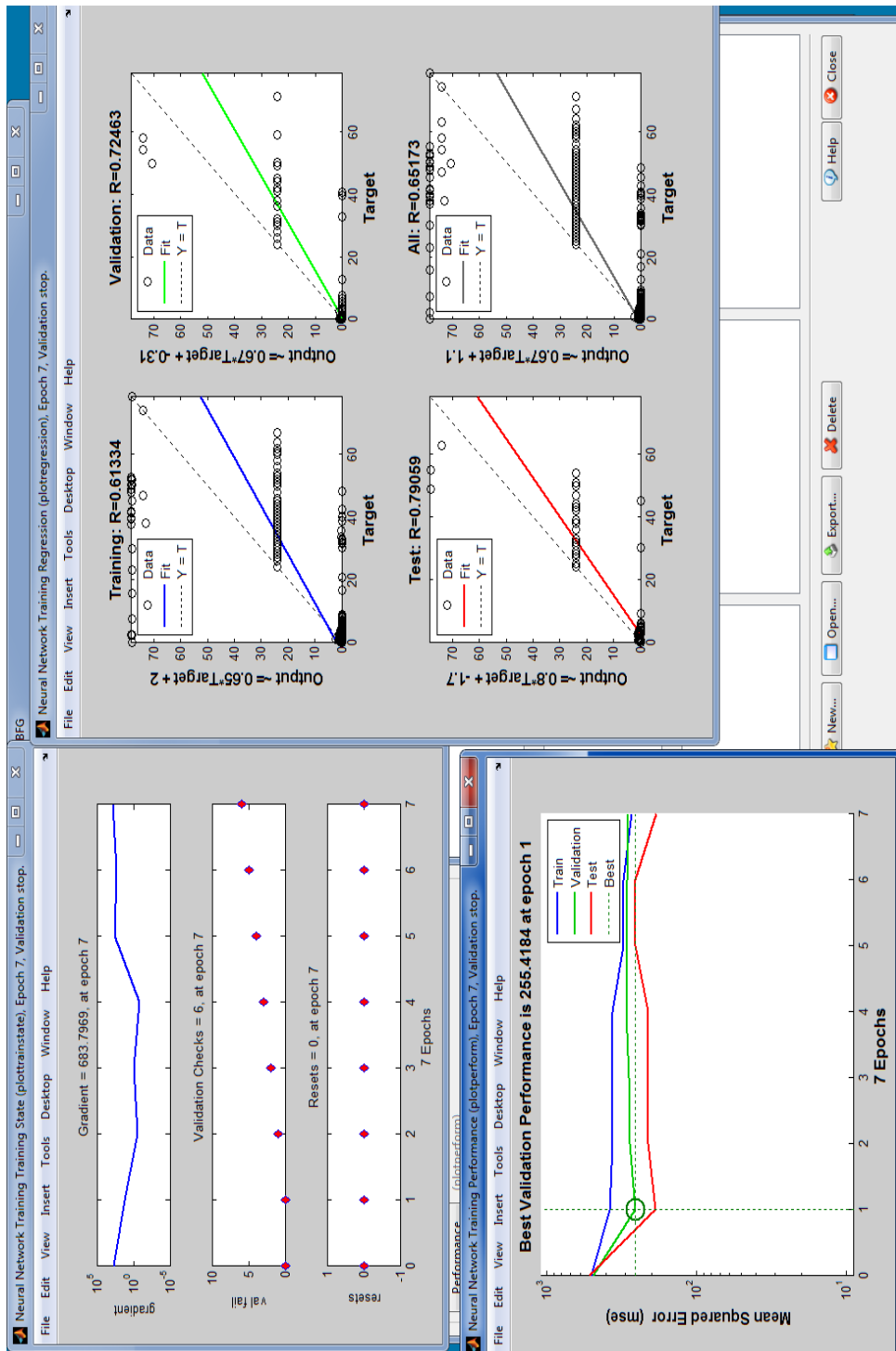


Figure 7.5: Train output for TrainBFG function

7.2.5 Scope of Prediction

The prediction of the tribological parameters was divided into two groups: a) covering the specific wear rate, roughness, and interface temperature and b) focusing on the friction coefficient only. In both groups, the input parameters were material type, load and sliding distances. A comprehensive study was conducted on the first group to identify the optimum model for prediction. The same model was used for predicting the friction coefficient. Several steps were followed to gain the optimum model:

1. For the tribological parameters (a non-linear complex problem), the feed-forward back propagation network needed to be considered in developing the model
2. Input and target data were imported to the model
3. Different training functions were considered to gain the optimum training function
4. Different adaption learning functions were considered to gain the optimum
5. Different performance functions were considered to gain the optimum
6. The number of layers were also considered. In the literature one or two layers are recommended (Nasir, T et al. 2010)
7. Number of neurons was considered to gain the optimum.

7.3 Optimisation of the ANN Model

At the initial stage of the model, all the parameters of the ANN model will be discussed and optimised for predicting the specific wear rate, temperature and the roughness of the materials for different sliding distances, applied load and materials.

7.3.1 ANN for Wear, Temperature And Roughness Prediction

7.3.1.1 Optimum Training Function

The first model was developed and consisted of two hidden layers. The first hidden layer contains 10 neurons and the second contains three neurons as the default option by the Matlab. To investigate the training function performance, different training functions were considered to gain the optimum, i.e. TRAINBFG, TRAINBR, TRAINCGF, TRAINCGB, TRAINGD, TRAINGDM, TRAINDGA. The definition of each function is given in Table 7.2. The details and algorithm of each training function in the section are given in approximate nonlinear functions and generalised complex data relationships in MATLAB tool. For each training function, the performance of the model was determined based on time, training, validation, test and the combination of all in terms of 'R', which indicates the relationship between the outputs and targets. The details of the results are given in Appendix B.

Table 7.2: Terms of the Training Function

TRAINBFG	BFGS quasi-Newton backpropagation
TRAINBR	Bayesian regulation backpropagation
TRAINCGB	Conjugate gradient backpropagation with Powell-Beale restarts
TRAINCGF	Conjugate gradient backpropagation with Fletcher-Reeves updates
TRAINCGP	Conjugate gradient backpropagation with Polak-Ribière updates
TRAINGD	Gradient descent backpropagation
TRAINGDA	Gradient descent with adaptive learning rate backpropagation
TRAINGDM	Gradient descent with momentum backpropagation
TRAINGDX	Gradient descent with momentum and adaptive learning rate backpropagation
TRAINLM	Levenberg-Marquardt backpropagation
TRAINOSS	One-step secant backpropagation
TRAINRP	Resilient backpropagation
TRAINSCG	Scaled conjugate gradient backpropagation

The minimum achieved error in the prediction process was represented by the performance of the model. The performances of the training functions are presented in Figure 7.6, showing the training, validation, testing and combination. The time consumed by the functions are all the same (less than a second) except TRAINCGP, which consumed about 200 sec for the trainings. In term of performance, Figure 7.6 clearly shows that TRAINSCG had the best performance compared to the others. Similar findings were reported by Vijay, Pai and Sriram (2010) when an ANN was used to monitor rolling element bearing using vibration signals. Moreover, Nasir, T et al. (2010) reported similar findings when ANN was used to predict the friction coefficient of glass fibre reinforced polyester composites in different orientations considering different operating parameters. In light of this, TRAINRP is recommended for future ANN development for tribological application and it will be used for the rest of this study. Its main advantages are that it updates weight and bias values according to the resilient back propagation algorithm and it can train any network as long as its weight, net input and transfer functions have derivative functions (Guide 2002; Pan & Lee 2012).

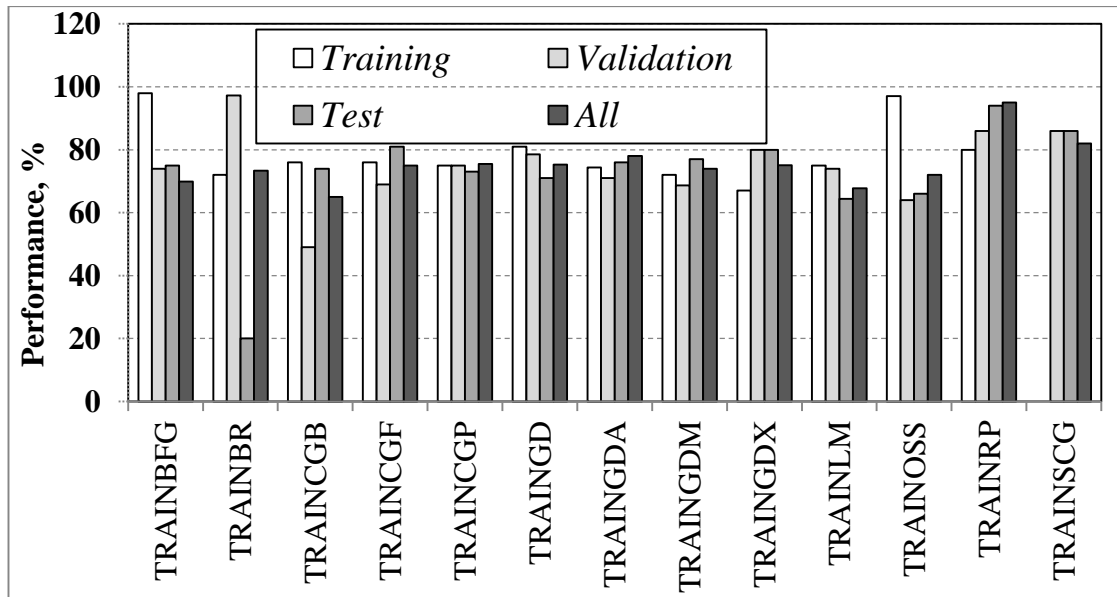


Figure 7.6: The performance of the ANN model training function to predict the specific wear rate, interface temperature and roughness for different sliding distances, materials and applied loads

7.3.1.2 Optimum Adaption Learning Function

In the previous section, the selection of the optimum training function was based on the LEARNGD adaption function. There were two learning functions in the ANN modelling: the LEARNGDM or LEARNGD. The differences between them were that LEARNGDM calculates the weight change for the neuron from the neuron's input and error, the weight learning rate and momentum constant MC, according to gradient descent with momentum. Meanwhile, LEARNGD determined the weight change for the neuron from the neuron's input and error, and the weight learning rate according to the gradient descent. In this study, both functions were used with the optimum training function (TRAINRP).

Figure 7.7 displays the regression of two networks developed with a forward back propagation network using TRAINRP as a training function and a) LEARNGD or b) LEARNGDM as adaption learning function. In the figures, the test, validation, training were all are almost the same, i.e. LEARNGD introduces $R = 0.95$, while with LEARNGDM, $R = 0.94$. Based on this, LEARNGD will be used as the adaption function for future models.

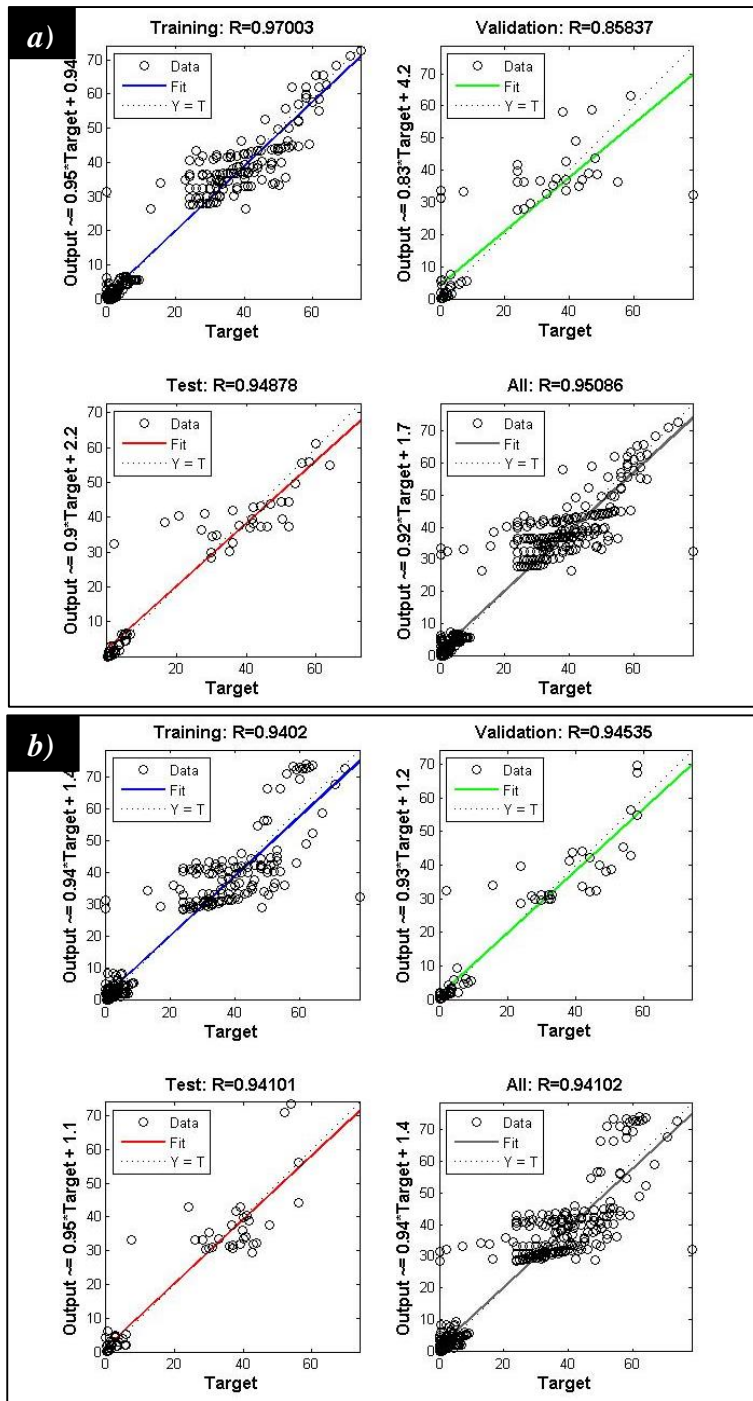


Figure 7.7: The performance of the feed-forward back propagation network using TRAINRP as training function and a) LEARNGD or b) LEARNGDM as adaption learning function

7.3.1.3 Optimum Performance Function

There are three performance functions in the ANN models (Matlab tool box): MSE (Mean squared normalised error performance), MSEREG (consists of MSE and biases), SSE (Sum squared error performance). To identify the optimum performance of the feed-forward back propagation network using TRAINRP as a training function and LEARNGD as an adaption learning function, the performance of the network was tested using three different performance functions. The performance (%) of each model was determined based on the mean square error $\times 100$. The results are presented in Figure 7.8 showing the performance of the network using the three

performance functions. The figure reveals that there is no remarkable difference between the three functions, but MSEREG shows slightly better performance compared to MSDE and SSE, which was due to the consideration of the biases in the performance. Therefore, MSEREG will be used as the performance function for the future work to identify the optimum number of layers.

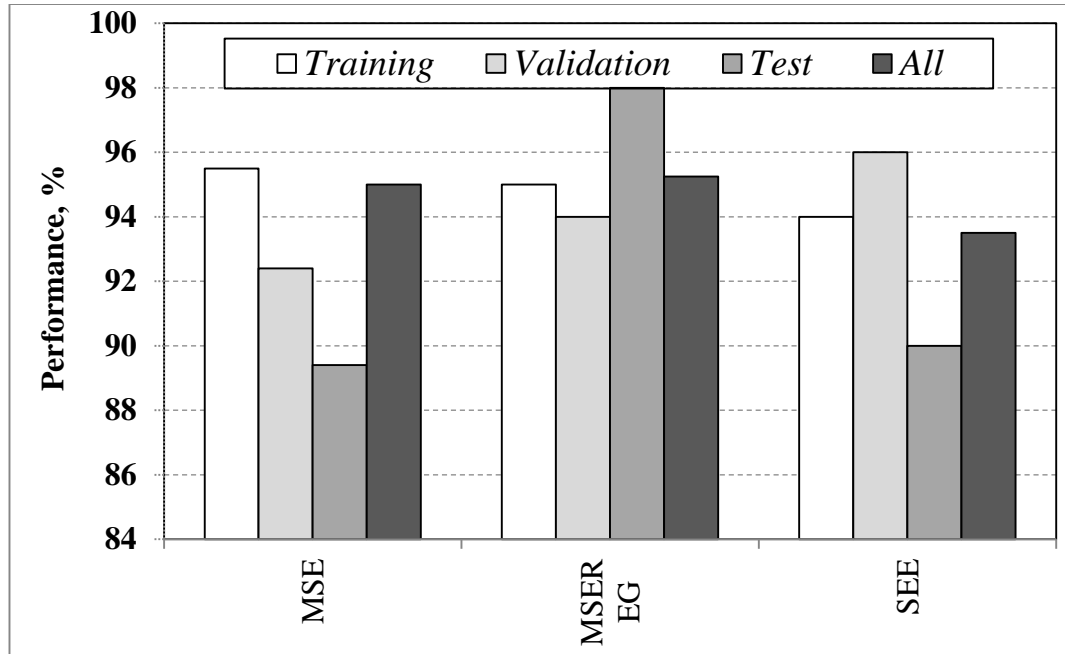


Figure 7.8: The performance of the feed-forward back propagation network using TRAINRP as training function, LEARNGD as adaption learning function with different performance functions.

7.3.1.4 Optimum Numbers of Neurons

In most of the works reporting the possibility of using ANN models in predicting different engineering problems, (Lingaraju et al. 2011; Liu et al. 2014; Zhang et al. 2003; Zhang, Friedrich & Velten 2002), the number of neurons greatly influenced the developed models' performance and there is no clear conclusion on the optimum number of neurons. However, all of these works reported that optimization needs to be considered. In some cases, a small number of neurons is not able to predict the data; in addition, a larger number may also fail to predict the data as well.

To find the optimum number of neurons in the ANN model, the feed-forward back propagation network using TRAINRP as training function LEARNGD as adaption learning function, and MSEREG performance function was developed with different numbers of neurons (2-20). The performance of the models is displayed in Figure 7.9 showing the training, validation, test and the combination of all performance. The figure indicates that 10 neurons can be considered to be the optimum numbers of neurons in ANN model.

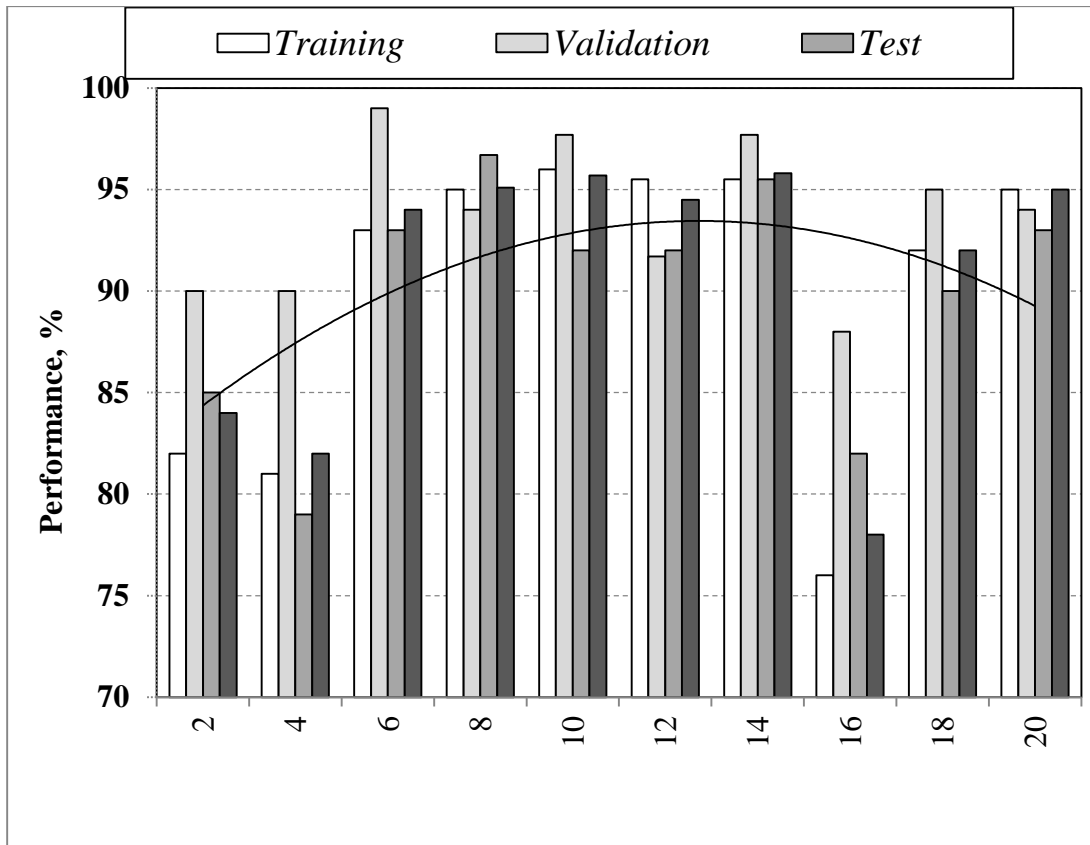


Figure 7.9: The performance of the feed-forward back propagation network using TRAINRP as training function, LEARNGD as adaption learning function and MSEREG as performance function with different numbers of neurons

7.3.1.5 Summary of the Optimum ANN Model for Wear, Temperature and Roughness

In light of the above sections, the optimum ANN model is a feed-forward back propagation network using TRAINRP as the training function, LEARNGD as the adaption learning function, MSEREG as the performance function with 10 neurons. In this model, the performance of the model is shown in Figure 7.10. The figure shows the performance of the ANN in predicting the specific wear rate, temperature and the roughness as a function of the sliding distance with one input of sliding distance. One can see that the R was always greater than 0.9 which represents good performance of the optimum model.

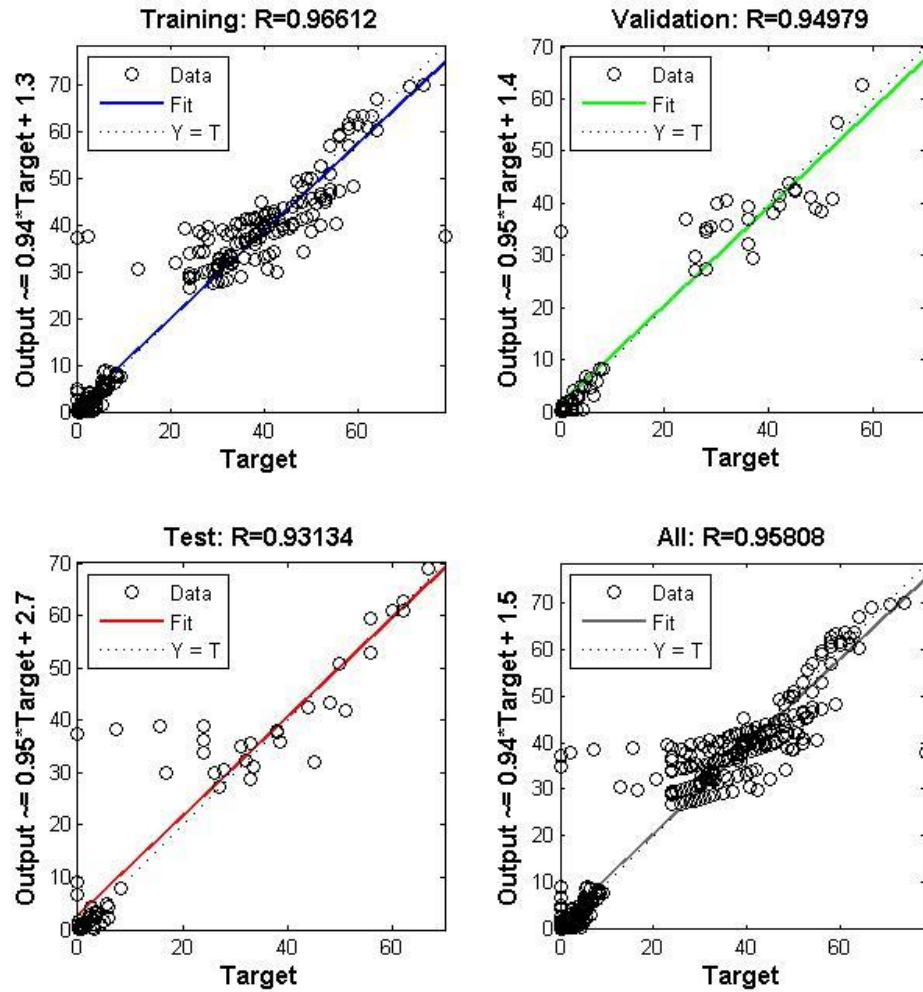


Figure 7.10: The performance of the optimum model to predict the specific wear rate, interface temperature and the roughness under different applied loads and sliding distances

7.3.2 Optimum ANN Model for Friction Coefficient

In developing the ANN model to predict the specific wear rate, interface temperature and roughness of the surface, it was found that feed-forward back propagation network using TRAINRP as the training function, LEARNGD as the adaption learning function, and MSEREG as the performance functions with 10 neurons is the optimum. For developing the ANN model for friction coefficient prediction, the same model is used. However, due to the huge data (about 12000 for each tested parameter) in the friction coefficient, the training of the ANN was arranged in several stages, i.e. each data for each material was trained individually for the same model. In the trainings of the specific wear rate, interface temperature and the roughness, the training time was less than one sec. Meanwhile, in training the ANN with one set of the friction coefficient, about 7 minutes was required for the trainings, Figure 7.11. Furthermore, the performance of the ANN is relatively poor with the first set of the data, Figure 7.12a. Moreover, the ANN performance significantly deteriorated when the model trained with all the data, Figure 7.12b.

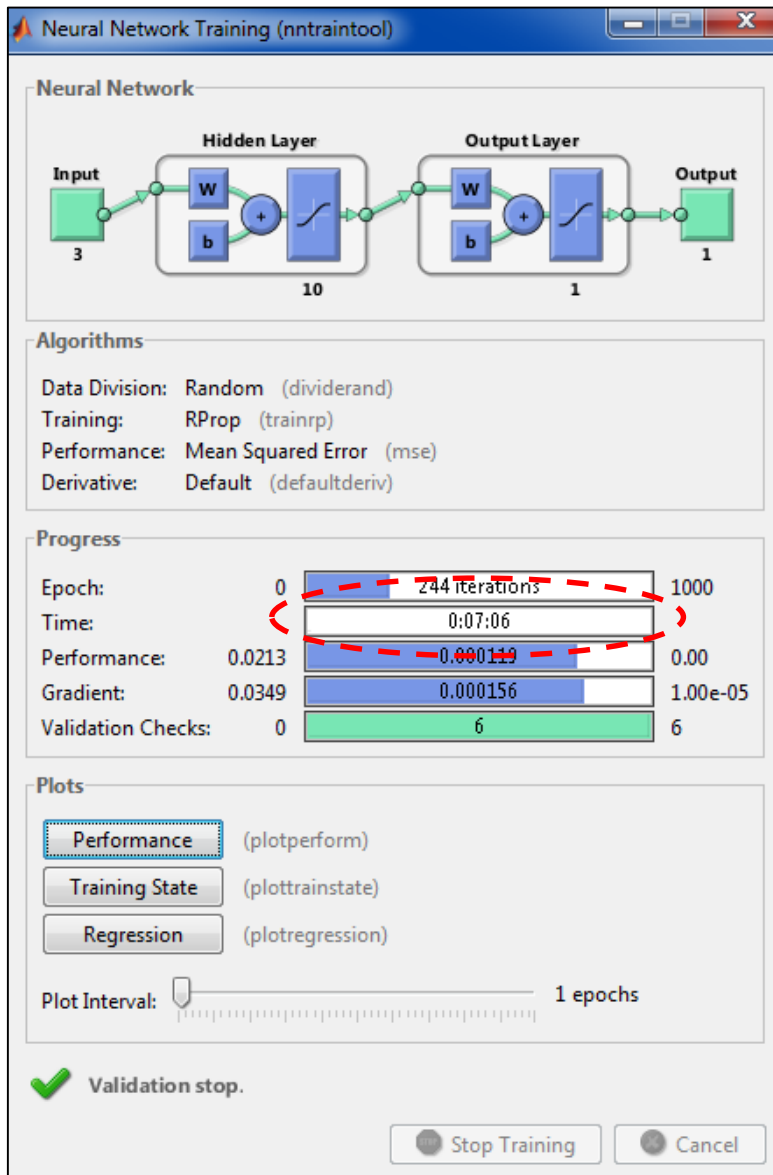


Figure 7.11: Required training time for ANN to predict the friction coefficient

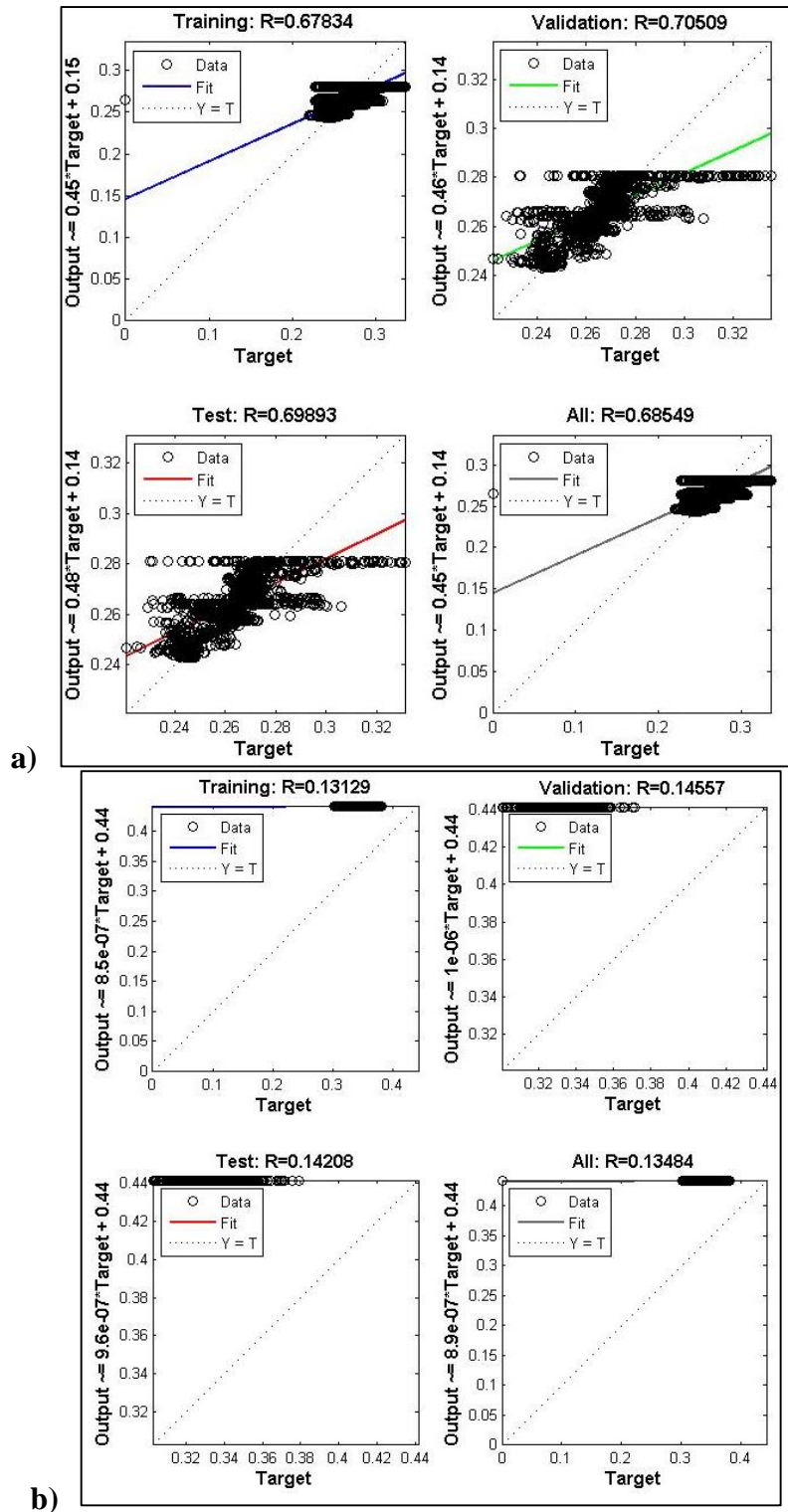


Figure 7.12: Regression of ANN results in predicting the friction coefficient with different numbers of data

7.3.2.1 Optimum Training Function for Friction Coefficient Prediction

Based on the findings in the previous section, it was necessary to identify the optimum training function for the friction coefficient prediction. Therefore, a similar procedure in finding the optimum training function to the specific wear rate was used for the friction coefficient. The performance of the ANN against a different number of frictional data is presented in Figure 7.13 for different training functions. The

figure clearly shows that the increase in the number of data above about 60000 significantly worsened the ANN model performance with the usage of training function. From the literature, it has been reported that the increase in the number of data improves the prediction and training performance of the ANN (Muthukrishnan & Davim 2009; Nasir, T et al. 2010; Zhang & Friedrich 2003). Meanwhile, the current study found that the higher number of data \gg 25000 worsens the performance of the ANN for all the available training functions. It is suggested that an ANN model be developed for individual materials and parameters to reduce the input data which may improve the prediction performance.

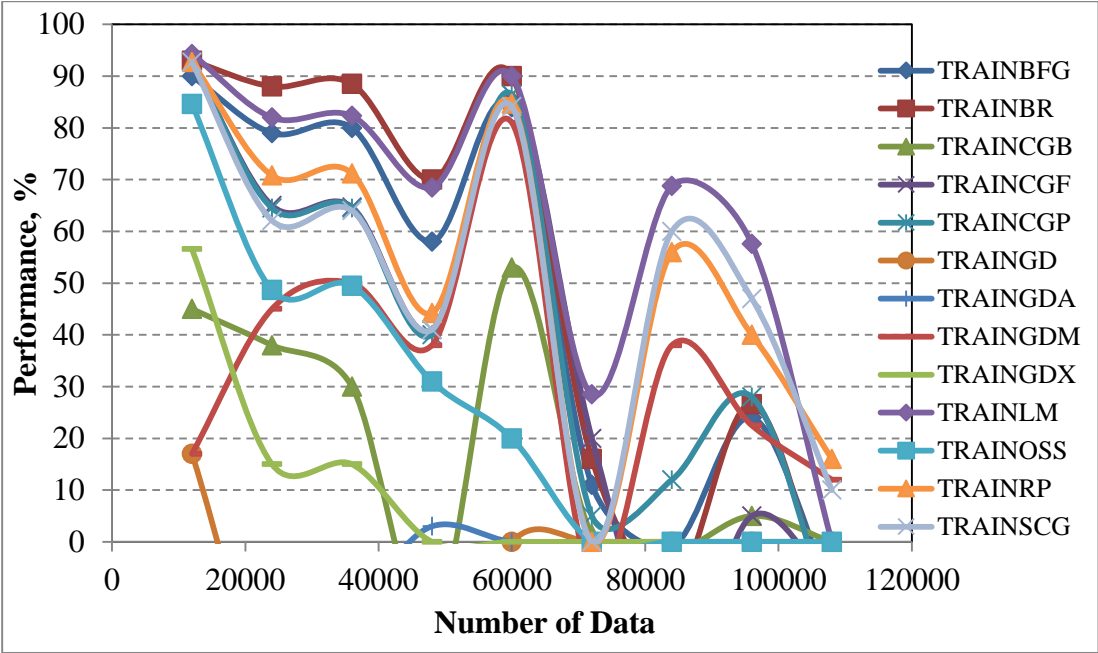


Figure 7.13: Performance of the ANN to predict the friction coefficient using different training functions and numbers of data

Figure 7.14 displays the performance of the frictional ANN models for different training functions considering individual input data for each operating parameter for the brass material only. One can see that there are remarkable differences between the performance of the ANN with all the input data (Figure 7.13) and applied loads (Figure 7.14) since the ANN performs much better with relatively less data. This will be recommended for future work and will be used for the future of this study as well. In other words, for the friction coefficient prediction, less data is required for the prediction. The figure also indicates that TRAINBR performs much better than others which are recommended for this work as well.

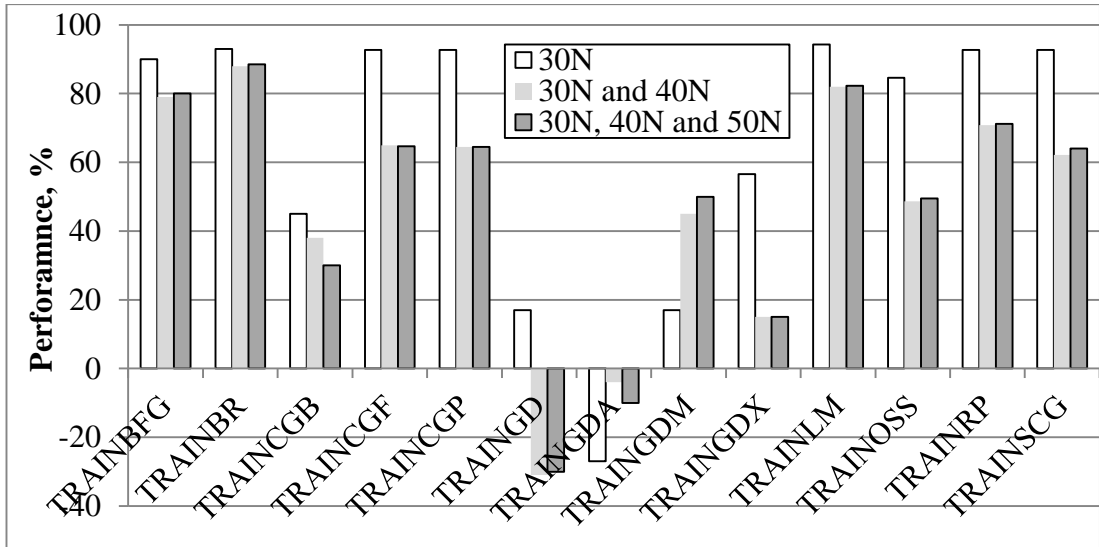


Figure 7.14 Performance of the ANN to predict the friction coefficient using different applied loads

7.3.2.2 Optimum Performance Function for Friction Coefficient Prediction

For the influence of the performance function on the frictional prediction using the ANN based on the BR training function, the performance of the ANN model was tested using MSE, MSEREG and SEE performance functions and the results are displayed in Figure 7.15. The figure shows that both MSE and SEE exhibits the same high performance for the ANN compared to the MSEREG. In the development of the ANN to predict the wear performance, MSEREG was the optimum function for the highest performance of the ANN compared to the MSE and SEE. In other words, MSEREG is not a suitable performance function when the data is large in amount compared to the MSE. For the friction coefficient prediction model, MSE was selected as optimum function. In the next section, the optimum number of neurons is discussed.

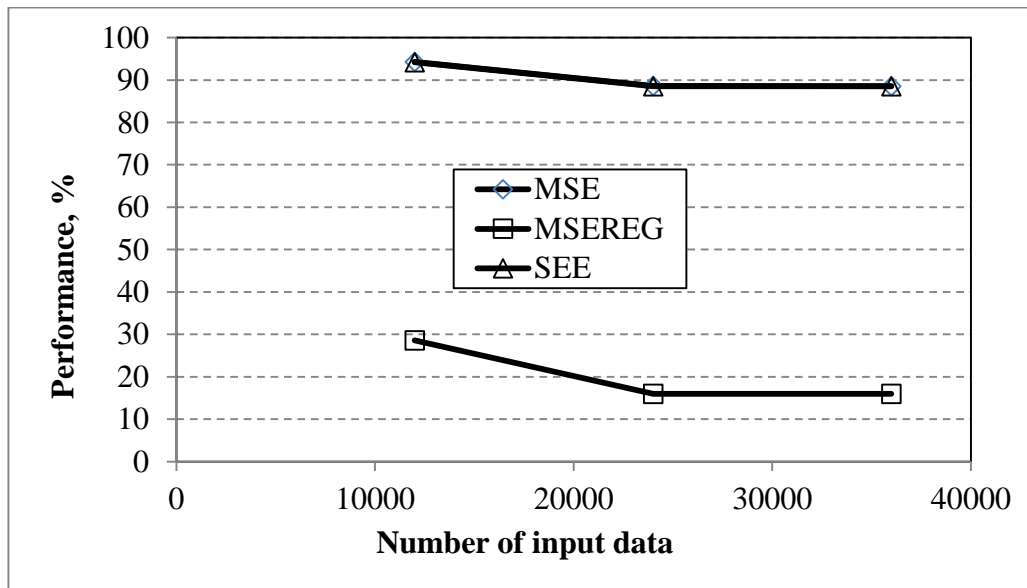


Figure 7.15: Performance of the ANN to predict the friction coefficient using BR training function for different performance functions and different numbers of input data

7.3.2.3 Optimum Number of Neurons in the Hidden Layer for Friction Coefficient Prediction

For the influence of the number of neurons on the performance of the ANN for predicting the friction coefficient, Figure 7.16 shows the influence of number of neurons in the hidden layer on the performance of the ANN model. For the three sets of input of data, increase in the performance to the ANN model could be seen with the increase in the number of neurons especially at the first range of the trend. An increase in the number of neurons more than 10 neurons showed no remarkable impact on the performance of the ANN model. When the ANN model was developed for wear prediction, an increase in the number of neurons by more than 10 neurons slightly reduced the performance of the ANN model (Figure 7.9).

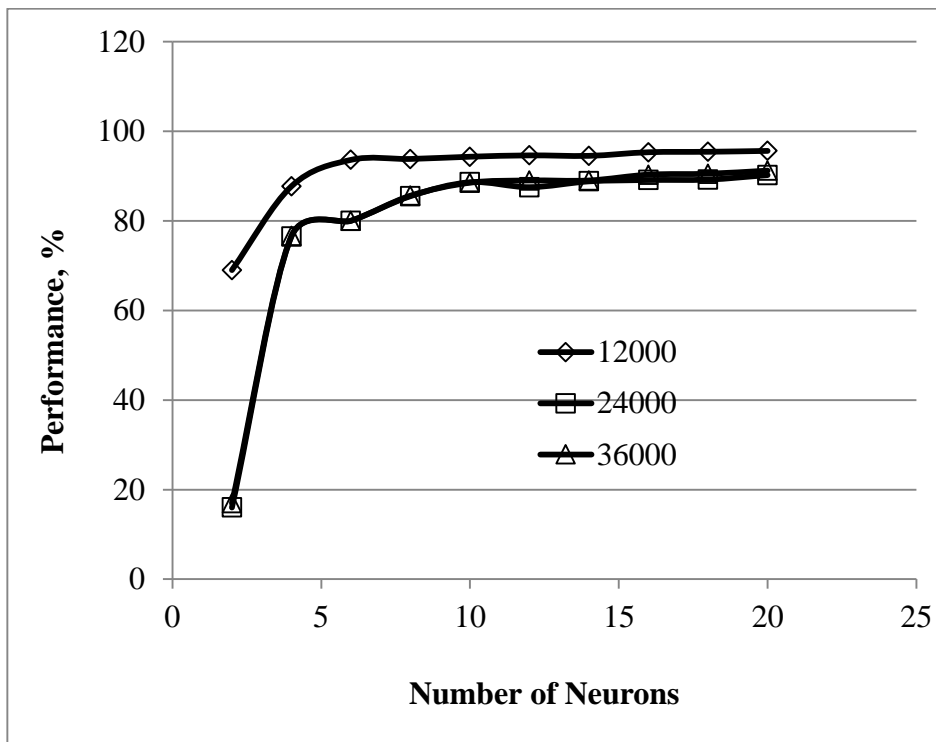


Figure 7.16: Performance of the ANN to predict the friction coefficient using BR training function and MSE performance function with different numbers of neurons and input data

7.3.2.4 Summary of the Friction Coefficient Prediction using the ANN

In light of the above sections, the optimum ANN model for the friction coefficient prediction consists of feed forward back propagation, training function of TRAINBR, adaption learning function of LEARNGD performance function of MSE and 10 neurons in the hidden layer. The regression of the ANN model is presented in Figure 7.17 illustrating that total performance is about 87.5 %, and the error percentage is about 12.5%. Further to this, Figure 7.18 shows the variation in the friction coefficient for both the real experimental data and the predicted results. It is obvious that there is an error in the prediction and this leads to a conclusion that sometimes the ANN approach is not a good technique for predicting huge amounts of data such as friction coefficients. In the literature, the frictional data has been reduced to be suitable for the ANN approach (Nasir, T et al. 2010) In the current study, the frictional data is about 12000 for each operating parameters which makes it difficult and complicated to predict using an ANN. In the ANN the weight in the

configuration may impact on the prediction results. In Figure 7.18, it seems that the predicted data is always higher than the measured which is due to the default weight used in the model. Reduce the value of the weight is not recommended as it may impact on other prediction values of the friction coefficient.

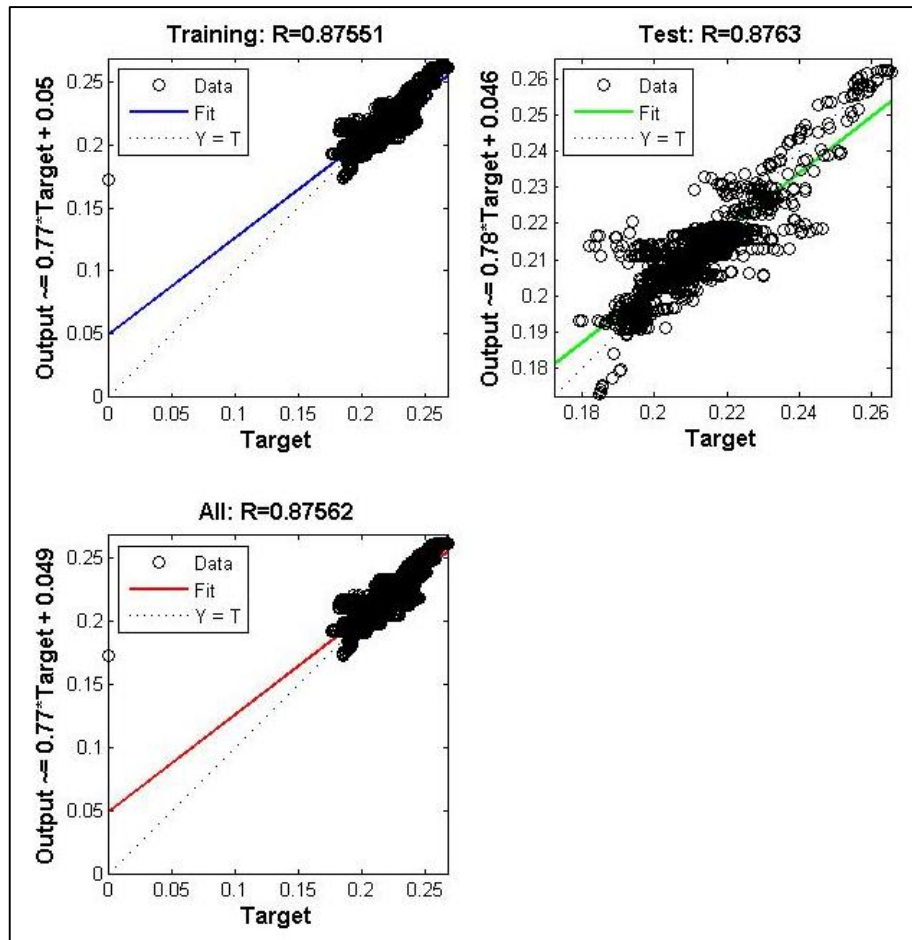


Figure 7.17: Performance of the optimum ANN mode for the friction coefficient prediction

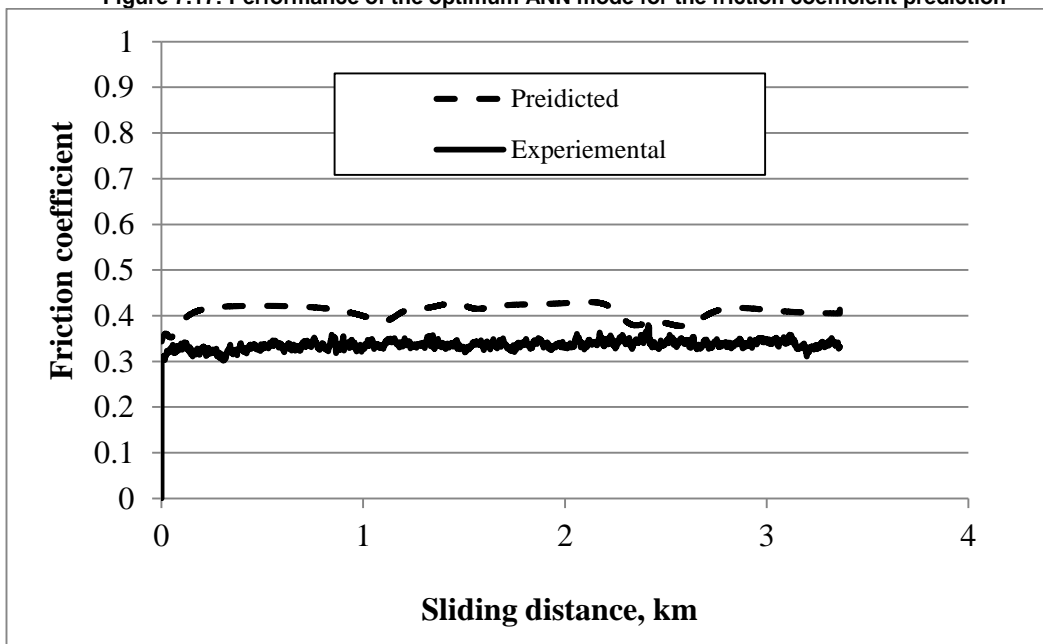


Figure 7.18: Real experimental data for friction coefficient of aluminium at 30 N applied load in comparing to the predicted data

7.4 Prediction of Specific Wear Rate

The experimental work was conducted at different applied loads of 30 N, 40 N and 50 N, sliding distance (0 – 10.8 km) for brass, the aluminium and mild steel materials. The results of the experiments were specific wear rate, interface temperature and the surface roughness. The experimental data was used to build the ANN model. For the specific wear rate, interface temperature and roughness prediction of those materials are displayed in Figures 7.19-7.21 at different operating parameters. Different applied loads of 35 N, 45 N and 55 N were selected for the prediction at the same sliding distance. From the literature, an ANN approach can be used to predict data within the input range (Wang, Ma & Wu 2013; Yang et al. 2013; Yousef, Mourad & Hilal-Alnaqbi 2011).

For the brass material, Figure 7.19 shows the specific wear rate, roughness of the rubbed brass surface after testing and interface temperature against sliding distances for both predicted and experimental data. The figure shows that the trend of the specific wear rate at the applied load of 35 N and 45N was similar to the experimental data which indicates that the ANN approach is able to identify the trend of the data with the input range. However, with the applied load of 55 N (outside the range of the input data), the trend of the specific wear rate seems to be incorrect, since there is an increase in the specific wear rate with the increase of the sliding distance. From the experimental works and literature, steady state can be reached after a certain sliding distance. In the current experimental data, the steady state was achieved after about 3-4 km which was predicted for the 35 N and the 45 N applied load as well but failed with the 55N since it was outside the range of the input. In other words, it can recommend that ANN is able to predict the trend and behaviour of the specific wear rates for the material considering the fact that the parameters should be within the range of the input data (Wang, Ma & Wu 2013; Yang et al. 2013; Yousef, Mourad & Hilal-Alnaqbi 2011). Similar to the specific wear, the interface temperature and the roughness prediction showed some disturbance in the data when the applied load of 55N was used compared to the 35 N and 45 N. In addition, the reason is that the 55 N applied load was out of the input data range associated with the fact that at the running in stage too much disturbance in the frictional values experimentally observed. This has been reported previously when the friction coefficient of polymer composites was predicted using ANN models (Nasir, T et al. 2010).

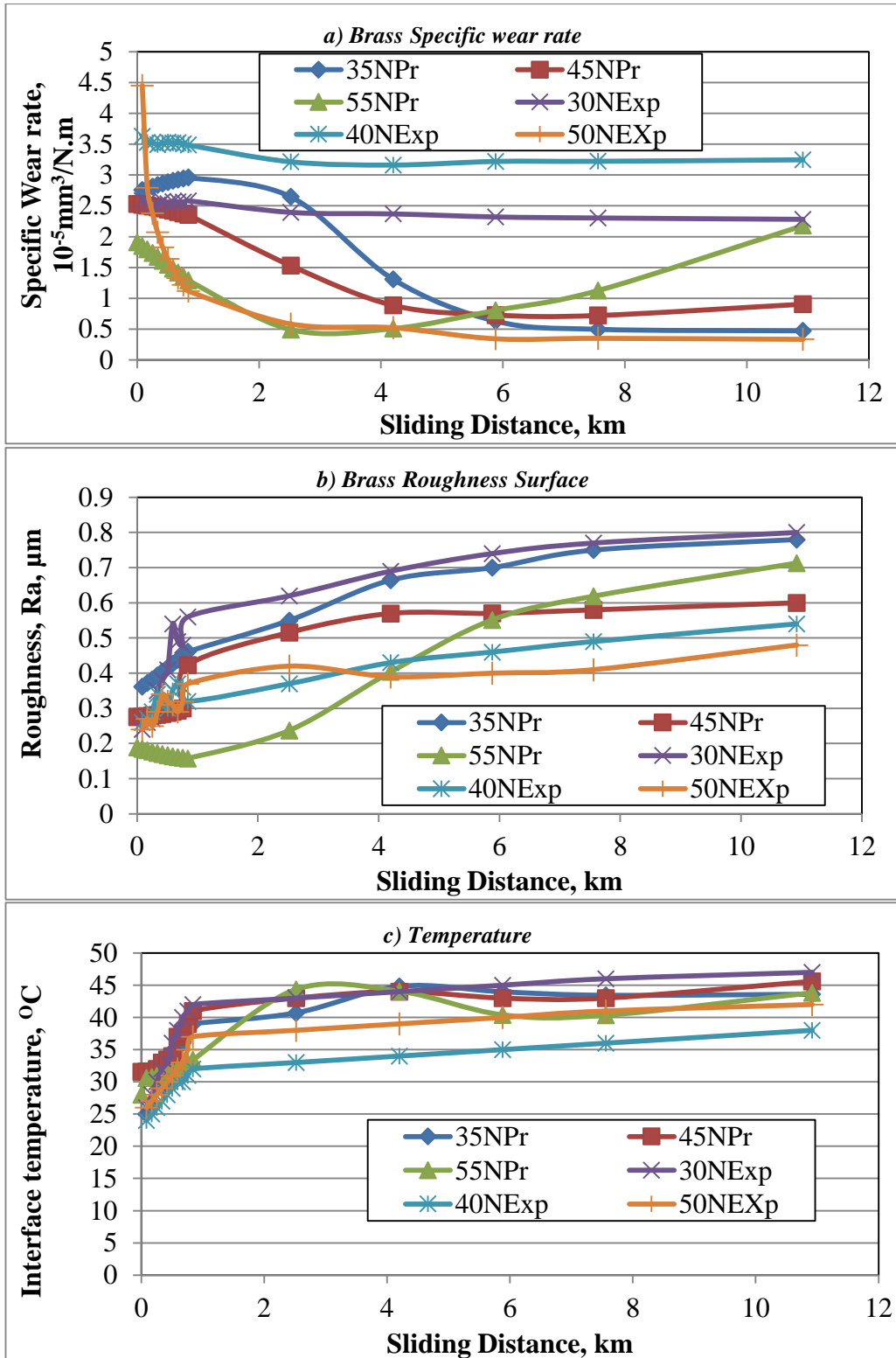


Figure 7.19: Real experimental data and predicted data for brass materials at different operating parameters

Similar to the brass prediction data, aluminium showed similar trends for the specific wear rate, roughness, and interface temperature, Figure 7.20. The trend of the specific wear of the predicted data was close to the experiment. One can see that the prediction of the 55 N applied load was still within the experimental data and there was slight disturbance in the trend after about 6 km. There could be two different reasons for these disturbances in the specific wear rate which are either the ANN

understood that the steady state of the specific wear rate was not yet reached or it was a wrong prediction technique. From a technical point of view, the predicted data under the load of 35 N and 45 N can be accepted as it is in agreement with the ones obtained for the brass. However, for the 55 N since it was outside the range and the trend is not clear, it can be omitted and cannot be accepted in understanding the wear behaviour of material.

The mild steel prediction results are displayed in Figure 7.21. The figure shows that the trend of the specific wear rate and the values of the predicted data were close to the experimental one except for the 55 N applied load which was out of the input range, i.e. similar findings were concluded in the case of the brass and the aluminium materials. However, the predicted data for the roughness and the interface temperature were very close to the experimental in term of trend and value for all the applied loads.

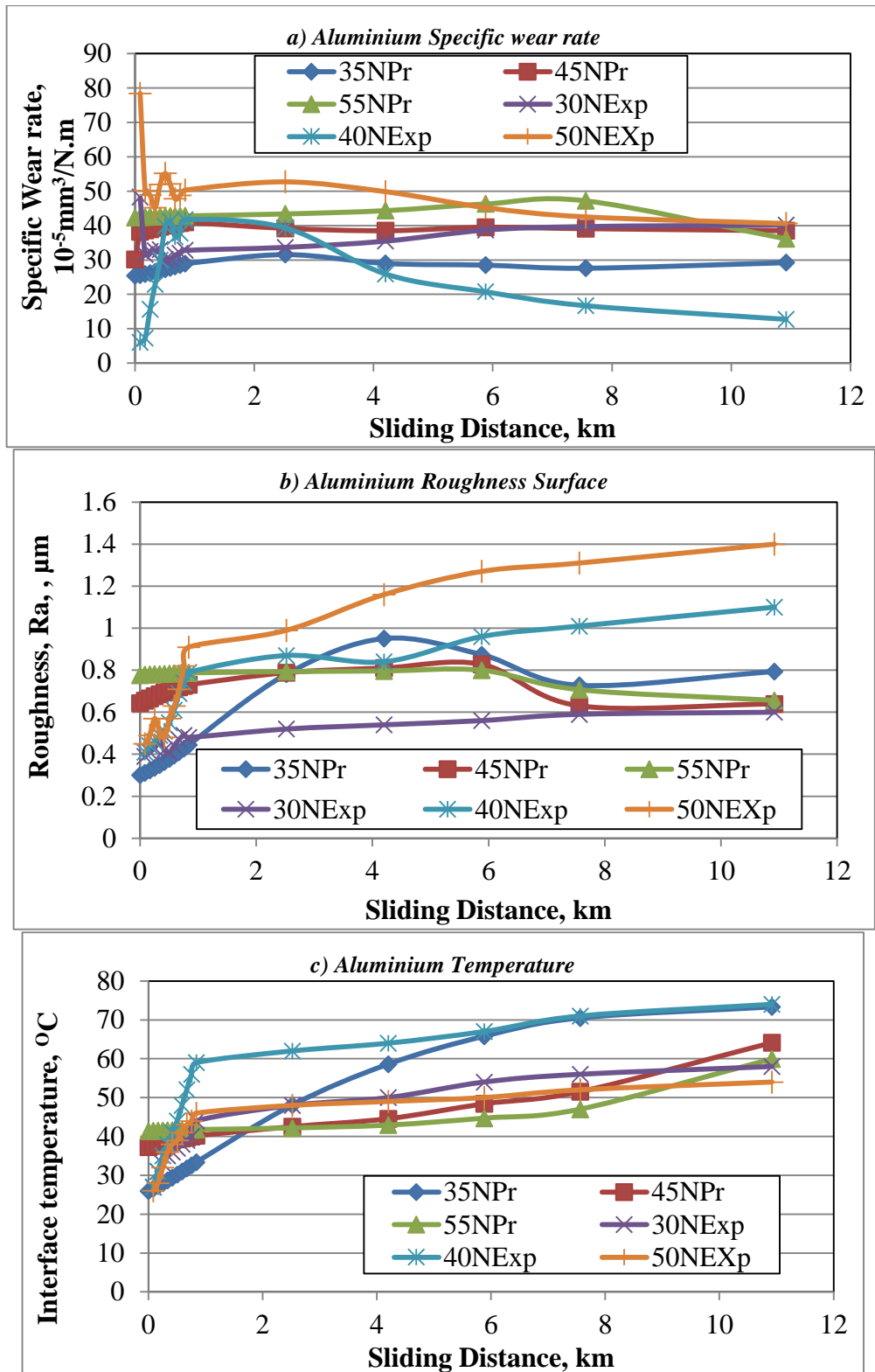


Figure 7.20: Real experimental data and predicted data for aluminium materials at different operating parameters

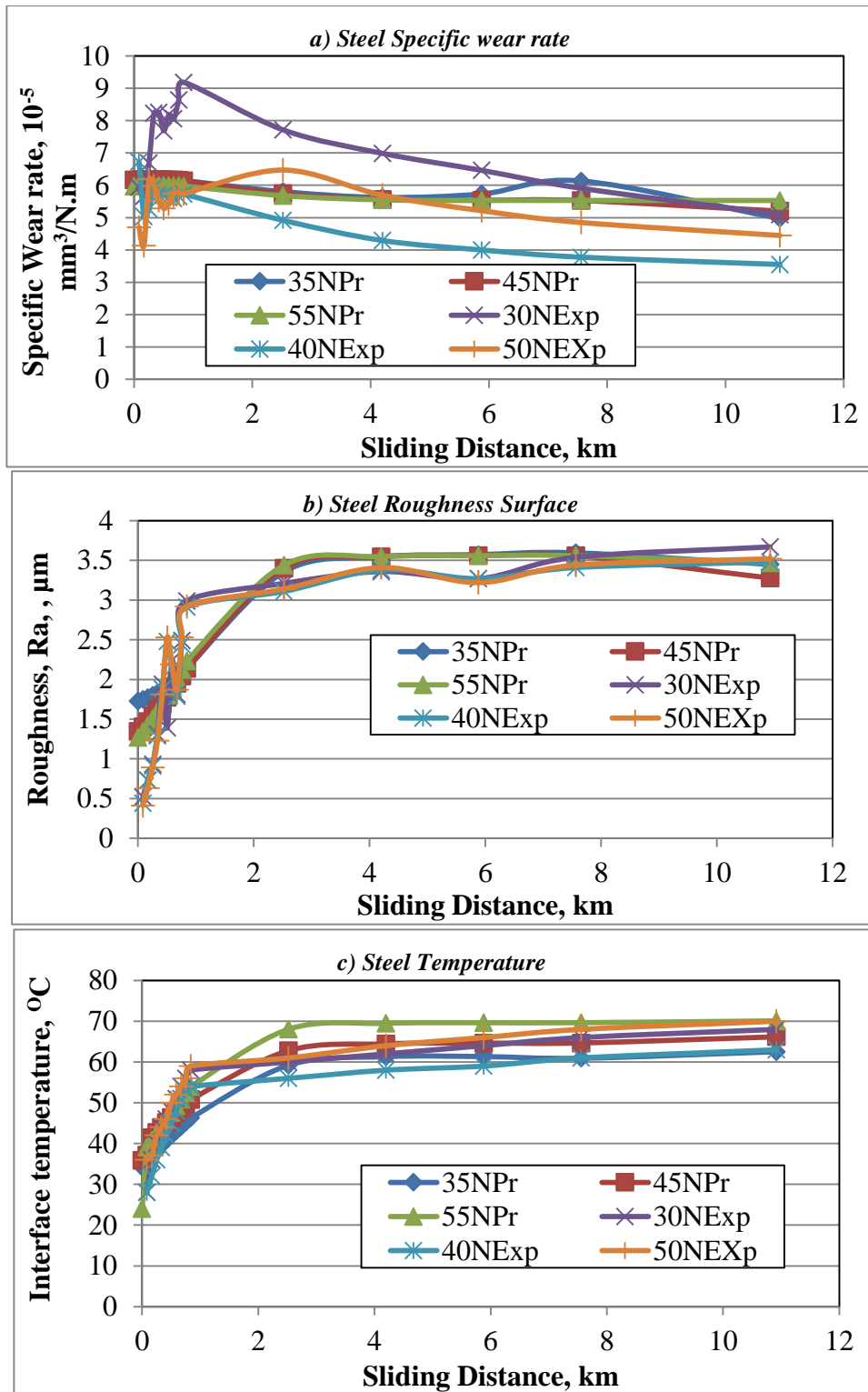


Figure 7.21: Real experimental data and predicted data for mild steel materials at different operating parameters

7.5 Chapter Summary

In this chapter the possibility of using an ANN as a tool for predicting tribological results was comprehensively studied considering different input parameters (material, applied load and sliding distance) and outputs (specific wear rate, interface temperature, roughness and friction coefficient). The main findings of this attempt can be summarised as:

- Attention and time should be paid to considering several steps in developing optimum ANN models in terms of training function, adaption function, performance function and number of neurons. For the current study, the model for predicting the wear rate was found to be inapplicable for the friction coefficient as the different number of inputs impacted the training function
- The Training function and number of inputs is the key to controlling the performance of ANN models. For a small amount of data (specific wear rate, roughness and interface temperature), TRAINRP was the optimum training function with 10 neurals, which achieved a performance of up to 95%. Conversely, due to the huge amount of data for the friction coefficient (above 12000 x 9), TRAINRP and other training functions did not perform as the performance dropped to the zero. TRAINBR managed to gain good friction coefficient prediction performance (about 95%, for 12000 x 3 inputs)
- Performance functions had less impact on the ANN models for predicting the specific wear rate, interface temperature, roughness as MSE, MSEREG and SEE exhibited relatively similar performances of about 95%. However, for friction coefficient prediction (large number of input data), MSEREG performance was performed poorly (below 20%), meanwhile, SEE and MSE performed well (over 90%)
- All the developed models for all the parameters showed poor performance when there were less than 10 neurons. For the specific wear rate, interface temperature and roughness, increasing the number of neurons to more than 10 showed a slight improvement (about 0.5%) in the performance of the ANN. Meanwhile, for the friction coefficient prediction, the increase in the number of neurons to more than 10 neurons reduced the performance of the ANN. In term of prediction, the optimum models of ANN for friction and specific wear rate, interface temperature and roughness showed very good correlations and prediction results with the consideration that the predicted values should be within the input range of values. For the current study, the ANN was able to predict the tribological data for the applied loads of 35 N and 45 N for different sliding distances. However, poor predictions in terms of trend and value were found when the applied load was outside the range of the input data (55 N).

Chapter 8: Conclusions and Recommendations

8.1 Conclusions

The conclusions of this thesis are divided below based on the research areas covered.

The literature review concluded that:

- There are demands for alternative lubricants to replace synthetic lubricants. WCO is a promising candidate for this purpose. WCOs are available everywhere in large quantities and there is an issue regarding their disposal. Despite previous attempts to convert WCOs into biofuels for diesel engines, issues relating to the impact of the fuel on engine components have limited its usage. Consequently, the current study was motivated to explore the use of WCO as a lubricant
- There is confusion and contradiction in current research presenting wear data in terms of wear rate, weight or volume loss, specific wear rate, and wear resistance. Previous results and recommendations pertaining to the dry adhesive wear behaviour of different metals were presented
- The ANN approach was found to be a promising tool for predicting the tribological behaviour of materials. As there are arguments in the literature about the number of inputs required to gain good predictable outputs, it was decided that this study would use a variety of models

Dry adhesive tests on brass, aluminium and mild steel led to the following conclusions:

- The specific wear rate versus the sliding distance can be divided into two regions, running in and steady state. After about 4 km sliding distance, adaption between the asperities in contact was established and a steady state was reached for almost all the materials
- The friction coefficient was almost steady for all the materials except the aluminium/stainless steel, which exhibited slight fluctuations due to the continuous modifications on its surface despite the steady state for the wear achieved
- The wear mechanism varies for each type of material. Mild steel rubbed against stainless steel exhibited an abrasive wear mechanism due to the presence of hard debris in the interface. Meanwhile, aluminium showed a pure adhesive nature when it was rubbed against a stainless steel counterface. Brass introduced abrasive wear associated with plastic deformation.

Regarding WCO as a lubricant, it can be concluded that:

- WCO with its blends has a significant impact on the wear and frictional performance of brass, aluminium and mild steel metals compared to dry contact conditions. At room temperature, the presence of the lubricant in the interface significantly reduced the specific wear rate and the friction coefficient for all the materials since it acted as a cleaner for the rubbing area and reduced the interaction between the asperities in contact

- The blend ratio of the WCO with the SO affected the wear and the friction coefficient of the selected material, especially at room temperature. This was mainly due to the fact that the viscosity of WCO is less than that of fully synthetic oil or its blends. High viscosity oil resulted in a significant reduction in the specific wear rate and the friction coefficient (i.e. a correlation was found between wear performance and viscosity)
- The wear mechanism for brass was predominant in the polishing process; meanwhile, an abrasion nature was observed for aluminium and mild steel
- The temperature of the lubricant was the most significant element in controlling the wear and frictional performance of the selected materials. This was mainly due to the reduction in the viscosity of all the blends at an elevated temperature, particularly at 80°C. This resulted in increased contact between the rubbed surfaces (reducing separation), leading to high friction associated with high material removal especially for mild steel and aluminium.
- At an elevated temperature, brass exhibited a slight abrasion nature and polishing was the dominant wear mechanism. Three body abrasion wear mechanisms were observed when testing the mild steel and aluminium. The presence of hard debris (mild steel) in the lubricant acted as a third body in the interface, and deteriorated the metal surface and increased the roughness of the counterface
- From testing in the journal bearing setup, WCO and its blends were found to be a very competitive candidate compared to industrial oils. Pressure and temperature distributions showed comparable results across all the selected lubricant blends. However, fully synthetic oil had the lowest lubricant temperature, giving it an advantage over others. In comparing the results of this study to those of industrial oils in the available literature, WCO was found to have the ability to be used as a lubricant for journal bearings. Moreover, the waste cooking oil and its blends exhibited similar a trend, in terms of oil pressure, with the fully synthetic oil. Despite of the fact that there was a slight increase in the oil pressure in the case of the pure waste cooking oil, the journal bearing worked without any issue and was able to carry the loads.

The ANN study concluded that:

- A great deal of time and research is required to determine the optimum training, adaption and performance functions, and the number of neurons for the optimum ANN model. There is no unique model that can be used for all the cases. The model for predicting wear was found to be inapplicable for the friction coefficient due to the differences in the number of inputs
- The Training function and the amount of input data is the key in controlling the performance of the ANN models. For wear prediction (small amount of data, specific wear rate, roughness and interface temperature), TRAINRP was found to be the optimum training function with 10 neurons. At this parameter, the ANN performance was found to be more than 95%. Meanwhile, the friction coefficient (data is above 12000 x 9), TRAINRP was not the optimum. However, TRAINBR managed to gain a good friction coefficient prediction performance (about 95%) considering (12000 x 3) inputs

- With regard to the influence of the number of neurons, all the developed models showed poor performance with less than 10 neurons. However, a large number of neurons may reduce the function of the ANN as seen in the case of the friction coefficient prediction. Therefore, the optimisation process should be also considered in selecting the number of neurons.
- Optimum ANN models showed very good correlation and prediction results if the predicted inputs were within the range of the trained data. For the current study, the ANN was able to predict the tribological data for different applied loads within the range (e.g. 35–45 N) considering different sliding distances. However, poor prediction of wear and friction was found when the applied load was outside the range of the input data (e.g. 55 N).

8.2 Recommendations

Some recommendations for future study are given as follows:

- Wear data should be presented in the form of specific wear rate for better understanding and comparison rather than the different forms used previously
- The durability of the oil and its interaction with the surfaces of metals require further study. Examining the chemical modifications may shed light on the separation process during the rubbing process especially at elevated temperature
- The influence of chemisorbed and EP additives on the wear and frictional data is recommended as such additives greatly impact on the ability to establish well adhered film on the rubbed surfaces
- For ANNs, it is important to thoroughly investigate the optimum model to predict tribological results especially with the large differences in input data.

References

- Abdelbary, A, Abouelwafa, MN, El Fahham, IM & Hamdy, AH 2012, 'Modeling the wear of Polyamide 66 using artificial neural network', *Materials & Design*, vol. 41, no. 0, pp. 460-9.
- Abdul Aziz, SM, Wahi, R, Ngaini, Z & Hamdan, S 2013, 'Bio-oils from microwave pyrolysis of agricultural wastes', *Fuel Processing Technology*, vol. 106, no. 0, pp. 744-50.
- Abdullah, MA, Saleman, SA, Tamaldin, N & Suhaimi, MS 2013, 'Reducing Wear and Friction by Means of Lubricants Mixtures', *Procedia Engineering*, vol. 68, no. 0, pp. 338-44.
- Adhvaryu, A & Erhan, SZ 2002, 'Epoxidized soybean oil as a potential source of high-temperature lubricants', *Industrial Crops and Products*, vol. 15, no. 3, pp. 247-54.
- Adhvaryu, A, Erhan, SZ & Perez, JM 2004, 'Tribological studies of thermally and chemically modified vegetable oils for use as environmentally friendly lubricants', *Wear*, vol. 257, no. 3–4, pp. 359-67.
- Agach, M, Delbaere, S, Marinkovic, S, Estrine, B & Nardello-Rataj, V 2012, 'Characterization, stability and ecotoxic properties of readily biodegradable branched oligoesters based on bio-sourced succinic acid and glycerol', *Polymer Degradation and Stability*, vol. 97, no. 10, pp. 1956-63.
- Ahmad, MA, Kasolang, S & Dwyer-Joyce, R 2013, 'The Effects of Oil Supply Pressure at Different Groove Position on Frictional Force and Torque in Journal Bearing Lubrication', *Procedia Engineering*, vol. 68, no. 0, pp. 70-6.
- Ahmad, MA, Kasolang, S & Dwyer-Joyce, RS 2014, 'Experimental study on the effects of oil groove location on temperature and pressure profiles in journal bearing lubrication', *Tribology International*, vol. 74, no. 0, pp. 79-86.
- Ahmad, MA, Kasolang, S, Dwyer-Joyce, R & Jumahat, A 2013, 'The Effects of Oil Supply Pressure at different Groove Position on Temperature and Pressure Profile in Journal Bearing', *Jurnal Teknologi*, vol. 66, no. 3.
- Ahmed, DI, Kasolang, S, Salem, S, Khidhir, BA & Yousif, B 2013, 'Prediction of Maximum Oil-Film Pressure in Journal Bearing using Fuzzy Logic and Particle Swarm Optimization approaches', *Australian Journal of Basic & Applied Sciences*, vol. 7, no. 4.
- Allmaier, H, Priestner, C, Reich, FM, Pribsch, HH & Novotny-Farkas, F 2013, 'Predicting friction reliably and accurately in journal bearings—extending the EHD simulation model to TEHD', *Tribology International*, vol. 58, no. 0, pp. 20-8.
- Alvarez-Vera, M, Ortega-Saenz, JA & Hernandez-Rodríguez, MAL 2013, 'A study of the wear performance in a hip simulator of a metal–metal Co–Cr alloy with different boron additions', *Wear*, vol. 301, no. 1–2, pp. 175-81, viewed 2013/5//.

Amamoto, Y & Goto, H 2006, 'Friction and wear of carbon steel near T1-transition under dry sliding', *Tribology International*, vol. 39, no. 8, pp. 756-62.

Amirat, M, Zaïdi, H, Djamaï, A, Necib, D & Eyidi, D 2009, 'Influence of the gas environment on the transferred film of the brass (Cu64Zn36)/steel AISI 1045 couple', *Wear*, vol. 267, no. 1-4, pp. 433-40.

Anghel, V, Bovington, C & Spikes, HA 1999, 'Thick-boundary-film formation by friction modifier additives', *Lubrication Science*, vol. 11, no. 4, pp. 313-35, Scopus.

Asadauskas, S & Erhan, SZ 1999, 'Depression of pour points of vegetable oils by blending with diluents used for biodegradable lubricants', *Journal of the American Oil Chemists' Society*, vol. 76, no. 3, pp. 313-6.

ASTM G77-98 Standard Test Method for Ranking Resistance of Materials to Sliding Wear Using Block-on-Ring Wear Test, WC.

Atabani, AE, Silitonga, AS, Ong, HC, Mahlia, TMI, Masjuki, HH, Badruddin, IA & Fayaz, H 2013, 'Non-edible vegetable oils: A critical evaluation of oil extraction, fatty acid compositions, biodiesel production, characteristics, engine performance and emissions production', *Renewable and Sustainable Energy Reviews*, vol. 18, no. 0, pp. 211-45.

Balasubramaniam, B, Sudalaiyadum Perumal, A, Jayaraman, J, Mani, J & Ramanujam, P 2012, 'Comparative analysis for the production of fatty acid alkyl esterase using whole cell biocatalyst and purified enzyme from *Rhizopus oryzae* on waste cooking oil (sunflower oil)', *Waste Management*, vol. 32, no. 8, pp. 1539-47.

Bang, K-B, Kim, J-H & Cho, Y-J 2010, 'Comparison of power loss and pad temperature for leading edge groove tilting pad journal bearings and conventional tilting pad journal bearings', *Tribology International*, vol. 43, no. 8, pp. 1287-93.

Batani, MR, Szpunar, JA, Wang, X & Li, DY 2005, 'The effect of wear and corrosion on internal crystalline texture of carbon steel and stainless steel', *Wear*, vol. 259, no. 1-6, pp. 400-4, viewed 2005/8//.

Beltzer, M & Jahanmir, S 1988, 'Effect of additive molecular structure on friction', *Lubrication Science*, vol. 1, no. 1, pp. 3-26.

Beran, E 2008, 'Experience with evaluating biodegradability of lubricating base oils', *Tribology International*, vol. 41, no. 12, pp. 1212-8.

Berglund, K, Marklund, P & Larsson, R 2010, 'Lubricant ageing effects on the friction characteristics of wet clutches', *Proceedings of the Institution of Mechanical Engineers, Part J: Journal of Engineering Tribology*, vol. 224, no. 7, pp. 639-47.

Bermúdez, MD, Martínez-Nicolás, G, Carrión, FJ, Martínez-Mateo, I, Rodríguez, JA & Herrera, EJ 2001, 'Dry and lubricated wear resistance of mechanically-alloyed aluminium-base sintered composites', *Wear*, vol. 248, no. 1-2, pp. 178-86.

Bezergianni, S, Dimitriadis, A & Chrysikou, LP 2014, 'Quality and sustainability comparison of one- vs. two-step catalytic hydroprocessing of waste cooking oil', *Fuel*, vol. 118, no. 0, pp. 300-7.

- Bhushan, B 2000, *Modern Tribology Handbook, Two Volume Set*, Taylor & Francis.
- Bhushan, B 2013a, *Principles and Applications of Tribology, Second Edition*.
- Bhushan, B 2013b, *Introduction to Tribology, Second Edition*.
- Binu, KG, Shenoy, BS, Rao, DS & Pai, R 2014, 'A Variable Viscosity Approach for the Evaluation of Load Carrying Capacity of Oil Lubricated Journal Bearing with TiO₂ Nanoparticles as Lubricant Additives', *Procedia Materials Science*, vol. 6, no. 0, pp. 1051-67.
- Biresaw, G & Bantchev, G 2008, 'Effect of chemical structure on film-forming properties of seed oils', *Journal of Synthetic Lubrication*, vol. 25, no. 4, pp. 159-83, Scopus.
- Birol, Y 2013, 'Sliding wear of CrN, AlCrN and AlTiN coated AISI H13 hot work tool steels in aluminium extrusion', *Tribology International*, vol. 57, no. 0, pp. 101-6.
- Birol, Y & Isler, D 2011, 'Abrasive wear performance of AlCrN-coated hot work tool steel at elevated temperatures under three-body regime', *Wear*, vol. 270, no. 3-4, pp. 281-6.
- Blum, MM & Ovaert, TC 2012, 'Experimental and numerical tribological studies of a boundary lubricant functionalized poro-viscoelastic PVA hydrogel in normal contact and sliding', *Journal of the Mechanical Behavior of Biomedical Materials*, vol. 14, no. 0, pp. 248-58.
- Bonny, K, De Baets, P, Perez, Y, Vleugels, J & Lauwers, B 2010, 'Friction and wear characteristics of WC-Co cemented carbides in dry reciprocating sliding contact', *Wear*, vol. 268, no. 11-12, pp. 1504-17.
- Borugadda, VB & Goud, VV 2014, 'Epoxidation of Castor Oil Fatty Acid Methyl Esters (COFAME) as a Lubricant base Stock Using Heterogeneous Ion-exchange Resin (IR-120) as a Catalyst', *Energy Procedia*, vol. 54, no. 0, pp. 75-84.
- Bouyer, J & Fillon, M 2011, 'Experimental measurement of the friction torque on hydrodynamic plain journal bearings during start-up', *Tribology International*, vol. 44, no. 7-8, pp. 772-81.
- Brito, FP, Miranda, AS, Claro, JCP, Teixeira, JC, Costa, L & Fillon, M 2014, 'The role of lubricant feeding conditions on the performance improvement and friction reduction of journal bearings', *Tribology International*, vol. 72, no. 0, pp. 65-82.
- Brockwell, K, Dmochowski, W & Decamillo, S 2004, 'An investigation of the steady-state performance of a pivoted shoe journal bearing with ISO VG 32 and VG 68 oils', *Tribology Transactions*, vol. 47, no. 4, pp. 480-8.
- Budinski, KG & Ives, LK 2005, 'Measuring abrasion resistance with a fixed abrasive loop', *Wear*, vol. 258, no. 1-4 SPEC. ISS., pp. 133-40.
- Burwell Jr, JT 1957, 'Survey of possible wear mechanisms', *Wear*, vol. 1, no. 2, pp. 119-41.

- Busse, M & Schlarb, AK 2013, 'Chapter 22 - A novel neural network approach for modeling tribological properties of polyphenylene sulfide reinforced on different scales', in K Friedrich & AK Schlarb (eds), *Tribology of Polymeric Nanocomposites (Second Edition)*, Butterworth-Heinemann, Oxford, pp. 779-93.
- Cao, L, Wang, J, Liu, K & Han, S 2014, 'Ethyl acetoacetate: A potential bio-based diluent for improving the cold flow properties of biodiesel from waste cooking oil', *Applied Energy*, vol. 114, no. 0, pp. 18-21.
- Cassar, G, Banfield, S, Avelar-Batista Wilson, JC, Housden, J, Matthews, A & Leyland, A 2012, 'Micro-abrasion wear testing of triode plasma diffusion and duplex treated Ti-6Al-4V alloy', *Wear*, vol. 274-275, no. 0, pp. 377-87.
- Castro, W, Perez, JM, Erhan, SZ & Caputo, F 2006, 'A study of the oxidation and wear properties of vegetable oils: soybean oil without additives', *Journal of the American Oil Chemists' Society*, vol. 83, no. 1, pp. 47-52.
- Cerda Varela, A, Bjerregaard Nielsen, B & Santos, IF 2013, 'Steady state characteristics of a tilting pad journal bearing with controllable lubrication: Comparison between theoretical and experimental results', *Tribology International*, vol. 58, no. 0, pp. 85-97.
- Chapman, I 2014, 'The end of Peak Oil? Why this topic is still relevant despite recent denials', *Energy Policy*, vol. 64, no. 0, pp. 93-101.
- 'Chapter 3 - Lubricants and Their Composition', 2014, in GW Stachowiak & AW Batchelor (eds), *Engineering Tribology (Fourth Edition)*, Butterworth-Heinemann, Boston, pp. 51-104.
- Chatra, KS, Jayadas, N & Kailas, SV 2012, 'Natural Oil-Based Lubricants', in *Green Tribology*, Springer, pp. 287-328.
- Chauhan, A, Sehgal, R & Sharma, RK 2010, 'Thermohydrodynamic analysis of elliptical journal bearing with different grade oils', *Tribology International*, vol. 43, no. 11, pp. 1970-7.
- Chauhan, A, Sehgal, R & Sharma, RK 2011, 'Investigations on the thermal effects in non-circular journal bearings', *Tribology International*, vol. 44, no. 12, pp. 1765-73.
- Cheenkachorn, K & Fungtammasan, B 2010, 'Development of engine oil using palm oil as a base stock for four-stroke engines', *Energy*, vol. 35, no. 6, pp. 2552-6.
- Cheng, Y-C, Chiu, YH, Wang, H-C, Chang, F-M, Chung, K-C, Chang, C-H & Cheng, K-S 2013, 'Using Akaike information criterion and minimum mean square error mode in compensating for ultrasonographic errors for estimation of fetal weight by new operators', *Taiwanese Journal of Obstetrics and Gynecology*, vol. 52, no. 1, pp. 46-52.
- Childs, PRN 2014, 'Chapter 5 - Journal Bearings', in PRN Childs (ed.), *Mechanical Design Engineering Handbook*, Butterworth-Heinemann, Oxford, pp. 139-200.
- Choi, H-Y, Lee, D-H & Lee, J 2013, 'Optimization of a railway wheel profile to minimize flange wear and surface fatigue', *Wear*, vol. 300, no. 1-2, pp. 225-33.

- Choo, JH, Forrest, AK & Spikes, HA 2007, 'Influence of organic friction modifier on liquid slip: A new mechanism of organic friction modifier action', *Tribology Letters*, vol. 27, no. 2, pp. 239-44, Scopus.
- Ciantar, C, Hadfield, M, Smith, AM & Swallow, A 1999, 'The influence of lubricant viscosity on the wear of hermetic compressor components in HFC-134a environments', *Wear*, vol. 236, no. 1–2, pp. 1-8.
- D'Annibale, F & Luongo, A 2013, 'A damage constitutive model for sliding friction coupled to wear', *Continuum Mechanics and Thermodynamics*, vol. 25, no. 2-4, pp. 503-22, Scopus.
- Dai, X, Zhang, K & Tang, C 2013, 'Friction and wear of pivot jewel bearing in oil-bath lubrication for high rotational speed application', *Wear*, vol. 302, no. 1–2, pp. 1506-13, viewed 2013/5//.
- De Barros, MI, Bouchet, J, Raoult, I, Le Mogne, T, Martin, JM, Kasrai, M & Yamada, Y 2003, 'Friction reduction by metal sulfides in boundary lubrication studied by XPS and XANES analyses', *Wear*, vol. 254, no. 9, pp. 863-70, Scopus.
- Delgado-Zamarreño, MM, González-Maza, I, Sánchez-Pérez, A & Carabias Martínez, R 2007, 'Analysis of synthetic phenolic antioxidants in edible oils by micellar electrokinetic capillary chromatography', *Food Chemistry*, vol. 100, no. 4, pp. 1722-7.
- Delgado, MA, García-Rico, C & Franco, JM 2014, 'The use of rosemary extracts in vegetable oil-based lubricants', *Industrial Crops and Products*, vol. 62, no. 0, pp. 474-80.
- Deligant, M, Podevin, P & Descombes, G 2011, 'CFD model for turbocharger journal bearing performances', *Applied Thermal Engineering*, vol. 31, no. 5, pp. 811-9.
- Demirbas, A 2006, 'Biodiesel production via non-catalytic SCF method and biodiesel fuel characteristics', *Energy Conversion and Management*, vol. 47, no. 15-16, pp. 2271-82.
- Dovi, VG, Friedler, F, Huisingh, D & Klemeš, JJ 2009, 'Cleaner energy for sustainable future', *Journal of Cleaner Production*, vol. 17, no. 10, pp. 889-95.
- Du, J, Zhang, G, Liu, T & To, S 2014, 'Improvement on load performance of externally pressurized gas journal bearings by opening pressure-equalizing grooves', *Tribology International*, vol. 73, no. 0, pp. 156-66.
- El-Tayeb, N, Yousif, B & Yap, T 2008, 'An investigation on worn surfaces of chopped glass fibre reinforced polyester through SEM observations', *Tribology International*, vol. 41, no. 5, pp. 331-40.
- Elangasinghe, MA, Singhal, N, Dirks, KN, Salmond, JA & Samarasinghe, S 'Complex time series analysis of PM10 and PM2.5 for a coastal site using artificial neural network modelling and k-means clustering', *Atmospheric Environment*, no. 0.

Elleuch, K, Elleuch, R, Mnif, R, Fridrici, V & Kapsa, P 2006, 'Sliding wear transition for the CW614 brass alloy', *Tribology International*, vol. 39, no. 4, pp. 290-6.

Erarslan, Y 2013, 'Wear performance of in-situ aluminum matrix composite after micro-arc oxidation', *Transactions of Nonferrous Metals Society of China*, vol. 23, no. 2, pp. 347-52.

Erhan, SZ, Sharma, BK & Perez, JM 2006, 'Oxidation and low temperature stability of vegetable oil-based lubricants', *Industrial Crops and Products*, vol. 24, no. 3, pp. 292-9.

Felder, E, Levrau, C, Mantel, M & Truong Dinh, N 2012, 'Identification of the work of plastic deformation and the friction shear stress in wire drawing', *Wear*, vol. 286, pp. 27-34.

Feser, T, Stoyanov, P, Mohr, F & Dienwiebel, M 2013, 'The running-in mechanisms of binary brass studied by in-situ topography measurements', *Wear*, vol. 303, no. 1–2, pp. 465-72.

Fischer, T & Tomizawa, H 1985, 'Interaction of tribochemistry and microfracture in the friction and wear of silicon nitride', *Wear*, vol. 105, no. 1, pp. 29-45.

Forati Rad, H, Amadeh, A & Moradi, H 2011, 'Wear assessment of plasma nitrided AISI H11 steel', *Materials & Design*, vol. 32, no. 5, pp. 2635-43.

Fox, NJ & Stachowiak, GW 2007, 'Vegetable oil-based lubricants—A review of oxidation', *Tribology International*, vol. 40, no. 7, pp. 1035-46.

Franco, Z & Nguyen, QD 2011, 'Flow properties of vegetable oil–diesel fuel blends', *Fuel*, vol. 90, no. 2, pp. 838-43.

Gajewski, J & Sadowski, T 2014, 'Sensitivity analysis of crack propagation in pavement bituminous layered structures using a hybrid system integrating Artificial Neural Networks and Finite Element Method', *Computational Materials Science*, vol. 82, no. 0, pp. 114-7.

Galle, J, Verhelst, S, Sierens, R, Goyos, L, Castaneda, R, Verhaege, M, Vervaeke, L & Bastiaen, M 2012, 'Failure of fuel injectors in a medium speed diesel engine operating on bio-oil', *Biomass and Bioenergy*, vol. 40, no. 0, pp. 27-35.

García-Zapateiro, LA, Franco, JM, Valencia, C, Delgado, MA & Gallegos, C 2013, 'Viscous, thermal and tribological characterization of oleic and ricinoleic acids-derived estolides and their blends with vegetable oils', *Journal of Industrial and Engineering Chemistry*, vol. 19, no. 4, pp. 1289-98.

Gava, GHS, Souza, RM, de Mello, JDB, de Macêdo, MCS & Scandian, C 2013, 'Effect of load partition and particle distribution on micro-abrasive wear mapping of two-phase metal matrix composites', *Wear*, vol. 301, no. 1–2, pp. 130-6, viewed 2013/5//.

Geitner, FK & Bloch, HP 2012, 'Chapter 3 - Machinery Component Failure Analysis', in FK Geitner & HP Bloch (eds), *Machinery Failure Analysis and Troubleshooting (Fourth Edition)*, Butterworth-Heinemann, Oxford, pp. 87-293.

Giannelos, PN, Sxizas, S, Lois, E, Zannikos, F & Anastopoulos, G 2005, 'Physical, chemical and fuel related properties of tomato seed oil for evaluating its direct use in diesel engines', *Industrial Crops and Products*, vol. 22, no. 3, pp. 193-9.

Gohar, R & Safa, MMA 2010, '5 - Fluid film lubrication', in H Rahnejat (ed.), *Tribology and Dynamics of Engine and Powertrain*, Woodhead Publishing, pp. 132-70.

Guide, MUs 2002, 'Neural network toolbox', *The MathWorks*.

Gyurova, LA & Friedrich, K 2011, 'Artificial neural networks for predicting sliding friction and wear properties of polyphenylene sulfide composites', *Tribology International*, vol. 44, no. 5, pp. 603-9.

Gyurova, LA, Miniño-Justel, P & Schlarb, AK 2010, 'Modeling the sliding wear and friction properties of polyphenylene sulfide composites using artificial neural networks', *Wear*, vol. 268, no. 5–6, pp. 708-14.

Haldar, SK, Ghosh, BB & Nag, A 2009, 'Studies on the comparison of performance and emission characteristics of a diesel engine using three degummed non-edible vegetable oils', *Biomass and Bioenergy*, vol. 33, no. 8, pp. 1013-8.

Hamrock, BJ, Schmid, SR & Jacobson, BO 2004, *Fundamentals of fluid film lubrication*, vol. 169, CRC press.

He, Z, Zhang, J, Zhang, G, Li, Z & Xie, W 2014, 'Crankshaft-bearing evolution indexes investigation and asperity contact identification based on neural network', *Applied Mathematical Modelling*, vol. 38, no. 2, pp. 506-23.

Hung, T-C, Chang, S-H, Hsu, S-P & Su, Y-T 2011, 'Reduction of tool wear during hydrodynamic polishing: A 'rock-and-roll' polishing strategy', *Journal of Materials Processing Technology*, vol. 211, no. 6, pp. 1069-75.

Iglesias, L, Laca, A, Herrero, M & Díaz, M 2012, 'A life cycle assessment comparison between centralized and decentralized biodiesel production from raw sunflower oil and waste cooking oils', *Journal of Cleaner Production*, vol. 37, no. 0, pp. 162-71.

Lubricant potentiality of degraded palm oil and effect of free fatty acid addition, Key Subjects <<http://www.scopus.com/inward/record.url?eid=2-s2.0-84891508135&partnerID=40&md5=6e32f328e2936ec9d8b12b72956108f6>>.

Imran, A, Masjuki, HH, Kalam, MA, Varman, M, Hasmelidin, M, Mahmud, KAHA, Shahir, SA & Habibullah, M 2013, 'Study of Friction and Wear Characteristic of Jatropha Oil Blended Lube Oil', *Procedia Engineering*, vol. 68, no. 0, pp. 178-85.

Jacobs, W, Boonen, R, Sas, P & Moens, D 2014, 'The influence of the lubricant film on the stiffness and damping characteristics of a deep groove ball bearing', *Mechanical Systems and Signal Processing*, vol. 42, no. 1–2, pp. 335-50.

Jahangiri, M, Hashempour, M, Razavizadeh, H & Rezaie, HR 2012, 'Application and conceptual explanation of an energy-based approach for the modelling and prediction of sliding wear', *Wear*, vol. 274–275, no. 0, pp. 168-74.

- Jamli, MR, Ariffin, AK & Wahab, DA 2014, 'Integration of feedforward neural network and finite element in the draw-bend springback prediction', *Expert Systems with Applications*, vol. 41, no. 8, pp. 3662-70.
- Jayasinghe, P & Hawboldt, K 2012, 'A review of bio-oils from waste biomass: Focus on fish processing waste', *Renewable and Sustainable Energy Reviews*, vol. 16, no. 1, pp. 798-821.
- Jayed, MH, Masjuki, HH, Saidur, R, Kalam, MA & Jahirul, MI 2009, 'Environmental aspects and challenges of oilseed produced biodiesel in Southeast Asia', *Renewable and Sustainable Energy Reviews*, vol. 13, no. 9, pp. 2452-62.
- Kasolang, S, Ahmad, MA, Joyce, R-D & Tai, CFM 2012, 'Preliminary Study of Pressure Profile in Hydrodynamic Lubrication Journal Bearing', *Procedia Engineering*, vol. 41, no. 0, pp. 1743-9.
- Kasolang, S, Ahmed, DI, Dwyer-Joyce, RS & Yousif, BF 2013, 'Performance analysis of journal bearings using ultrasonic reflection', *Tribology International*, vol. 64, no. 0, pp. 78-84.
- Kato, K 2000, 'Wear in relation to friction — a review', *Wear*, vol. 241, no. 2, pp. 151-7.
- Kazmi, A 2011, *Advanced oil crop biorefineries*, RSC Publishing.
- Khondee, N, Tathong, S, Pinyakong, O, Powtongsook, S, Chatchupong, T, Ruangchainikom, C & Luepromchai, E 2012, 'Airlift bioreactor containing chitosan-immobilized *Sphingobium* sp. P2 for treatment of lubricants in wastewater', *Journal of Hazardous Materials*, vol. 213–214, no. 0, pp. 466-73.
- Khonsari, MM & Booser, ER 2008, *Applied Tribology: Bearing Design and Lubrication*, Wiley.
- Kim, JE 2014, 'Energy security and climate change: How oil endowment influences alternative vehicle innovation', *Energy Policy*, vol. 66, no. 0, pp. 400-10.
- Kim, SW, Koo, BS, Ryu, JW, Lee, JS, Kim, CJ, Lee, DH, Kim, GR & Choi, S 2013, 'Bio-oil from the pyrolysis of palm and *Jatropha* wastes in a fluidized bed', *Fuel Processing Technology*, vol. 108, no. 0, pp. 118-24.
- Kreivaitis, R, Gumbytė, M, Kazancev, K, Padgurskas, J & Makarevičienė, V 2013, 'A comparison of pure and natural antioxidant modified rapeseed oil storage properties', *Industrial Crops and Products*, vol. 43, no. 0, pp. 511-6.
- Krishnaveni, K, Sankara Narayanan, TSN & Seshadri, SK 2005, 'Electroless Ni–B coatings: preparation and evaluation of hardness and wear resistance', *Surface and Coatings Technology*, vol. 190, no. 1, pp. 115-21.
- Kumar, M & Bijwe, J 2011, 'Composite friction materials based on metallic fillers: Sensitivity of μ to operating variables', *Tribology International*, vol. 44, no. 2, pp. 106-13.

- Kumaran, ST & Uthayakumar, M 2013, 'Investigation on the dry sliding friction and wear behavior of AA6351-SiC-B4C hybrid metal matrix composites', *Proceedings of the Institution of Mechanical Engineers, Part J: Journal of Engineering Tribology*, p. 1350650113508103.
- Larsen, TØ, Andersen, TL, Thorning, B & Vigild, ME 2008, 'The effect of particle addition and fibrous reinforcement on epoxy-matrix composites for severe sliding conditions', *Wear*, vol. 264, no. 9-10, pp. 857-68.
- Lawal, S, Choudhury, I & Nukman, Y 2012, 'Application of vegetable oil-based metalworking fluids in machining ferrous metals—A review', *International Journal of Machine Tools and Manufacture*, vol. 52, no. 1, pp. 1-12.
- Lawal, SA, Choudhury, IA & Nukman, Y 2013, 'A critical assessment of lubrication techniques in machining processes: a case for minimum quantity lubrication using vegetable oil-based lubricant', *Journal of Cleaner Production*, vol. 41, no. 0, pp. 210-21.
- Leiro, A, Vuorinen, E, Sundin, KG, Prakash, B, Sourmail, T, Smanio, V, Caballero, FG, Garcia-Mateo, C & Elvira, R 2013, 'Wear of nano-structured carbide-free bainitic steels under dry rolling–sliding conditions', *Wear*, vol. 298–299, no. 0, pp. 42-7.
- Leonard, BD, Ghosh, A, Sadeghi, F, Shinde, S & Mittelbach, M 2014, 'Third body modeling in fretting using the combined finite-discrete element method', *International Journal of Solids and Structures*, vol. 51, no. 6, pp. 1375-89.
- Li, J, Ma, H, Ren, T, Zhao, Y, Zheng, L, Ma, C & Han, Y 2008, 'The tribological chemistry of polysulfides in mineral oil and synthetic diester', *Applied Surface Science*, vol. 254, no. 22, pp. 7232-6.
- Li, L, Li, T, Liu, JJ, Tian, ZY, Zhang, GZ & Fu, ZY 2013, 'Study on Wear Ratio Analysis of Materials by Computer Image Technology', *Advanced Materials Research*, vol. 763, pp. 220-2.
- Li, X, Zhu, Y & Xiao, G 'Application of artificial neural networks to predict sliding wear resistance of Ni-TiN nanocomposite coatings deposited by pulse electrodeposition', *Ceramics International*, no. 0.
- Lingaraju, D, Ramji, K, Rao, NBRM & lakshmi, UR 2011, 'Characterization and prediction of some engineering properties of polymer - Clay/Silica hybrid nanocomposites through ANN and regression models', *Procedia Engineering*, vol. 10, no. 0, pp. 9-18.
- Liu, H, Zhou, M, Zhou, Y, Wang, S, Li, G, Jiang, L & Dan, Y 2014, 'Aging life prediction system of polymer outdoors constructed by ANN. 1. Lifetime prediction for polycarbonate', *Polymer Degradation and Stability*, vol. 105, no. 0, pp. 218-36.
- Liu, W, Zhu, J & Liang, Y 2005, 'Effect of bridged cyclotriphosphazenes as lubricants on the tribological properties of a steel-on-steel system', *Wear*, vol. 258, no. 5–6, pp. 725-9.

- LiuJie, X, Davim, JP & Cardoso, R 2007, 'Prediction on tribological behaviour of composite PEEK-CF30 using artificial neural networks', *Journal of Materials Processing Technology*, vol. 189, no. 1–3, pp. 374-8.
- Louaisil, K, Dubar, M, Deltombe, R, Dubois, A & Dubar, L 2009, 'Analysis of interface temperature, forward slip and lubricant influence on friction and wear in cold rolling', *Wear*, vol. 266, no. 1–2, pp. 119-28.
- Luna, FMT, Rocha, BS, Rola Jr, EM, Albuquerque, MCG, Azevedo, DCS & Cavalcante Jr, CL 2011, 'Assessment of biodegradability and oxidation stability of mineral, vegetable and synthetic oil samples', *Industrial Crops and Products*, vol. 33, no. 3, pp. 579-83.
- Luo, Y, Yang, L & Tian, M 2013, 'Influence of Bio-Lubricants on the Tribological Properties of Ti6Al4V Alloy', *Journal of Bionic Engineering*, vol. 10, no. 1, pp. 84-9.
- Madankar, CS, Pradhan, S & Naik, SN 2013, 'Parametric study of reactive extraction of castor seed (*Ricinus communis* L.) for methyl ester production and its potential use as bio lubricant', *Industrial Crops and Products*, vol. 43, no. 0, pp. 283-90.
- Majdoub, F, Martin, JM, Belin, M, Perret-Liaudet, J & Iovine, R 2014, 'Effect of Temperature on Lubricated Steel/Steel Systems With or Without Fatty Acids Additives Using an Oscillating Dynamic Tribometer', *Tribology Letters*.
- Majumdar, BC & Saha, AK 1974, 'Temperature distribution in oil journal bearings', *Wear*, vol. 28, no. 2, pp. 259-66.
- Martín-Alfonso, JE & Franco, JM 2014, 'Ethylene-vinyl acetate copolymer (EVA)/sunflower vegetable oil polymer gels: Influence of vinyl acetate content', *Polymer Testing*, vol. 37, no. 0, pp. 78-85.
- Martínez, FJ, Canales, M, Izquierdo, S, Jiménez, MA & Martínez, MA 2012, 'Finite element implementation and validation of wear modelling in sliding polymer–metal contacts', *Wear*, vol. 284–285, no. 0, pp. 52-64.
- Máscia, R, Ramos Neto, FF, Neto, TFB & Franco, SD 2013, 'Effects of pressure and counterbody hardness in the abrasive wear behavior of tool steels', *Wear*, vol. 303, no. 1–2, pp. 412-8.
- McQueen, JS, Gao, H, Black, ED, Gangopadhyay, AK & Jensen, RK 2005, 'Friction and wear of tribofilms formed by zinc dialkyl dithiophosphate antiwear additive in low viscosity engine oils', *Tribology International*, vol. 38, no. 3, pp. 289-97.
- Meireles, MR, Almeida, PE & Simões, MG 2003, 'A comprehensive review for industrial applicability of artificial neural networks', *Industrial Electronics, IEEE Transactions on*, vol. 50, no. 3, pp. 585-601.
- Mejía, JD, Salgado, N & Orrego, CE 2013, 'Effect of blends of Diesel and Palm-Castor biodiesels on viscosity, cloud point and flash point', *Industrial Crops and Products*, vol. 43, no. 0, pp. 791-7.

Mendelsohn, R & Neumann, JE 2004, *The impact of climate change on the United States economy*, Cambridge University Press.

Miller, NE 1980, 'Adhesive wear polishing of molybdenum alloy', *Metallography*, vol. 13, no. 2, pp. 135-42.

Minami, I, Furesawa, T, Kubo, T, Nanao, H & Mori, S 2008, 'Investigation of tribochemistry by means of stable isotopic tracers: Mechanism for durability of monomolecular boundary film', *Tribology International*, vol. 41, no. 11, pp. 1056-62, Scopus.

'Mixed-fiber diets and cholesterol metabolism in middle-aged men', 1991, *Nutrition Reviews*, vol. 49, no. 3, pp. 80-2, item: 1647508.

Mobarak, HM, Niza Mohamad, E, Masjuki, HH, Kalam, MA, Al Mahmud, KAH, Habibullah, M & Ashraful, AM 2014, 'The prospects of biolubricants as alternatives in automotive applications', *Renewable and Sustainable Energy Reviews*, vol. 33, no. 0, pp. 34-43.

Morris, B, Zou, L, Royle, M, Simpson, D & Shelton, JC 2011, 'Quantifying the wear of acetabular cups using coordinate metrology', *Wear*, vol. 271, no. 7-8, pp. 1086-92.

Mortier, RM, Fox, MF & Orszulik, ST 2010, *Chemistry and technology of lubricants*, Springer Science+ Business Media.

Moshkovich, A, Perfilyev, V, Lapsker, I & Rapoport, L 2014, 'Friction, wear and plastic deformation of Cu and α/β brass under lubrication conditions', *Wear*, vol. 320, no. 1-2, pp. 34-40.

Muralidharan, K, Vasudevan, D & Sheeba, KN 2011, 'Performance, emission and combustion characteristics of biodiesel fuelled variable compression ratio engine', *Energy*, vol. 36, no. 8, pp. 5385-93.

Muthukrishnan, N & Davim, JP 2009, 'Optimization of machining parameters of Al/SiC-MMC with ANOVA and ANN analysis', *Journal of Materials Processing Technology*, vol. 209, no. 1, pp. 225-32.

Muzakkir, SM, Lijesh, KP & Hirani, H 2014, 'Tribological failure analysis of a heavily-loaded slow speed hybrid journal bearing', *Engineering Failure Analysis*, vol. 40, no. 0, pp. 97-113.

Muzakkir, SM, Hirani, H, Thakre, GD & Tyagi, MR 2011, 'Tribological failure analysis of journal bearings used in sugar mills', *Engineering Failure Analysis*, vol. 18, no. 8, pp. 2093-103.

Myshkin, N, Petrokovets, M & Kovalev, A 2006, 'Tribology of polymers: adhesion, friction, wear, and mass-transfer', *Tribology International*, vol. 38, no. 11, pp. 910-21.

Nagendramma, P & Kaul, S 2012, 'Development of ecofriendly/biodegradable lubricants: An overview', *Renewable and Sustainable Energy Reviews*, vol. 16, no. 1, pp. 764-74.

- Nampi, PP, Kume, S, Hotta, Y, Watari, K, Itoh, M, Toda, H & Matsutani, A 2011, 'The effect of polyvinyl alcohol as a binder and stearic acid as an internal lubricant in the formation, and subsequent sintering of spray-dried alumina', *Ceramics International*, vol. 37, no. 8, pp. 3445-50.
- Nasir, T, Yousif, BF, McWilliam, S, Salih, ND & Hui, LT 2010, 'An artificial neural network for prediction of the friction coefficient of multi-layer polymeric composites in three different orientations', *Proceedings of the Institution of Mechanical Engineers, Part C: Journal of Mechanical Engineering Science*, vol. 224, no. 2, pp. 419-29.
- Nasir, T, Yousif, B, McWilliam, S, Salih, N & Hui, L 2010, 'An artificial neural network for prediction of the friction coefficient of multi-layer polymeric composites in three different orientations', *Proceedings of the Institution of Mechanical Engineers, Part C: Journal of Mechanical Engineering Science*, vol. 224, no. 2, pp. 419-29.
- Neville, A, Morina, A, Haque, T & Voong, M 2007, 'Compatibility between tribological surfaces and lubricant additives-How friction and wear reduction can be controlled by surface/lube synergies', *Tribology International*, vol. 40, no. 10-12 SPEC. ISS., pp. 1680-95, Scopus.
- Nishio, U, Somaya, K & Yoshimoto, S 2011, 'Numerical calculation and experimental verification of static and dynamic characteristics of aerostatic thrust bearings with small feedholes', *Tribology International*, vol. 44, no. 12, pp. 1790-5.
- Núñez, N, Martín-Alfonso, JE, Valencia, C, Sánchez, MC & Franco, JM 2012, 'Rheology of new green lubricating grease formulations containing cellulose pulp and its methylated derivative as thickeners', *Industrial Crops and Products*, vol. 37, no. 1, pp. 500-7.
- P. Suh, N 1973, 'The delamination theory of wear', *Wear*, vol. 25, no. 1, pp. 111-24.
- Pączelt, I, Kucharski, S & Mróz, Z 2012, 'The experimental and numerical analysis of quasi-steady wear processes for a sliding spherical indenter', *Wear*, vol. 274-275, no. 0, pp. 127-48.
- Pan, X & Lee, B 2012, 'A comparison of support vector machines and artificial neural networks for mid-term load forecasting', in *Industrial Technology (ICIT), 2012 IEEE International Conference on: proceedings of the Industrial Technology (ICIT), 2012 IEEE International Conference on IEEE*, pp. 95-101.
- Panagopoulos, CN, Georgiou, EP & Simeonidis, K 2012, 'Lubricated wear behavior of leaded $\alpha+\beta$ brass', *Tribology International*, vol. 50, no. 0, pp. 1-5.
- Panpanit, S & Visvanathan, C 2001, 'The role of bentonite addition in UF flux enhancement mechanisms for oil/water emulsion', *Journal of Membrane Science*, vol. 184, no. 1, pp. 59-68.
- Paredes, X, Comuñas, MJP, Pensado, AS, Bazile, J-P, Boned, C & Fernández, J 2014, 'High pressure viscosity characterization of four vegetable and mineral hydraulic oils', *Industrial Crops and Products*, vol. 54, no. 0, pp. 281-90.

- Patil, P, Deng, S, Isaac Rhodes, J & Lammers, PJ 2010, 'Conversion of waste cooking oil to biodiesel using ferric sulfate and supercritical methanol processes', *Fuel*, vol. 89, no. 2, pp. 360-4.
- Pehan, S, Jerman, MS, Kegl, M & Kegl, B 2009, 'Biodiesel influence on tribology characteristics of a diesel engine', *Fuel*, vol. 88, no. 6, pp. 970-9.
- Pop, L, Puşcaş, C, Bandur, G, Vlase, G & Nuţiu, R 2008, 'Basestock oils for lubricants from mixtures of corn oil and synthetic diesters', *Journal of the American Oil Chemists' Society*, vol. 85, no. 1, pp. 71-6.
- Prasad, BK 2007, 'Investigation into sliding wear performance of zinc-based alloy reinforced with SiC particles in dry and lubricated conditions', *Wear*, vol. 262, no. 3–4, pp. 262-73.
- Prasad, BK 2011, 'Sliding wear response of a grey cast iron: Effects of some experimental parameters', *Tribology International*, vol. 44, no. 5, pp. 660-7.
- Prasad, BK, Modi, OP & Yegneswaran, AH 2008, 'Wear behaviour of zinc-based alloys as influenced by alloy composition, nature of the slurry and traversal distance', *Wear*, vol. 264, no. 11–12, pp. 990-1001.
- Preis, V, Behr, M, Handel, G, Schneider-Feyrer, S, Hahnel, S & Rosentritt, M 2012, 'Wear performance of dental ceramics after grinding and polishing treatments', *Journal of the Mechanical Behavior of Biomedical Materials*, vol. 10, no. 0, pp. 13-22.
- Quinchia, LA, Delgado, MA, Valencia, C, Franco, JM & Gallegos, C 2009, 'Viscosity modification of high-oleic sunflower oil with polymeric additives for the design of new biolubricant formulations', *Environmental Science and Technology*, vol. 43, no. 6, pp. 2060-5, Scopus.
- Quinchia, LA, Delgado, MA, Valencia, C, Franco, JM & Gallegos, C 2010, 'Viscosity modification of different vegetable oils with EVA copolymer for lubricant applications', *Industrial Crops and Products*, vol. 32, no. 3, pp. 607-12.
- Quinchia, LA, Delgado, MA, Franco, JM, Spikes, HA & Gallegos, C 2012, 'Low-temperature flow behaviour of vegetable oil-based lubricants', *Industrial Crops and Products*, vol. 37, no. 1, pp. 383-8.
- Quinchia, LA, Delgado, MA, Reddyhoff, T, Gallegos, C & Spikes, HA 2014, 'Tribological studies of potential vegetable oil-based lubricants containing environmentally friendly viscosity modifiers', *Tribology International*, vol. 69, no. 0, pp. 110-7.
- Rahman, S, Masjuki, H, Kalam, M, Abedin, M, Sanjid, A & Imtenan, S 2014, 'Effect of idling on fuel consumption and emissions of a diesel engine fuelled by *Jatropha* biodiesel blends', *Journal of Cleaner Production*.
- Rao, RN, Das, S, Mondal, DP, Dixit, G & Tulasi Devi, SL 2013, 'Dry sliding wear maps for AA7010 (Al–Zn–Mg–Cu) aluminium matrix composite', *Tribology International*, vol. 60, no. 0, pp. 77-82.

- Rizwanul Fattah, IM, Masjuki, HH, Liaquat, AM, Ramli, R, Kalam, MA & Riazuddin, VN 2013, 'Impact of various biodiesel fuels obtained from edible and non-edible oils on engine exhaust gas and noise emissions', *Renewable and Sustainable Energy Reviews*, vol. 18, no. 0, pp. 552-67.
- Ronkainen, H, Varjus, S & Holmberg, K 1998, 'Friction and wear properties in dry, water-and oil-lubricated DLC against alumina and DLC against steel contacts', *Wear*, vol. 222, no. 2, pp. 120-8.
- Rudnick, L 2006, *Automotives Gear Lubricants, Synthetics, mineral oils, and bio-based lubricants: chemistry and technology*, Taylor and Francis, Florida.
- Rudnick, LR 2010, *Lubricant additives: chemistry and applications*, CRC Press.
- Sadaka, S & Boateng, AA 2009, *Pyrolysis and Bio-oil*, [Cooperative Extension Service], University of Arkansas, US Department of Agriculture and county governments cooperating.
- Salih, N, Salimon, J & Yousif, E 2011, 'The physicochemical and tribological properties of oleic acid based triester biolubricants', *Industrial Crops and Products*, vol. 34, no. 1, pp. 1089-96, Scopus.
- Salimon, J, Salih, N & Yousif, E 2012, 'Triester derivatives of oleic acid: The effect of chemical structure on low temperature, thermo-oxidation and tribological properties', *Industrial Crops and Products*, vol. 38, no. 0, pp. 107-14.
- Sánchez, R, Franco, JM, Delgado, MA, Valencia, C & Gallegos, C 2011, 'Thermal and mechanical characterization of cellulosic derivatives-based oleogels potentially applicable as bio-lubricating greases: Influence of ethyl cellulose molecular weight', *Carbohydrate Polymers*, vol. 83, no. 1, pp. 151-8.
- Seireg, S 1998, *Friction and Lubrication in Mechanical Design*, Taylor & Francis.
- Shahabuddin, M, Masjuki, HH & Kalam, MA 2013, 'Experimental Investigation into Tribological Characteristics of Bio-Lubricant Formulated from Jatropha Oil', *Procedia Engineering*, vol. 56, no. 0, pp. 597-606.
- Shahabuddin, M, Masjuki, HH, Kalam, MA, Bhuiya, MMK & Mehat, H 2013, 'Comparative tribological investigation of bio-lubricant formulated from a non-edible oil source (Jatropha oil)', *Industrial Crops and Products*, vol. 47, no. 0, pp. 323-30.
- Sharma, BK, Adhvaryu, A & Erhan, SZ 2009, 'Friction and wear behavior of thioether hydroxy vegetable oil', *Tribology International*, vol. 42, no. 2, pp. 353-8.
- Sharma, RV & Dalai, AK 2013, 'Synthesis of bio-lubricant from epoxy canola oil using sulfated Ti-SBA-15 catalyst', *Applied Catalysis B: Environmental*, vol. 142-143, no. 0, pp. 604-14, viewed 2013/11//.
- Shashidhara, Y & Jayaram, S 2010, 'Vegetable oils as a potential cutting fluid—An evolution', *Tribology International*, vol. 43, no. 5, pp. 1073-81.

Shashidhara, YM & Jayaram, SR 2010, 'Vegetable oils as a potential cutting fluid—An evolution', *Tribology International*, vol. 43, no. 5–6, pp. 1073-81, viewed 2010/6//.

Shi, X, Zhai, W, Wang, M, Xu, Z, Yao, J, Song, S & Wang, Y 2014, 'Tribological behaviors of NiAl based self-lubricating composites containing different solid lubricants at elevated temperatures', *Wear*, vol. 310, no. 1–2, pp. 1-11.

Shipway, PH & Ngao, NK 2003, 'Microscale abrasive wear of polymeric materials', *Wear*, vol. 255, no. 1-6, pp. 742-50.

Singh, AK 2011, 'Castor oil-based lubricant reduces smoke emission in two-stroke engines', *Industrial Crops and Products*, vol. 33, no. 2, pp. 287-95.

Slavkovic, R, Jugovic, Z, Dragicevic, S, Jovicic, A & Slavkovic, V 2013, 'An application of learning machine methods in prediction of wear rate of wear resistant casting parts', *Computers & Industrial Engineering*, vol. 64, no. 3, pp. 850-7.

Smith, EH, Weston-Hays, J, Middlebrook, B, Hatton, DR, Herraty, TG, Eliades, P, Stevens, KT, Davies, A, Lewis, MWJ & Sherrington, I 1994, '9 - Tribology', in *Mechanical Engineers Reference Book (Twelfth Edition)*, Butterworth-Heinemann, Oxford, pp. 9/1-9/132.

Solghar, AA, Brito, F & Claro, J 2014, 'An experimental investigation on the influence of deactivation of a groove on the performance of a twin groove journal bearing', *Proceedings of the Institution of Mechanical Engineers, Part J: Journal of Engineering Tribology*, p. 1350650113518521.

Spikes, HA & Olver, AV 2002, 'Mixed lubrication—Experiment and theory', in MPGD D. Dowson & AA Lubrecht (eds), *Tribology Series*, Elsevier, vol. Volume 40, pp. 95-113.

Spinelli, D, Jez, S & Basosi, R 2012, 'Integrated Environmental Assessment of sunflower oil production', *Process Biochemistry*, vol. 47, no. 11, pp. 1595-602.

Stachowiak, G & Batchelor, AW 2013, *Engineering tribology*, Butterworth-Heinemann.

Suarez, PAZ, Moser, BR, Sharma, BK & Erhan, SZ 2009, 'Comparing the lubricity of biofuels obtained from pyrolysis and alcoholysis of soybean oil and their blends with petroleum diesel', *Fuel*, vol. 88, no. 6, pp. 1143-7.

Syahrullail, S, Kamitani, S & Shakirin, A 2013, 'Performance of Vegetable Oil as Lubricant in Extreme Pressure Condition', *Procedia Engineering*, vol. 68, no. 0, pp. 172-7.

Syahrullail, S, Zubil, B, Azwadi, C & Ridzuan, M 2011, 'Experimental evaluation of palm oil as lubricant in cold forward extrusion process', *International journal of mechanical sciences*, vol. 53, no. 7, pp. 549-55.

Syahrullail, S, Zubil, BM, Azwadi, CSN & Ridzuan, MJM 2011, 'Experimental evaluation of palm oil as lubricant in cold forward extrusion process', *International Journal of Mechanical Sciences*, vol. 53, no. 7, pp. 549-55.

- Szolwinski, MP & Farris, TN 1996, 'Mechanics of fretting fatigue crack formation', *Wear*, vol. 198, no. 1, pp. 93-107.
- Talebian-Kiakalaieh, A, Amin, NAS & Mazaheri, H 2013, 'A review on novel processes of biodiesel production from waste cooking oil', *Applied Energy*, vol. 104, no. 0, pp. 683-710.
- Tang, Z & Li, S 'A review of recent developments of friction modifiers for liquid lubricants (2007–present)', *Current Opinion in Solid State and Materials Science*, no. 0.
- Tang, Z & Li, S 2014, 'A review of recent developments of friction modifiers for liquid lubricants (2007–present)', *Current Opinion in Solid State and Materials Science*, vol. 18, no. 3, pp. 119-39.
- Tewari, A 2012, 'Load dependence of oxidative wear in metal/ceramic tribocouples in fretting environment', *Wear*, vol. 289, no. 0, pp. 95-103.
- Ting, C-C & Chen, C-C 2011, 'Viscosity and working efficiency analysis of soybean oil based bio-lubricants', *Measurement*, vol. 44, no. 8, pp. 1337-41.
- Trezona, R, Allsopp, D & Hutchings, I 1999, 'Transitions between two-body and three-body abrasive wear: influence of test conditions in the microscale abrasive wear test', *Wear*, vol. 225, pp. 205-14.
- Tseng, WJ, Liu, D-M & Hsu, C-K 1999, 'Influence of stearic acid on suspension structure and green microstructure of injection-molded zirconia ceramics', *Ceramics International*, vol. 25, no. 2, pp. 191-5.
- Turhan, H 2005, 'Adhesive wear resistance of Cu–Sn–Zn–Pb bronze with additions of Fe, Mn and P', *Materials Letters*, vol. 59, no. 12, pp. 1463-9.
- Tylczak, JH & Oregon, A 1992, 'Abrasive wear', *ASM Handbook*, vol. 18, pp. 184-6.
- Umanath, K, Palanikumar, K & Selvamani, ST 2013, 'Analysis of dry sliding wear behaviour of Al6061/SiC/Al₂O₃ hybrid metal matrix composites', *Composites Part B: Engineering*, vol. 53, no. 0, pp. 159-68.
- Ünlü, BS & Atik, E 2007, 'Determination of friction coefficient in journal bearings', *Materials & Design*, vol. 28, no. 3, pp. 973-7.
- Vasheghani Farahani, M, Emadoddin, E, Emamy, M & Honarbakhsh Raouf, A 2014, 'Effect of grain refinement on mechanical properties and sliding wear resistance of extruded Sc-free 7042 aluminum alloy', *Materials & Design*, vol. 54, no. 0, pp. 361-7.
- Velkavrh, I & Kalin, M 2012, 'Comparison of the effects of the lubricant-molecule chain length and the viscosity on the friction and wear of diamond-like-carbon coatings and steel', *Tribology International*, vol. 50, no. 0, pp. 57-65.
- Velkavrh, I, Kalin, M & Vižintin, J 2009, 'The influence of viscosity on the friction in lubricated DLC contacts at various sliding velocities', *Tribology International*, vol. 42, no. 11–12, pp. 1752-7.

Vengudusamy, B, Green, JH, Lamb, GD & Spikes, HA 2012, 'Behaviour of MoDTC in DLC/DLC and DLC/steel contacts', *Tribology International*, vol. 54, pp. 68-76, Scopus.

Vijay, G, Pai, PS & Sriram, N 2010, 'Artificial Neural Network based Condition Monitoring of Rolling Element Bearing using Vibration Signals', *Advances in Mechanical Engineering*, p. 449.

Wang, A & Rack, H 1991, 'Dry sliding wear in 2124 Al-SiC_w/17-4 PH stainless steel systems', *Wear*, vol. 147, no. 2, pp. 355-74.

Wang, B, Ma, JH & Wu, YP 2013, 'Application of artificial neural network in prediction of abrasion of rubber composites', *Materials & Design*, vol. 49, no. 0, pp. 802-7.

Wang, L, Zhou, J, Duszcyk, J & Katgerman, L 2012, 'Identification of a friction model for the bearing channel of hot aluminium extrusion dies by using ball-on-disc tests', *Tribology International*, vol. 50, no. 0, pp. 66-75.

Wang, SQ, Wei, MX & Zhao, YT 2010, 'Effects of the tribo-oxide and matrix on dry sliding wear characteristics and mechanisms of a cast steel', *Wear*, vol. 269, no. 5-6, pp. 424-34.

Wang, SQ, Wang, L, Zhao, YT, Sun, Y & Yang, ZR 'Mild-to-severe wear transition and transition region of oxidative wear in steels', *Wear*, no. 0.

Wang, YQ, Afsar, AM, Jang, JH, Han, KS & Song, JI 2010, 'Room temperature dry and lubricant wear behaviors of Al₂O₃f/SiCp/Al hybrid metal matrix composites', *Wear*, vol. 268, no. 7-8, pp. 863-70.

Wang, Z, Dohda, K & Haruyama, Y 2006, 'Effects of entraining velocity of lubricant and sliding velocity on friction behavior in stainless steel sheet rolling', *Wear*, vol. 260, no. 3, pp. 249-57.

Wei, MX, Wang, SQ, Wang, L, Cui, XH & Chen, KM 2011, 'Effect of tempering conditions on wear resistance in various wear mechanisms of H13 steel', *Tribology International*, vol. 44, no. 7-8, pp. 898-905.

Wieleba, W 2002, 'The statistical correlation of the coefficient of friction and wear rate of PTFE composites with steel counterface roughness and hardness', *Wear*, vol. 252, no. 9-10, pp. 719-29.

Xiao, Y, Shi, W, Luo, J & Liao, Y 2014, 'The tribological performance of TiN, WC/C and DLC coatings measured by the four-ball test', *Ceramics International*, vol. 40, no. 5, pp. 6919-25.

Xin, L, Gaoliang, P & Zhe, L 2014, 'Prediction of seal wear with thermal-structural coupled finite element method', *Finite Elements in Analysis and Design*, vol. 83, no. 0, pp. 10-21.

Yaakob, Z, Mohammad, M, Alherbawi, M, Alam, Z & Sopian, K 2013, 'Overview of the production of biodiesel from Waste cooking oil', *Renewable and Sustainable Energy Reviews*, vol. 18, no. 0, pp. 184-93.

- Yang, D, Peng, X, Zhong, L, Cao, X, Chen, W, Zhang, X, Liu, S & Sun, R 2014, "Green" films from renewable resources: Properties of epoxidized soybean oil plasticized ethyl cellulose films', *Carbohydrate Polymers*, vol. 103, no. 0, pp. 198-206.
- Yang, X-w, Zhu, J-c, Nong, Z-s, He, D, Lai, Z-h, Liu, Y & Liu, F-w 2013, 'Prediction of mechanical properties of A357 alloy using artificial neural network', *Transactions of Nonferrous Metals Society of China*, vol. 23, no. 3, pp. 788-95.
- Yao, N, Zhang, P, Song, L, Kang, M, Lu, Z & Zheng, R 2013, 'Stearic acid coating on circulating fluidized bed combustion fly ashes and its effect on the mechanical performance of polymer composites', *Applied Surface Science*, vol. 279, no. 0, pp. 109-15.
- Yasseri, SF, Bahai, H, Bazargan, H & Aminzadeh, A 2010, 'Prediction of safe sea-state using finite element method and artificial neural networks', *Ocean Engineering*, vol. 37, no. 2-3, pp. 200-7.
- Yilmaz, N 2011, 'Temperature-dependent viscosity correlations of vegetable oils and biofuel-diesel mixtures', *Biomass and Bioenergy*, vol. 35, no. 7, pp. 2936-8.
- Yousef, BF, Mourad, A-HI & Hilal-Alnaqbi, A 2011, 'Prediction of the Mechanical Properties of PE/PP Blends Using Artificial Neural Networks', *Procedia Engineering*, vol. 10, no. 0, pp. 2713-8.
- Yousif, B & El-Tayeb, N 2010, 'Wet adhesive wear characteristics of untreated oil palm fibre-reinforced polyester and treated oil palm fibre-reinforced polyester composites using the pin-on-disc and block-on-ring techniques', *Proceedings of the Institution of Mechanical Engineers, Part J: Journal of Engineering Tribology*, vol. 224, no. 2, pp. 123-31.
- Yousif, BF 2013a, 'Design of newly fabricated tribological machine for wear and frictional experiments under dry/wet condition', *Materials & Design*, vol. 48, no. 0, pp. 2-13.
- Yousif, BF 2013b, 'Editorial for SI: Materials, design and tribology', *Materials & Design*, vol. 48, no. 0, p. 1.
- Yousif, BF & El-Tayeb, NSM 2008, 'Wear and friction characteristics of CGRP composite under wet contact condition using two different test techniques', *Wear*, vol. 265, no. 5-6, pp. 856-64.
- Yousif, BF & Chin, CW 2012, 'Epoxy composite based on kenaf fibers for tribological applications under wet contact conditions', *Surface Review and Letters*, vol. 19, no. 5.
- Yousif, BF, Devadas, A & Yusaf, TF 2009, 'Adhesive wear and frictional behavior of multilayered polyester composite based on Betelnut fiber mats under wet contact conditions', *Surface Review and Letters*, vol. 16, no. 3, pp. 407-14.
- Yusaf, TF, Yousif, BF & Elawad, MM 2011, 'Crude palm oil fuel for diesel-engines: Experimental and ANN simulation approaches', *Energy*, vol. 36, no. 8, pp. 4871-8.

- Zerrouki, AA, Aïfa, T & Baddari, K 2014, 'Prediction of natural fracture porosity from well log data by means of fuzzy ranking and an artificial neural network in Hassi Messaoud oil field, Algeria', *Journal of Petroleum Science and Engineering*, vol. 115, no. 0, pp. 78-89.
- Zhang, H, Wang, Q & Mortimer, SR 2012, 'Waste cooking oil as an energy resource: Review of Chinese policies', *Renewable and Sustainable Energy Reviews*, vol. 16, no. 7, pp. 5225-31.
- Zhang, Z & Friedrich, K 2003, 'Artificial neural networks applied to polymer composites: a review', *Composites Science and Technology*, vol. 63, no. 14, pp. 2029-44.
- Zhang, Z, Friedrich, K & Velten, K 2002, 'Prediction on tribological properties of short fibre composites using artificial neural networks', *Wear*, vol. 252, no. 7–8, pp. 668-75.
- Zhang, Z, Barkoula, NM, Karger-Kocsis, J & Friedrich, K 2003, 'Artificial neural network predictions on erosive wear of polymers', *Wear*, vol. 255, no. 1–6, pp. 708-13, viewed 2003/9//.
- Zhao, X, Liu, J, Zhu, B, Luo, Z & Miao, H 1997, 'Effects of lubricants on friction and wear of Ti(CN)1045 steel sliding pairs', *Tribology International*, vol. 30, no. 3, pp. 177-82.
- Zhu, H, Jar, C, Song, J, Zhao, J, Li, J & Xie, Z 2012, 'High temperature dry sliding friction and wear behavior of aluminum matrix composites (Al₃Zr+ α -Al₂O₃)/Al', *Tribology International*, vol. 48, no. 0, pp. 78-86.
- Zmitrowicz, A 2005, 'Wear debris: a review of properties and constitutive models', *Journal of Theoretical and Applied Mechanics*, vol. 43, no. 1, pp. 3-35.

Appendix A: Detailed Drawings of the Components of the Hybrid Tribology Machine

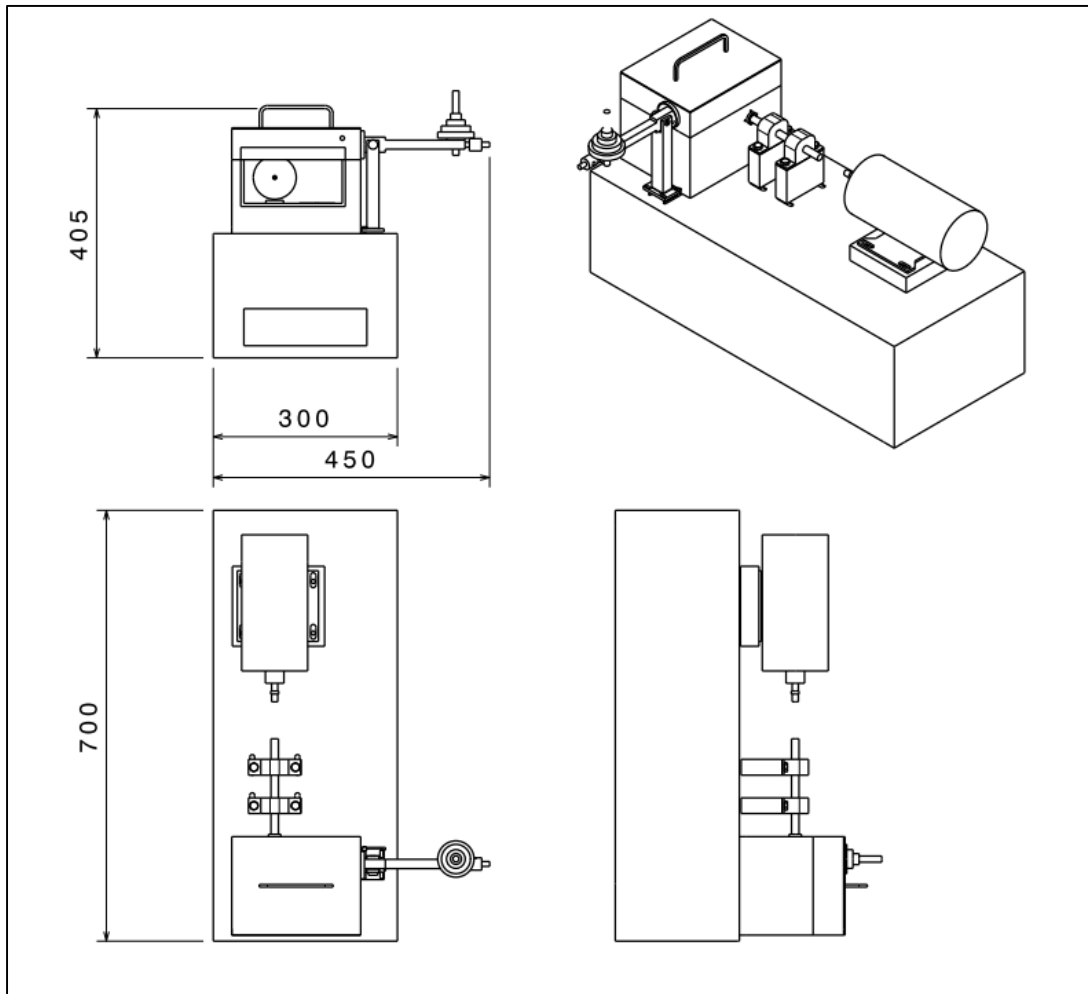


Figure A.1: Overview of the hybrid tribology machine showing the main dimensions.

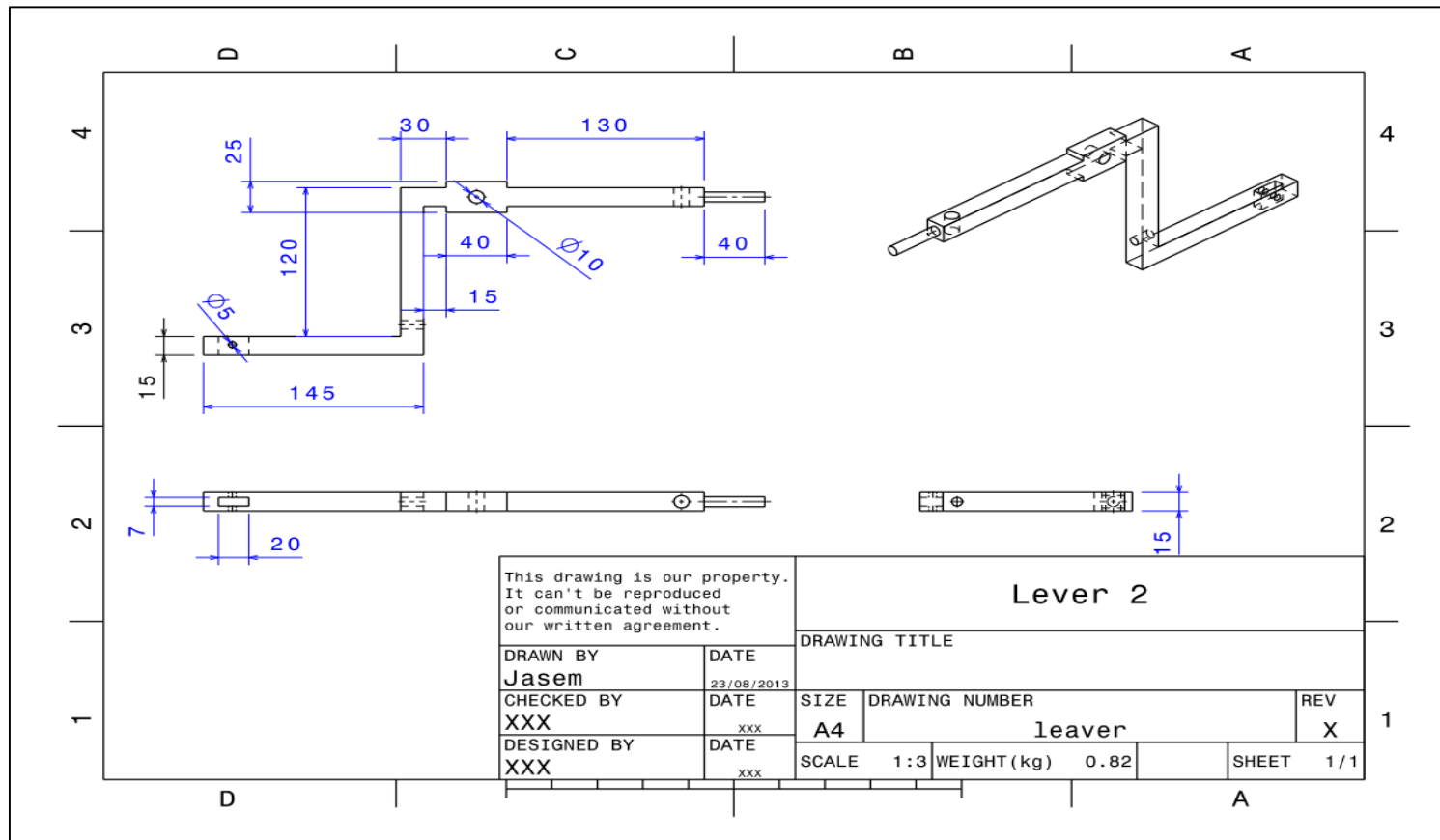


Figure A.2: Two-dimensional views of the lever for the hybrid tribology machine with the ISO.

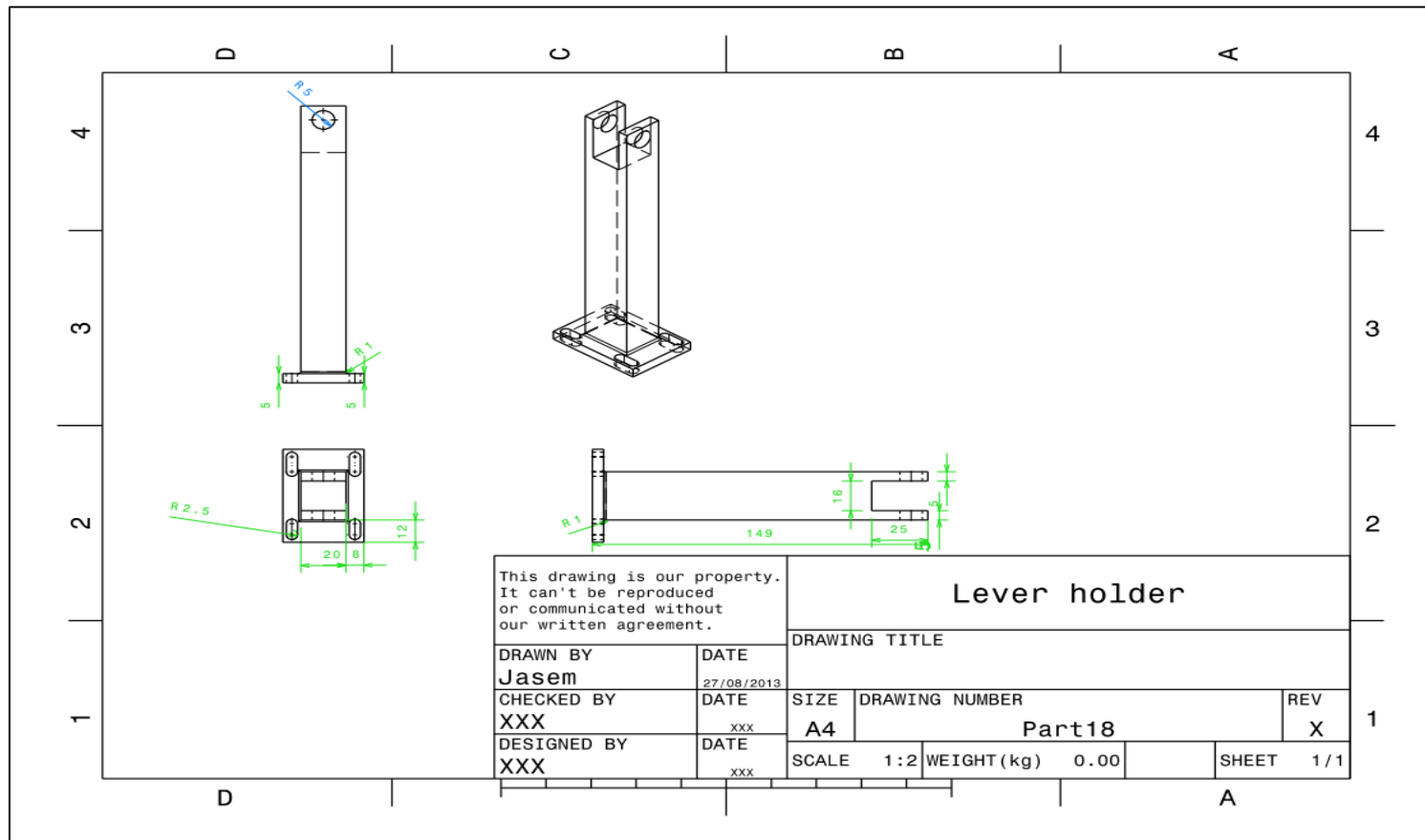


Figure A.3: Two-dimensional views of the lever holder for the hybrid tribology machine with the ISO.

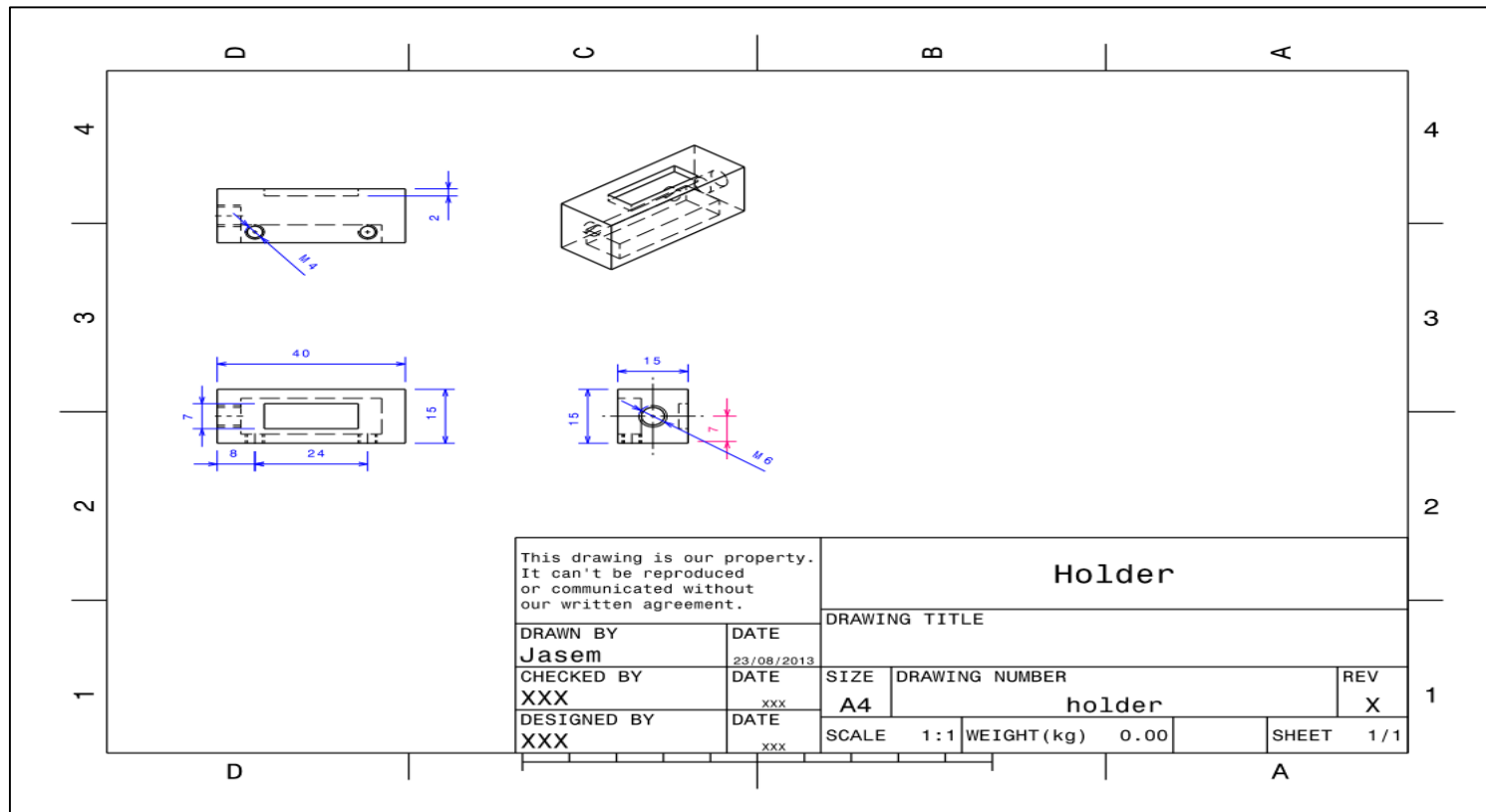


Figure A.4: Two-dimensional views of the sample holder for the hybrid tribology machine with the ISO.

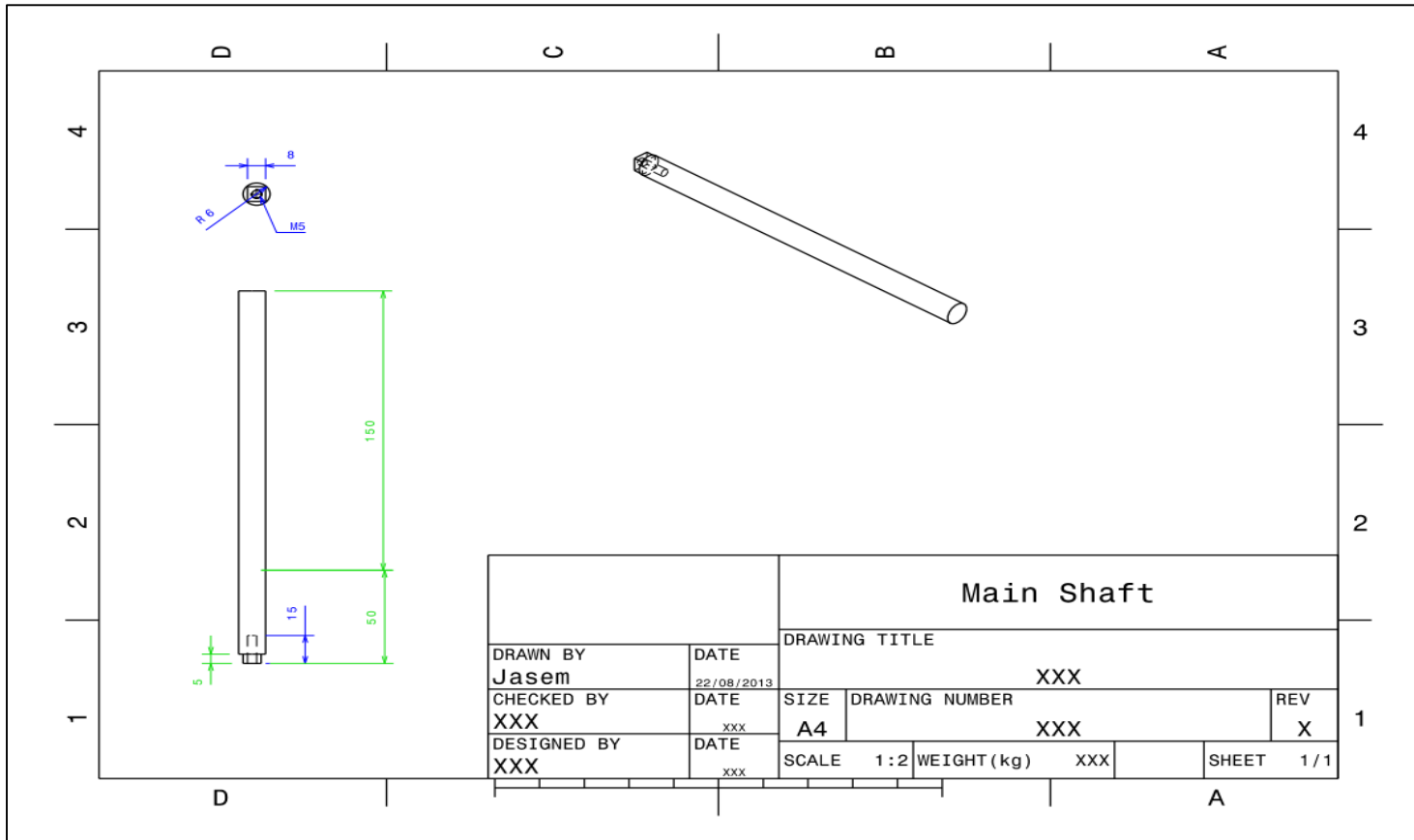


Figure A.5: The main shaft connecting the counterface and the motor through the coupling.

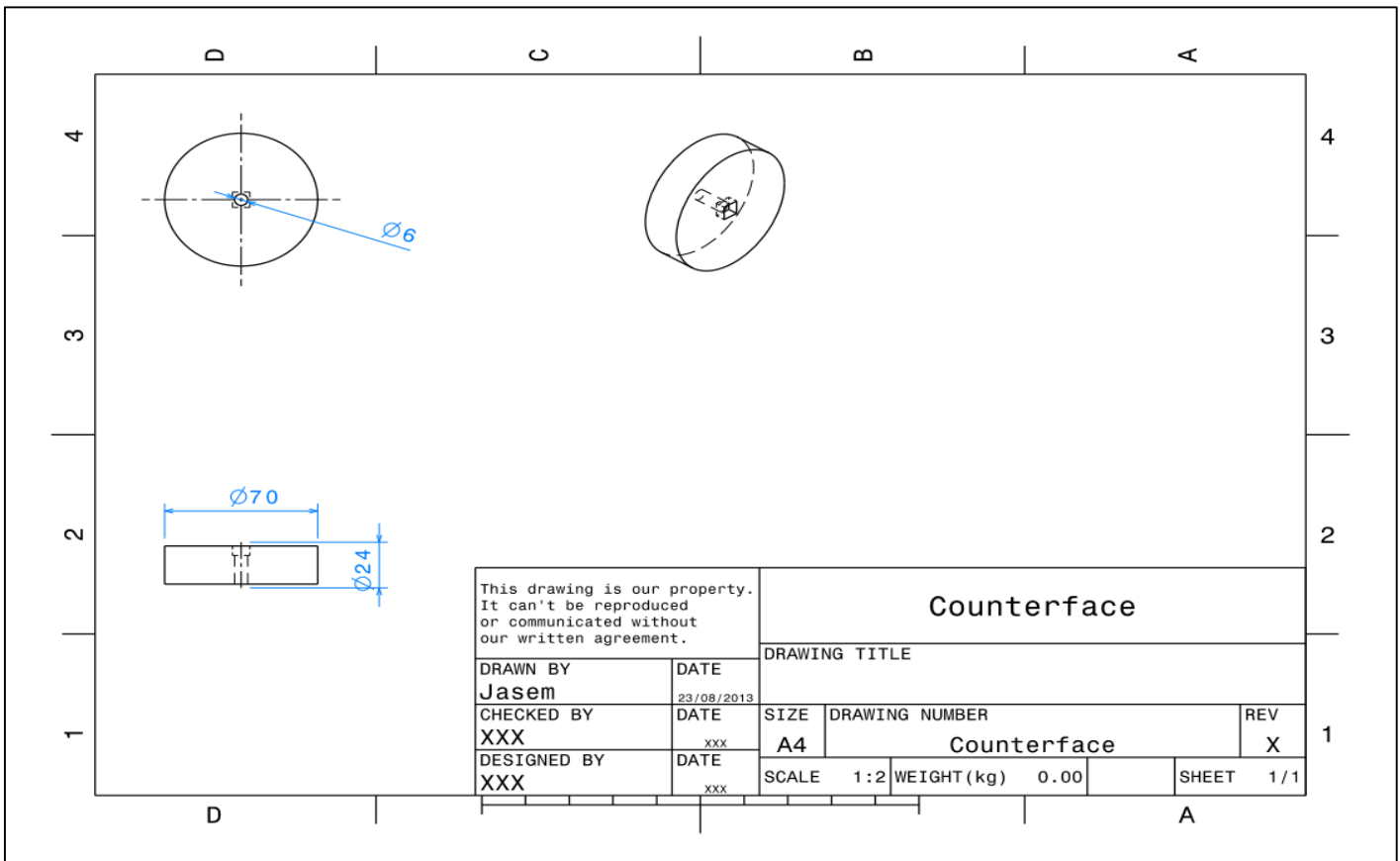


Figure A.6: Two-dimensional views of the counterface for the hybrid tribology machine with the ISO.

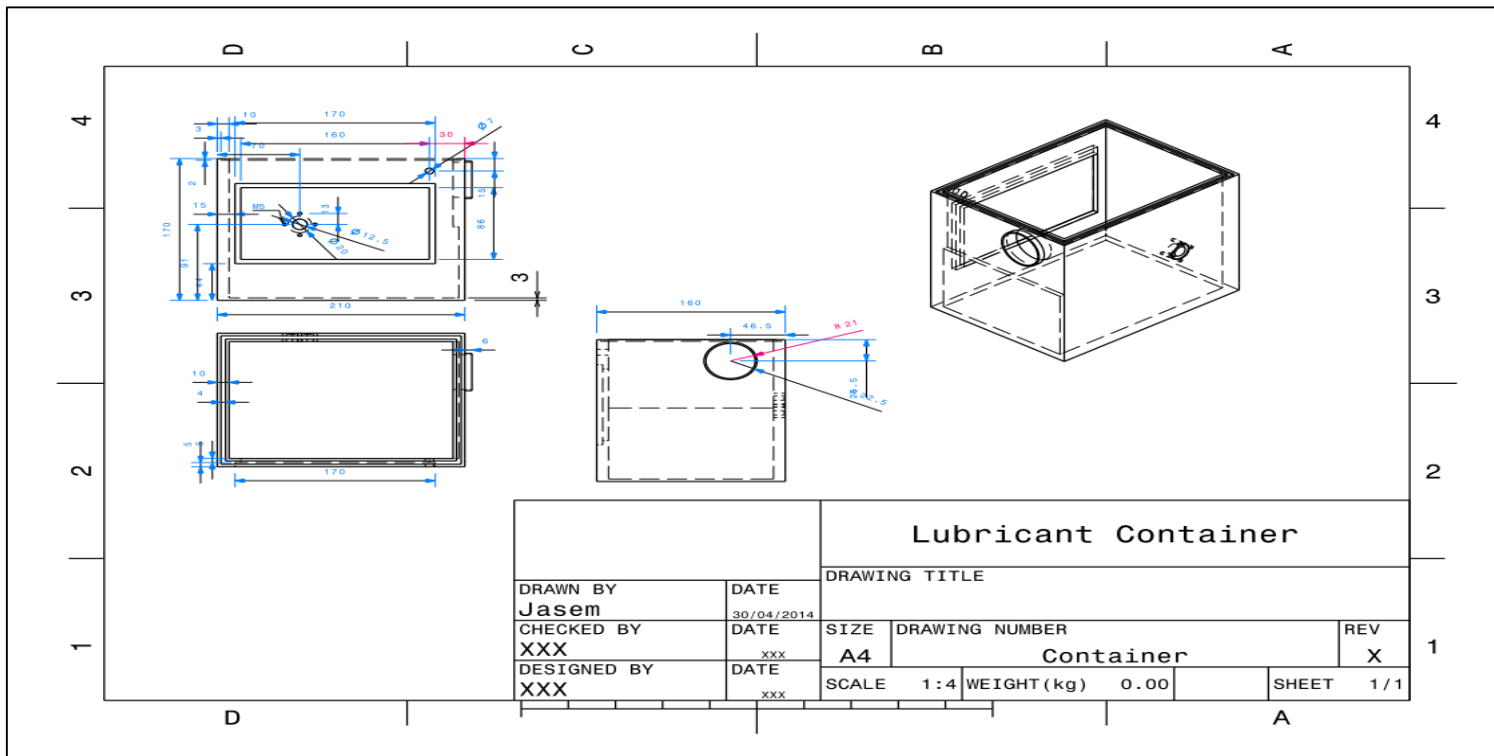


Figure A.7: Two-dimensional views of the lubricant container for the hybrid tribology machine with the ISO.

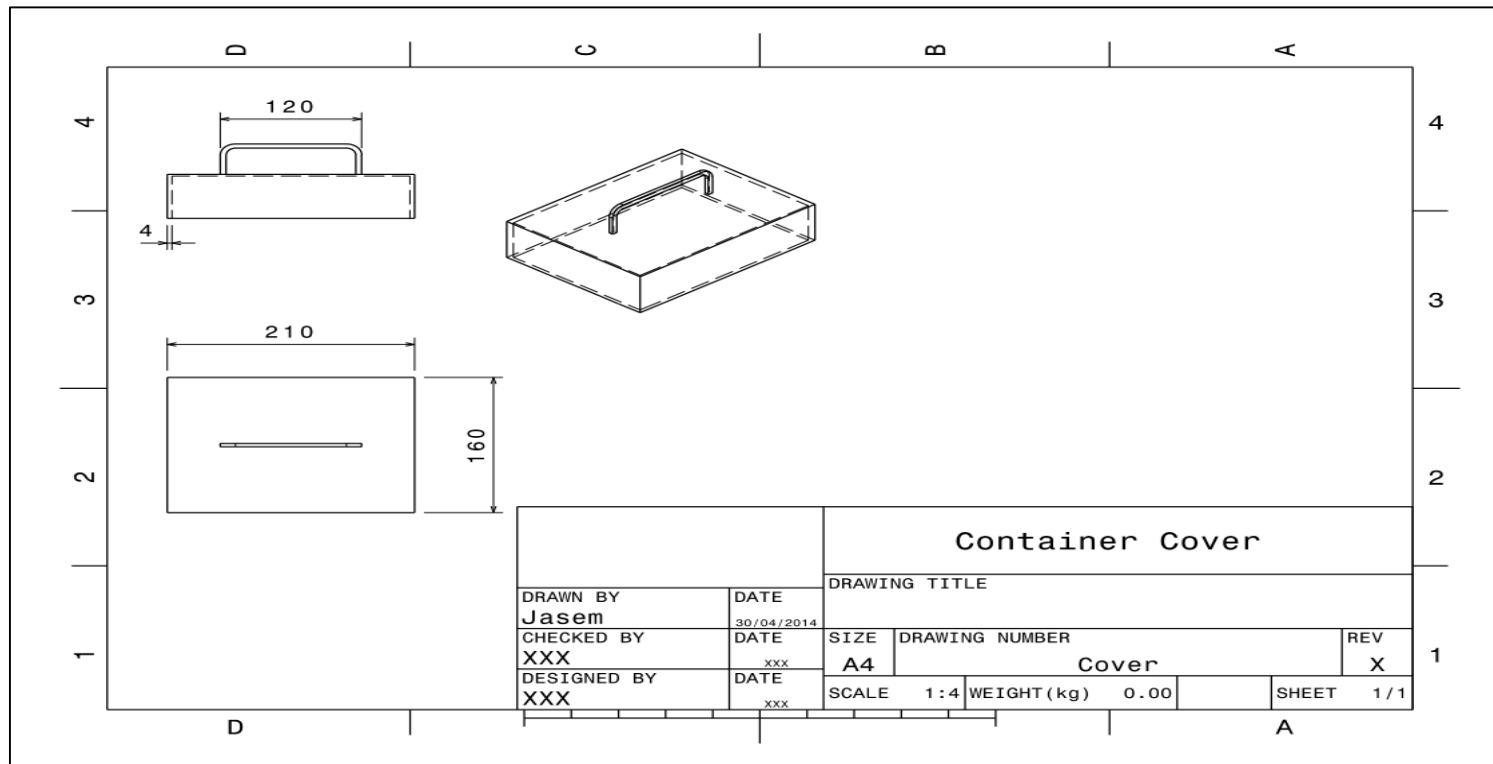


Figure A.8: Two-dimensional views of the machine cover for the hybrid tribology machine with the ISO.

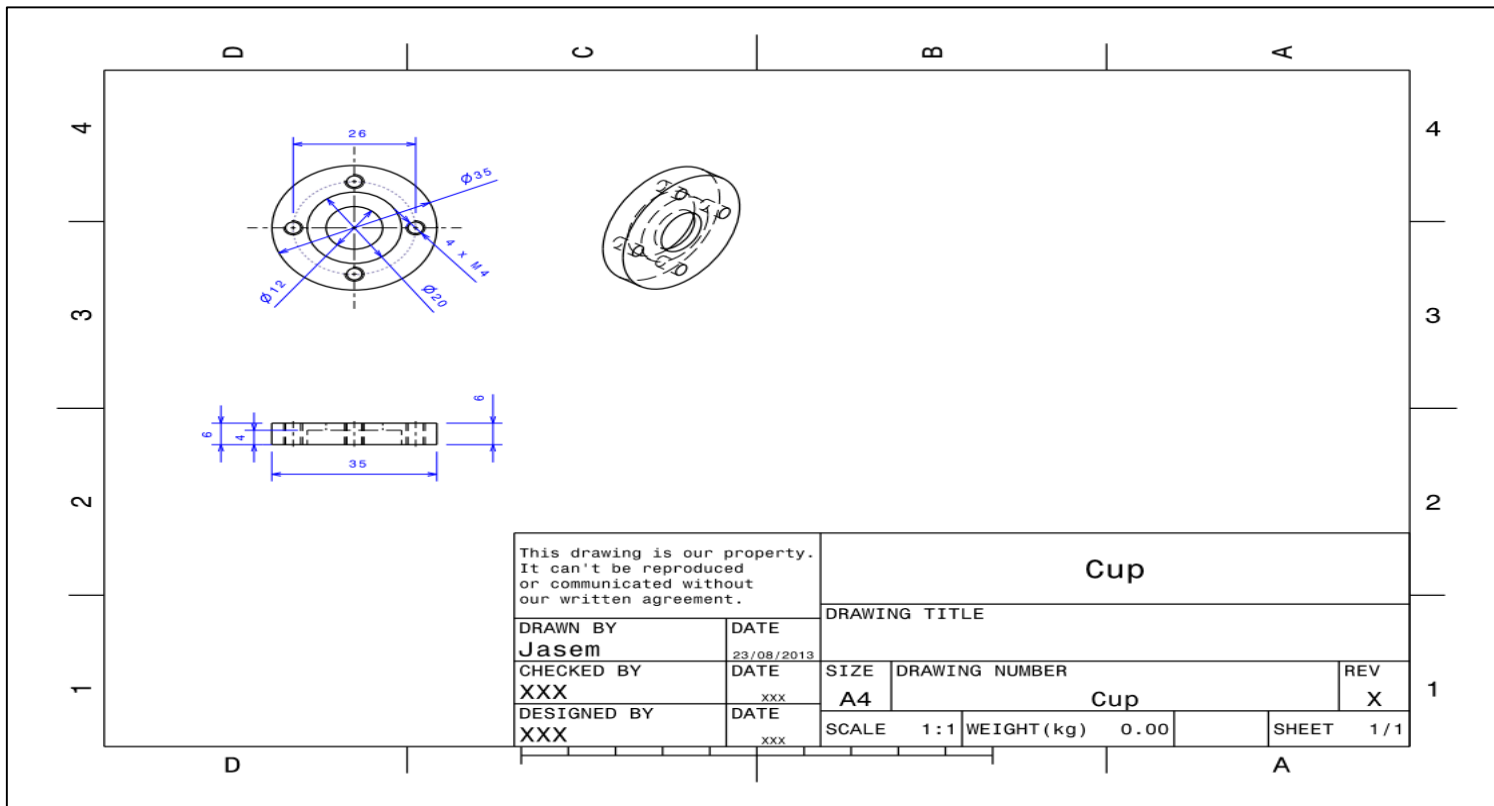


Figure A.9: The seal cup for the hole in which the main shaft enters the lubricant container.

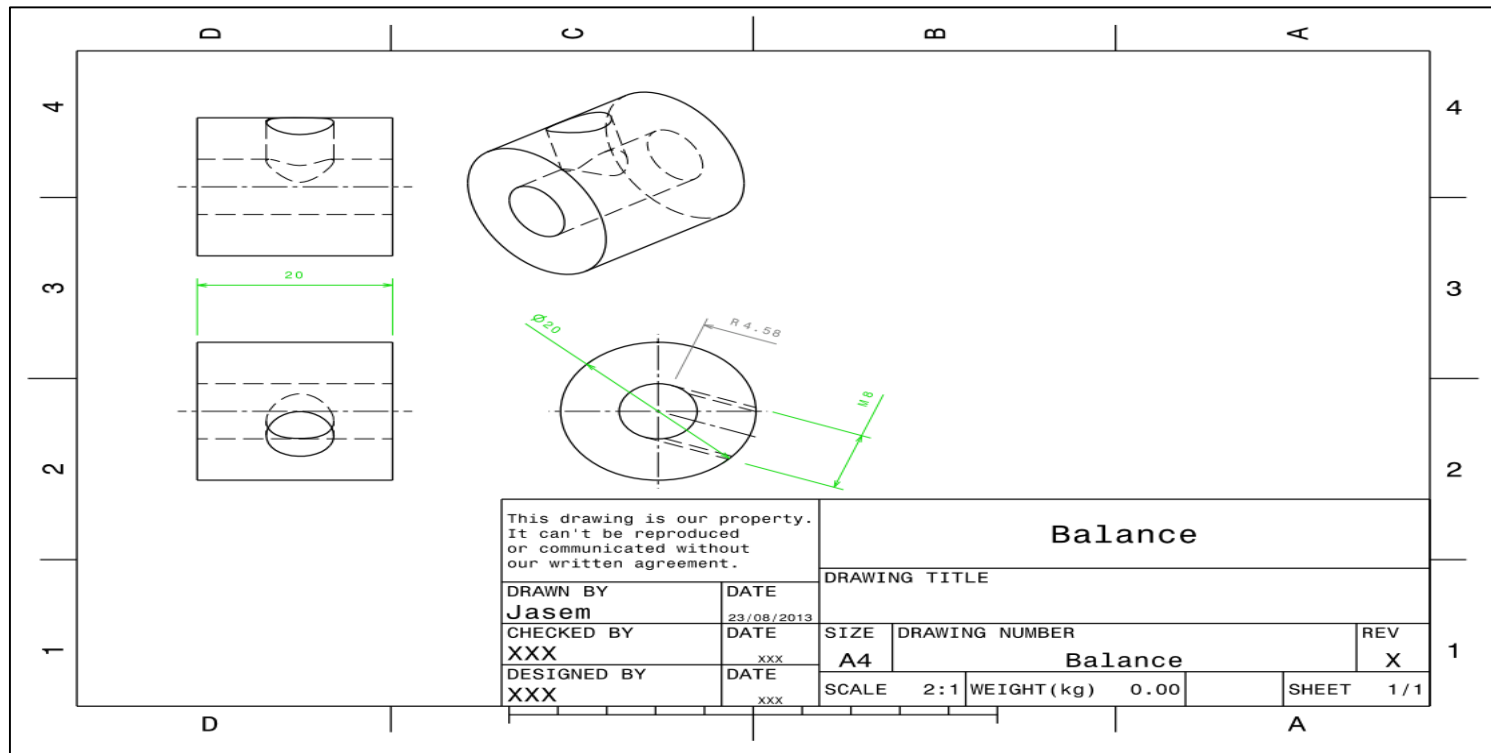


Figure A.10: The balancing weight that is attached to the main lever of the machine.

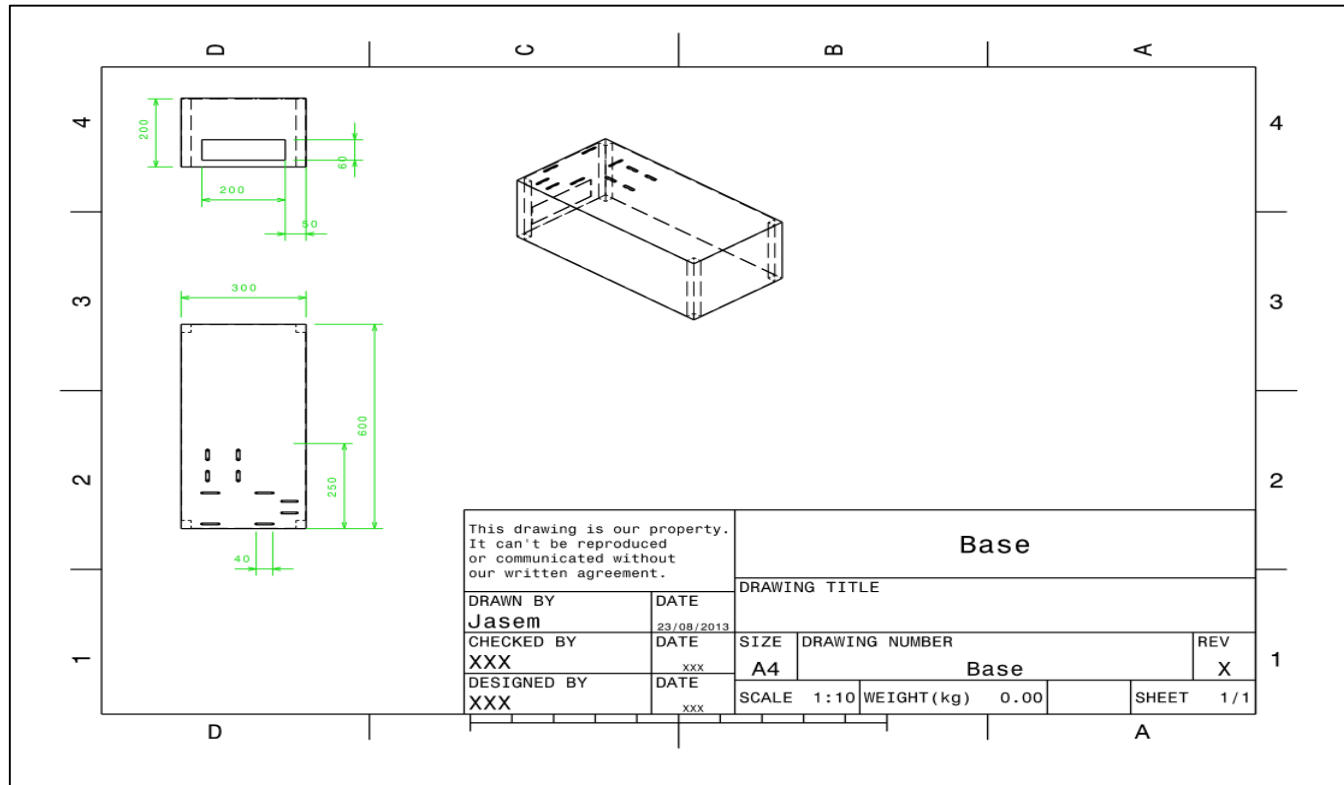


Figure A.11: The main frame of the machine showing the base with the generated slots to attach the components.

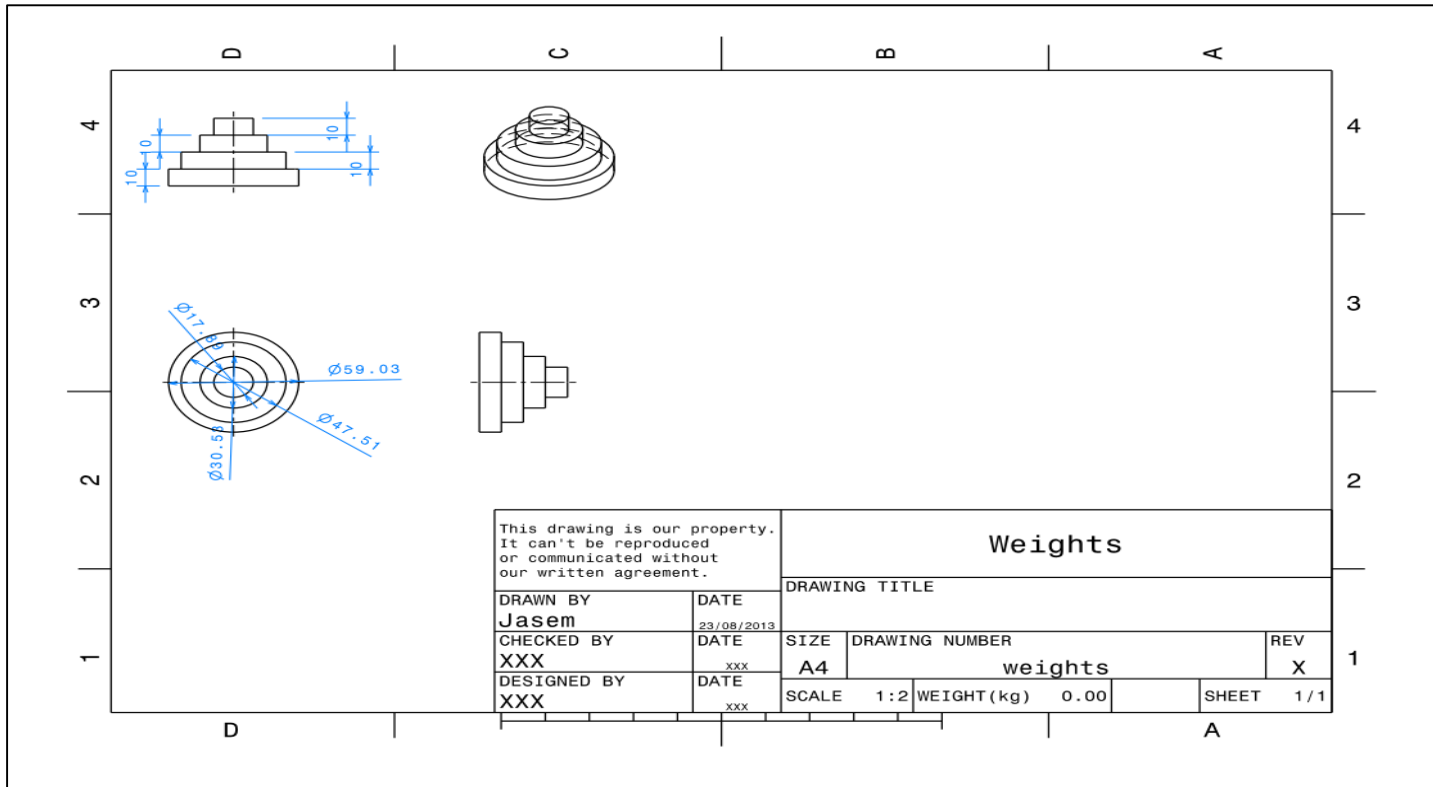


Figure A.12: The designed weights for the new machine.

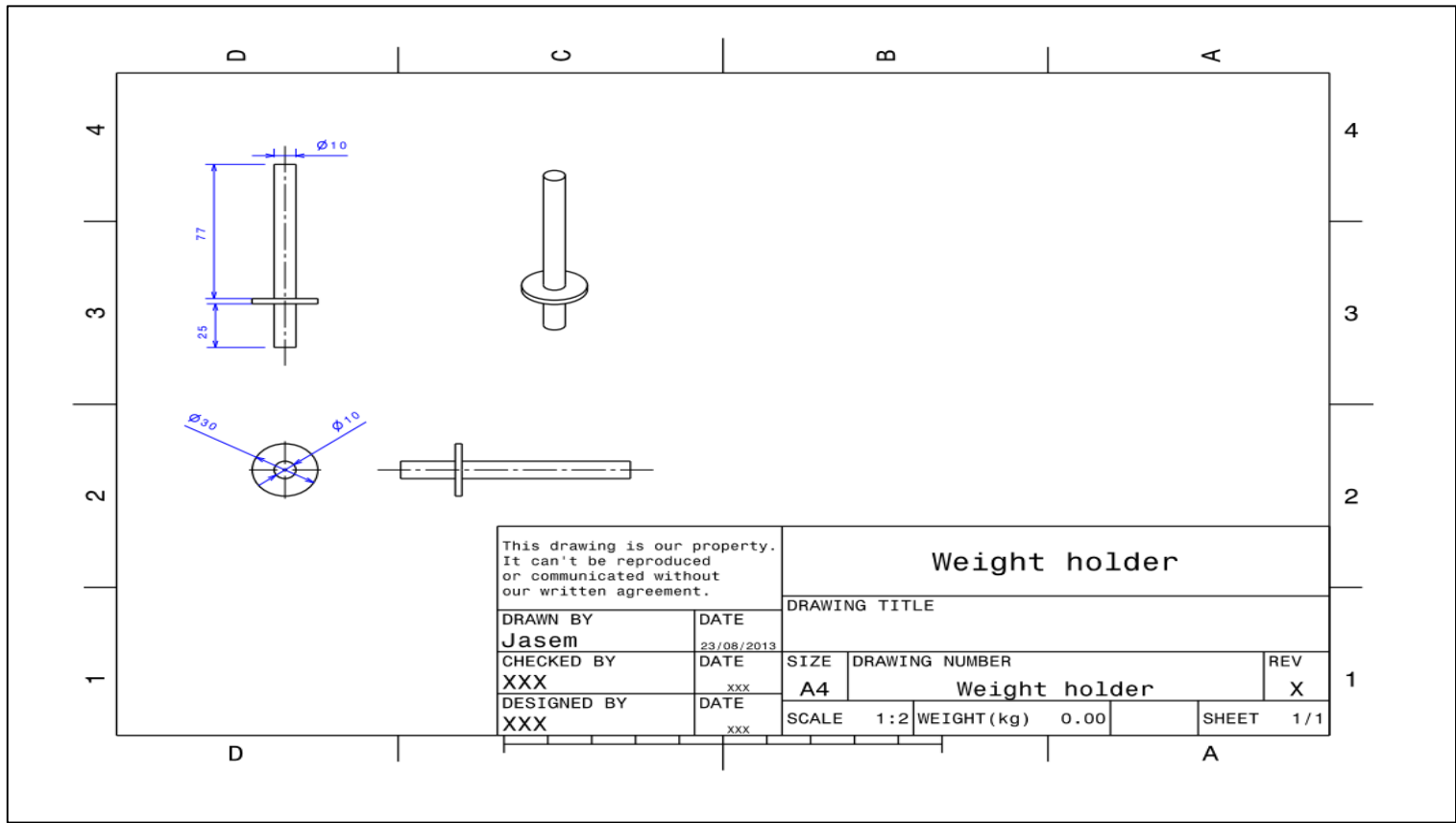


Figure A.13: The weight holder for the new machine.

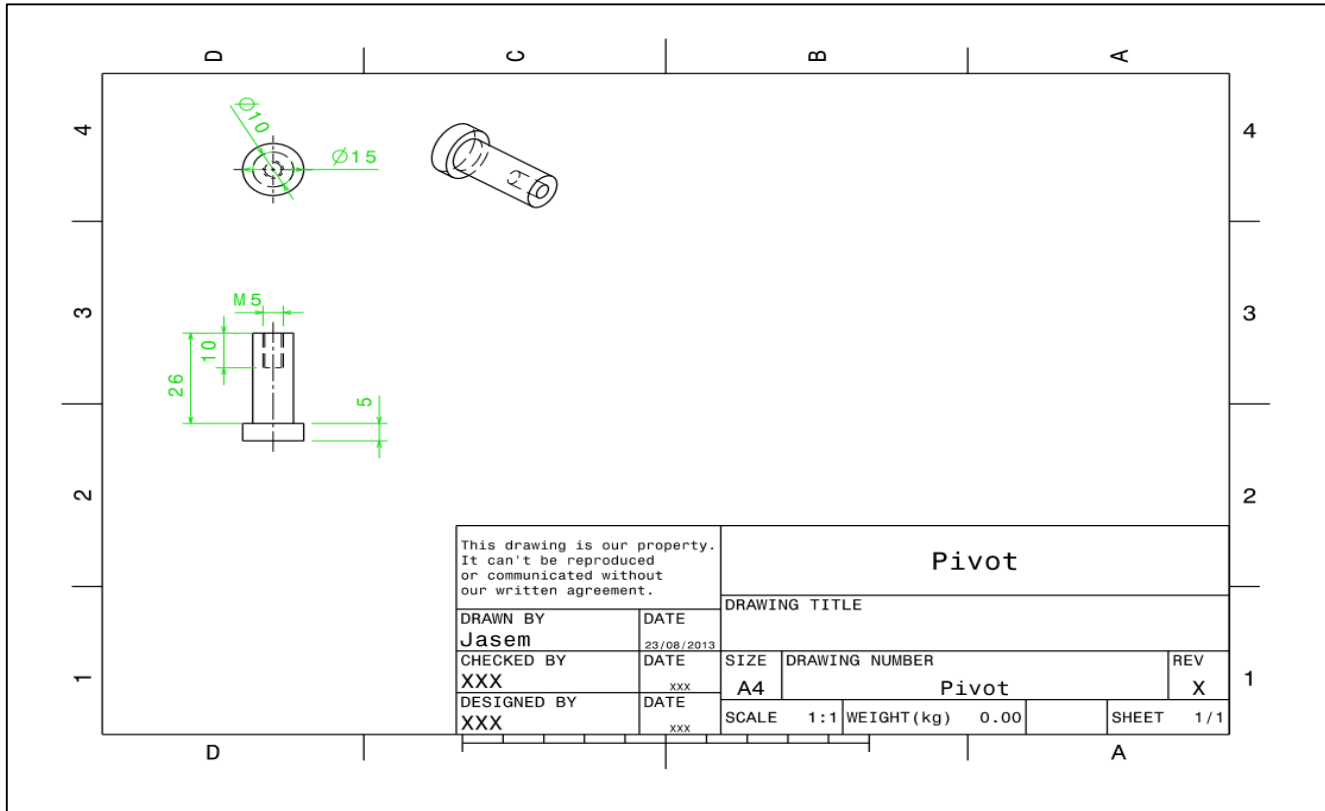


Figure A.14: The pivot for the new machine.

Appendix B: Details of the ANN models

B.1 The Performance of Different Training Functions

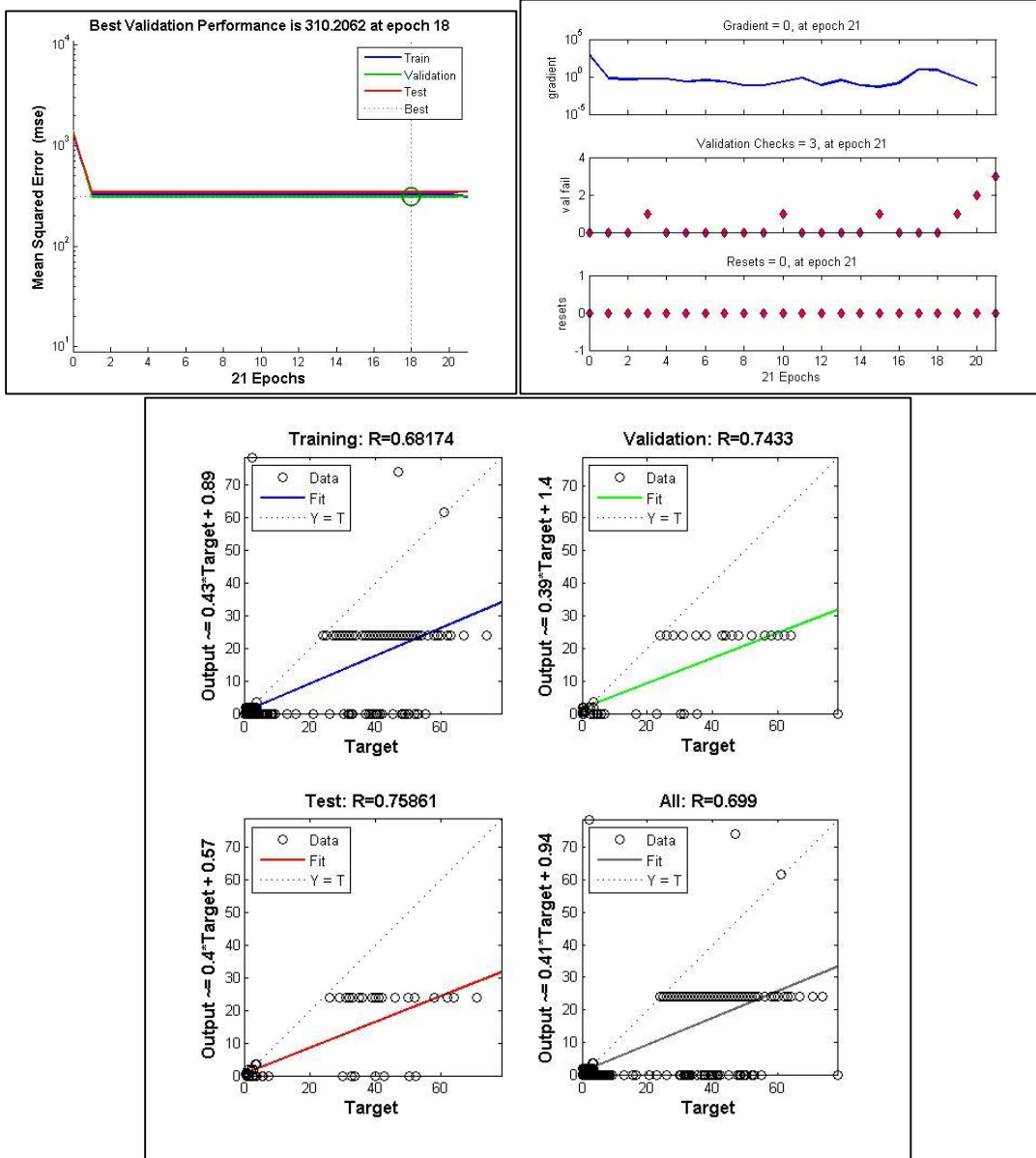


Figure B.1: Performance of Trainbfg.

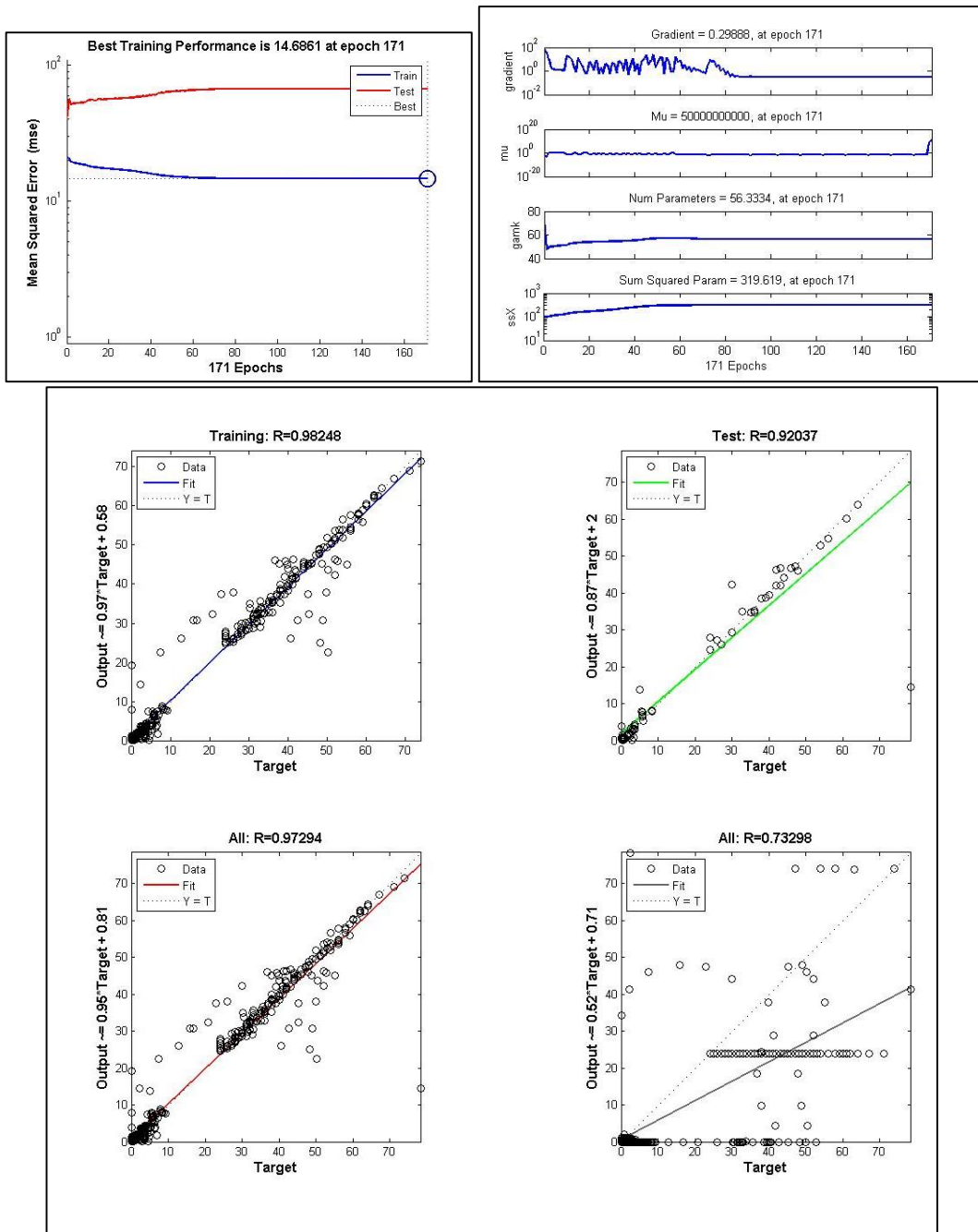


Figure B.2: Performance of Trainbr.

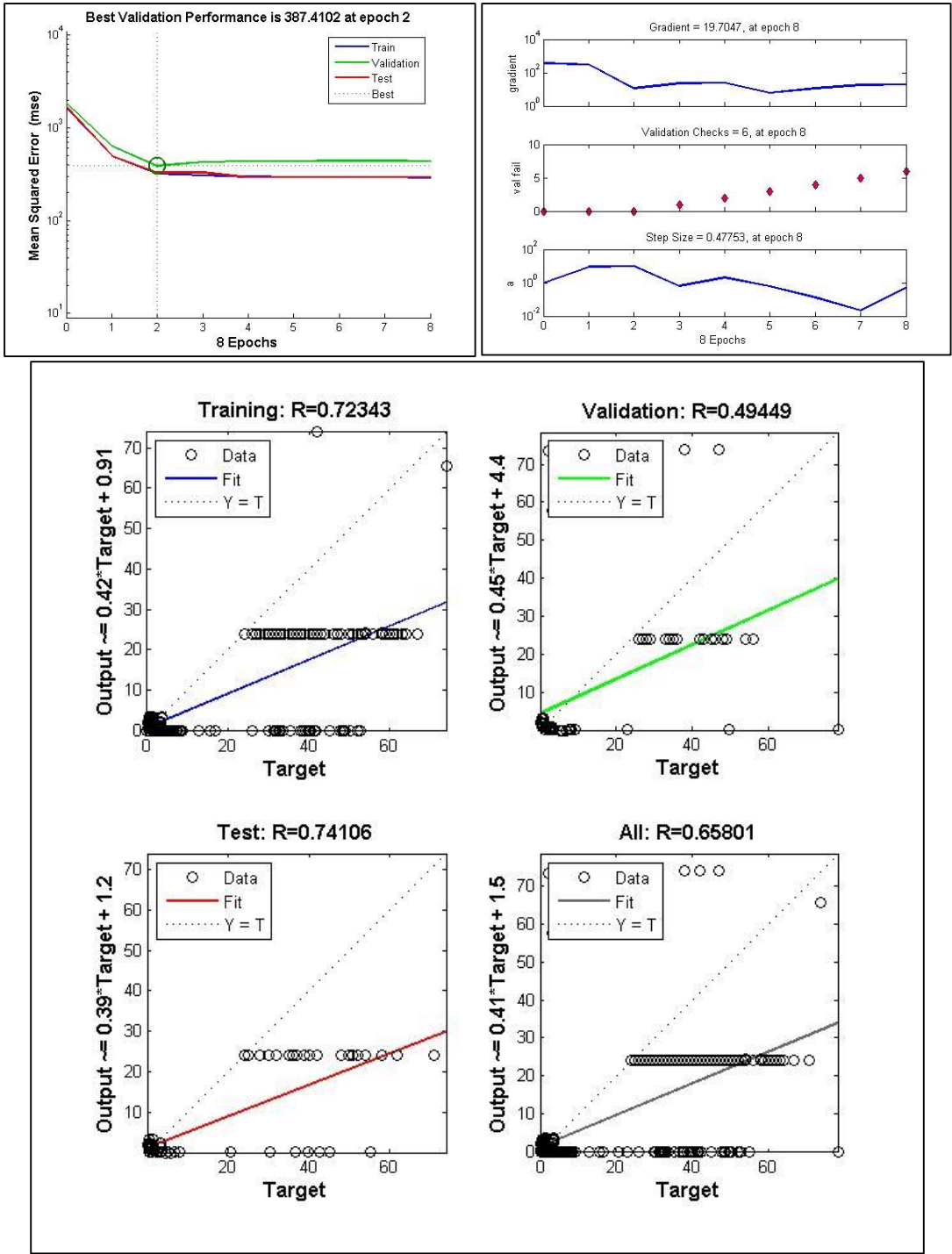


Figure B.3: Performance of Traincgb.

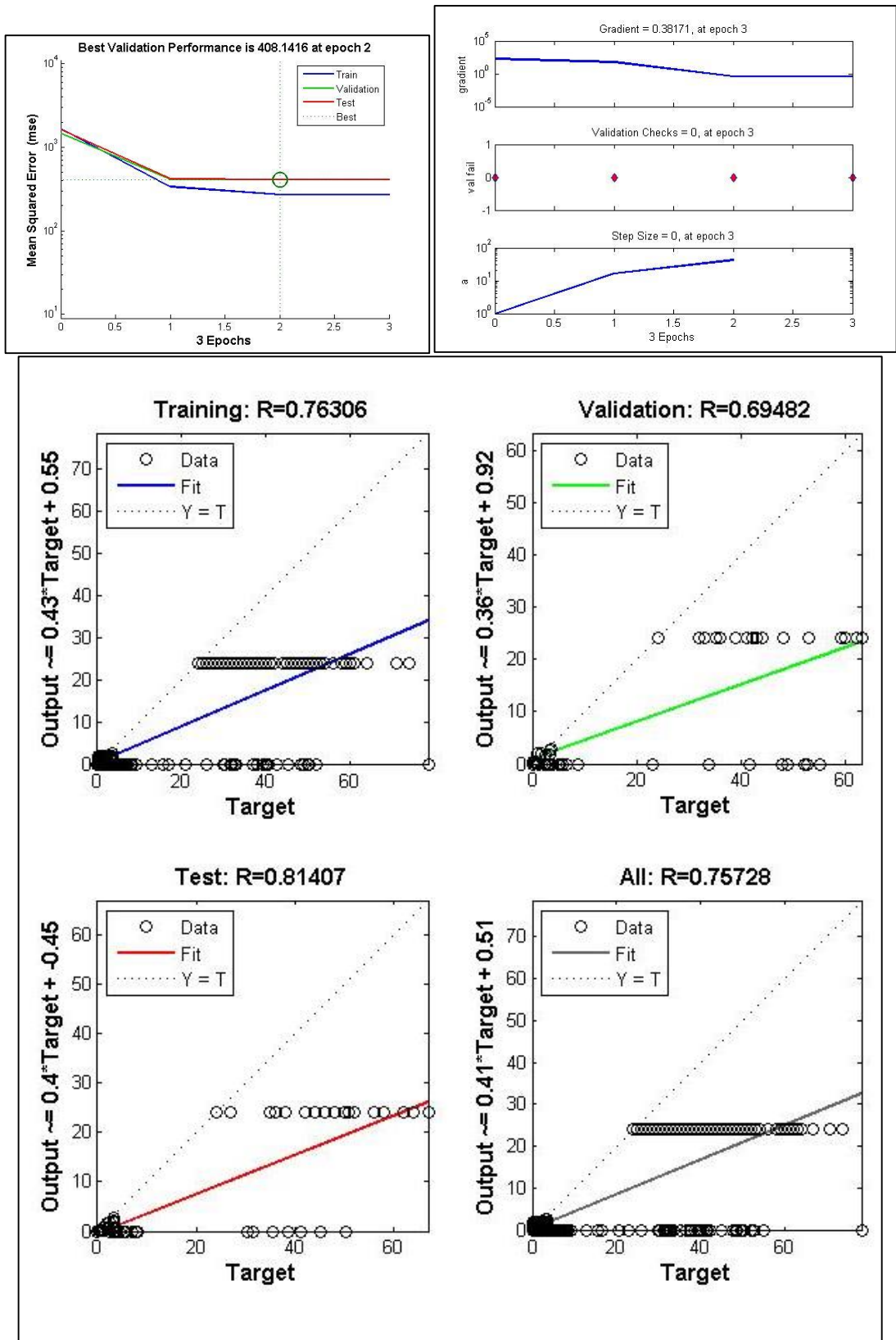


Figure B.4: Performance of Traincgf.

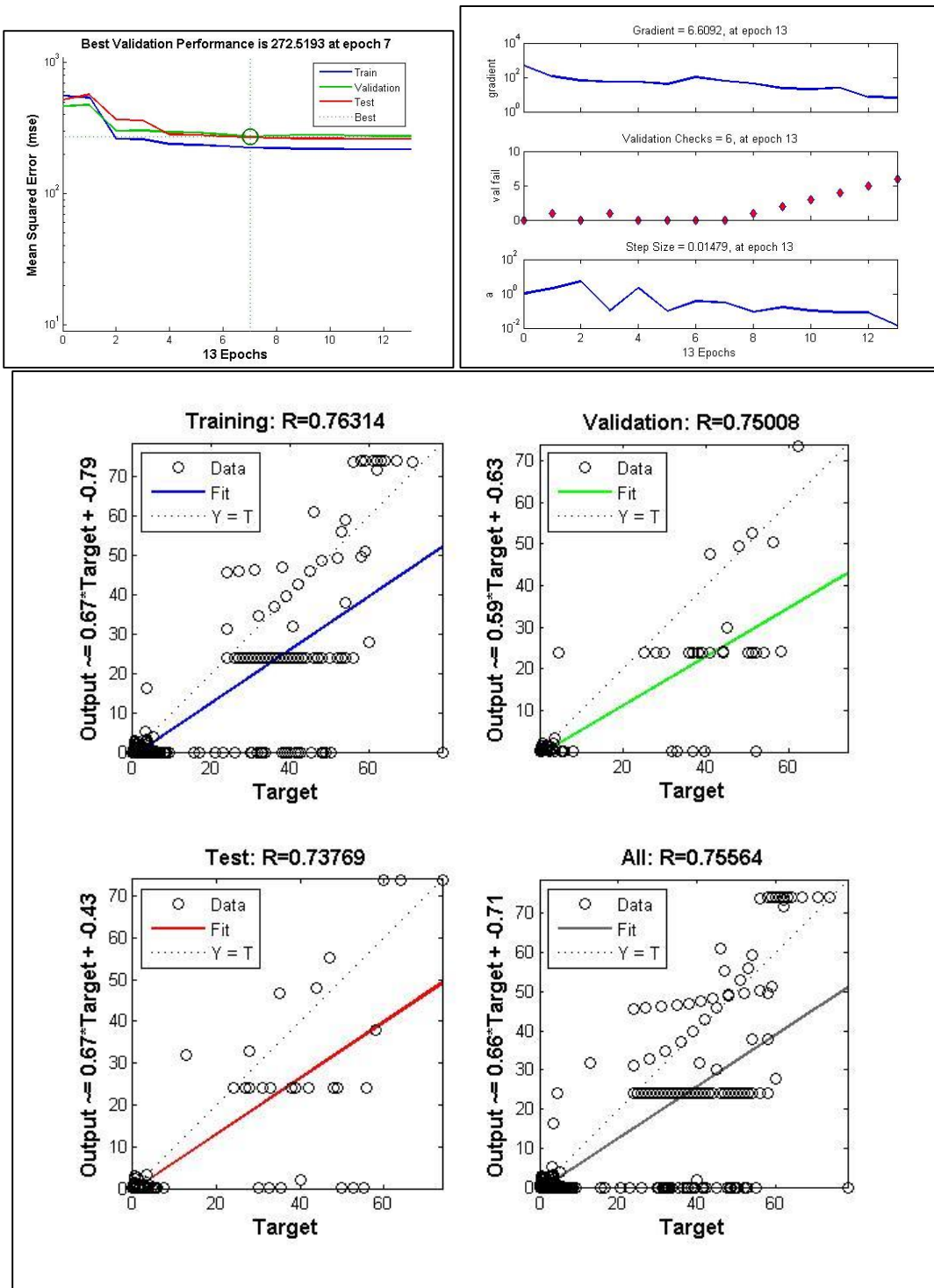


Figure B.5: Performance of Traincgp.

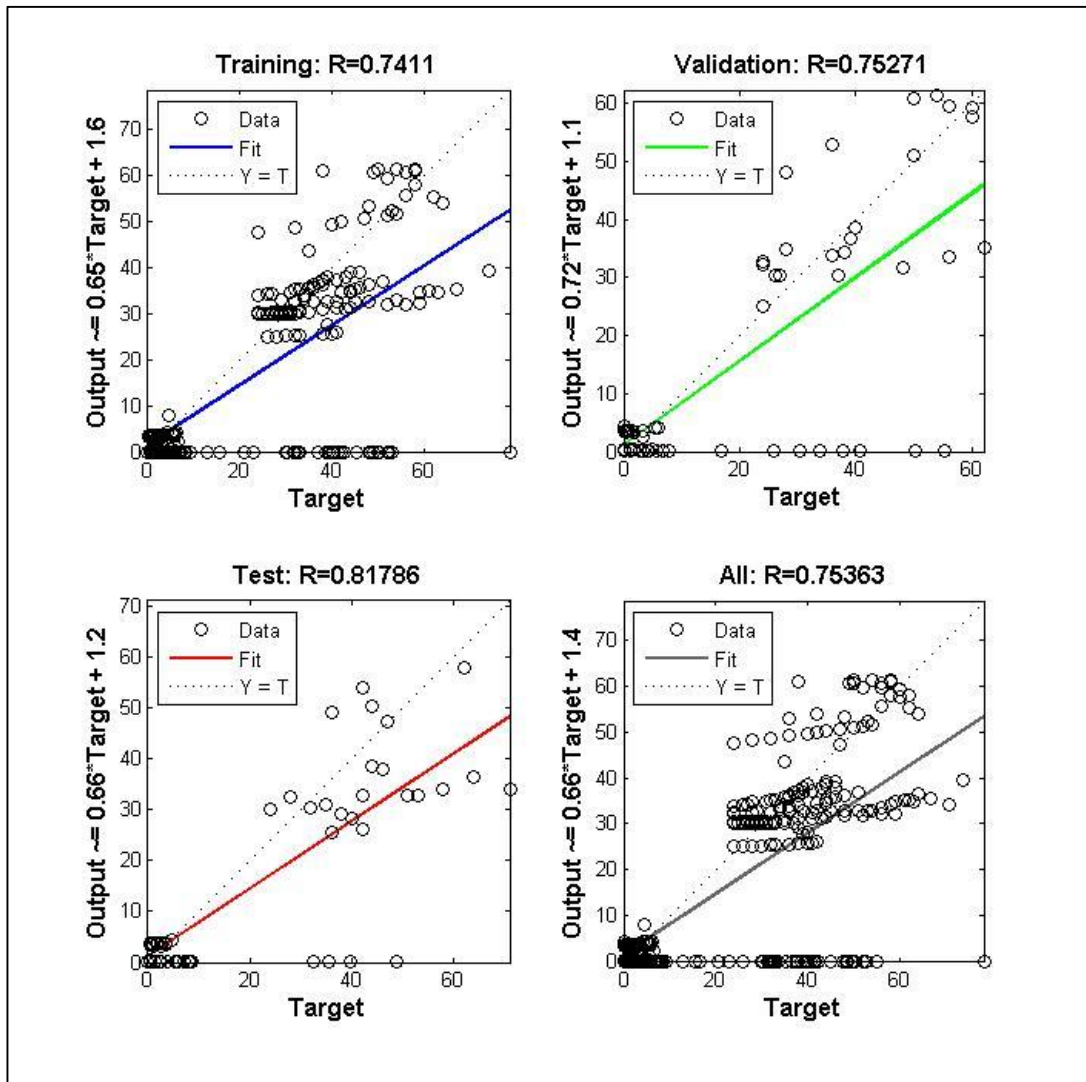
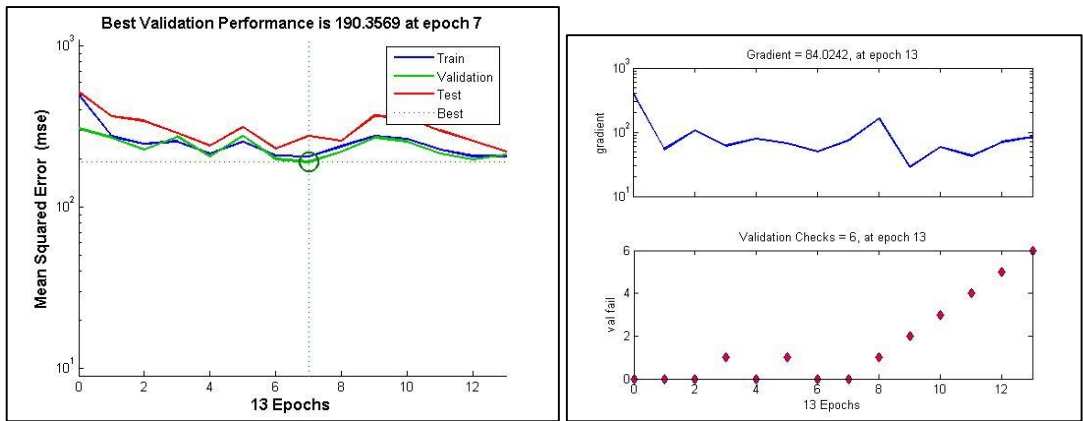


Figure B.6: Performance of Traingd.

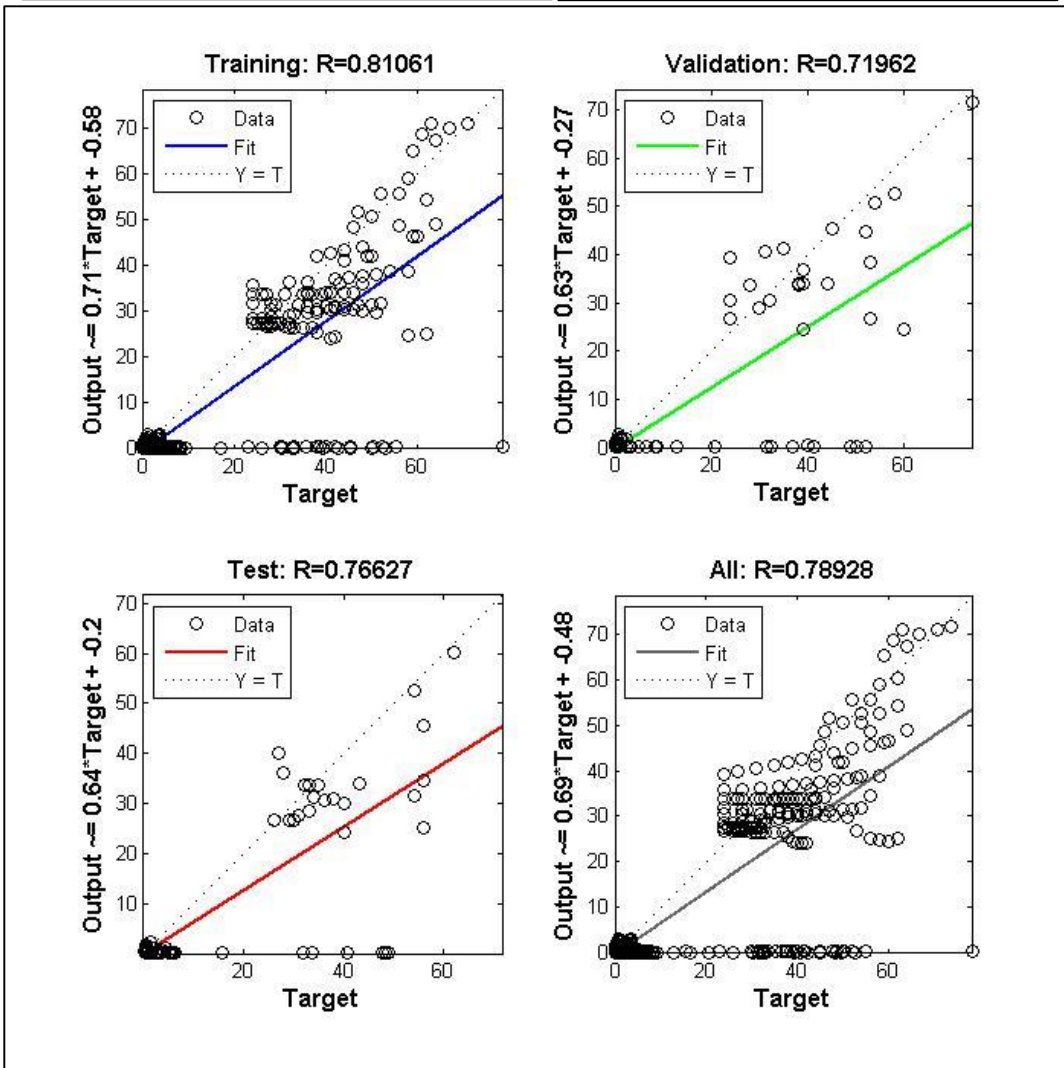
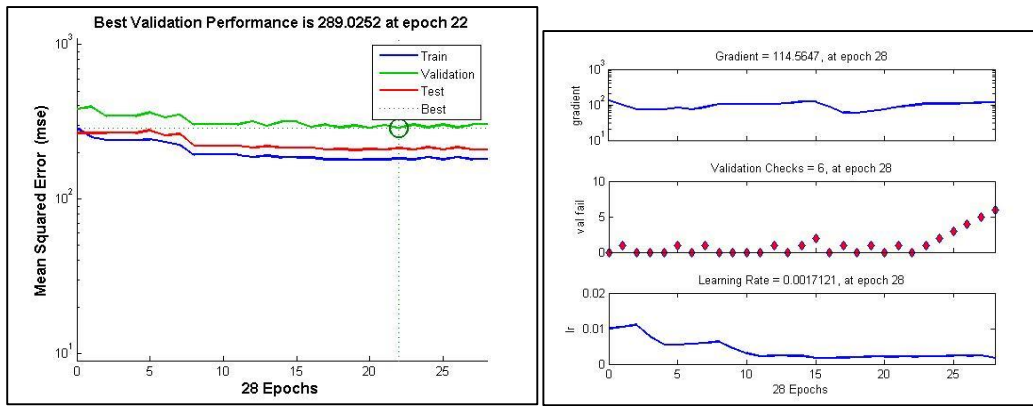


Figure B.7: Performance of Traingda.

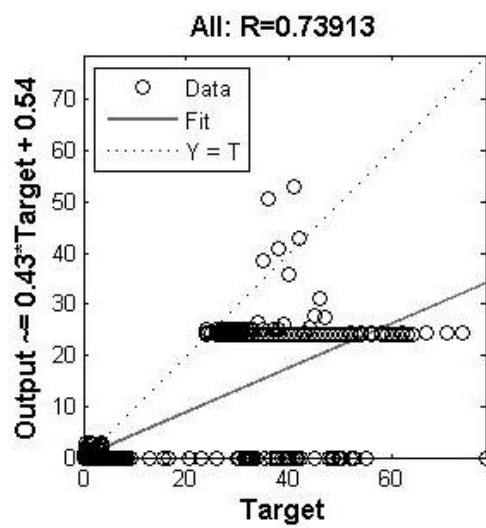
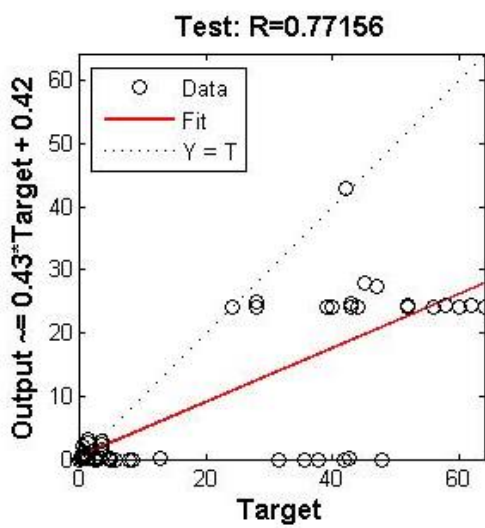
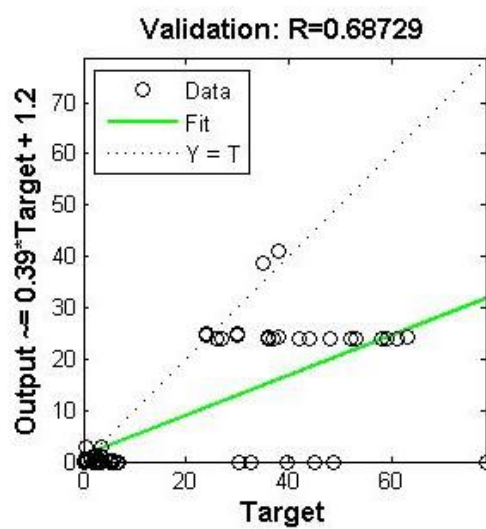
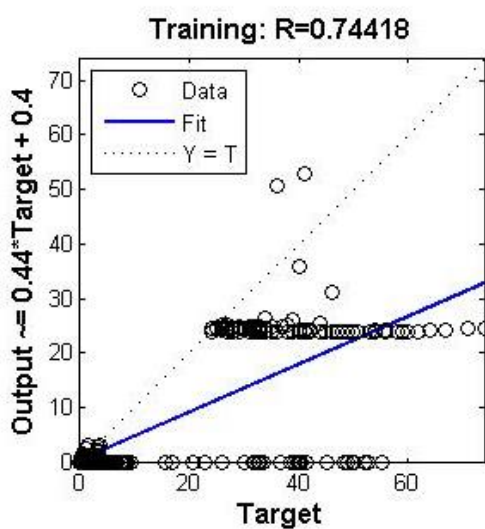
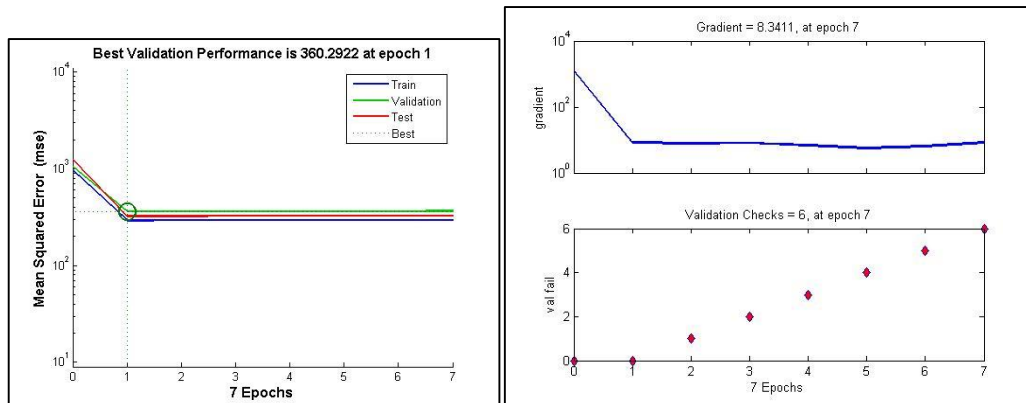


Figure B.8: Performance of Traingdm.

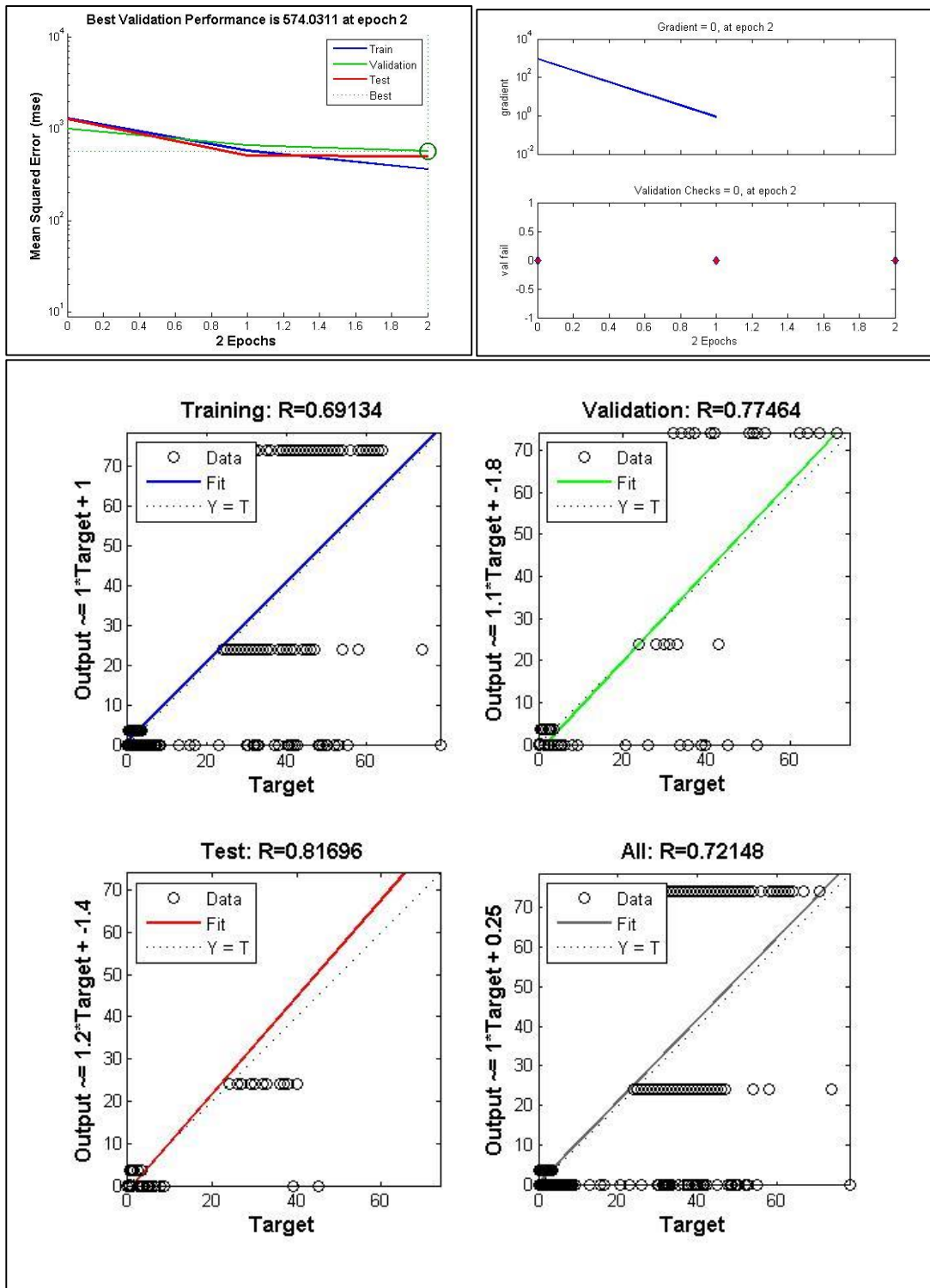


Figure B.9: Performance of Trainoss.

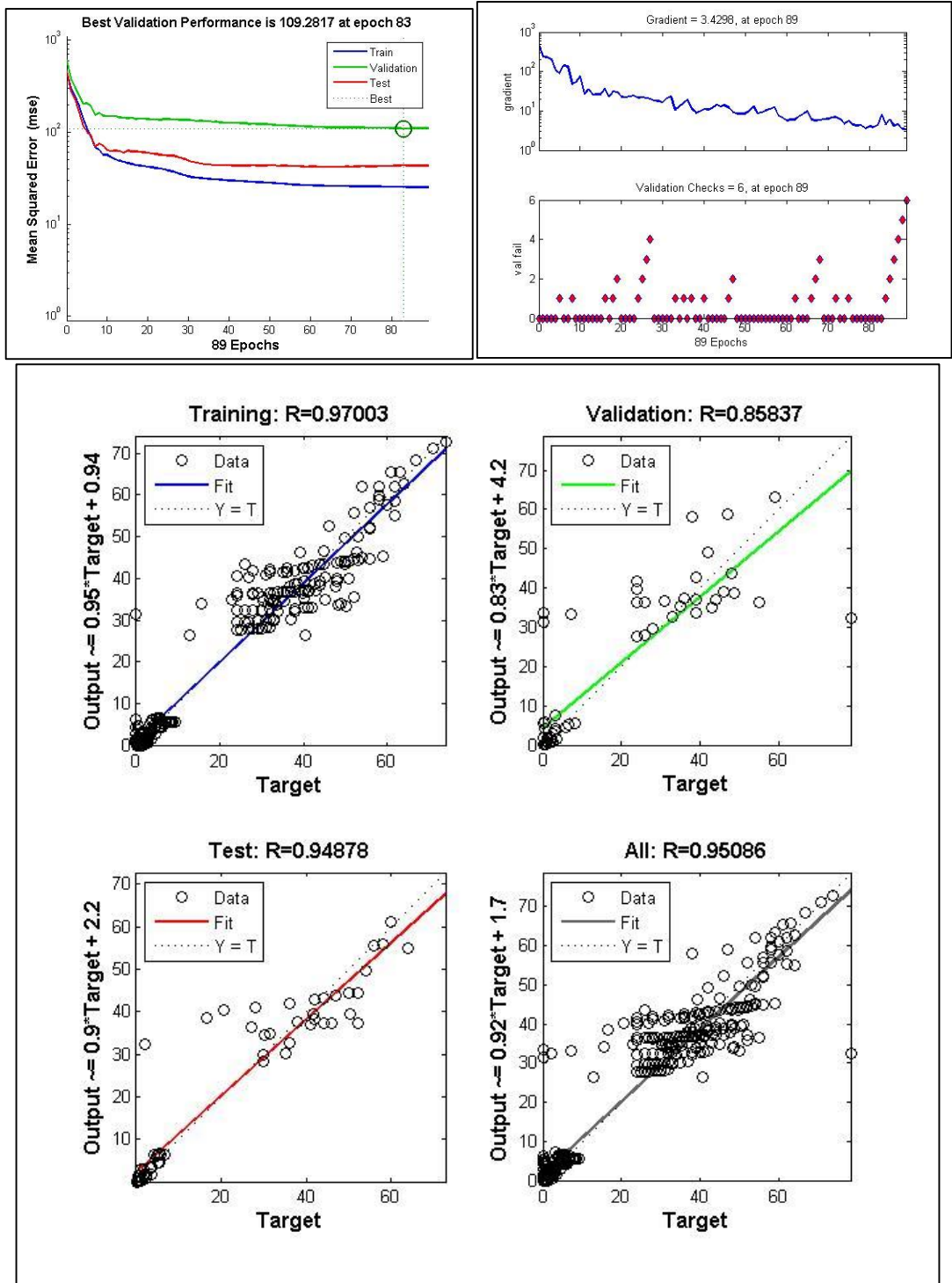


Figure B.10: Performance of Trainrp.

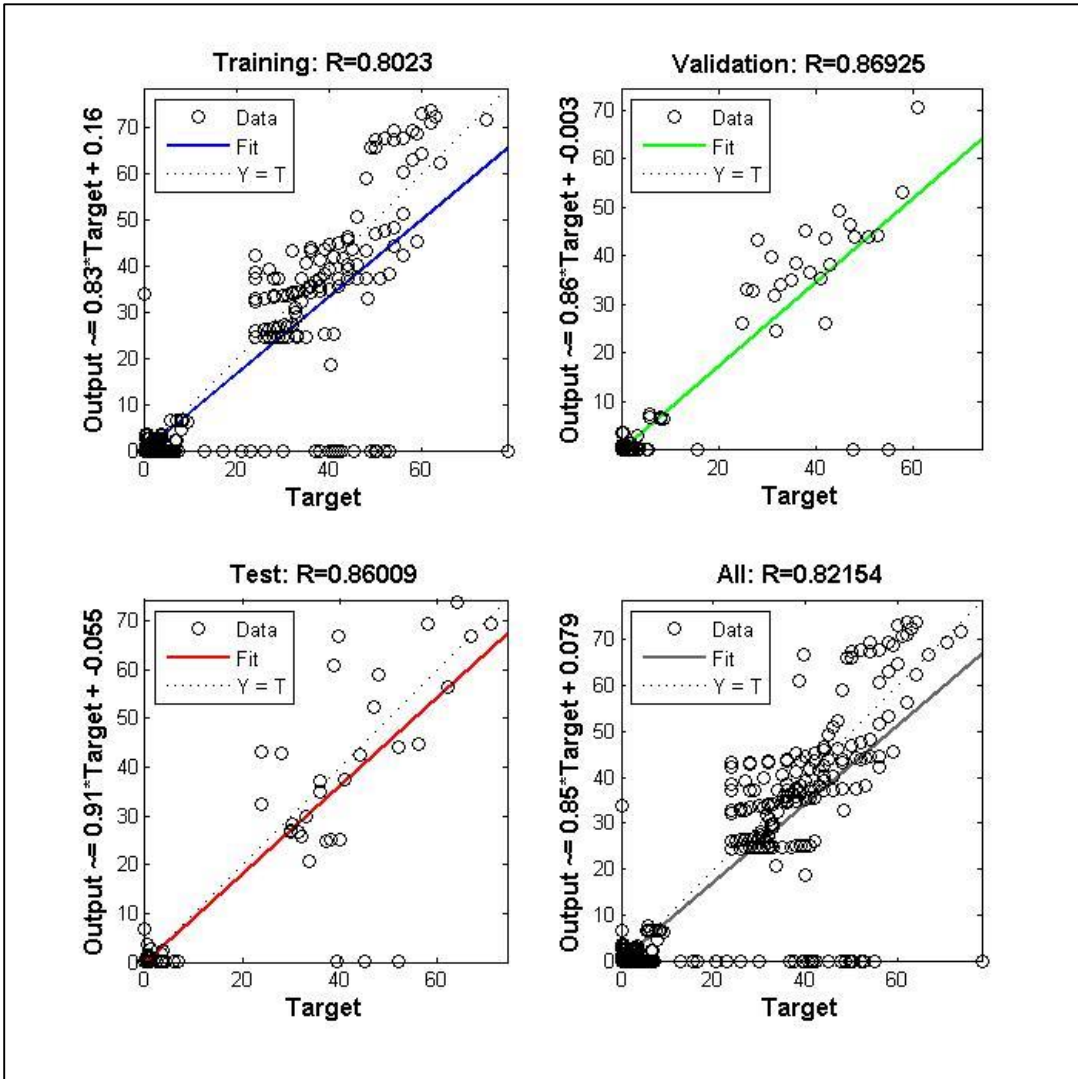
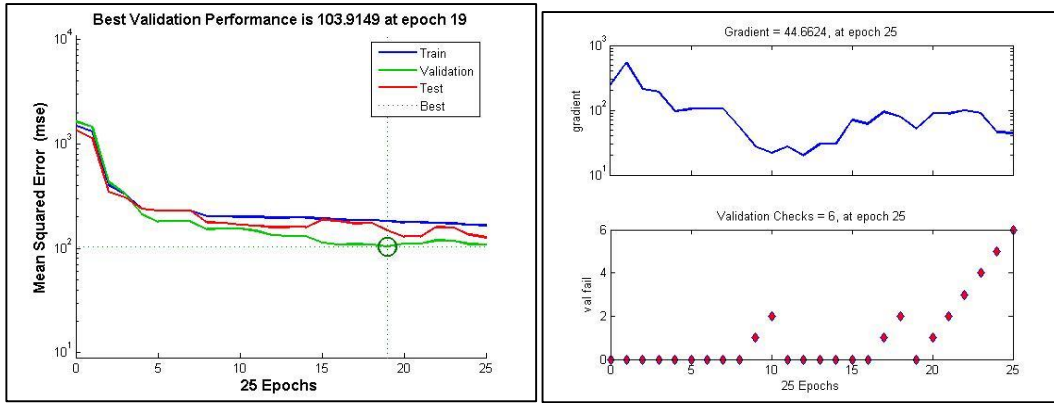


Figure B.11: Performance of Trainscg.

B.2 Optimum Performance Function

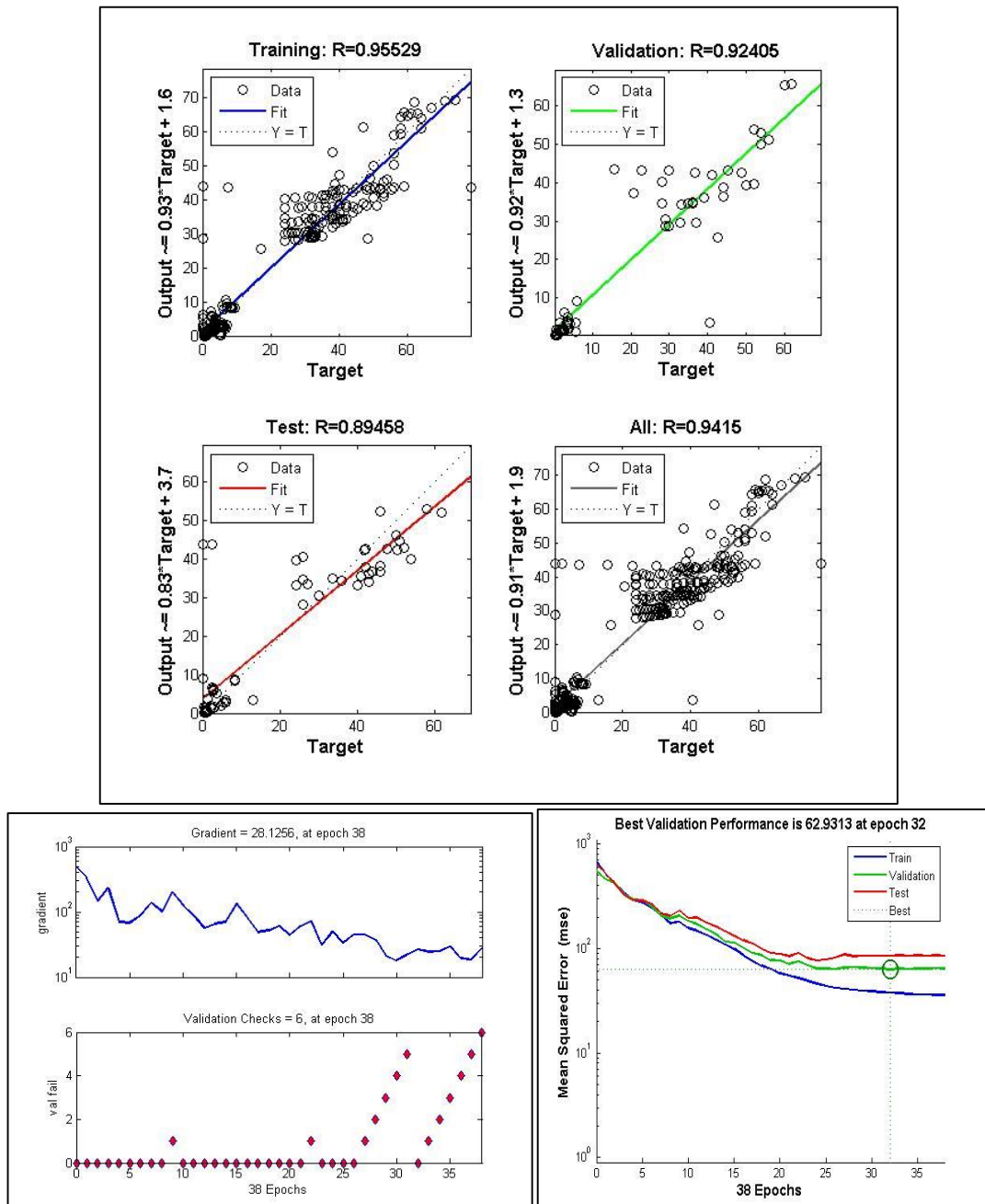


Figure B.12: Performance of MES.

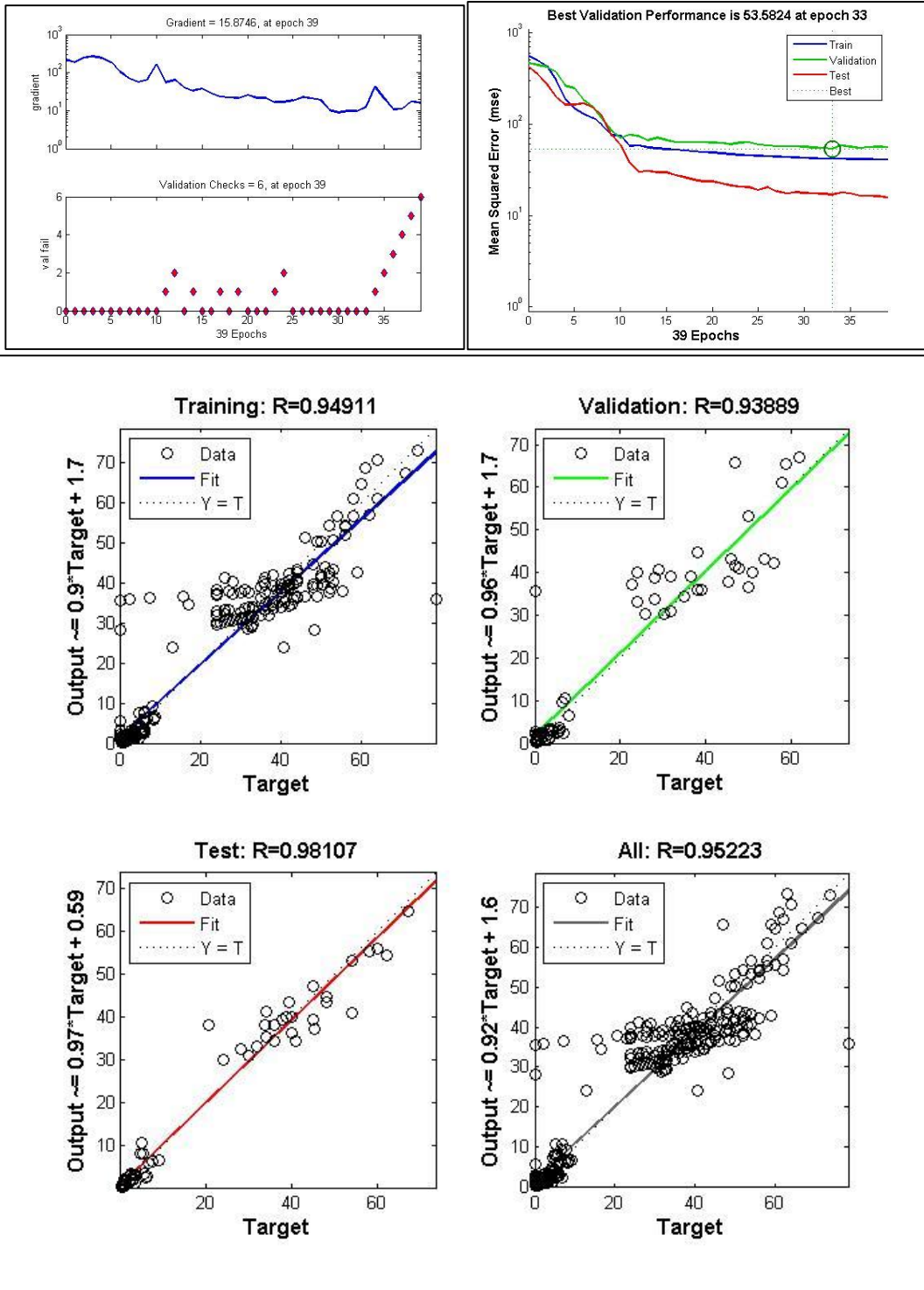


Figure B.13: Performance of MSEREG.

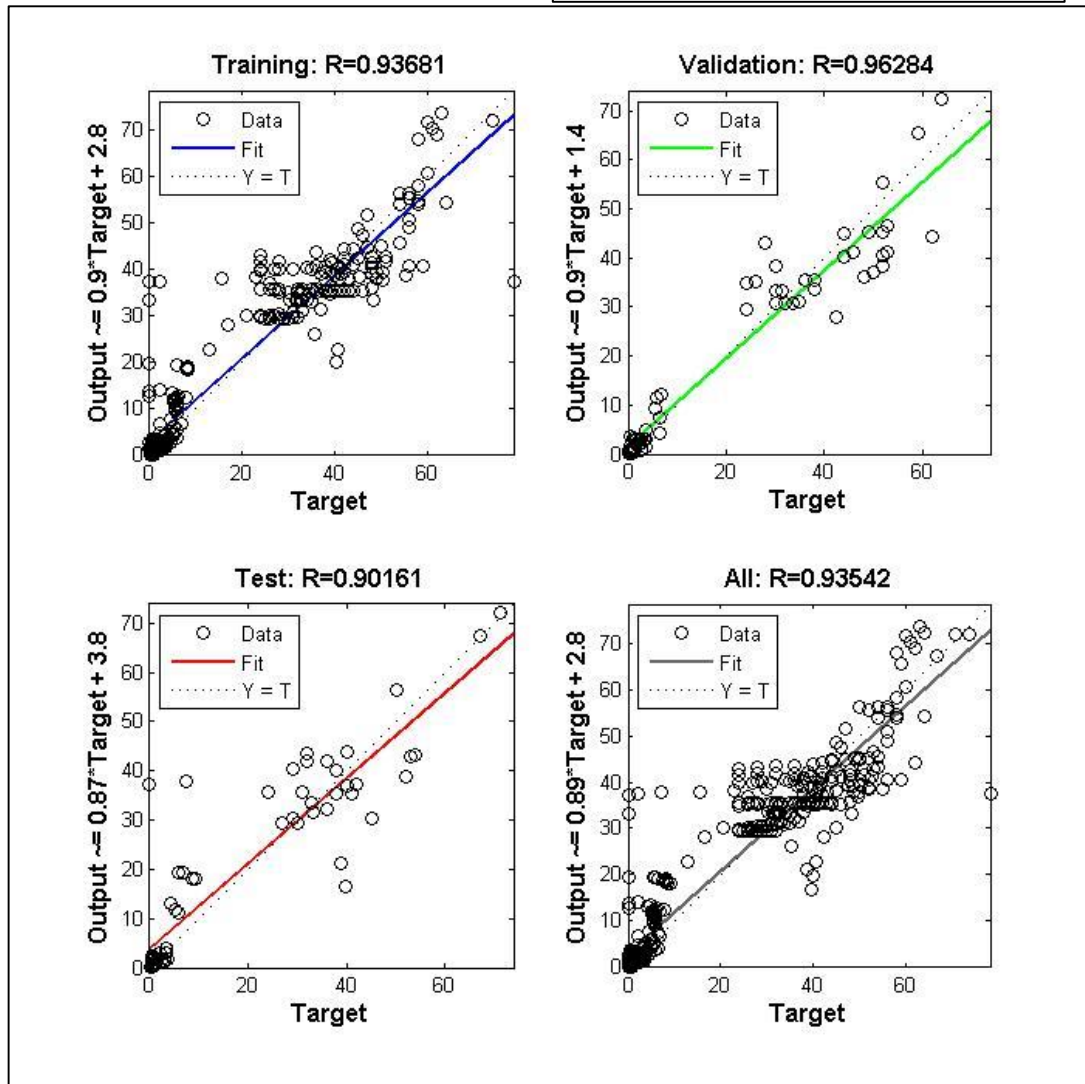
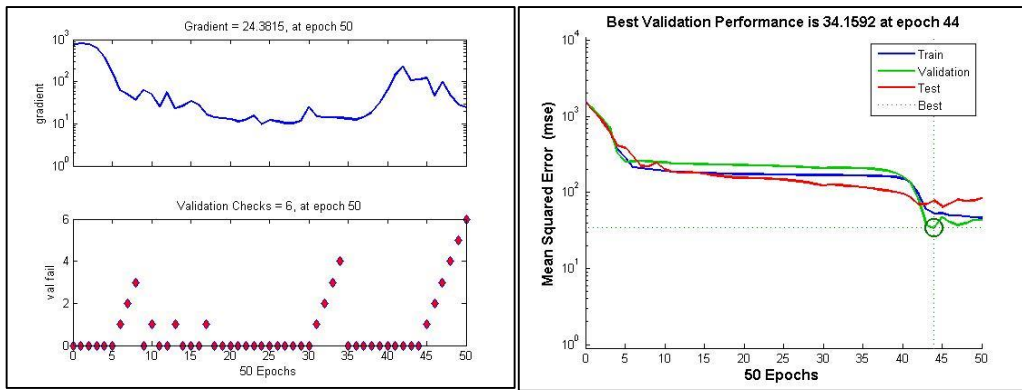


Figure B.14: Performance of SSE.

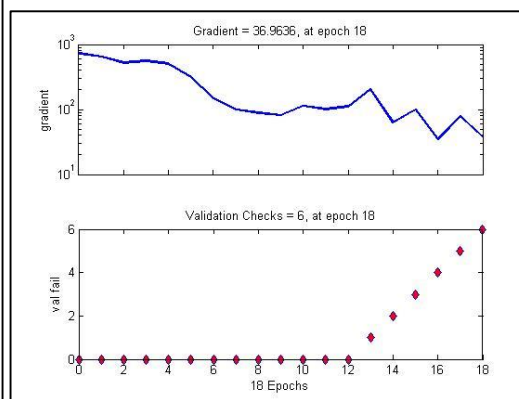
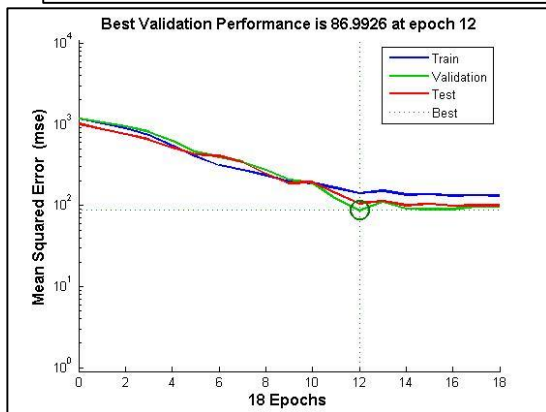
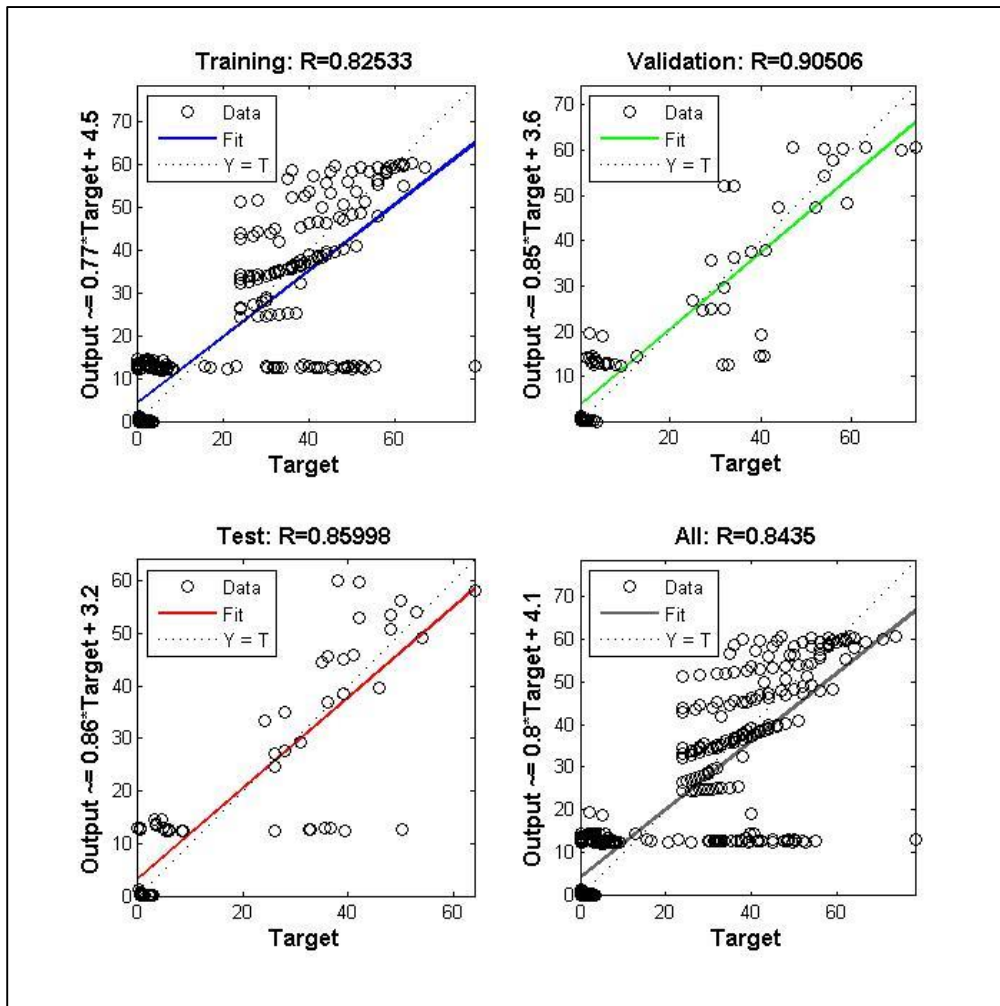


Figure B.15: Performance of ANN model with 2 Neurons in the hidden layer.

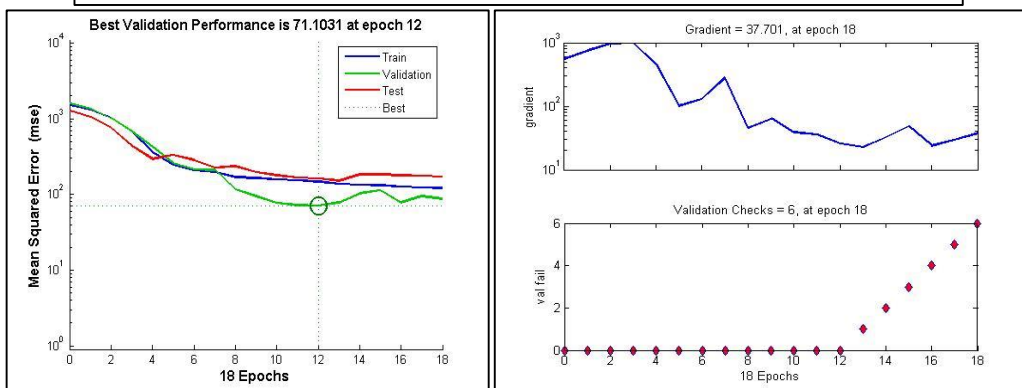
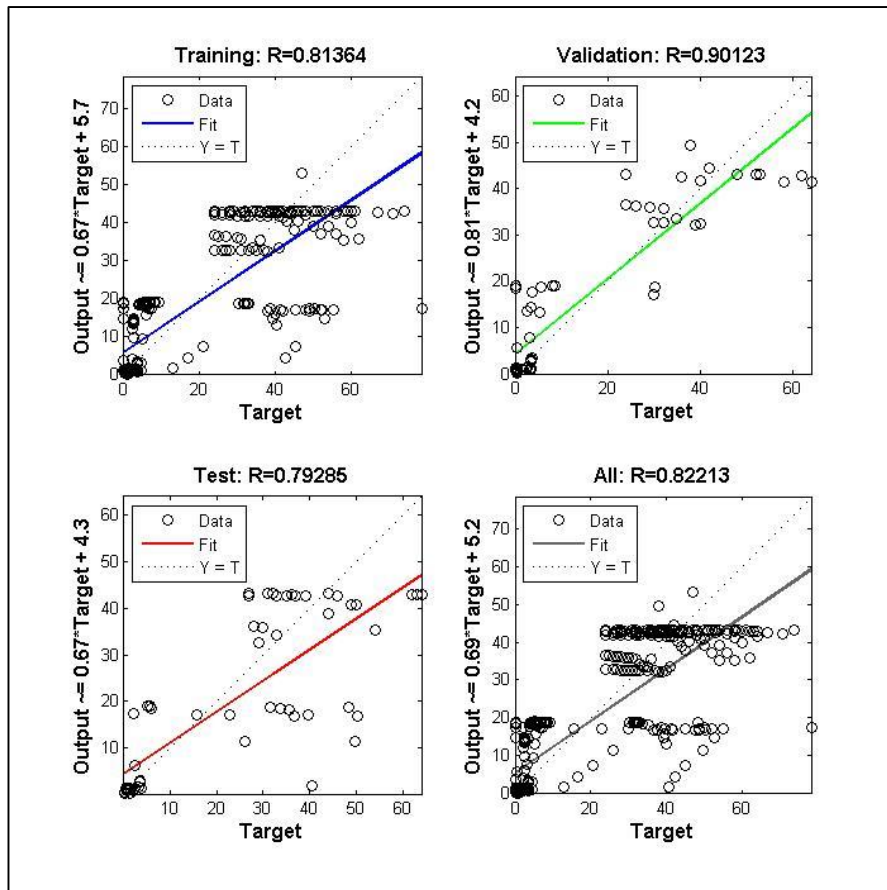


Figure B.16: Performance of ANN model with 4 Neurons in the hidden layer.

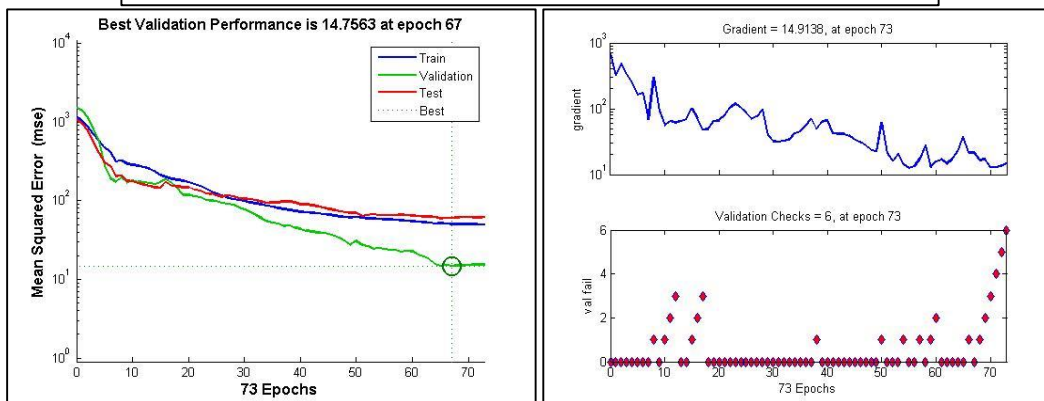
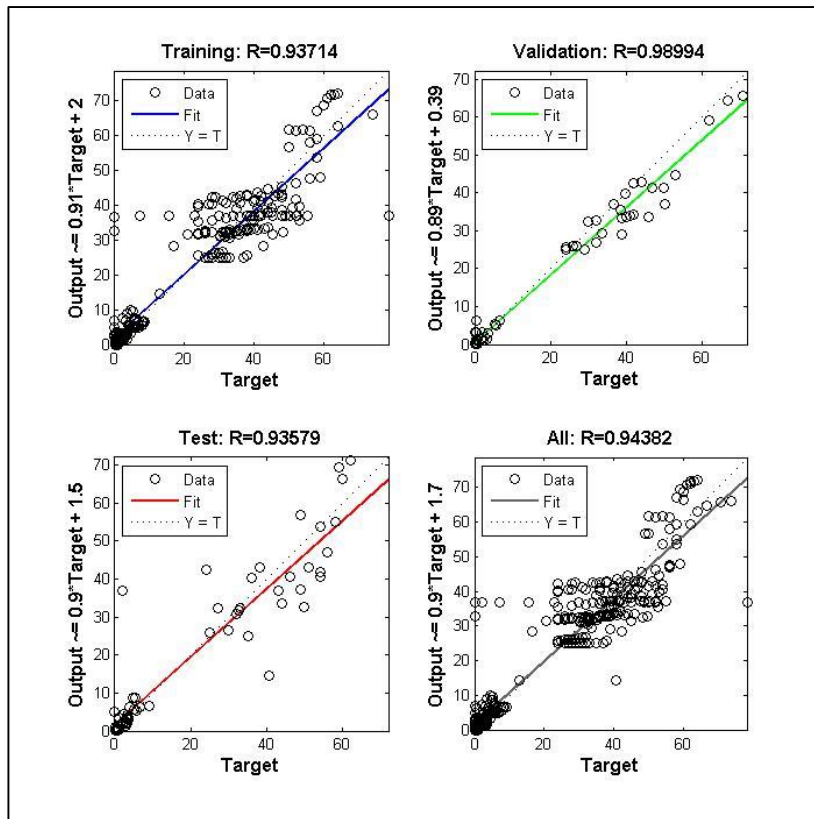


Figure B.17: Performance of ANN model with 6 Neurons in the hidden layer.

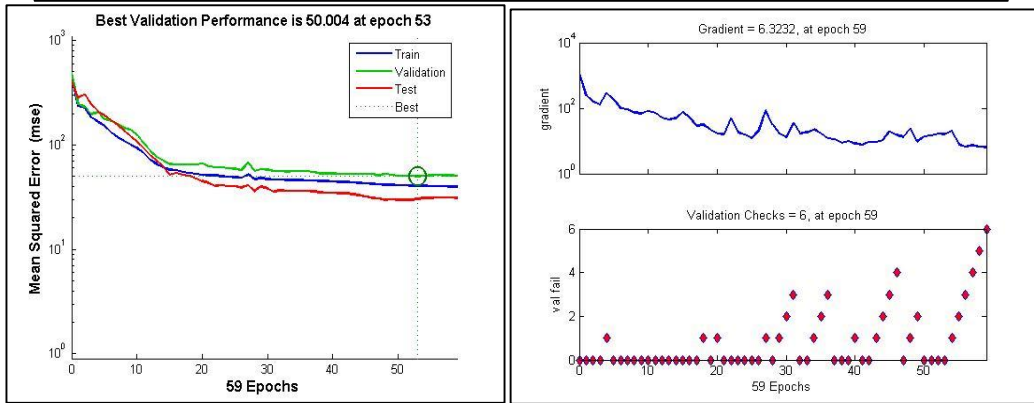
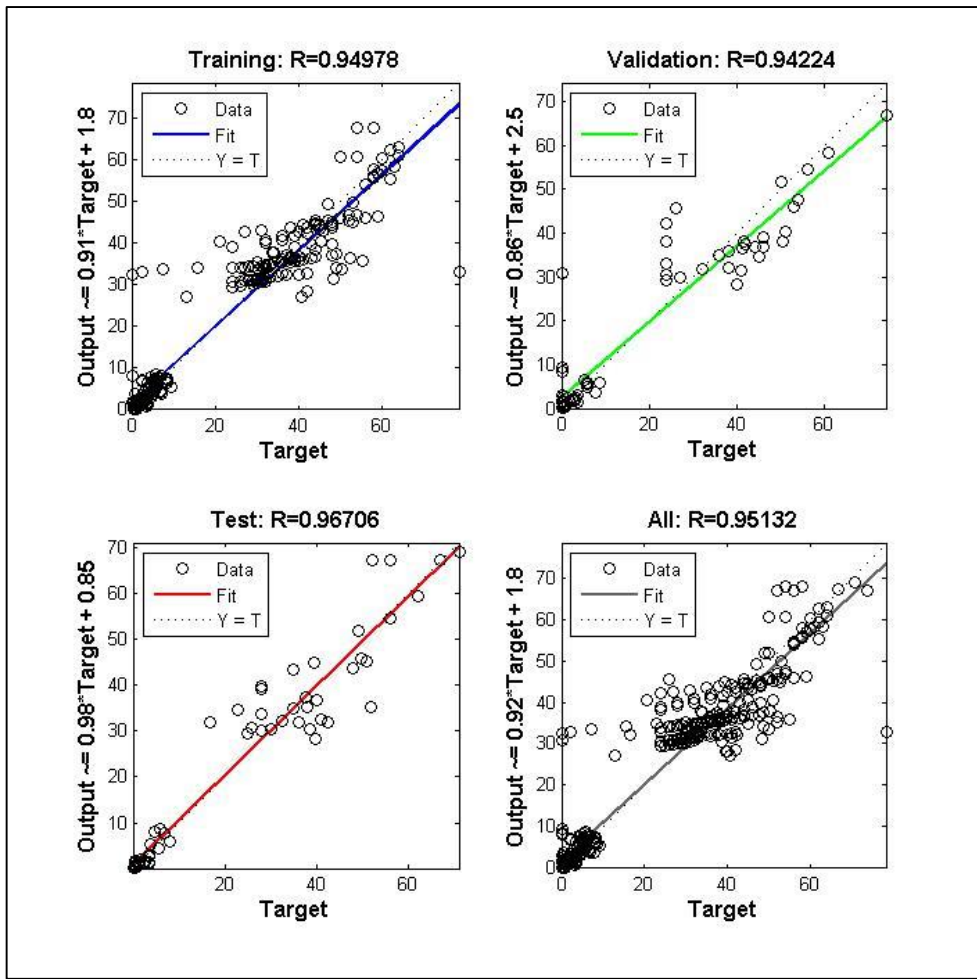


Figure B.18: Performance of ANN model with 8 Neurons in the hidden layer.

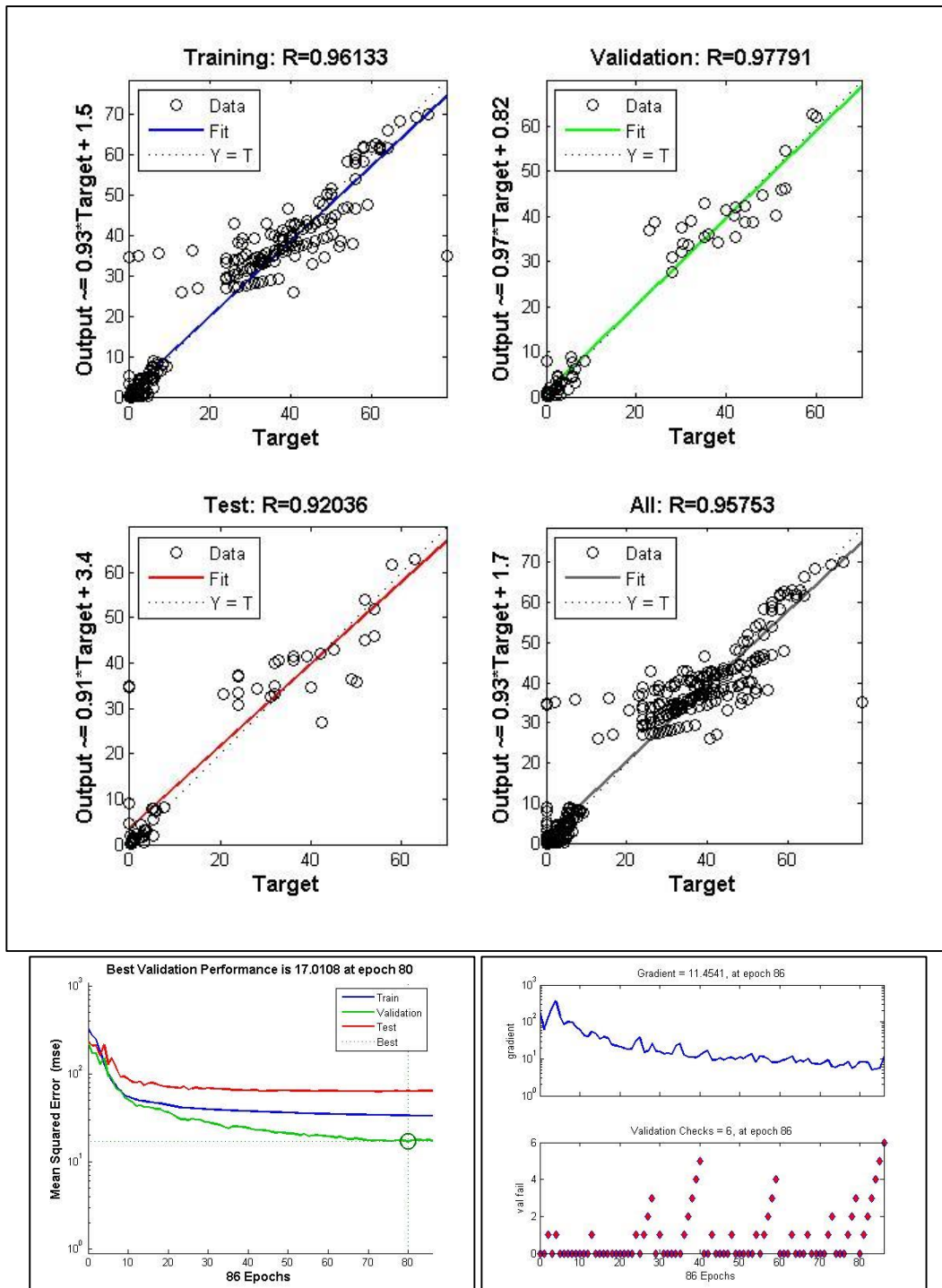


Figure B.19: Performance of ANN model with 10 Neurons in the hidden layer.

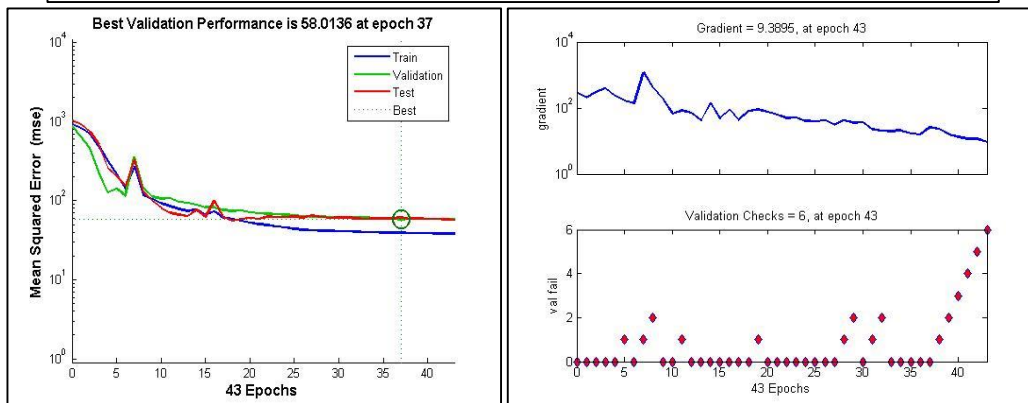
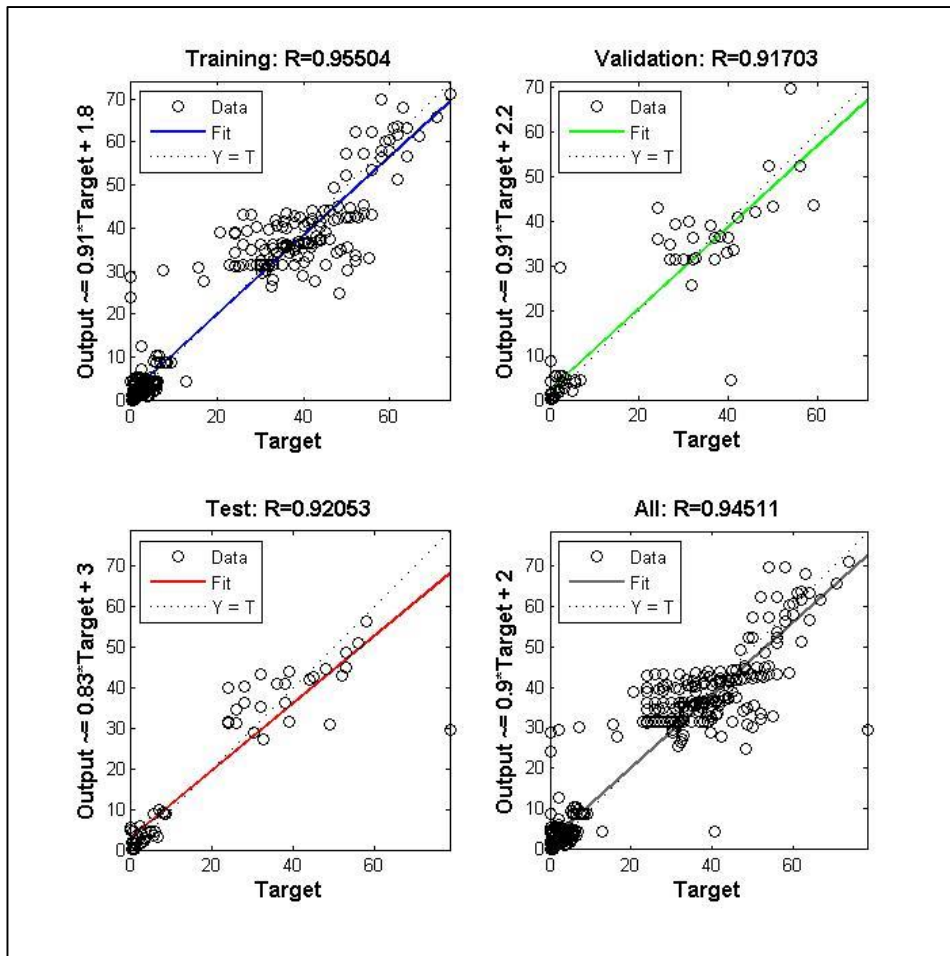


Figure B.20: Performance of ANN model with 12 Neurons in the hidden layer.

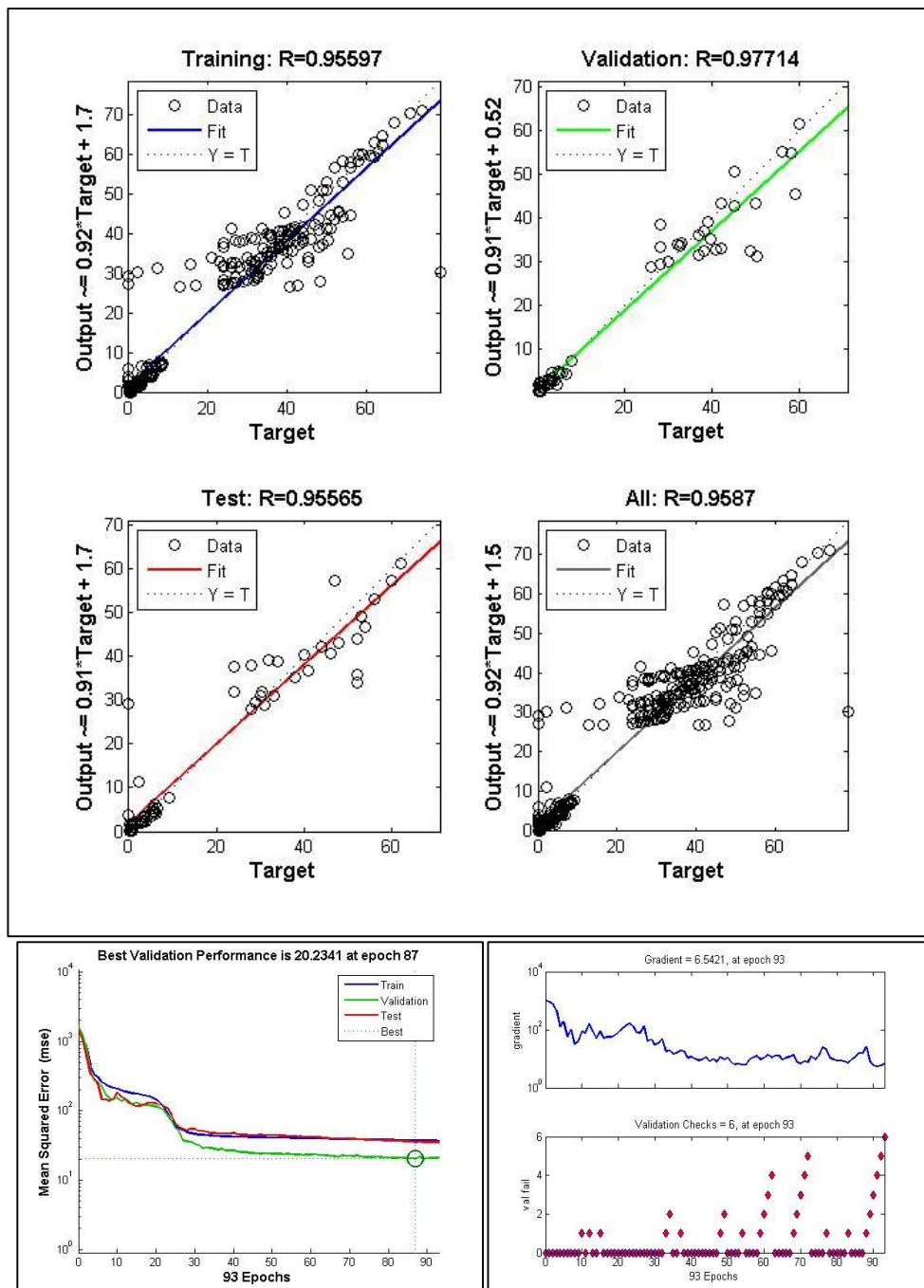


Figure B.21: Performance of ANN model with 14 Neurons in the hidden layer.

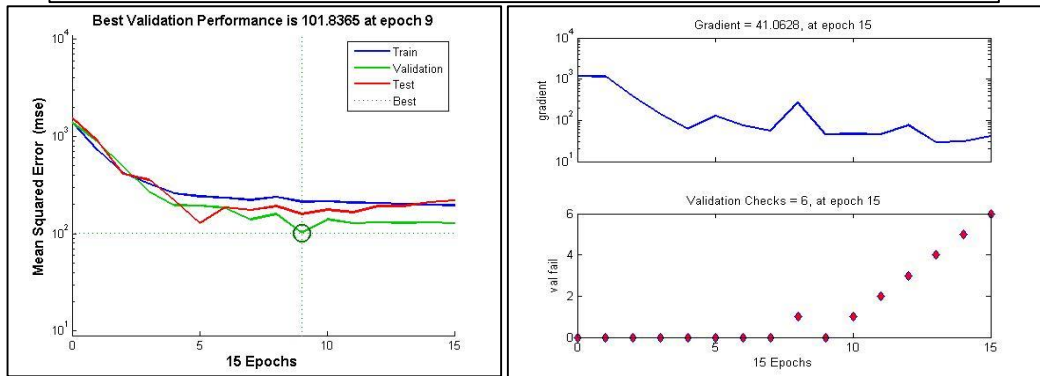
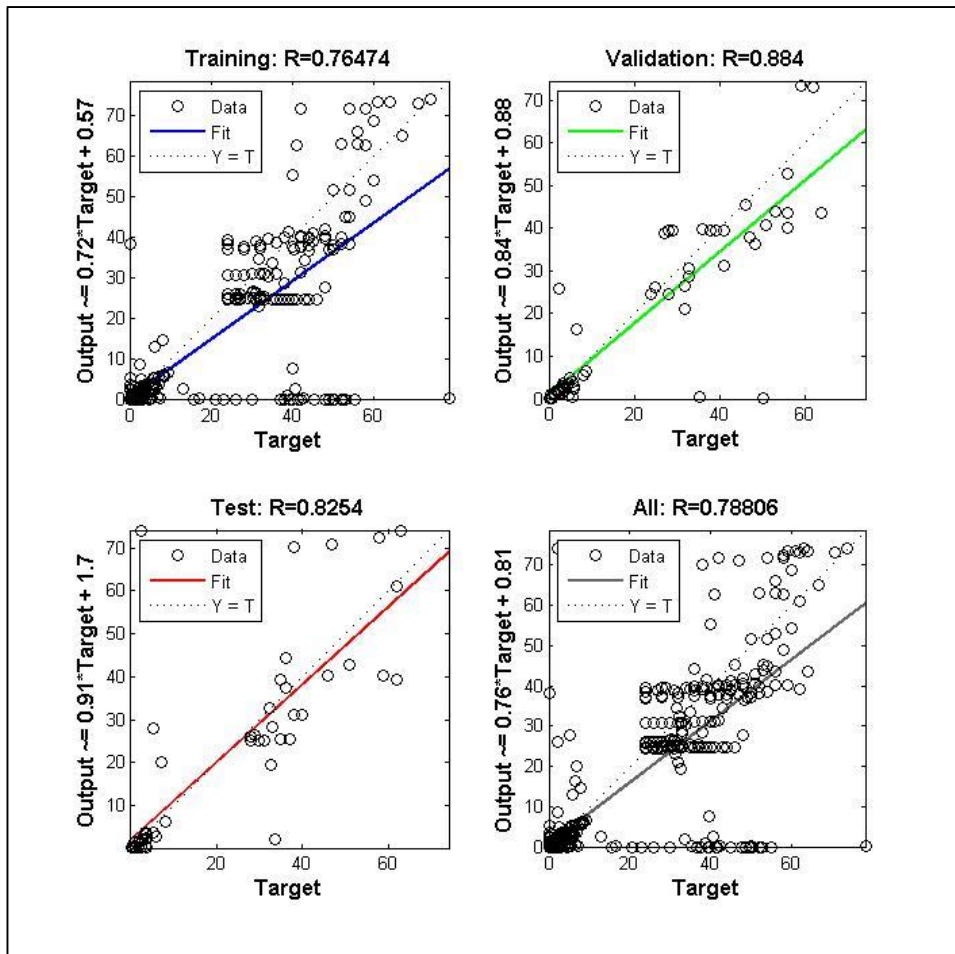


Figure B.22: Performance of ANN model with 16 Neurons in the hidden layer.

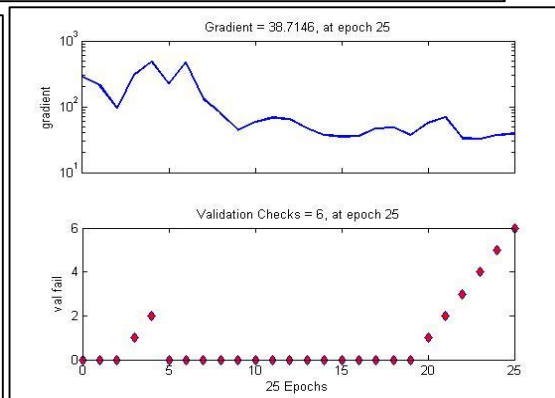
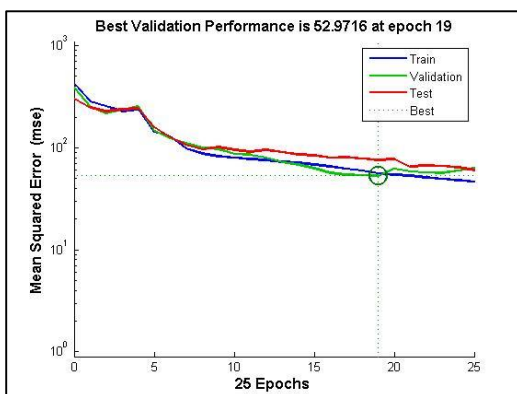
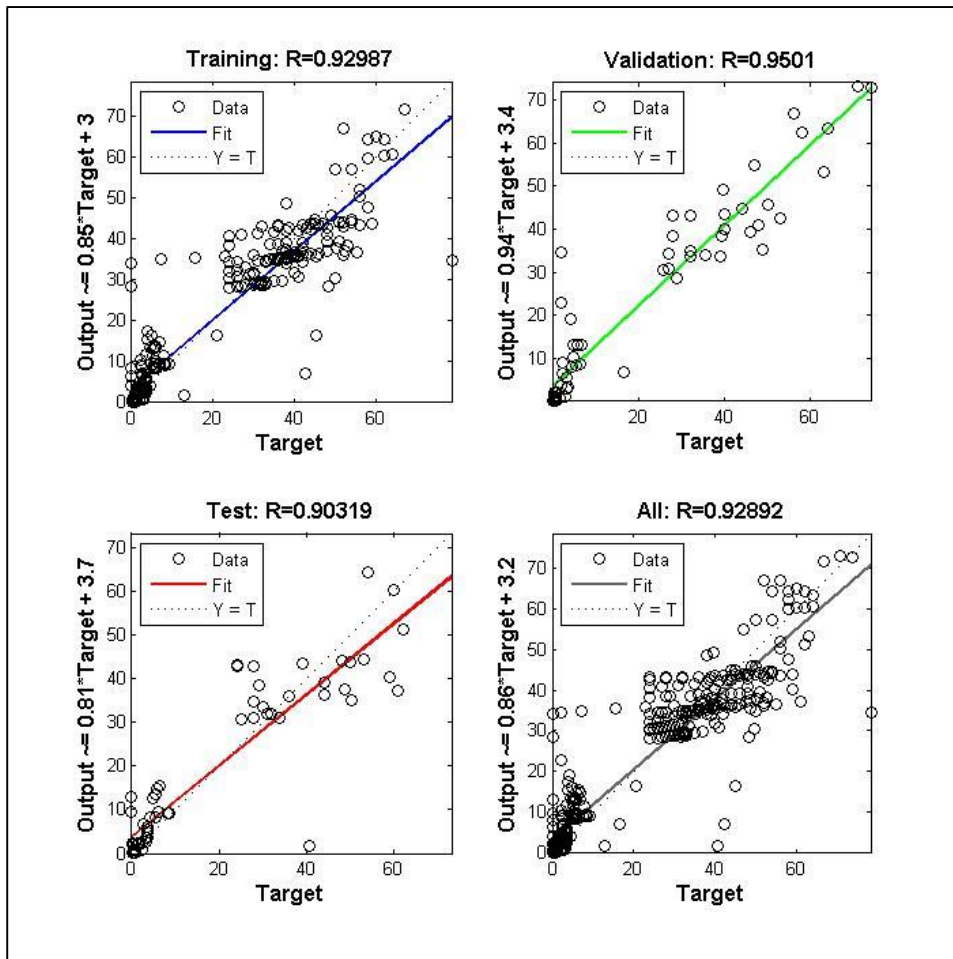


Figure B.23: Performance of ANN model with 18 Neurons in the hidden layer.

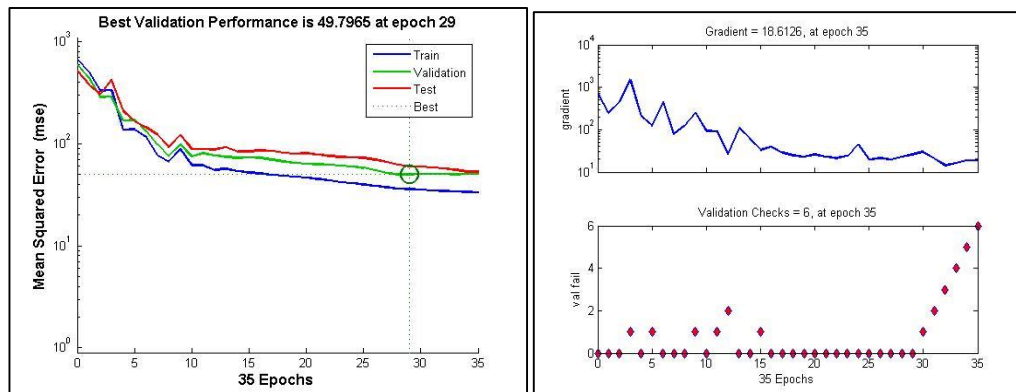
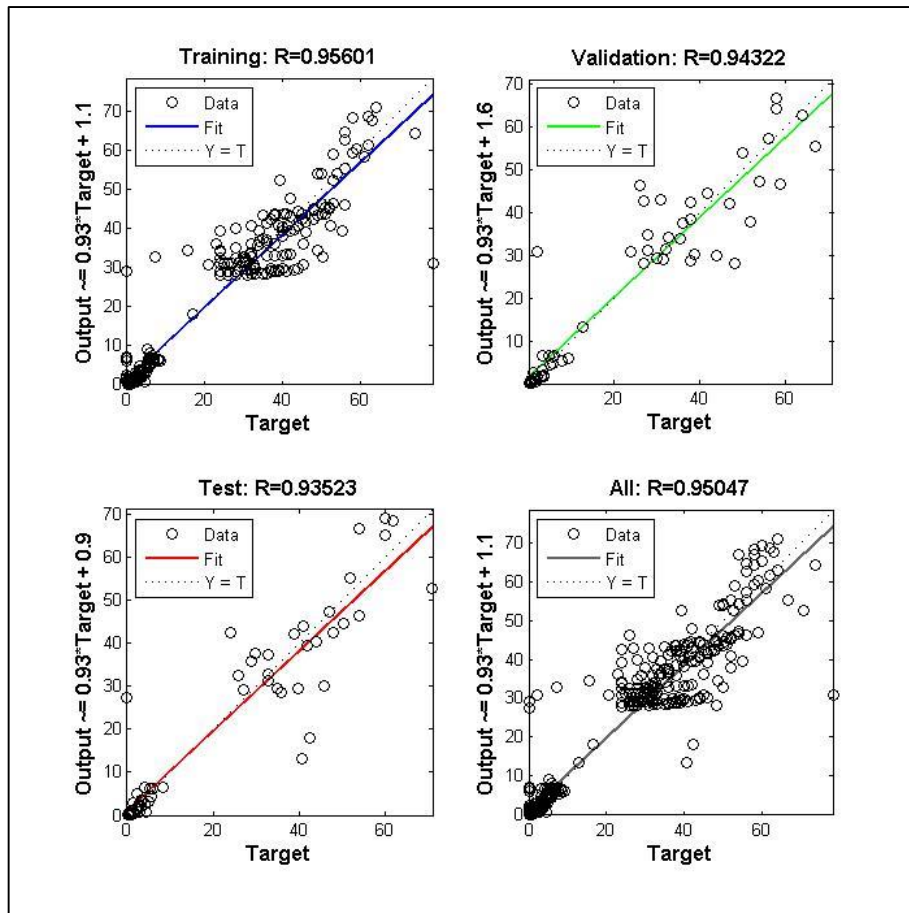


Figure B.24: Performance of ANN model with 20 Neurons in the hidden layer.